6. TSPA-LA MODEL DESCRIPTION

This *Total System Performance Assessment Model/Analysis for the License Application* (TSPA-LA) of the Yucca Mountain repository system is a systematic probabilistic analysis that synthesizes site characterization data, repository design information, process models, abstractions, and analyses. More specifically, U.S. Nuclear Regulatory Commission (NRC) Proposed Rules 10 CFR 63.2 (1) [DIRS 178394] and 10 CFR 63.2 (2) and (3) [DIRS 180319] define three activities as part of performance assessment (PA):

"Performance assessment means an analysis that:

1. Identifies the features, events, processes (FEPs) (except human intrusion), and sequences of events and processes (except human intrusion) that might affect the Yucca Mountain disposal system and their probabilities of occurring;

2. Examines the effects of those FEPs, and sequences of events and processes upon the performance of the Yucca Mountain disposal system; and

3. Estimates the dose incurred by the reasonably maximally exposed individual, including the associated uncertainties, as a result of releases caused by all significant FEPs, and sequences of events and processes, weighted by their probability of occurrence."

The first activity determines what representations of possible future states of the repository (i.e., scenario classes) are sufficiently important to warrant quantitative analysis. For the TSPA-LA, nominal and event scenario classes are analyzed. The Nominal Scenario Class incorporates all FEPs (Appendix I), except those FEPs associated with early failures of the waste packages (WPs) or drip shields (DSs) and disruptive events. The Early Failure Scenario Class addresses FEPs that describe the potential for DS and WP early failure in the absence of disruptive events. The TSPA-LA Model includes two scenario classes that address the possibility that disruptive events may occur at or near the repository and that these events may affect repository performance. In addition, the NRC Proposed Rule 10 CFR 63.322 [DIRS 180319] requires the U.S. Department of Energy (DOE) to assess a Human Intrusion Scenario and 10 CFR 63.321 [DIRS 178394] provides the performance standard for the Human Intrusion Scenario. Section 6.1.1 summarizes the scenario class development process adopted for the TSPA-LA, including the basis for identification and screening of potentially relevant FEPs. Section 6.1.2 summarizes the selection of the scenario classes. The following scenario classes are included in the TSPA-LA.

Nominal Scenario Class (Section 6.3)—The Nominal Scenario Class uses the TSPA-LA Model components to describe all included FEPs that are nominally expected to occur. The Nominal Scenario Class encompasses all processes affecting the integrity of the WPs containing spent nuclear fuel (SNF) and high-level (radioactive) nuclear waste (HLW) in the absence of disruptive events. These processes include WP degradation because of corrosion mechanisms including general corrosion, stress corrosion cracking (SCC), localized corrosion, and microbially influenced corrosion (MIC).

Early Failure Scenario Class (Section 6.4)—The Early Failure Scenario Class describes performance of the repository system in the event of early failures of the DSs or WPs due to

manufacturing or material defects or to pre-emplacement operations including improper heat treatment. Early failure events are addressed by two modeling cases: (1) the Drip Shield Early Failure (EF) Modeling Case that includes an early failure of one or more DSs that then assumes localized corrosion of the WP(s) beneath the failed DS(s) and the subsequent release of radionuclides to the groundwater, and (2) the Waste Package EF Modeling Case that includes an early failure of one or more WPs and the subsequent release of radionuclides to the groundwater.

Igneous Scenario Class (Section 6.5)—This class considers those FEPs associated with igneous activity. This scenario class includes two modeling cases: (1) the Igneous Intrusion Modeling Case with releases of radionuclides to groundwater, and (2) the Volcanic Eruption Modeling Case with releases of radionuclides to the atmosphere. The Igneous Intrusion Modeling Case assumes that a dike intersects the repository and destroys DSs and WPs in those drifts intruded by magma, exposing the waste forms to percolating water and mobilizing radionuclides. The Volcanic Eruption Modeling Case represents the fraction of igneous intrusions in which a volcanic eruption also occurs.

Seismic Scenario Class (Section 6.6)—The Seismic Scenario Class describes performance of the repository system in the event of seismic activity capable of disrupting repository emplacement drifts and the engineered barrier system (EBS). This scenario class includes processes captured in the Nominal Scenario Class, as well as damage to DSs and WPs as a function of the magnitude of the seismic event(s). Seismic disruption of the repository is addressed in two modeling cases. The first modeling case represents the DSs and WPs that fail from nominal processes, as well as mechanical damage associated with seismic vibratory ground motion. This modeling case is referred to as the Seismic Ground Motion (GM) Modeling Case. The Seismic GM Modeling Case includes drift degradation and subsequent effects of accumulating rubble. The Seismic GM Modeling Case also includes the effects of SCC of the WPs and diffusion of mobilized radionuclides through WP cracks and WP rupturing with the potential to have both advection and diffusion of mobilized radionuclides through the rupture opening. The second modeling case considers the WPs that are breached because of fault displacement. This modeling case is referred to as the Seismic Fault Displacement (FD) Modeling Case. The Seismic FD Modeling Case includes breaching of WPs and DSs by the displacement along faults, as well as nominal failures of the DSs and WPs. Seismic ground motion damage of the DSs and WPs is excluded from this modeling case. This modeling case includes advection and diffusion of mobilized radionuclides out of the breached WP.

Human Intrusion Scenario (Section 6.7)—The Human Intrusion Scenario describes performance of the repository system in the event that subsurface exploratory drilling disrupts the repository. Human intrusion disruption of the repository is addressed by a single modeling case.

The second and third PA activities defined by the NRC Proposed Rule 10 CFR 63.2 (2) and (3) [DIRS 180319] require the development of a TSPA Model that describes overall system behavior and clearly displays the extent to which uncertainty in the understanding of the repository system affects the description of system behavior. The Yucca Mountain repository system is a combination of integrated processes that are conceptualized and modeled as a collection of coupled model components. For the TSPA-LA Model, eight principal model

components are combined to evaluate repository system performance for Nominal, Early Failure, Igneous, and Seismic Classes and the Human Intrusion Scenario. The model components are:

- Unsaturated Zone (UZ) Flow
- EBS Environment
- WP and DS Degradation
- Waste Form Degradation and Mobilization
- EBS Flow and Transport
- UZ Transport
- Saturated Zone (SZ) Flow and Transport
- Biosphere.

The TSPA-LA Model components and their supporting abstraction models and analyses are illustrated on Figure 6-1. The model components are in the top row of the figure, with submodels and abstractions below the model component level. As shown, model components are composed of a collection of submodels (e.g., process models, analyses, or abstractions) that together represent a key component of the repository system. Submodels are implemented in the TSPA-LA Model to represent each abstraction, analysis, or process model included in the TSPA-LA Model. Note that submodels have arrows on the left side illustrating links to the parent model component. Figure 6-1 also illustrates specific information that is used to analyze the disruptive event scenario classes. Note that the Nominal, Early Failure, Igneous (except volcanic eruption), and Seismic Scenario Classes and the Human Intrusion Scenario use many of the same submodels and parameters. Each of the model components included in the TSPA-LA Model quantifies uncertainty in the underlying processes and input parameters, or bounds that uncertainty appropriately by selecting parameters and parameter values that bound potential consequences of the TSPA-LA Model from an overall performance perspective (i.e., that bound the expected dose to the receptor). Input uncertainty in the TSPA-LA Model is explicitly represented by assigning probability distributions to parameters representing epistemic and aleatory uncertainty. Because many of the TSPA-LA Model inputs are uncertain, the TSPA-LA Model uses a probabilistic framework to implement the model components and submodels. The treatment of uncertainty and the probabilistic framework used in implementing the TSPA-LA Model is discussed further in Section 6.1.3.

Section 6 Structure—The primary goals of Section 6 are to describe: (1) how the model components and their submodels, illustrated on Figure 6-1, are integrated in the TSPA-LA Model, and (2) how the TSPA-LA Model is implemented to estimate the dose incurred by the reasonably maximally exposed individual (RMEI) due to radionuclide releases in the Nominal, Early Failure, Igneous, and Seismic Scenario Classes and the Human Intrusion Scenario. The contents of Section 6 are summarized as follows.

Section 6.1 develops the basis for a detailed description of the TSPA-LA Model and its implementation for the Nominal, Early Failure, Igneous, and Seismic Scenario Classes and the Human Intrusion Scenario. The following topics are presented:

- FEP analysis for the TSPA-LA Model and the formation and screening of scenario classes (Section 6.1.1)

- Descriptions of scenario classes and their treatment in the TSPA-LA Model (Section 6.1.2)
- Treatment of uncertainty in the TSPA-LA Model analyses (Section 6.1.3)
- A description of the TSPA-LA Model structure and design (Section 6.1.4)
- TSPA-LA Model file architecture (Section 6.1.5).

Section 6.2 introduces alternative conceptual models (ACMs) for the TSPA-LA Model, including a general discussion of ACMs. Detailed evaluations of the ACMs are included in Sections 6.3, 6.4, 6.5, 6.6, and 6.7.

Section 6.3 provides detailed descriptions of the TSPA-LA Model components and submodels. The model component and submodel descriptions include:

- A discussion of how submodels are connected to other submodels and model components in the TSPA-LA Model.
- A description of the conceptual model on which the submodel is based.
- A description of the submodel abstractions.
- A description of how the abstractions are implemented in the TSPA-LA Model.
- An evaluation of the consistency and reasonable and technically defensible conservatism in assumptions and parameters used in the TSPA-LA Model. Assumptions and parameter values that are different among submodels in the TSPA-LA Model are documented.
- A summary of ACMs that were considered in the development of the conceptual model.

The focus of Section 6.3 is on the TSPA-LA Model components and submodels and their implementation in the Nominal Scenario Class. The majority of these submodels are applied in the same manner to evaluate the consequences of the Early Failure, Igneous, and Seismic Scenario Classes and the Human Intrusion Scenario.

Section 6.3 provides a discussion on the consistency of modeling assumptions for each model component. This section also includes explanations of the differences in model assumptions between different model abstractions, and it discusses their impact on the TSPA-LA Model.

Section 6.3 discusses reasonable and technically defensible conservatisms associated with the TSPA-LA Model for each model component. The list of reasonable and technically defensible conservatisms in each subsection focuses on those aspects of the TSPA-LA Model that result in estimates of performance that either:

- Overestimate the consequences of processes that have potential to degrade subsystem performance

- Underestimate the effects of processes that might result in improved subsystem performance.

The reasonable and technically defensible conservatisms presented in Sections 6.3, 6.4, 6.5, 6.6, and 6.7, in respect to how they impact the TSPA-LA Model at the submodel level, are primarily associated with assumptions from supporting analysis and model reports rather than on the overall TSPA-LA Model performance. These reasonable and technically defensible conservatisms may or may not have a direct impact on the performance of the TSPA-LA Model. Validation of the TSPA-LA Model consists of a sequence of activities that are designed to build confidence in the results of the model (Section 7, Volume II). An important function of the TSPA-LA Model is to assimilate the conservatisms identified in the supporting analysis and model reports to evaluate their significance (either quantitatively or qualitatively) to performance. The Performance Margin Analysis (PMA) presented in Section 7.7.4 quantifies the impact of submodel representations and assumed conservatisms with respect to the overall performance. Additionally, TSPA-LA Model uncertainties identified in Sections 6.3, 6.4, 6.5, 6.6, and 6.7 will affect the assessment of total system performance and must be taken into account. A discussion presented in Section 7.4 and Appendix K includes information regarding the impacts of these uncertainties on those estimates (e.g., uncertainty in the estimate of mean annual dose).

Sections 6.4, 6.5, 6.6, and 6.7 describe how the consequences of the Early Failure, Igneous, and Seismic Scenario Classes and the Human Intrusion Scenario, respectively, are evaluated, including modifications to the model components described in Section 6.3. Each scenario class section includes discussions that are specific to each case that outline the differences between the Nominal Scenario Class model components and submodels and those used to model the Early Failure, Igneous and Seismic Scenario Classes, and the Human Intrusion Scenario. Sections 6.4, 6.5, 6.6, and 6.7 also include a discussion of the consistency of model assumptions and conservatisms specific to each scenario class.

Model Terminology—A variety of model components and submodels are discussed in Section 6. Use of the word model, without any qualification, will be restricted to the TSPA-LA Model itself. A number of elements were identified within the TSPA-LA Model. The elements shown on Figure 1-3, commonly referred to as the TSPA wheel, have been identified by the TSPA-LA modeling team as particularly important. The items indicated by icons on Figure 1-3 will be referred to as model components. These model components were chosen because they provide a useful framework for discussing and reviewing the TSPA-LA Model and the process level models that support the TSPA-LA Model. All other parts of the TSPA-LA Model will be referred to as submodels. The distinction between the terms model components and submodels are, to a certain extent, arbitrary, but they have been introduced to try to improve the clarity of the discussion within Section 6. Submodels in the TSPA-LA Model are composed of one or more process models, analyses, or abstractions. Table 6-1 maps the principal model components of the TSPA-LA Model from Figure 6-1 to each submodel discussed in Sections 6.1.4, 6.3, 6.4, 6.5, 6.6, and 6.7. Additionally, the process model, analysis, or abstraction that feeds each submodel is listed in Table 6-1 and discussed in Sections 6.3, 6.4, 6.5, 6.6, and 6.7. The term process model is used throughout Section 6.0 as a generalized term for a mathematical model that represents an event, phenomenon, process, or component, evaluated within an analysis and model report. The process model moniker is used here to identify the detailed computational

models that form the basis of the data, analysis, and abstractions implemented with the TSPA-LA Model.

Table 6-1. TSPA-LA Model Discretization

Figure 6-1		Section 6				Referenced Analyses/Models	
TSPA-LA Principal Model Components		Subsection			Submodel for TSPA-LA	Abstraction/Process Model(s)/Analysis(es)	Reference
Unsaturated Zone Flow Model Component	Site-Scale UZ Flow	Mountain-Scale UZ Flow	6.3.1		UZ Flow Fields Abstraction	UZ Flow Fields Abstraction	1
						Site-Scale UZ Flow Process Model	
						Active Fracture Model	
						Dual-Permeability UZ Flow Model	
	Infiltration Analysis				Infiltration Submodel	Infiltration Model Abstraction	2
						Infiltration Process Model	2
	Climate Analysis				Climate Submodel	Future Climate Analysis	3
	Drift Seepage	Drift-Scale UZ Flow	6.3.3	6.3.3.1	Drift Seepage Submodel	Drift Seepage Abstraction	4,5
						Drift Seepage Abstraction including Drift Collapse	
						TH Seepage Process Model	
	Drift Wall Condensation			6.3.3.2	Drift Wall Condensation Submodel	In-Drift Natural Convection and Condensation Process Model	7
						Drift Wall Condensation Abstraction	
EBS Environment Model Component	EBS Thermal-Hydrologic Environment	EBS TH Environment	6.3.2		EBS TH Environment Submodel	MSTHM Process Model	6
						MSTHM Abstraction	
	EBS Chemical Environment	EBS Chemical Environment	6.3.4		EBS Chemical Environment Submodel	EBS P&CE Abstraction	8
						IDPS Process Model	15

Table 6-1. TSPA-LA Model Discretization (Continued)

Figure 6-1		Section 6				Referenced Analyses/Models	
TSPA-LA Principal Model Components		Subsection			Submodel for TSPA-LA	Abstraction/Process Model(s)/Analysis(es)	Reference
WP and DS Degradation Model Component	WAPDEG	WP and DS Degradation	6.3.5	6.3.5.1	WP and DS Degradation Submodel	WP General Corrosion Abstraction	10,11,12
						WP MIC Abstraction	
						WP SCC Abstraction	
						DS General Corrosion Abstraction	
	Localized Corrosion on WP Outer Surface			6.3.5.2	Localized Corrosion Initiation Submodel	Localized Corrosion Initiation Abstraction	
						Localized Corrosion Penetration Rate Abstraction	
Waste Form Degradation and Mobilization Model Component	Radionuclide Inventory	WF Degradation and Mobilization	6.3.7	6.3.7.1	Radionuclide Inventory Submodel	Initial Radionuclide Inventory Screening Analysis	20,35
						Initial Radionuclide Inventory Abstraction	20,35
	In-Package Chemistry			6.3.7.2	In-Package Chemistry Submodel	In-Package Chemistry Abstraction	21
	Cladding Degradation			6.3.7.3	Cladding Degradation	Cladding Degradation Abstraction	22
	CSNF, DSNF, HLW Degradation			6.3.7.4	Waste Form Degradation Submodel	CSNF WF Degradation Abstraction	23
						DSNF WF Degradation Abstraction	24
						HLW Glass Degradation Abstraction	25
	Dissolved Radionuclide Concentration Limits			6.3.7.5	Dissolved Concentration Limits Submodel	Dissolved Concentration Limits Abstraction	26
	WF & EBS Colloids			6.3.7.6	Engineered Barrier System Colloids Submodel	WF and In-Drift Colloid Concentration Abstraction	27

Table 6-1. TSPA-LA Model Discretization (Continued)

Figure 6-1		Section 6			Referenced Analyses/Models	
TSPA-LA Principal Model Components		Subsection		Submodel for TSPA-LA	Abstraction/Process Model(s)/Analysis(es)	Reference
EBS Flow and Transport Model Component	EBS Flow	EBS Flow	6.3.6	EBS Flow Submodel	EBS Flow Abstraction	13
	EBS Transport	EBS Transport	6.3.8	EBS Transport Submodel	EBS Transport Abstraction	13
					Single Continuum Invert Abstraction	
					Mass of Corrosion Products Abstraction	
					Waste Form Water Volume Abstraction	22,25
				EBS-UZ Interface Submodel	EBS-UZ Interface Abstraction	13
Unsaturated Zone Transport Model Component	UZ Transport (Particle Tracking)	UZ Transport	6.3.9	UZ Transport Submodel	Active Fracture Model Abstraction	14
					Particle Tracking Model Abstraction	
					Dual-Continuum Transport Model Abstraction	
					UZ Transport Abstraction	
SZ Flow and Transport Model Component	3-D SZ Flow and Transport	SZ Transport	6.3.10	SZ Flow and Transport Submodel	3-D SZ Flow and Transport Process Model	17,18
					3-D SZ Flow and Transport Abstraction	16
	1-D SZ Flow and Transport				SZ Convolute Abstraction	
					1-D SZ Flow and Transport Abstraction	
Biosphere Model Component	Nominal BDCFs	Biosphere	6.3.11	Biosphere Submodel	Biosphere Process Model	19
	Groundwater Protection Conversion Factors				Groundwater Exposure Case Abstraction	
	Disruptive Events BDCFs				Volcanic Ash Exposure Case Abstraction	

Table 6-1. TSPA-LA Model Discretization (Continued)

Figure 6-1		Section 6				Referenced Analyses/Models	
TSPA-LA Principal Model Components		Subsection			Submodel for TSPA-LA	Abstraction/Process Model(s)/Analysis(es)	Reference
Events	Early Failure	Early Failure Scenario Class	DS Early Failure	6.4.1	DS Early Failure Submodel	Abstraction of DS Failures from Undetected Defects	28
			WP Early Failure	6.4.2	WP Early Failure Submodel	Abstraction of WP Failures from Undetected Defects	28
	Igneous Activity	Igneous Scenario Class	Igneous Intrusion Modeling Case	6.5.1	Igneous Intrusion Submodel	Igneous Activity Analysis	29
					Igneous Event Time and Probability Submodel	Annual Frequency Abstraction	
					Igneous Intrusion EBS Damage Submodel	Number of WP Hit by Igneous Events Abstraction	30
					EBS TH Environment Submodel Modifications for Igneous Intrusion	Dike Drift Interactions Analysis	9
					EBS Chemical Environment Submodel Modifications for Igneous Intrusion	Unevaporated Seepage Chemistry Abstraction	
						Basalt Chemistry Abstraction	
					Mean Annual Dose for Igneous Intrusion	Calculation of Expected Dose	Section 6.1.2 Appendix J

Table 6-1. TSPA-LA Model Discretization (Continued)

Figure 6-1		Section 6				Referenced Analyses/Models	
TSPA-LA Principal Model Components		Subsection			Submodel for TSPA-LA	Abstraction/Process Model(s)/Analysis(es)	Reference
Events (continued)	Igneous Activity (continued)	Igneous Scenario Class	Volcanic Eruption	6.5.2	Volcanic Eruption Submodel	Eruptive Processes Analysis	31,32
					Volcanic Interaction with the Repository Submodel	Number of WP Hit by Eruptive Conduits Analysis	30
					Atmospheric Transport Submodel	Atmospheric Dispersal and Deposition of Tephra Analysis	32,33
						ASHPLUME Model Abstraction	
					Tephra Redistribution Submodel	Redistributed Tephra Abstraction	
					Volcanic Ash Exposure Submodel	Mean Annual Dose for Volcanic Eruption Abstraction	31
	Seismic Activity	Seismic Scenario Class		6.6.1	Ground Motion Damage	Seismic Damage Abstraction	34
					Fault Displacement Damage		
				6.6.2.1	Drift Seepage Submodel and Drift Wall Condensation Submodel Modifications for Seismic Disruption	Drift Seepage Abstraction including Drift Collapse	4,5

Table 6-1. TSPA-LA Model Discretization (Continued)

Figure 6-1		Section 6				Referenced Analyses/Models	
TSPA-LA Principal Model Components		Subsection			Submodel for TSPA-LA	Abstraction/Process Model(s)/Analysis(es)	Reference
Events (continued)	Seismic Activity (continued)	Seismic Scenario Class (continued)		6.6.2.2	EBS TH Environment Submodel Modifications for Seismic Disruption	Collapsed Drift TH Abstraction	6
				6.6.2.3	WP and DS Degradation Submodel Modifications for Seismic Disruption	WP and DS Degradation Submodel	10,11,12
				6.6.2.4	WP Localized Corrosion Initiation Submodel for Seismic Disruption	Localized Corrosion Initiation Analysis	10
	Human Intrusion	Human Intrusion Scenario		6.7	Human Intrusion Submodel	10CFR Part 63.322 & 63.321	36

Table 6-1. TSPA-LA Model Discretization (Continued)

Figure 6-1	Section 6		Referenced Analyses/Models	
TSPA-LA Principal Model Components	**Subsection**	**Submodel for TSPA-LA**	**Abstraction/Process Model(s)/Analysis(es)**	**Reference**

NOTES:

1 UZ *Flow Models and Submodels* (SNL 2007 [DIRS 184614]).
2 *Simulation of Net Infiltration for Present-Day and Potential Future Climates* (SNL 2007 [DIRS 182145]).
3 *Future Climate Analysis* (BSC 2004 [DIRS 170002]).
4 *Abstraction of Drift Seepage* (SNL 2007 [DIRS 181244]).
5 *Seepage Model for PA Including Drift Collapse* (BSC 2004 [DIRS 167652]).
6 *Multiscale Thermohydrologic Model* (SNL 2007 [DIRS 181383]).
7 *In-Drift Natural Convection and Condensation* (SNL 2007 [DIRS 181648]).
8 *Engineered Barrier System: Physical and Chemical Environment* (SNL 2007 [DIRS 177412]).
9 *Dike/Drift Interactions* (SNL 2007 [DIRS 177430]).
10 *General Corrosion and Localized Corrosion of Waste Package Outer Barrier* (SNL 2007 [DIRS 178519]).
11 *Stress Corrosion Cracking of Waste Package Outer Barrier and Drip Shield Materials* (SNL 2007 [DIRS 181953]).
12 *General Corrosion and Localized Corrosion of the Drip Shield* (SNL 2007 [DIRS 180778]).
13 *EBS Radionuclide Transport Abstraction* (SNL 2007 [DIRS 177407]).
14 *Particle Tracking Model and Abstraction of Transport Processes* (SNL 2008 [DIRS 184748]).
15 *In Drift Precipitates/Salts Model* (SNL 2007 [DIRS 177411]).
16 *Saturated Zone Flow and Transport Model Abstraction* (SNL 2008 [DIRS 183750]).
17 *Saturated Zone Site-Scale Flow Model* (SNL 2007 [DIRS 177391]).
18 *Site-Scale Saturated Zone Transport* (SNL 2007 [DIRS 177392]).
19 *Biosphere Model Report* (SNL 2007 [DIRS 177399]).
20 *Initial Radionuclides Inventory* (SNL 2007 [DIRS 180472]).
21 *In-Package Chemistry Abstraction* (SNL 2007 [DIRS 180506]).
22 *Cladding Degradation Summary for LA* (SNL 2007 [DIRS 180616]).
23 *CSNF Waste Form Degradation: Summary Abstraction* (BSC 2004 [DIRS 169987]).
24 *DSNF and Other Waste Form Degradation Abstraction* (BSC 2004 [DIRS 172453]).
25 *Defense HLW Glass Degradation Model* (BSC 2004 [DIRS 169988]).
26 *Dissolved Concentration Limits of Radioactive Elements* (SNL 2007 [DIRS 177418]).

Table 6-1. TSPA-LA Model Discretization (Continued)

Figure 6-1	Section 6		Referenced Analyses/Models	
TSPA-LA Principal Model Components	**Subsection**	**Submodel for TSPA-LA**	**Abstraction/Process Model(s)/Analysis(es)**	**Reference**

27 *Waste Form and In-Drift Colloids-Associated Radionuclide Concentrations: Abstraction and Summary* (SNL 2007 [DIRS 177423]).

28 *Analysis of Mechanisms for Early Waste Package/Drip Shield Failures* (SNL 2007 [DIRS 178765]).

29 *Characterize Framework for Igneous Activity at Yucca Mountain, Nevada* (BSC 2004 [DIRS 169989]).

30 *Number of Waste Packages Hit by Igneous Events* (SNL 2007 [DIRS 177432]).

31 *Characterize Eruptive Processes at Yucca Mountain, Nevada* (SNL 2007 [DIRS 174260]).

32 *Atmospheric Dispersal and Deposition of Tephra from a Potential Volcanic Eruption at Yucca Mountain, Nevada* (SNL 2007 [DIRS 177431]).

33 *Redistribution of Tephra and Waste by Geomorphic Processes Following a Potential Volcanic Eruption at Yucca Mountain, Nevada* (SNL 2007 [DIRS 179347]).

34 *Seismic Consequence Abstraction* (SNL 2007 [DIRS 176828]).

35 *MOX Spent Nuclear Fuel and LaBS Glass for TSPA-LA* (SNL 2007 [DIRS 177422]).

36 NRC Proposed Rule at 10 CFR 63.321 [DIRS 178394] and 63.322 [DIRS 180319].

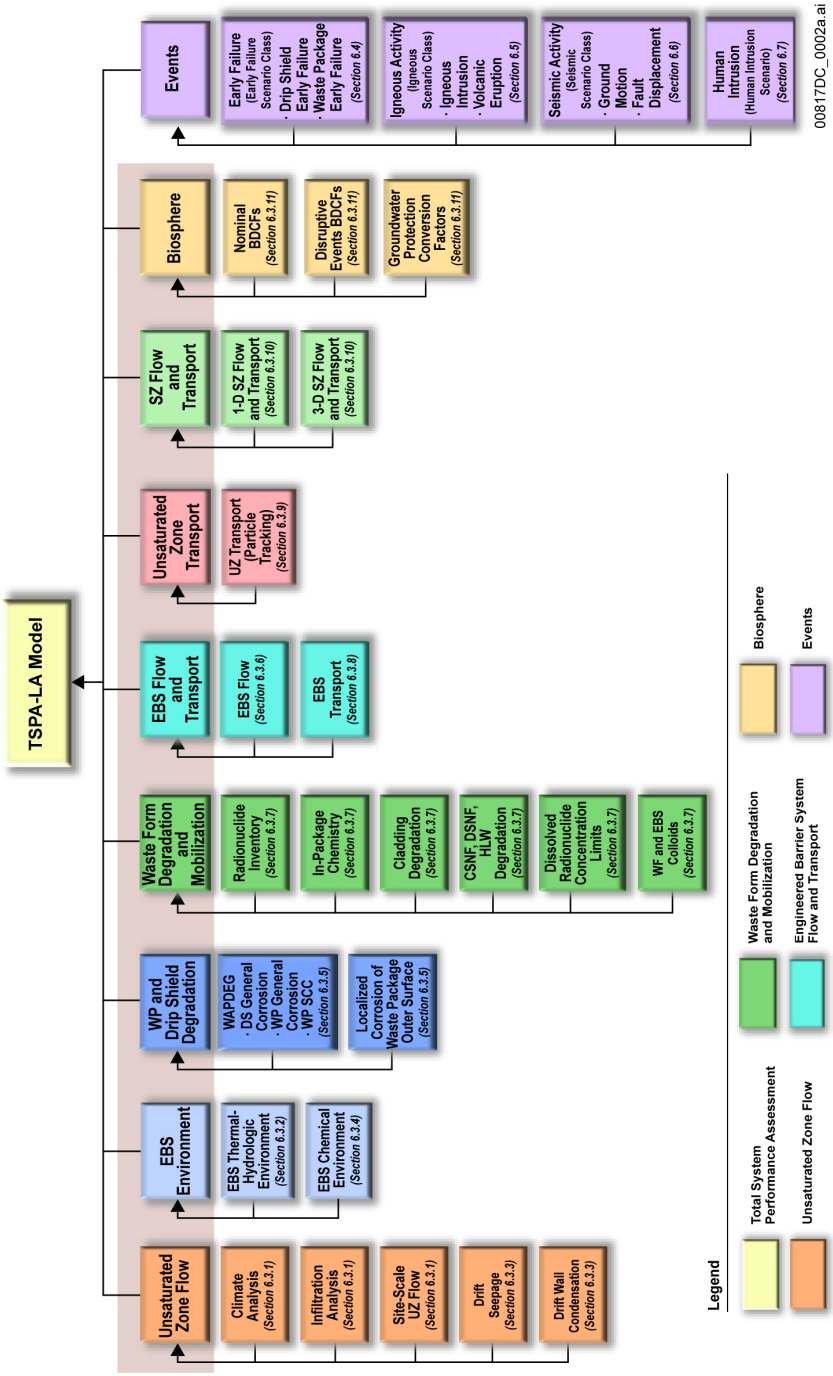

Figure 6-1. TSPA-LA Principal Model Components and Submodels

INTENTIONALLY LEFT BLANK

6.1 CONCEPTUAL DESIGN

The TSPA-LA Model evaluates the repository system performance for four scenario classes and for a human intrusion scenario. The TSPA-LA Model is exercised using modeling cases (discussed in detail in Section 6.1.2) that represent the scenario-specific conditions over which the repository performance can be assessed. The remainder of Section 6.1 provides a conceptual overview of the FEPs related to the TSPA-LA Model (Section 6.1.1), the scenario classes and modeling cases (Section 6.1.2), a discussion on the treatment of uncertainty in the TSPA-LA Model (Section 6.1.3), the individual model components and submodels that comprise the model scenario classes and modeling cases (Section 6.1.4), and the architecture of the TSPA-LA Model (Section 6.1.5). As noted in *Yucca Mountain Review Plan, Final Report* (NRC 2003 [DIRS 163274], Section 2.2), the model abstraction review process ends with a review of how the abstracted submodels are implemented in the TSPA-LA Model. This section provides overview information to facilitate this review and, in particular, an overview of the integration of model components and submodels that describe processes and conditions in different parts of the Yucca Mountain repository system.

Section 6 provides a text-based description of the TSPA-LA Model. For a complete representation of the conceptual basis and mathematical implementation of the TSPA-LA Model, and for full traceability to the source information used to develop the model, the reader should use the text of Section 6 in conjunction with complementary tools that are provided in this report and on the accompanying digital video disk (DVD). The following information tools should be used together while reading Section 6:

- Model Components and Submodels, listed in Table 6-1
- Model Implementation Descriptions, mapped in Table 6.1.5-1
- The GoldSim model file (available on DVD)
- The TSPA Input Database (available on DVD)
- Parameter Entry Forms (PEFs) (available within the TSPA Input Database on DVD)
- Appendix I—FEPs Mapped to TSPA-LA GoldSim model file.

Understanding the conceptual basis for the TSPA-LA Model begins with a review of the FEPs development and screening process, described in Section 6.1.1. Potentially relevant FEPs are identified and evaluated, consistent with available field and laboratory data for the Yucca Mountain site, for inclusion into process models documented in a suite of analysis and model reports. Appendix I provides a roadmap between the conceptualization represented by included FEPs and the mathematical implementation in the GoldSim model file. Appendix I identifies one or more locations where included FEPs are implemented within the GoldSim model file. The appendix also identifies documentation that provides additional information on the conceptualization and mathematical representation of each included FEP.

Table 6-1 provides the roadmap through the conceptual structure of the TSPA-LA Model. The table identifies the process models and associated analyses that support the TSPA-LA Model and gives the principal references. The table also identifies the abstractions that were developed for implementation into the TSPA-LA Model. These elements are mapped to the conceptual structure of the TSPA-LA Model, as defined in Section 6.3. All of this information is mapped to the conceptual structure provided by the TSPA wheel (Figure 1-3), illustrating how the details of

the TSPA-LA Model conceptualization relate to the high-level conceptual structure that has formed the basis for analysis and discussion of the Yucca Mountain repository system for many years.

The mathematical implementation of the conceptualization presented in Table 6-1 is discussed in Section 6.3 and documented in the GoldSim model file. Table 6.1.5-1 presents the suite of submodels that were developed to implement the abstractions identified in Table 6-1. Table 6.1.5-1 includes the locations within the GoldSim model file, to view the actual implementation of the submodels. The model file also includes documentation of the submodel implementation. Decisions made during the implementation of the submodels have resulted in slight differences between the model structure defined in Table 6.1.5-1 and the model structure defined in Section 6.3, and these differences are resolved in Table 6-1. Collectively, stepping from Figure 6-1 to Table 6-1 to Table 6.1.5-1 and Section 6.3 associates an increase in the detail provided by looking at smaller and smaller logical segments of the model. The basic idea is that the principal model components from Figure 6-1 may be comprised of one or more submodels (listed on Figure 6-1 and in Table 6-1), which may be comprised of one or more abstractions, analyses, or process models (listed in Tables 6-1 and 6.1.5-1). The reader can follow the roadmap, terminating in the model file, which provides the greatest detail of the implementation.

The annual dose results generated from the GoldSim model file undergo further processing to calculate the distribution of expected annual doses for each scenario class, where the term "expected annual dose" refers to the expectation of annual dose over aleatory uncertainty conditional on each epistemic realization. Section 6.1.2 outlines these calculations, which are implemented in the EXDOC_LA software [DIRS 182102]. The representation of the two types of uncertainty is discussed in Section 6.1.3. The distributions of expected annual dose from each scenario class are combined to form a distribution of total expected annual dose. The mean of this distribution of total expected annual dose is the quantity compared to the regulatory standard specified in 10 CFR 63.303(a) [DIRS 178394] for the period within 10,000 years after disposal, and the median of this distribution is the quantity compared to the regulatory standard specified in 10 CFR 63.303(b) [DIRS 178394] for the period after 10,000 years of disposal.

Parameters connect the model, as implemented in the GoldSim model file, to the field and laboratory measurements that provide the basic data for the TSPA-LA Model. All parameters included in the TSPA-LA Model are documented in the TSPA Input Database, which is a Microsoft Access Database included in the DVD. The parameter database provides the linkage between the description of the parameter, the parameter values used by the model, and the model structure defined in Table 6.1.5-1. Information provided for each parameter includes a brief description, the identification of parameter type (i.e., constant, table, or stochastic), and information on parameter source. The source information includes the source data tracking number (DTN) or the analysis and model report, as well as information on any modifications made to the source information. Traceability to the specific location of source values is provided by the PEFs that are included in the database. The PEFs provide a roadmap to a specific location within a DTN or the analysis and model report where a parameter value can be found.

The database also identifies the submodel where the parameter is implemented within the model file. Many parameters are included in calculations at multiple locations within the model file,

but the database identifies at least one location, which is the primary location where the parameter value is brought into the model.

Most of the information from the TSPA Input Database is also captured in the GoldSim model file. At the location where a parameter is implemented in the model file, the information from the database about DTNs or analysis and model report sources and parameter types can be obtained by moving the cursor over the parameter icon. Thus, information from the database and the PEFs is linked through the GoldSim model file. The database description on page 6.1-2 provides details.

There are differences in assumptions and parameter sets used in the TSPA-LA Model that have arisen in the development of the abstractions and process models. Most of these differences are due to the use of conservative assumptions in the process model or analysis when uncertainty is difficult to quantify. Assumptions made within the TSPA-LA Model are consistent between the various submodels, assumptions, and parameter values that differ between submodels and are documented as part of the discussion of each submodel implementation in Section 6.3. Evaluating potential impacts from these assumptions with respect to the mean annual dose is conducted through a series of processes described in Section 7.4 (Uncertainty Characterization), Section 7.7.1 (Analysis of Single Realizations), Section 7.7.4 (Performance Margin Analysis), and Section 8.3 (Results of Barrier Capability). To enhance understanding of the complex interactions within the TSPA-LA Model, a discussion of consistency among model components and submodels and identification of conservative assumptions in abstractions, process models, and parameter sets is presented, along with each submodel described in Section 6.3.

The tools discussed above, in conjunction with review of Section 6.0, all provide the reader with a complete representation of the conceptual basis and mathematical implementation of the TSPA-LA Model, and full traceability to the source information used to develop the model.

INTENTIONALLY LEFT BLANK

6.1.1 Features, Events, and Processes Screening and Scenario Development

This section describes the identification and screening of features, events, and processes (FEPs) for the TSPA-LA Model and the development of scenario classes used to estimate repository performance in the TSPA-LA.

For the TSPA-LA Model, FEP analysis and scenario development follows a five-step approach (Figure 6.1.1-1):

Step 1. Identify and classify the FEPs potentially relevant to the long-term performance of the disposal system.

Step 2. Evaluate the FEPs to identify those FEPs that should be included in the TSPA-LA and those that can be excluded from the TSPA.

Step 3. Form appropriate scenario classes from the FEPs that were included in the TSPA. Disruptive events are used to form scenario classes.

Step 4. Construct the calculation of total mean annual dose.

Step 5. Specify the implementation of the scenario classes in the computational modeling for the TSPA-LA and document the treatment of FEPs that were included.

FEP analysis, which includes Steps 1 and 2 above, addressed scenario analysis acceptance Criteria 1 and 2, respectively, as outlined in *Yucca Mountain Review Plan, Final Report* (NRC 2003 [DIRS 163274], Section 2.2.1.2.1.3). Scenario development, which includes Steps 3 and 4 above, addressed scenario analysis acceptance Criteria 3 and 4, respectively, as outlined in *Yucca Mountain Review Plan, Final Report* (NRC 2003 [DIRS 163274], Section 2.2.1.2.1.3). Section 6.1.2 outlines the calculation of total mean annual dose using the scenario classes, addressing Step 4 above. Sections 6.1.3 and 6.1.4 describe the implementation of each scenario class in the model components and submodels incorporated into the TSPA-LA Model (Step 5 above).

6.1.1.1 Features, Events, Processes, Scenarios, and Scenario Classes

Features are physical, chemical, thermal, or temporal characteristics of the site or repository system. For the purposes of screening FEPs for the TSPA-LA, a feature is defined as an object, structure, or condition that has the potential to affect disposal system performance (SNL 2008 [DIRS 179476], Appendix A). Examples of features are the WP and fracture systems or faults.

Processes are phenomena and activities that have gradual, continuous interactions with the system being modeled. For the purposes of screening FEPs for the TSPA-LA Model, a process is defined as a natural or human-caused phenomenon that has the potential to affect disposal system performance and that operates during all or a significant part of the period of performance (SNL 2008 [DIRS 179476], Appendix A). Percolation of water into the unsaturated rock layers above the repository is an example of a process.

Events are occurrences that have a specific starting time and, usually, a duration shorter than the time being simulated in a model. Events are also defined as uncertain occurrences that take place within a short time relative to the time frame of a model. For the purposes of screening FEPs for the TSPA-LA Model, an event is defined as a natural or human-caused phenomenon that has a potential to affect disposal system performance and that occurs during an interval that is short compared to the period of performance (SNL 2008 [DIRS 179476], Appendix A). An earthquake is an example of an event.

The identification, classification, and screening of a comprehensive list of FEPs potentially relevant to the postclosure performance of the Yucca Mountain Repository was an iterative process based on site-specific information, design, and regulations. The iterative FEP analysis process was initiated to support the TSPA for the Site Recommendation (TSPA-SR) and continued through the TSPA-LA FEP analysis, as described in *Features, Events, and Processes for the Total System Performance Assessment: Methods* (SNL 2008 [DIRS 179476], Section 6.1.4.1).

A scenario is a well-defined, connected sequence of FEPs that can be thought of as describing possible future conditions in the repository system. Scenarios can be undisturbed where the performance is the expected or nominal performance of the system, or disturbed if altered by events such as volcanism or seismicity (NRC 2003 [DIRS 163274], Section 3). There is an infinite number of possible future states, and for scenario development to be useful, the process must generate scenarios that can be aggregated into a manageable number of scenario classes representative of the range of futures potentially relevant to the PA of the repository (SNL 2008 [DIRS 179476], Section 6.3).

A scenario class is a set of related scenarios that share sufficient similarities to usefully aggregate them for the purposes of analysis. The number and breadth of scenario classes depend on the resolution at which scenarios were defined. Coarsely defined scenarios result in fewer broad scenario classes, whereas narrowly defined scenarios result in many scenario classes. The objective of scenario development is to define a limited set of scenario classes that can be quantitatively analyzed while maintaining comprehensive coverage of the range of possible future states of the repository system. The process of scenario development is described by Cranwell et al. (1990 [DIRS 101234], Section 2.4).

The following sections provide summaries of the TSPA-LA FEP analysis and scenario development steps.

6.1.1.2 Step 1: Identification and Classification of Features, Events and Processes

In Step 1 of the FEP analysis and scenario development process, FEPs potentially relevant to postclosure performance are identified and classified. The primary objectives of FEP identification and classification are to develop a comprehensive set of FEPs for subsequent screening, to uncover missing FEPs and interactions, and to provide a framework for developing and organizing scenario classes.

An initial list of FEPs relevant to Yucca Mountain was developed from a comprehensive list of FEPs from radioactive waste disposal programs in other countries (BSC 2005 [DIRS 173800],

Section 2.1.1). The list was supplemented with additional Yucca Mountain-specific FEPs from project literature, technical workshops, and reviews (BSC 2005 [DIRS 173800], Sections 2.1.1). This process is illustrated on Figure 6.1.1-2. This initial FEP list, developed to support TSPA-SR, contained 328 FEPs (BSC 2002 [DIRS 159684], Table FEPS). This list was revised for TSPA-LA in part with an application of a hybrid procedure that included reclassification, refinement, and audits against other recently published international lists. Additional analyses and refinements were conducted during the transition from the TSPA-SR FEP list to the TSPA-LA FEP list (DTN: MO0706SPAFEPLA.001_R0 [DIRS 181613]).

The TSPA-SR FEP classification was derived from a Nuclear Energy Agency classification scheme (NEA 1999 [DIRS 152309], pp. 28 to 34) that was based on a combination of the classification schemes listed in *Development of the Total System Performance Assessment-License Application Features, Events, and Processes* (BSC 2005 [DIRS 173800], Section 2.1.2). The TSPA-SR classification was a layered scheme, with different layers categorized by cause, field of effects, and causative factors, location, scientific discipline, radionuclide transfer agent, and/or radionuclide mobilization. As a check on comprehensiveness, TSPA-SR FEPs were also classified according to technical subject area (i.e., a combination of locations and physical field of effect). The alternate classification did not result in the identification of any additional FEPs. For TSPA-LA, yet another classification scheme was applied based on a mapping between Yucca Mountain Project (YMP) specific features (i.e., locations and fields of effect) and processes (i.e., radionuclide mobilization and causative factors). The revised approach improved traceability by relating FEPs directly to YMP specific technical subject areas rather than to generic international groupings.

These FEP identification actions resulted in a comprehensive TSPA-LA FEP list containing 374 FEPs (DTN: MO0706SPAFEPLA.001_R0 [DIRS 181613]).

6.1.1.3 Step 2: Screening of FEPs

In Step 2 of the FEP analysis and scenario development process, the list of FEPs identified and classified in Step 1 was screened to determine which FEPs should be included or excluded from the TSPA-LA analysis. A FEP can be excluded based on any one of the following three FEP screening criteria, which derive from NRC Proposed Rule 10 CFR Part 63 ([DIRS 178394] and [DIRS 180319]), as described below:

1. Low Probability (10 CFR 63.342(a) and (b) [DIRS 178394])—Performance assessments shall exclude events that have less than one chance in 10,000 of occurring over 10,000 years. FEPs meeting this criterion may be excluded (screened out) from the TSPA-LA on the basis of low probability. For example, the impact of large meteorites was excluded because of low probability.

2. Low Consequence (10 CFR 63.114(e) and (f) [DIRS 178394])—FEPs may be excluded (screened out) from the TSPA-LA on the basis of low consequence if the omission of a FEP would not significantly change the magnitude or time of radiological exposures or radionuclide releasesFor example, gas generation from waste form decay is excluded because of low consequence, even though the process is certain to occur.

3. By Regulation—FEPs may also be excluded if they are inconsistent with regulations that specify repository system characteristics, concepts, and definitions. The regulations most commonly used for screening TSPA-LA FEPs are those pertaining to the characteristics, concepts, and definitions of the reference biosphere, geologic setting, RMEI, and human intrusion ((NRC 2003 [DIRS 163274], Section 2.2.1.2.1.3, Acceptance Criterion 2) and (SNL 2008 [DIRS 179476], Section 6)).

In addition, according to 10 CFR 63.342(c) [DIRS 178394], PAs conducted to show compliance of FEPs with individual protection standards following permanent closure and affected by human intrusion shall project the continued effects of all included FEPs beyond 10,000 years after closure until the period of geologic stability, including seismic and igneous events covered under the probability limits of 10 CFR 63.342(a) [DIRS 178394].

The FEP screening process included input from subject matter experts, as documented in the *LA FEP List and Screening* (DTN: MO0706SPAFEPLA.001_R0 [DIRS 181613]). The FEP screening process is described in *Features, Events, and Processes for the Total System Performance Assessment: Methods* (SNL 2008 [DIRS 179476], Section 6). A second report, *Features, Events, and Processes for the Total System Performance Assessment: Analyses* (SNL 2008 [DIRS 183041]), contains tables that identify the relevant FEP analysis reports for each FEP and indicate whether or not each FEP is included in the TSPA-LA Model or was screened out.

Appendix I contains additional information on all FEPs that were included in the TSPA-LA Model. This appendix provides a mapping between the FEPs documentation and implementation of the FEP in the TSPA-LA Model. Table I-2 identifies each included FEP, by FEP number, and provides a brief explanation of how the FEP is included. The actual inclusion of the FEP may be by direct implementation in the TSPA-LA Model file, implementation within a dynamically linked library (DLL), or by inclusion in a process model abstraction. Table I-2 identifies a path to the location of each included FEP within the TSPA-LA Model file. Table I-2 includes information on how each FEP was implemented and identifies supporting documentation where additional information is available, explaining the implementation of the included FEP.

6.1.1.4 Step 3: Formation of Scenario Classes

All FEPs screened in during the formal identification and screening for Step 1 and Step 2 are used for TSPA-LA scenario development and are incorporated into scenario classes (Sections 6.3, 6.4, 6.5, 6.6, and 6.7). For the purpose of scenario class formation, features and processes generally are present in all possible repository futures. In contrast, events may or may not occur in every future of the repository system. For this reason, scenario classes are distinguished by events, while the features and processes are generally applicable across all scenario classes.

The three retained events that have been identified for inclusion in the TSPA-LA are:

- Early failure
- Igneous
- Seismic.

These three events lead to the definition of three corresponding scenario classes for the TSPA-LA, and one additional scenario class accounting for repository futures in which none of the three events occur:

- Early Failure Scenario Class, A_E: the set of futures each of which includes one or more early failure events (i.e., one or more early failed WPs and/or one or more early failed DSs).
- Igneous Scenario Class, A_I: the set of futures each of which includes one or more igneous events.
- Seismic Scenario Class, A_S: the set of futures each of which includes one or more seismic events.
- Nominal Scenario Class, A_N: the set of futures each of which includes nominal features and processes (e.g., corrosion processes, such as general corrosion, localized corrosion, and SCC) but *no* events (i.e., no igneous and no seismic events and no early WP or DS failures).

The first three scenario classes are not mutually exclusive. Because the three types of events occur independently, many potential futures of the repository include events of different types, and such futures are included in more than one of the sets listed above. Section 6.1.2 explains how the four scenario classes listed above are aggregated from a set of mutually exclusive scenario classes and how total dose to the RMEI is correctly calculated using these four scenario classes.

6.1.1.5 Description of Scenario Classes and Modeling Cases

The scenario classes addressed by the TSPA-LA Model are distinguished by the type of event included in each scenario class. For example, the Early Failure Scenario Class accounts for all possible futures in which one or more early failures of DSs or WPs occur, the Igneous Scenario Class accounts for all possible futures in which one or more igneous events occur, and the Seismic Scenario Class accounts for all possible futures in which seismic events occur. In contrast, the Nominal Scenario Class accounts for all possible futures in which no early failures, igneous, or seismic events occur.

Each scenario class is implemented in the TSPA-LA Model by one or more modeling cases. The modeling cases that implement a scenario class are distinguished by different modes and extent of damage to the repository that could result from the occurrence of the events represented by the scenario class. The Early Failure Scenario Class is implemented in two modeling cases, the

Waste Package EF Modeling Case and the Drip Shield EF Modeling Case, because early failure of a DS has a different effect on the repository performance than early failure of a WP. Similarly, the Seismic Scenario Class is implemented in two modeling cases, one accounting for damage due to ground motion, and a second accounting for damage due to fault displacement. The Igneous Scenario Class also comprises two modeling cases, one for igneous intrusion and one for volcanic eruption.

Each scenario class accounts for FEPs that remain screened in after Step 2. The FEPs addressed by each scenario class, and the modeling cases used for each scenario class, are described below. In general, FEPs that describe a feature, such as the WP, or a process, such as flow in the UZ, are relevant to, and included in, more than one scenario class. In contrast, FEPs that describe an event, such as the occurrence of an igneous intrusion, are only included in the scenario class and modeling case that accounts for the effects of the event on repository performance. Thus, there is not a one-to-one association between FEPs and modeling cases.

A single FEP or related FEPs may be implemented differently in different scenario classes, model components, or portions of a model domain. These differing implementations are not inconsistencies; rather, they are reasonable simplifications that focus the model on things that matter and allow reasonable and technically defensible conservatism where information is controversial or lacking. In cases where a FEP is treated differently in different parts of the model, it is important that the impacts on the overall performance of any simplifications can be shown to be neutral or conservative for the purposes of each model component. For example, flow in fractured basalt is represented realistically for the purposes of a FEP screening argument (screening out hydrologic effects of the vertical dike on the grounds that flow in the dike will be insignificant), whereas flow through magma-filled drifts is represented conservatively. In another example, a radionuclide solubility model is applied in the WP and invert but is conservatively neglected in the UZ and SZ.

Nominal Scenario Class—The Nominal Scenario Class for the TSPA-LA Model includes all of the FEPs that were screened in according to the FEP screening process described in Section 6.1.1, except for those FEPs that are related to early failures, igneous activity, seismic activity, or a human intrusion. This scenario class, therefore, incorporates the important effects and system perturbations caused by climate change and repository heating that are projected to occur after repository closure. In addition, the Nominal Scenario Class considers that the WPs and DSs are subject to the EBS environment and will degrade with time. If the WPs and DSs breach and the waste forms are subsequently exposed to water, radionuclides may be mobilized and eventually be released from the repository. These radionuclides can then be transported by groundwater percolating through the UZ to the SZ and then to the accessible environment by water flowing in the SZ. The TSPA-LA Model includes FEPs associated with the biosphere in order to calculate annual dose to the RMEI. Accordingly, the TSPA-LA Model explicitly includes the following model components (Figure 6.1.1-3):

- UZ Flow
- EBS Environment
- WP and DS Degradation
- Waste Form Degradation and Mobilization
- EBS Flow and Transport

- UZ Transport
- SZ Flow and Transport
- Biosphere.

The FEPs included in these model components are addressed in one modeling case. This modeling case represents those WPs that fail because of corrosion processes (e.g., general corrosion, SCC, or localized corrosion). This modeling case is referred to as the Nominal Modeling Case. The Nominal Modeling Case quantifies repository performance in the absence of early failures or disruptive events before 10,000 years. For repository performance 10,000 years after closure, nominal processes are included in the Seismic GM Modeling Case, described below.

Early Failure Scenario Class—The Early Failure Scenario Class describes performance of the repository system in the event of early failures of the DSs or WPs due to manufacturing or material defects or to pre-emplacement operations including improper heat treatment. Early failure events are addressed by two modeling cases: (1) the Waste Package EF Modeling Case that considers the early failure of one or more WPs and the subsequent release of radionuclides to the groundwater; and (2) the Drip Shield EF Modeling Case that considers the early failure of one or more DSs that results in localized corrosion of the WPs beneath the failed DSs and the subsequent release of radionuclides to the groundwater.

The Waste Package EF Modeling Case accounts for the consequences of one or more WP failures at the time of repository closure due to manufacturing defects or damage during emplacement. WP early failure compromises the WP, exposing the waste forms to percolating water and mobilizing radionuclides. The released radionuclides may then be transported out of the repository, moved down through the UZ to the SZ, and then transported through the SZ to the accessible environment. The TSPA-LA Model components needed to calculate total system performance for the Waste Package EF Modeling Case include the following (Figure 6.1.1-4):

- UZ Flow
- EBS Environment
- WP and DS Degradation
- Waste Form Degradation and Mobilization
- EBS Flow and Transport
- UZ Transport
- SZ Flow and Transport
- Biosphere.

The FEPs associated with DS early failure and corrosion failure of WPs are not addressed in the Waste Package EF Modeling Case. Instead, these FEPs are accounted for in the Drip Shield EF and Nominal Modeling Cases.

The Drip Shield EF Modeling Case accounts for the consequences of one or more DS failures at the time of repository closure due to manufacturing defects or damage during emplacement. The WPs beneath the early failed DSs are assumed to be susceptible to localized corrosion, which compromises the WPs, exposing the waste forms to percolating water, and mobilizing radionuclides. The released radionuclides may then be transported out of the repository, moved down through the UZ to the SZ, and then be transported through the SZ to the accessible environment. The TSPA-LA Model components needed to calculate total system performance for the Drip Shield EF Modeling Case include the following (Figure 6.1.1-4):

- UZ Flow
- EBS Environment
- WP and DS Degradation
- Waste Form Degradation and Mobilization
- EBS Flow and Transport
- UZ Transport
- SZ Flow and Transport
- Biosphere.

The Drip Shield EF Modeling Case assumes that a WP underneath a failed DS experiences localized corrosion.

Igneous Scenario Class—The Igneous Scenario Class describes performance of the repository system in the event of igneous activity that disrupts the repository. Igneous disruption of the repository is addressed by two modeling cases: (1) the Igneous Intrusion Modeling Case that represents the interaction of intrusive magma with the repository and the release of radionuclides to the groundwater, and (2) the Volcanic Eruption Modeling Case that represents an eruption at the land surface and the release of radionuclides to the atmosphere.

The Igneous Intrusion Modeling Case models a dike intersecting the repository and compromising DSs and WPs in those drifts intruded by magma, exposing the waste forms to percolating water and mobilizing radionuclides. The released radionuclides may then be transported out of the repository, moved down through the UZ to the SZ, and then be transported through the SZ to the accessible environment. The TSPA-LA Model components, needed to calculate total system performance for the Igneous Intrusion Modeling Case, include the following, given that a certain number of WPs are destroyed by the intrusion (Figure 6.1.1-5):

- UZ Flow
- EBS Environment
- WP and DS Degradation
- Waste Form Degradation and Mobilization
- EBS Flow and Transport
- UZ Transport
- SZ Flow and Transport
- Biosphere.

The FEPs associated with corrosion failure of WPs prior to the disruption are included in the Igneous Intrusion Modeling Case. The FEPs associated with corrosion failure of WPs of undisrupted WPs after the disruption occurs are not included in the Igneous Intrusion Modeling Case. Instead, these FEPs are accounted for in the Nominal Modeling Case.

The Volcanic Eruption Modeling Case represents the fraction of igneous intrusions in which a volcanic eruption also occurs. For this modeling case, waste from WPs intersected by eruptive conduits is transported to the land surface, and tephra and entrained waste are discharged into the atmosphere, transported by wind currents, and deposited on the surface. The Volcanic Eruption Modeling Case also evaluates the fluvial and eolian redistribution of contaminated tephra deposited on the land surface. The TSPA-LA Model uses the following processes and model components to calculate repository system performance for the Volcanic Eruption Modeling Case (Figure 6.1.1-6):

- Volcanic interaction with the repository
- Atmospheric transport
- Tephra redistribution
- Biosphere.

Seismic Scenario Class—The Seismic Scenario Class describes performance of the repository system in the event of seismic activity capable of disrupting repository emplacement drifts and damaging the EBS. Radionuclides in damaged WPs may be mobilized and transported out of the repository, transported to the water table by the groundwater percolating through the UZ, and then transported to the accessible environment by water flowing in the SZ. The TSPA-LA Model components needed to calculate total system performance for the Seismic Scenario Class include the following (Figure 6.1.1-7):

- UZ Flow
- EBS Environment
- WP and DS Degradation
- Waste Form Degradation and Mobilization
- EBS Flow and Transport
- UZ Transport
- SZ Flow and Transport
- Biosphere.

Seismic disruption of the repository is addressed in two modeling cases. The first modeling case is the Seismic GM Modeling Case, which represents the consequences of mechanical damage associated with seismic vibratory ground motion. The Seismic GM Modeling Case includes: drift degradation and the effects on the EBS of accumulated rubble, the effects of SCC of the WPs and diffusion of mobilized radionuclides through WP cracks, and the effects of WP rupture with the potential to have both advection and diffusion of mobilized radionuclides through the rupture opening. Because corrosion processes accounted for in the Nominal Scenario Class have the potential to alter the repository's susceptibility to damage during a seismic ground motion event, the Seismic GM Modeling Case includes these nominal processes when calculating consequences after 10,000 years.

The second modeling case is the Seismic FD Modeling Case, which represents advection and diffusion of mobilized radionuclides out of WP breaches caused by a fault displacement. Seismic ground motion damage of the DSs and WPs is excluded from this modeling case.

6.1.1.6 Human Intrusion Scenario

In addition to the four scenario classes described above, the TSPA-LA considers a Human Intrusion Scenario as defined in NRC Proposed Rule 10 CFR 63.322 [DIRS 180319]. The Human Intrusion Scenario considers the intrusion of a single water or exploratory well into the repository, through the DS and WP, and into the underlying SZ. Human intrusion is not expected to occur during the first 10,000 years after repository closure (Section 6.3.7). NRC Proposed Rule 10 CFR 63.321 [DIRS 178394] describes the Individual Protection Standard for a Human Intrusion.

The Human Intrusion Scenario in implemented in a single modeling case, the Human Intrusion Modeling Case. This modeling case describes performance of the repository system in the event that subsurface exploratory drilling disrupts the repository. The Human Intrusion Modeling Case assumes that subsurface exploratory drilling activities intersect the repository and destroy a single DS and WP without being recognized by the drillers. After penetrating a thinned DS and WP, the drillers continue to bore a conduit through to the SZ. The drillers penetrate a DS and WP with an opening the size of the drill bit, thereby exposing the waste forms to percolating water and mobilizing radionuclides. The released radionuclides may then be transported out of the repository, move down through the borehole to the SZ, and then be transported through the SZ to the accessible environment. The TSPA-LA Model components needed to calculate total system performance for the Human Intrusion Modeling Case include the following, given that a certain WP is destroyed by the intrusion (Figure 6.1.1-8):

- UZ Flow
- EBS Environment
- WP and DS Degradation
- Waste Form Degradation and Mobilization
- EBS Flow and Transport
- UZ Transport (stylized)
- SZ Flow and Transport
- Biosphere.

The FEPs associated with corrosion failure of WPs prior to the disruption are not included in the Human Intrusion Modeling Case. The FEPs associated with corrosion failure of WPs and of undisrupted WPs after the disruption occurs are also not included in the Human Intrusion Modeling Case.

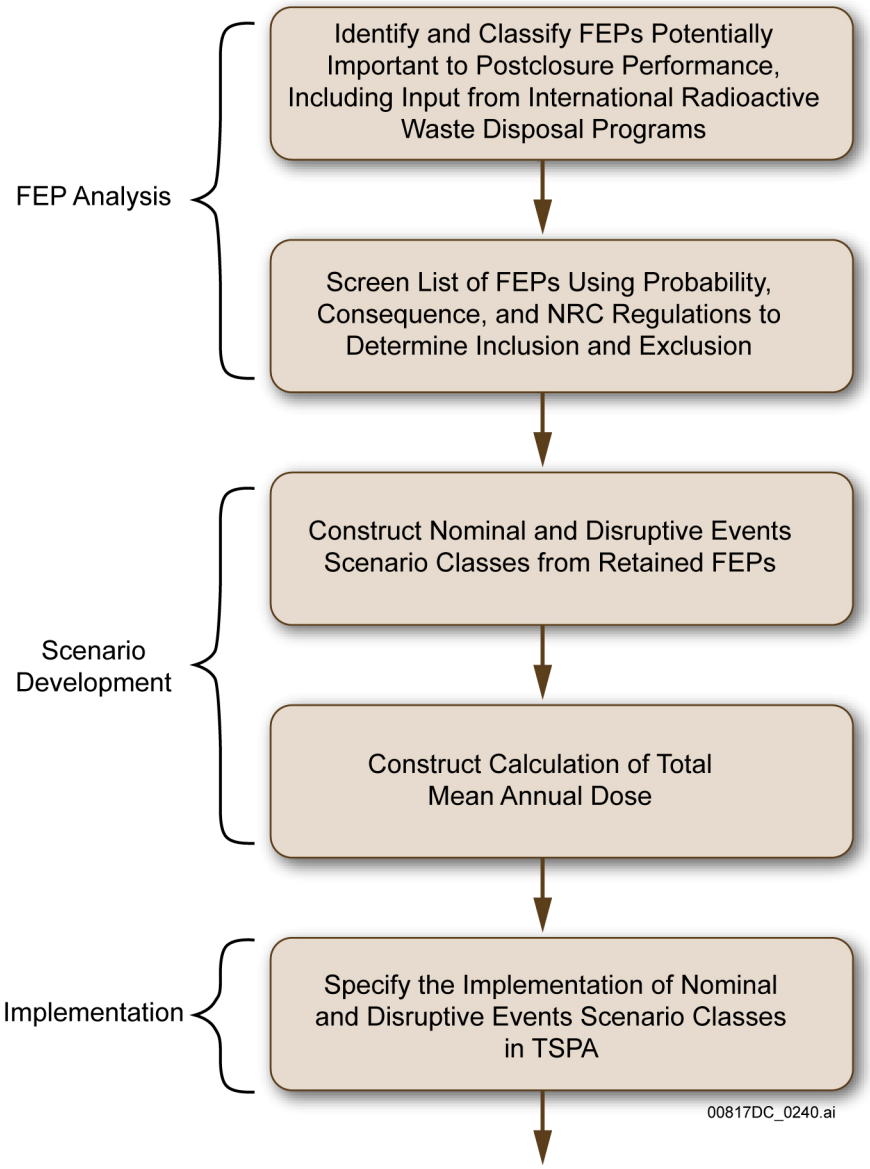

Figure 6.1.1-1. Steps in the Features, Events, and Processes Analysis and Scenario Selection Process

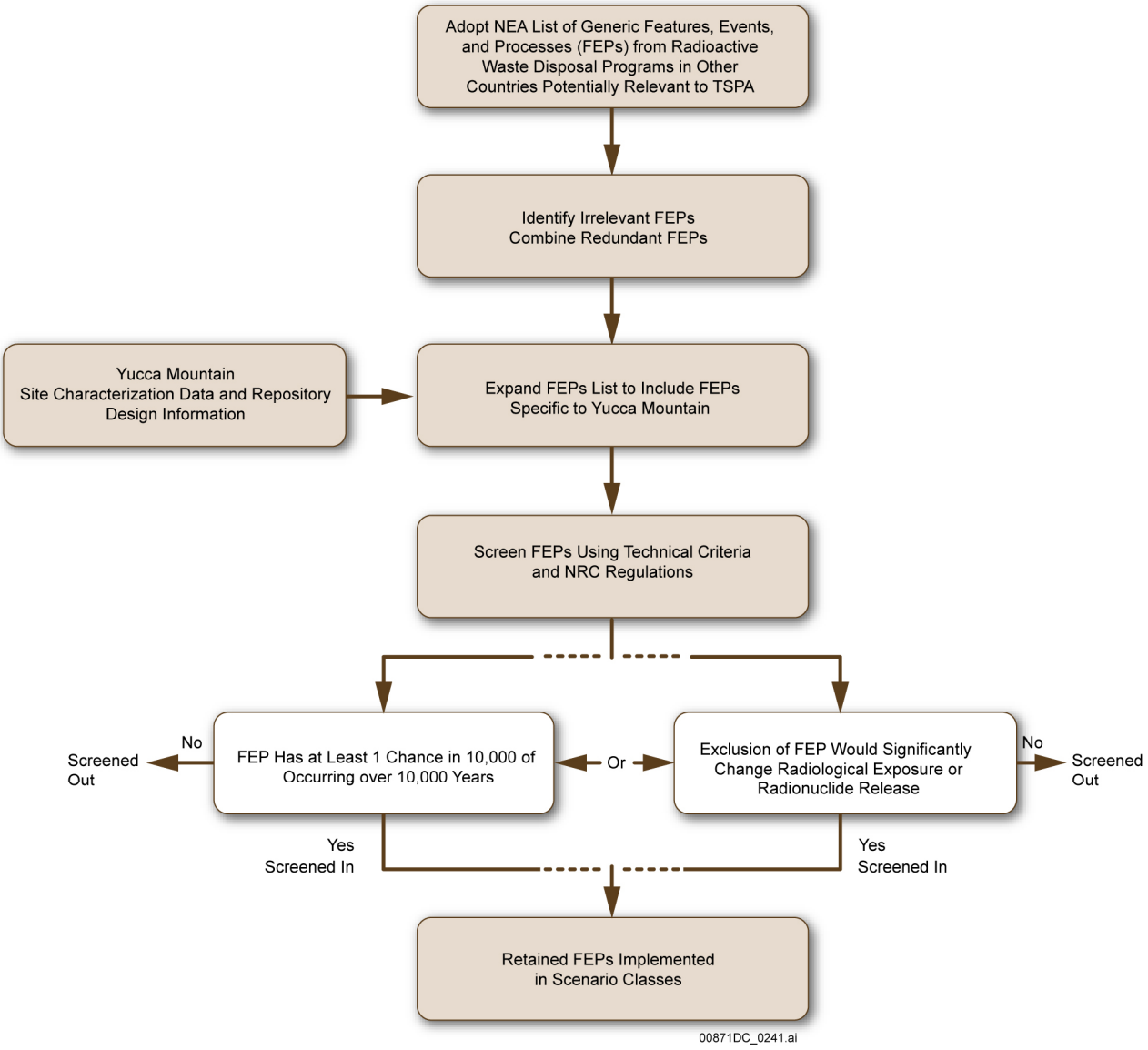

Figure 6.1.1-2. Schematic Illustration of the Features, Events, and Processes Analysis Method

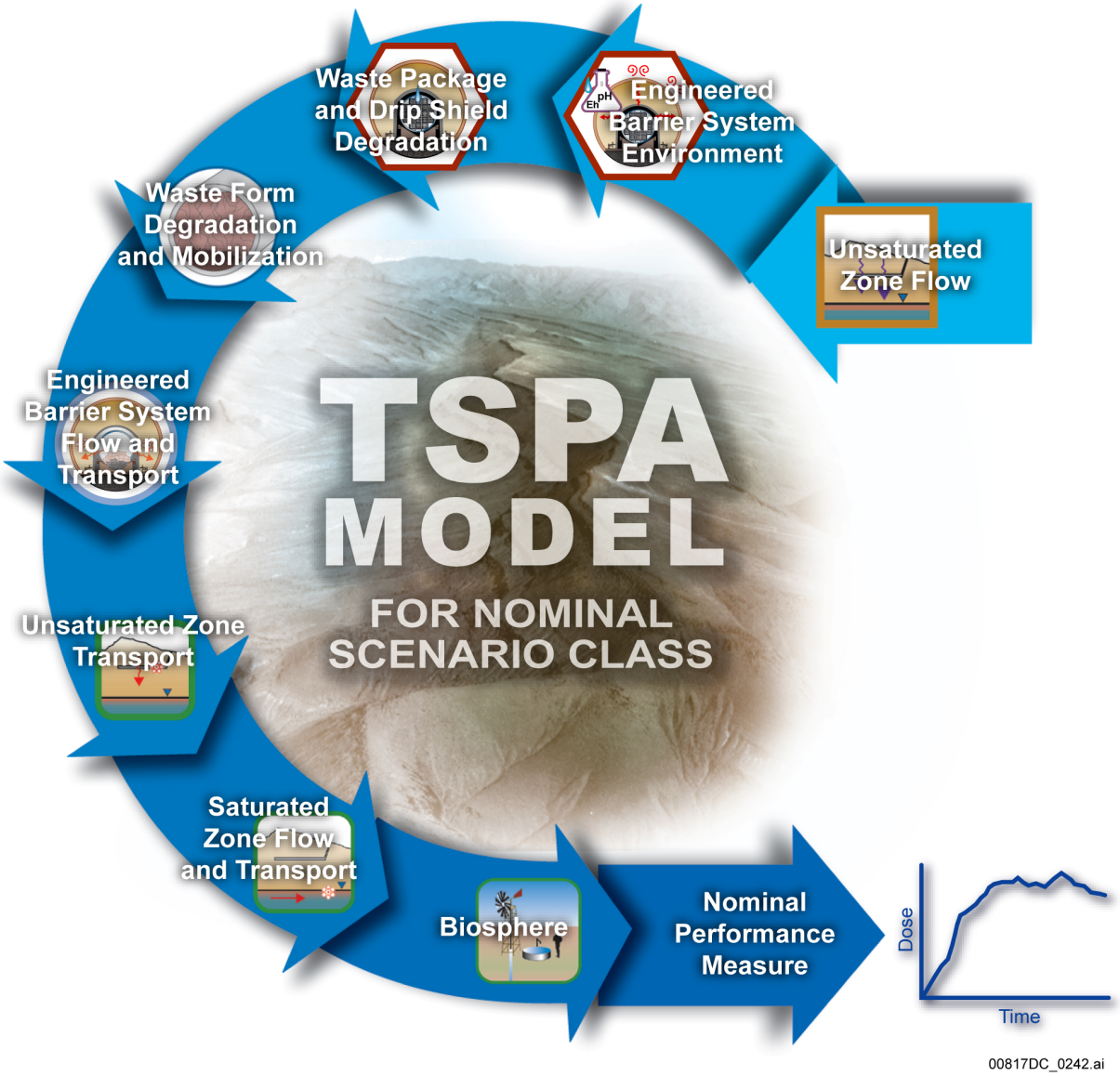

Figure 6.1.1-3. Schematic Representation of the TSPA-LA Model Components for the Nominal Scenario Class

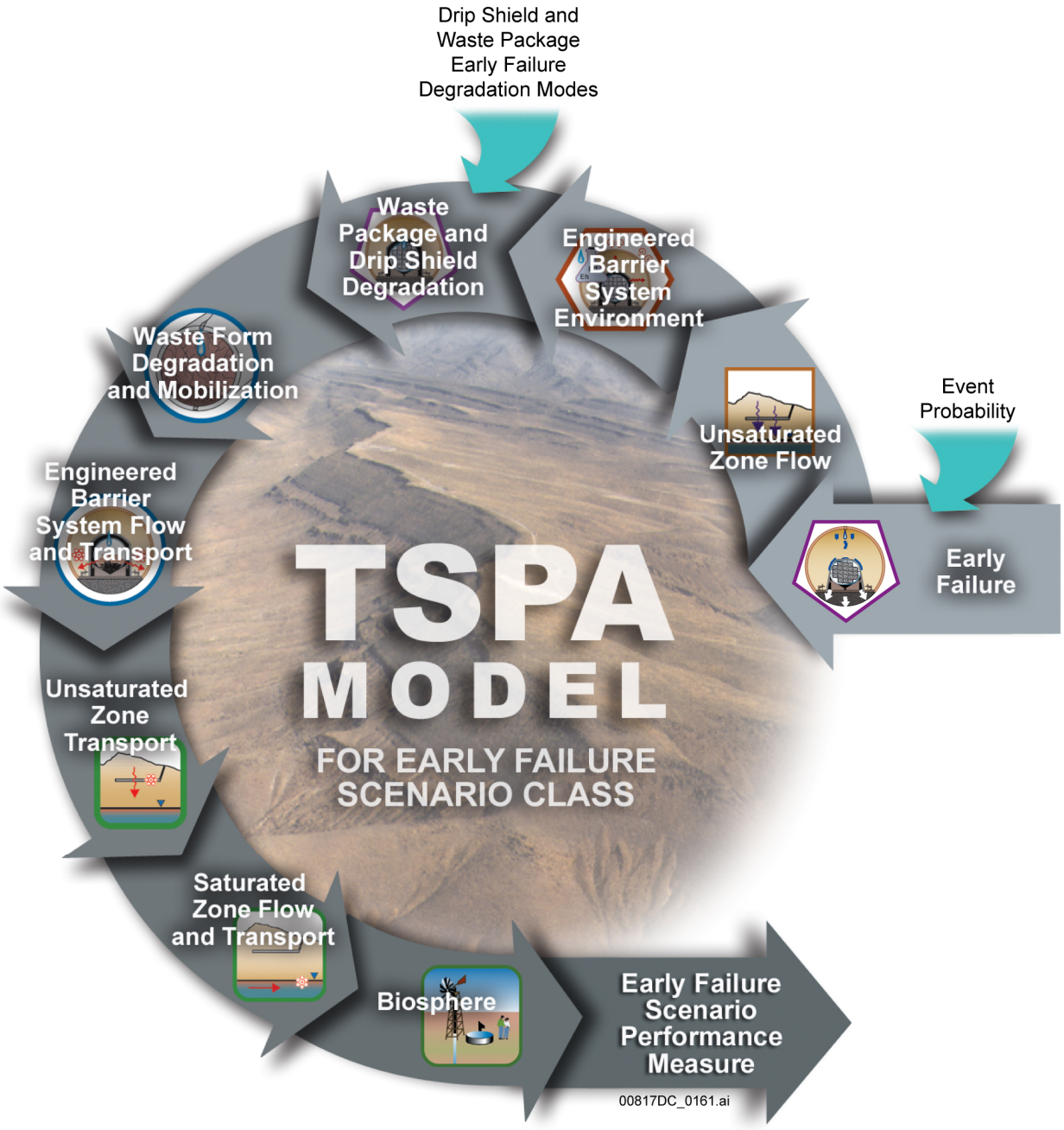

Figure 6.1.1-4. Schematic Representation of the TSPA-LA Model Components for the Early Failure Scenario Class

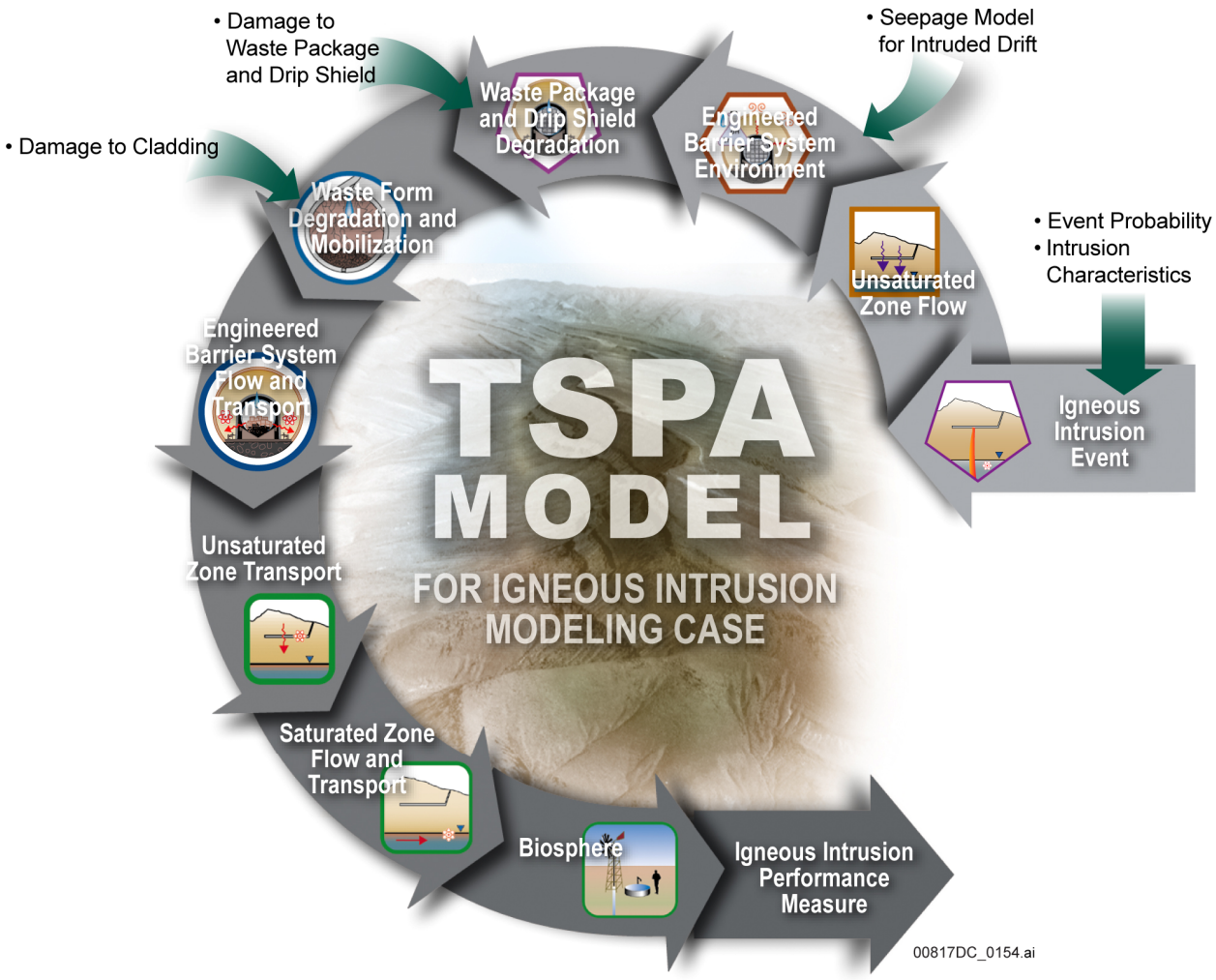

Figure 6.1.1-5. Schematic Representation of the TSPA-LA Model Components for the Igneous Intrusion Modeling Case

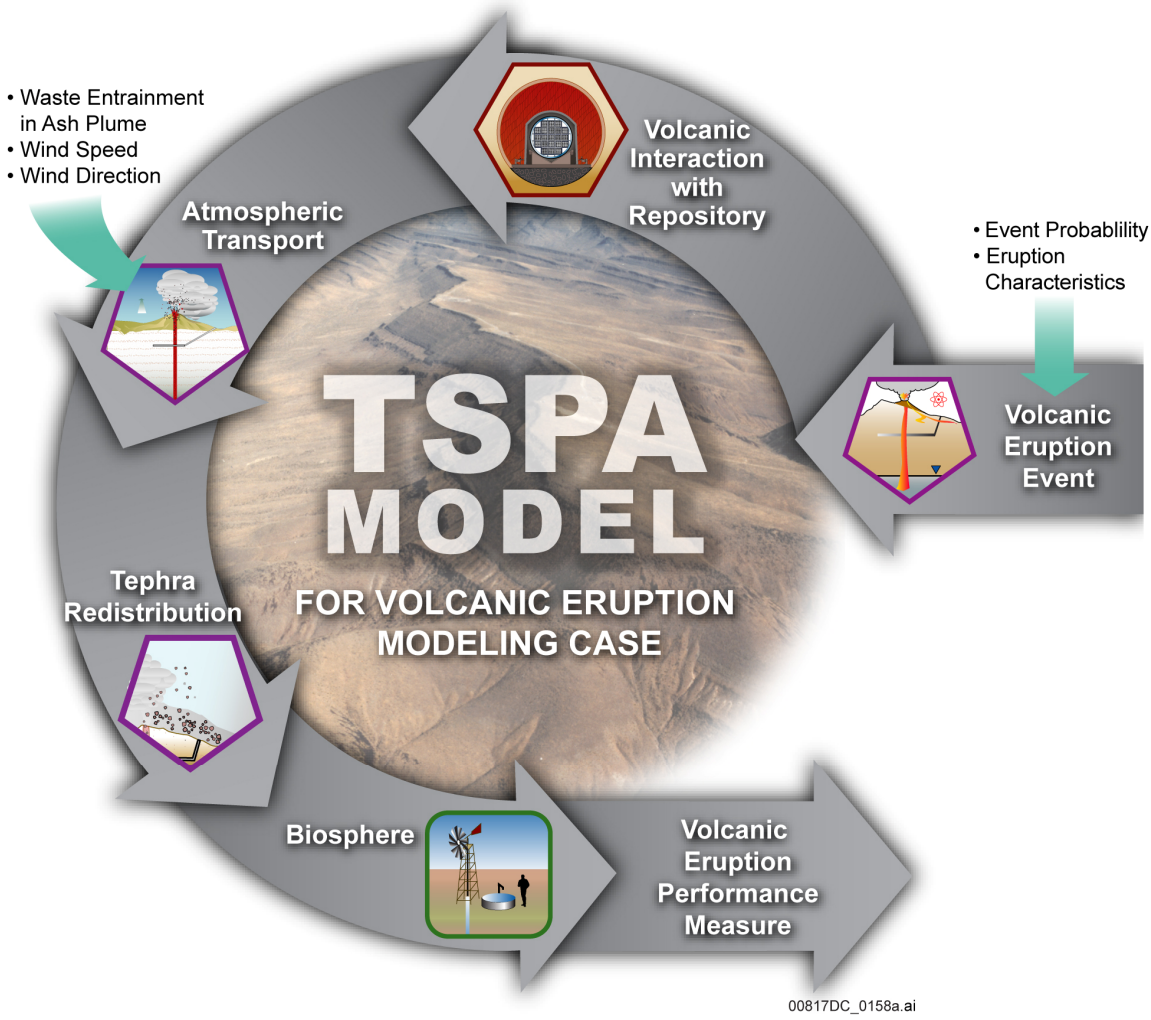

Figure 6.1.1-6. Schematic Representation of the TSPA-LA Model Components for the Volcanic Eruption Modeling Case

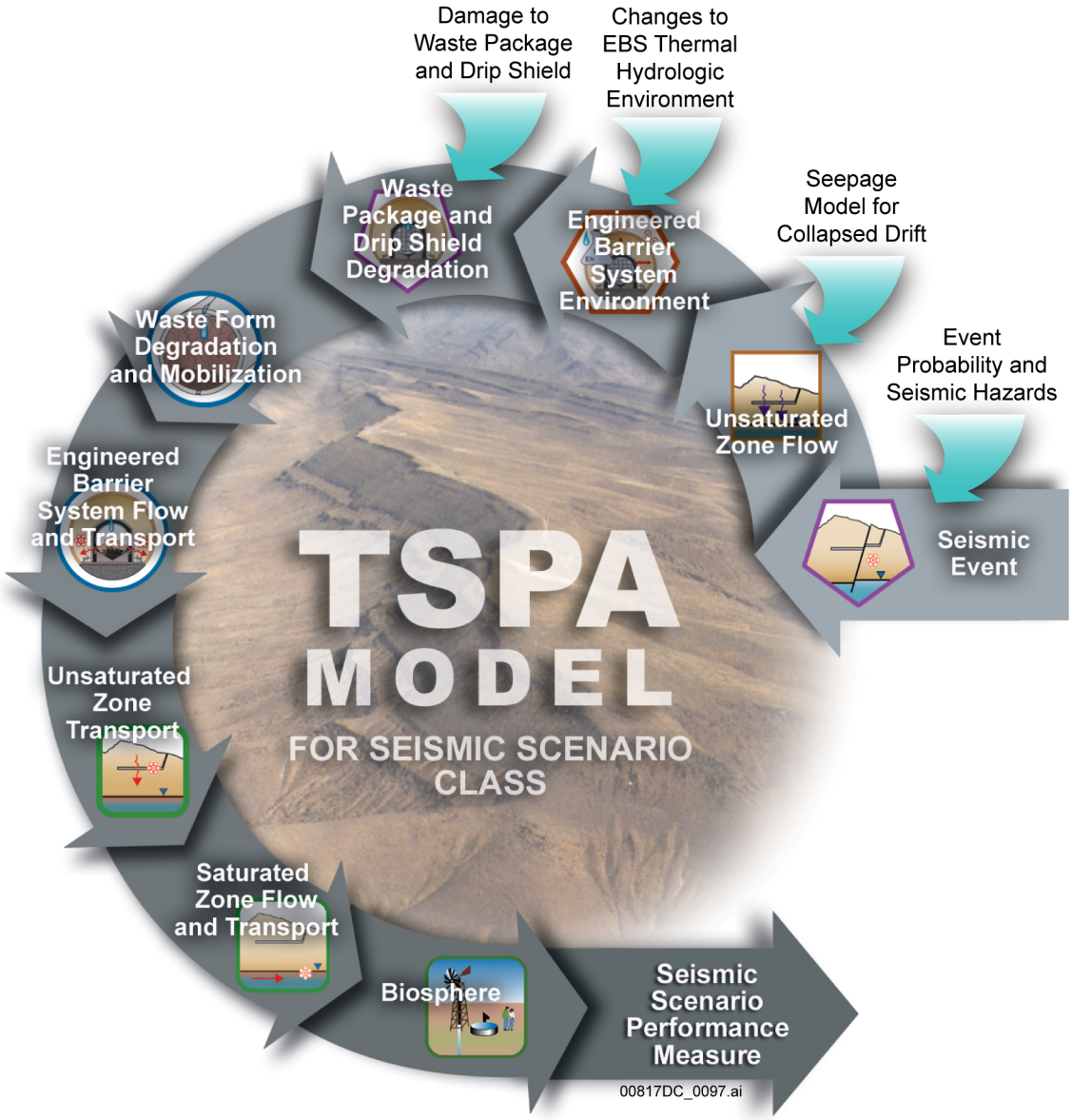

Figure 6.1.1-7. Schematic Representation of the TSPA-LA Model Components for the Seismic Scenario Class

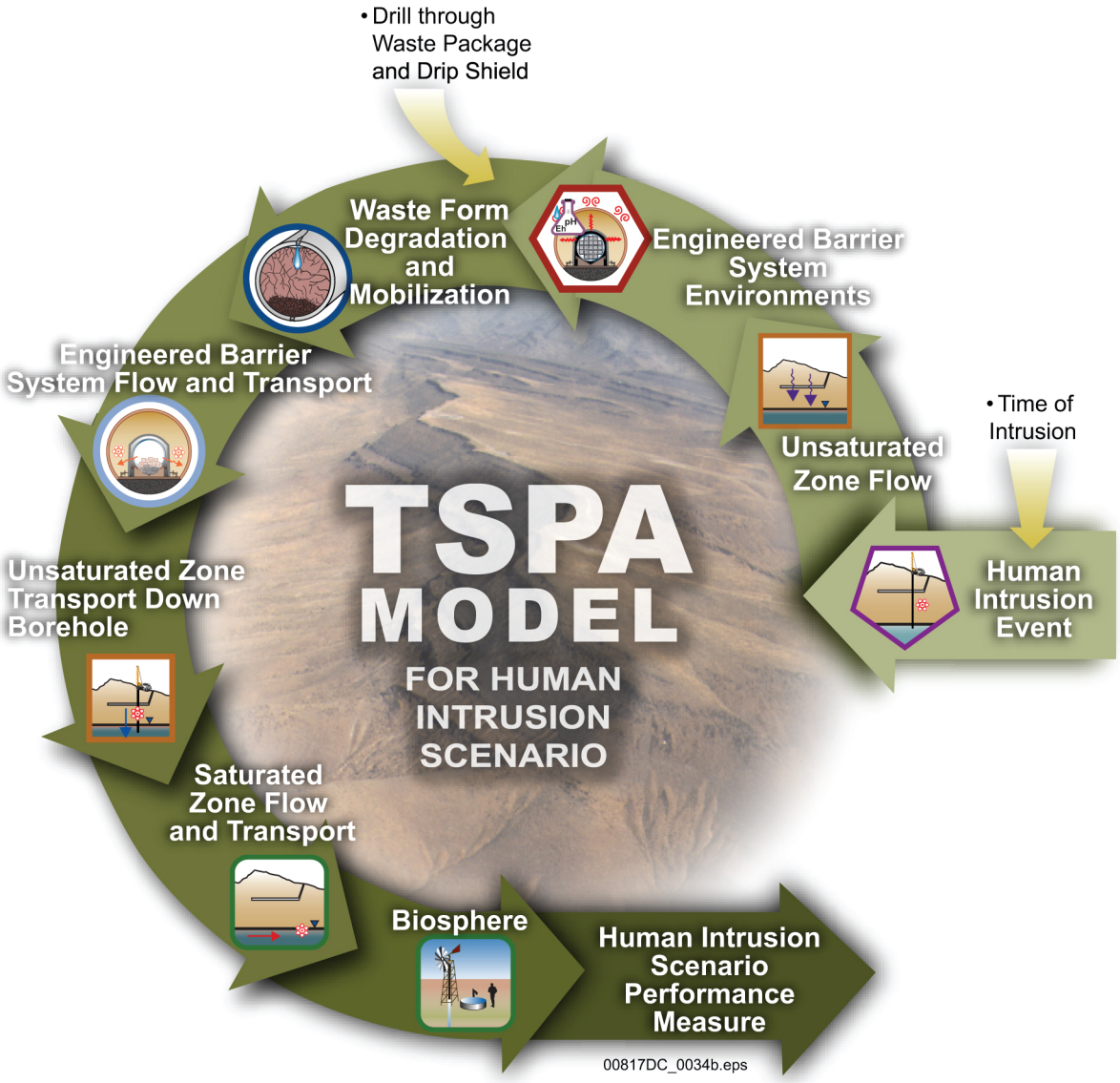

Figure 6.1.1-8. Schematic Representation of the TSPA-LA Model Components for the Human Intrusion Scenario

6.1.2 Calculation of Dose for the TSPA-LA Model

The identification and screening of FEPs is discussed in Section 6.1.1. The screening resulted in three retained events that are used to define scenario classes: early failure events, igneous events, and seismic events. Section 6.1.1 describes the scenario classes used to estimate repository performance in the TSPA-LA Model. The scenario classes are the Nominal Scenario Class, Early Failure Scenario Class, Igneous Scenario Class, and Seismic Scenario Class. A separate Human Intrusion Scenario is also described.

This section outlines the calculation of total mean annual dose and total median annual dose using the scenario classes defined in Section 6.1.1. Section 6.1.2.4 describes calculations for each of the individual modeling cases used in the TSPA-LA Model. Appendix J presents formal derivations for calculation of total mean annual dose and total median annual dose and the calculations performed for each modeling case.

6.1.2.1 Description of Uncertainty

The treatment of aleatory and epistemic uncertainty in the TSPA-LA Model is of particular importance to this discussion. In general, aleatory uncertainty derives from inherent uncertainty about future events, and epistemic uncertainty derives from lack of knowledge about quantities, models, or assumptions. Formally, aleatory uncertainty is characterized by a set $\mathcal{A} = \{\mathbf{a} : \mathbf{a} = [a_1, a_2, \ldots, a_{nA}]\}$ in which each vector $\mathbf{a} \in \mathcal{A}$ represents a possible future of the repository, and each a_j is a specific property of the future $\mathbf{a}$ (e.g., number of WP early failures, time of a seismic event). Each individual element a_i is described by a probability distribution, which conceptually leads to a density function $d_A(\mathbf{a})$ for the set $\mathcal{A}$. In this text it is useful to group the elements a_i of $\mathbf{a}$ into subsets corresponding to the modeling cases (e.g., denote by A_E the subset of elements that describe early failure events).

Similarly, epistemic uncertainty is characterized by a set $\mathcal{E} = \{\mathbf{e} : \mathbf{e} = [e_1, e_2, \ldots, e_{nE}]\}$ where each element e_i of $\mathbf{e}$ is an uncertain parameter (e.g., uncertainty in radionuclide solubility). Associated to each element e_i of $\mathbf{e}$ is a probability distribution, which taken together lead to a density function $d_E(\mathbf{e})$ for the set $\mathcal{E}$. Certain elements of $\mathbf{e}$ are used to characterize distributions for elements of $\mathbf{a}$ and thus are specific to certain modeling cases (e.g., the rate of occurrence for igneous events); other elements characterize uncertainty that applies to all modeling cases (e.g., uncertainty in radionuclide solubility). Where the distinction is important, it is useful to denote by $\mathbf{e}_A$ the subset of elements that influence aleatory uncertainty and to denote by $\mathbf{e}_M$ the elements e_i of $\mathbf{e}$ that are common to all modeling cases. The density function $d_A(\mathbf{a})$ is more correctly expressed as $d_A(\mathbf{a}|\mathbf{e}_A)$ to show the dependence of $\mathbf{a}$ on $\mathbf{e}_A$.

6.1.2.2 Calculation of Total Mean and Median Annual Dose

Total mean annual dose is defined as the expected value of dose to the RMEI, where the expectation is taken over both aleatory and epistemic uncertainty (Section 6.1.3). Total median

annual dose is estimated as the median of the distribution of expected dose to the RMEI, where the expectation is taken only over aleatory uncertainty. As specified in the proposed revision to 10 CFR 63.303 [DIRS 178394], total mean annual dose is the quantity compared to the regulatory standard for the period within 10,000 years after disposal, and total median annual dose is the quantity compared to the regulatory standard specified in 10 CFR 63.303(b) [DIRS 178394] for the period after 10,000 years of disposal. The calculations of total mean annual dose and total median annual dose are formally described in Appendix J Section J.4, which presents the mathematical definition of aleatory and epistemic uncertainty, the conceptual structure for the treatment of uncertainty, and the computational approach to the calculation of mean annual dose for each scenario class.

Calculation of total mean annual dose proceeds in a four-step process. First, a set of realizations of epistemic uncertainty are sampled from $\mathcal{E}$ consistent with the density function $d_E(\mathbf{e})$. Next, for each scenario class, a set of realizations of aleatory uncertainty, or futures, are selected from the set from $\mathcal{A}$ consistent with the density function $d_A(\mathbf{a})$. The contribution to total dose from each scenario class, $D_J(\tau|\mathbf{a},\mathbf{e})$, is computed as a function of time τ for each future $\mathbf{a}$ and each epistemic realization $\mathbf{e}$, where the subscript J in $D_J(\tau|\mathbf{a},\mathbf{e})$ indicates a particular scenario class. Third, for each scenario class and for each epistemic realization $\mathbf{e}$, the expected annual dose $\bar{D}_J(\tau|\mathbf{e})$ is computed where the expectation is taken over aleatory uncertainty. This expectation over aleatory uncertainty accounts for the probabilities that define each scenario class; thus, in the vernacular of previous TSPA analyses, $\bar{D}_J(\tau|\mathbf{e})$ is probability-weighted. Finally, total expected annual dose $\bar{D}(\tau|\mathbf{e})$ is computed for each epistemic realization $\mathbf{e}$ by summing expected annual doses over scenario classes, and total mean annual dose $\bar{\bar{D}}(\tau)$ is calculated as the expectation over epistemic uncertainty.

Total median annual dose $Q_{0.5}\left(\bar{D}(\tau|\mathbf{e})\right)$ is calculated as the median of the distribution of expected dose, where the expectation is taken only over aleatory uncertainty. Formally, at each time τ, the calculation of total expected annual dose produces a distribution $\left\{\bar{D}(\tau|\mathbf{e})\right\}$ of values of total expected annual dose, one value for each epistemic realization $\mathbf{e}$. The TSPA-LA Model estimates the total median annual dose to the RMEI by the median of the distribution $\left\{\bar{D}(\tau|\mathbf{e})\right\}$.

The quantity $\bar{D}(\tau|\mathbf{e})$ is formally described as the total expected annual dose conditional on epistemic uncertainty. For convenience, this text uses the less cumbersome term total expected annual dose to refer to $\bar{D}(\tau|\mathbf{e})$. The quantity $\bar{\bar{D}}(\tau)$ is technically also an expected value. Again, for convenience, and to distinguish this quantity in the text from the total expected annual dose $\bar{D}(\tau|\mathbf{e})$, this text uses the term total mean annual dose to refer to $\bar{\bar{D}}(\tau)$.

For an arbitrary future $\mathbf{a}$ and epistemic realization $\mathbf{e}$, total annual dose, $D(\tau|\mathbf{a},\mathbf{e})$, is approximated as:

$$D(\tau|\mathbf{a},\mathbf{e}) \cong D_N(\tau|\mathbf{a},\mathbf{e}) + D_E(\tau|\mathbf{a},\mathbf{e}) + D_I(\tau|\mathbf{a},\mathbf{e}) + D_S(\tau|\mathbf{a},\mathbf{e}) \quad \text{(Eq. 6.1.2-1)}$$

where

$D_N(\tau|\mathbf{a},\mathbf{e})$ = Dose at time τ resulting from nominal processes

$D_E(\tau|\mathbf{a},\mathbf{e})$ = Additional dose at time τ resulting from any early failures occurring in the future $\mathbf{a}$

$D_I(\tau|\mathbf{a},\mathbf{e})$ = Additional dose at time τ resulting from any igneous events occurring in the future $\mathbf{a}$

$D_S(\tau|\mathbf{a},\mathbf{e})$ = Additional dose at time τ resulting from any seismic events occurring in the future $\mathbf{a}$.

Equation 6.1.2-2 approximates total annual dose as the sum of dose resulting from nominal process and from events. The approximation relies on the simplifying assumption that the dose resulting from a combination of events is the sum of the doses resulting from each separate event; this approximation is justified in Section 6.1.2.3.

Total expected annual dose, $\overline{D}(\tau|\mathbf{e})$, is calculated as the expected value of $D(\tau|\mathbf{a},\mathbf{e})$ where the expectation is over the uncertainty in $\mathbf{a}$ (aleatory uncertainty). Written simply,

$$\begin{aligned}
\overline{D}(\tau|\mathbf{e}) &= \int_{\mathcal{A}} D(\tau|\mathbf{a},\mathbf{e})\, d_A(\mathbf{a})\, dA \\
&= \int_{\mathcal{A}} \left(D_N(\tau|\mathbf{a},\mathbf{e}) + D_E(\tau|\mathbf{a},\mathbf{e}) + D_I(\tau|\mathbf{a},\mathbf{e}) + D_S(\tau|\mathbf{a},\mathbf{e}) \right) d_A(\mathbf{a})\, dA \\
&= \int_{\mathcal{A}} D_N(\tau|\mathbf{a},\mathbf{e})\, d_A(\mathbf{a})\, dA + \int_{\mathcal{A}} D_E(\tau|\mathbf{a},\mathbf{e})\, d_A(\mathbf{a})\, dA \\
&\quad + \int_{\mathcal{A}} D_I(\tau|\mathbf{a},\mathbf{e})\, d_A(\mathbf{a})\, dA + \int_{\mathcal{A}} D_S(\tau|\mathbf{a},\mathbf{e})\, d_A(\mathbf{a})\, dA \\
&= \overline{D}_N(\tau|\mathbf{e}) + \overline{D}_E(\tau|\mathbf{e}) + \overline{D}_I(\tau|\mathbf{e}) + \overline{D}_S(\tau|\mathbf{e})
\end{aligned} \quad \text{(Eq. 6.1.2-2)}$$

where the dependence of $d_A(\mathbf{a})$ on $\mathbf{e}$ is omitted for brevity of notation. The quantity $\overline{D}_N(\tau|\mathbf{e})$ is the expected annual dose resulting from nominal processes. The quantities $\overline{D}_E(\tau|\mathbf{e})$, $\overline{D}_I(\tau|\mathbf{e})$, and $\overline{D}_S(\tau|\mathbf{e})$ are the expected values of the additional annual dose resulting from the occurrence of early failure, igneous, and seismic events, respectively. For brevity these quantities are frequently referred to as the expected annual dose for each scenario class, and the term "additional" is omitted for convenience.

Total mean annual dose, $\overline{\overline{D}}(\tau)$, is calculated as the expected value of $\overline{D}(\tau|\mathbf{e})$ where the expectation is over the uncertainty in $\mathbf{e}$ (epistemic uncertainty). $\overline{\overline{D}}(\tau)$ is calculated by:

$$\begin{aligned}\overline{\overline{D}}(\tau) &= \int_{\mathcal{E}} \overline{D}(\tau|\mathbf{e})\, d_E(\mathbf{e})\, dE \\ &\cong \frac{1}{N}\sum_{k=1}^{N} \overline{D}(\tau|\mathbf{e}_k)\end{aligned} \qquad \text{(Eq. 6.1.2-3)}$$

where $\{\mathbf{e}_k\}$ is a Latin hypercube sample (LHS) of the epistemic variables of size N consistent with the distributions defining each of the elements e_i of $\mathbf{e}$.

Due to the complexity of $D(\tau|\mathbf{a},\mathbf{e})$, evaluation of the integral in Equation 6.1.2-2 requires that the set of all futures A be divided into subsets, for which the integral can be numerically evaluated. The set A is first divided into eight mutually exclusive, or disjoint, sets of repository futures, defined by the events retained in the TSPA-LA Model (early failure, igneous, and seismic). A sequence of re-arranging terms in the integral, presented below, leads to the calculation of total expected annual dose as the sum of the expected annual dose for each of the four scenario classes $\{A_N, A_{EF}, A_I, A_S\}$ identified in Section 6.1.1.

The three retained events lead directly to the first three disjoint sets of repository futures:

- Early failure scenario set, S_{EF}: the set of futures each of which includes one or more early failure events (i.e., one or more early failed WPs and/or one or more early failed DSs), but no seismic or igneous events, and also includes nominal features and processes.

- Igneous scenario set, S_I: the set of futures each of which includes one or more igneous events, but no seismic or early failure events, and also includes retained nominal features and processes.

- Seismic scenario set, S_S: the set of futures each of which includes one or more seismic events, but no igneous or early failure events, and also includes retained nominal features and processes.

The three sets listed above describe only those futures in which a single type of event occurs, thus they are subsets of the scenario classes defined in Section 6.1.1. Because the events occur independently, there are many future states of the repository in which more than one type of event may occur. Therefore, four additional sets are defined to account for futures that include combinations of the three types of events:

- Early failure/Igneous scenario set, S_{EF+I}: the set of futures each of which includes one or more early failure events and one or more igneous events, but no seismic events.

- Early failure/Seismic scenario set, S_{EF+S}: the set of futures each of which includes one or more early failure events and one or more seismic events, but no igneous events.

- Igneous/seismic scenario set, S_{I+S}: the set of futures each of which includes one or more igneous events and one or more seismic events, but no early failure events, and also includes nominal features and processes.

- Igneous/seismic/early failure scenario set, S_{EF+I+S}: the set of futures each of which includes one or more early failure events and one or more seismic events and one or more igneous events, and also includes nominal features and processes.

Each of the four scenario sets listed above can also be defined in terms of intersections of the scenario classes listed in Section 6.1.1. Finally, it is possible that no events occur in the future of the repository. One more set of repository futures, defined as the complement of the union of the sets above, accounts for the futures in which no event occurs:

- Nominal scenario set, S_N: the set of futures each of which includes nominal features and processes (e.g., corrosion processes, such as general corrosion, localized corrosion, and SCC) but *no* events (i.e., no igneous or seismic events and no early WP or DS failures).

The eight sets of futures defined above partition the set of all futures of the repository into a collection of disjoint sets. The set of all futures is formally a probability space with a probability measure p_A derived from the distributions of the individual elements a_i of $\mathbf{a}$. Hence, a probability can be calculated for each of the eight disjoint sets $\{S_{EF}, S_I, S_S, S_{EF+I}, S_{EF+S}, S_{I+S}, S_{EF+I+S}, S_N\}$. Because the union of the eight sets equals all of A, and the eight sets are disjoint, the probabilities associated with each of the eight sets sum to exactly one.

These eight sets $\{S_{EF}, S_I, S_S, S_{EF+I}, S_{EF+S}, S_{I+S}, S_{EF+I+S}, S_N\}$ form a collection of scenario classes in and of themselves. Since these sets are disjoint and their union covers all futures of the repository, these sets meet the acceptance criteria for scenario classes specified in the *Yucca Mountain Review Plan, Final Report* (NRC 2003 [DIRS 163274]). Total expected annual dose could be calculated separately for these eight scenario classes, and then combined appropriately to estimate repository performance. However, the TSPA-LA Model calculation of total expected annual dose is simplified by aggregating these eight disjoint sets into the scenario classes identified in Section 6.1.1.

Partition the set of futures A into $\{S_{EF}, S_I, S_S, S_{EF+I}, S_{EF+S}, S_{I+S}, S_{EF+I+S}, S_N\}$ as defined above. Next, separate the integral in Equation 6.1.2-2 into a sum of eight integrals over the separate disjoint sets:

$$\begin{aligned}\bar{D}(\tau|\mathbf{e}) &= \int_{\mathcal{A}} D(\tau|\mathbf{a},\mathbf{e})\, d_A(\mathbf{a})\, dA \\ &= \int_{S_N} D(\tau|\mathbf{a},\mathbf{e})\, d_A(\mathbf{a})\, dA + \int_{S_{EF}} D(\tau|\mathbf{a},\mathbf{e})\, d_A(\mathbf{a})\, dA \\ &\quad + \int_{S_I} D(\tau|\mathbf{a},\mathbf{e})\, d_A(\mathbf{a})\, dA + \int_{S_S} D(\tau|\mathbf{a},\mathbf{e})\, d_A(\mathbf{a})\, dA \\ &\quad + \int_{S_{EF+I}} D(\tau|\mathbf{a},\mathbf{e})\, d_A(\mathbf{a})\, dA + \int_{S_{EF+S}} D(\tau|\mathbf{a},\mathbf{e})\, d_A(\mathbf{a})\, dA \\ &\quad + \int_{S_{I+S}} D(\tau|\mathbf{a},\mathbf{e})\, d_A(\mathbf{a})\, dA + \int_{S_{EF+I+S}} D(\tau|\mathbf{a},\mathbf{e})\, d_A(\mathbf{a})\, dA \\ &= \int_{\bigcup_J S_J} D(\tau|\mathbf{a},\mathbf{e})\, d_A(\mathbf{a})\, dA\end{aligned} \quad \text{(Eq. 6.1.2-4)}$$

where, for convenience in the presentation, $J = 1, 2, \ldots, 8$ is an index and the collection $\{S_J\}$ are the eight disjoint sets $\{S_{EF}, S_I, S_S, S_{EF+I}, S_{EF+S}, S_{I+S}, S_{EF+I+S}, S_N\}$.

Next, use Equation 6.1.2-1 in Equation 6.1.2-4 to obtain

$$\begin{aligned}\bar{D}(\tau|\mathbf{e}) &= \int_{\bigcup_J S_J} D(\tau|\mathbf{a},\mathbf{e})\, d_A(\mathbf{a})\, dA \\ &= \int_{\bigcup_J S_J} \left(D_N(\tau|\mathbf{a},\mathbf{e}) + D_E(\tau|\mathbf{a},\mathbf{e}) + D_I(\tau|\mathbf{a},\mathbf{e}) + D_S(\tau|\mathbf{a},\mathbf{e})\right) d_A(\mathbf{a})\, dA \\ &= \int_{\bigcup_J S_J} D_N(\tau|\mathbf{a},\mathbf{e})\, d_A(\mathbf{a})\, dA + \int_{\bigcup_J S_J} D_E(\tau|\mathbf{a},\mathbf{e})\, d_A(\mathbf{a})\, dA \\ &\quad + \int_{\bigcup_J S_J} D_I(\tau|\mathbf{a},\mathbf{e})\, d_A(\mathbf{a})\, dA + \int_{\bigcup_J S_J} D_S(\tau|\mathbf{a},\mathbf{e})\, d_A(\mathbf{a})\, dA\end{aligned}$$

(Eq. 6.1.2-5)

Consider first the integral involving $D_E(\tau|\mathbf{a},\mathbf{e})$. If a future $\mathbf{a}$ does not include any early failure events, there is no additional dose that can result from early failure. Thus, the quantity $D_E(\tau|\mathbf{a},\mathbf{e})$ is zero for any future $\mathbf{a}$ that does not include any early failure events. Using this observation, the term in Equation 6.1.2-5 that involves $D_E(\tau|\mathbf{a},\mathbf{e})$ is expanded as

$$\begin{aligned}\int_{\bigcup_J S_J} D_E(\tau|\mathbf{a},\mathbf{e})\, d_A(\mathbf{a})\, dA &= \sum_J \int_{S_J} D_E(\tau|\mathbf{a},\mathbf{e})\, d_A(\mathbf{a})\, dA \\ &= \int_{S_{EF}} D_E(\tau|\mathbf{a},\mathbf{e})\, d_A(\mathbf{a})\, dA + \int_{S_{EF+I}} D_E(\tau|\mathbf{a},\mathbf{e})\, d_A(\mathbf{a})\, dA \\ &\quad + \int_{S_{EF+S}} D_E(\tau|\mathbf{a},\mathbf{e})\, d_A(\mathbf{a})\, dA + \int_{S_{EF+I+S}} D_E(\tau|\mathbf{a},\mathbf{e})\, d_A(\mathbf{a})\, dA\end{aligned}$$

(Eq. 6.1.2-6)

since the integral of $D_E(\tau|\mathbf{a},\mathbf{e})$ over any of the sets $\{S_I, S_S, S_{I+S}, S_N\}$ is zero. Finally, by using the definition of the Early Failure Scenario Class, A_E, and the eight disjoint scenario sets, $\{S_{EF}, S_I, S_S, S_{EF+I}, S_{EF+S}, S_{I+S}, S_{EF+I+S}, S_N\}$, write $A_E = S_{EF} \cup S_{EF+I} \cup S_{EF+S} \cup S_{EF+I+S}$. Equation 6.1.2-6 becomes

$$\begin{aligned}
&\int_{S_{EF}} D_E(\tau|\mathbf{a},\mathbf{e})\, d_A(\mathbf{a})\, dA + \int_{S_{EF+I}} D_E(\tau|\mathbf{a},\mathbf{e})\, d_A(\mathbf{a})\, dA \\
&\quad + \int_{S_{EF+S}} D_E(\tau|\mathbf{a},\mathbf{e})\, d_A(\mathbf{a})\, dA + \int_{S_{EF+I+S}} D_E(\tau|\mathbf{a},\mathbf{e})\, d_A(\mathbf{a})\, dA \\
&\qquad = \int_{S_{EF} \cup S_{EF+I} \cup S_{EF+S} \cup S_{EF+I+S}} D_E(\tau|\mathbf{a},\mathbf{e})\, d_A(\mathbf{a})\, dA \qquad \text{(Eq. 6.1.2-7)} \\
&\qquad = \int_{A_E} D_E(\tau|\mathbf{a},\mathbf{e})\, d_A(\mathbf{a})\, dA \\
&\qquad = \bar{D}_E(\tau|\mathbf{e})
\end{aligned}$$

where $\bar{D}_E(\tau|\mathbf{e})$ is the expected annual dose due to early failures. Similar sequences of operations lead to the following expressions for the expected annual dose due to igneous events, $\bar{D}_I(\tau|\mathbf{e})$, and the expected annual dose due to seismic events, $\bar{D}_S(\tau|\mathbf{e})$:

$$\bar{D}_I(\tau|\mathbf{e}) = \int_{A_I} D_I(\tau|\mathbf{a},\mathbf{e})\, d_A(\mathbf{a})\, dA \qquad \text{(Eq. 6.1.2-8)}$$

$$\bar{D}_S(\tau|\mathbf{e}) = \int_{A_S} D_S(\tau|\mathbf{a},\mathbf{e})\, d_A(\mathbf{a})\, dA \qquad \text{(Eq. 6.1.2-9)}$$

where

$A_I = S_I \cup S_{EF+I} \cup S_{I+S} \cup S_{EF+I+S}$	is the Igneous Scenario Class.
$\bar{D}_I(\tau|\mathbf{e})$	is the expected annual dose due to igneous events.
$A_S = S_S \cup S_{EF+S} \cup S_{I+S} \cup S_{EF+I+S}$	is the Seismic Scenario Class.
$\bar{D}_S(\tau|\mathbf{e})$	is the expected annual dose due to seismic events.

The final quantity required for calculation of total expected annual dose is $\bar{D}_N(\tau|\mathbf{e})$, the expected annual dose for the Nominal Scenario Class. The Nominal Scenario Class excludes the occurrence of any events, and thus does not depend on any of the aleatory uncertainties that describe future events. The Nominal Scenario Class addresses other types of aleatory uncertainty describing the time, location and extent of damage to WP caused by corrosion processes. Moreover, these corrosion processes occur in every future of the repository. Hence,

$$\bar{D}_N(\tau|\mathbf{e}) = \int_{A} D_N(\tau|\mathbf{a},\mathbf{e})\, d_A(\mathbf{a})\, dA \qquad \text{(Eq. 6.1.2-10)}$$

where the aleatory uncertainty in Equation 6.1.2-10 describes spatial and temporal variability in waste package failure by corrosion processes. Using Equation 6.1.2-7 through Equation 6.1.2-10, Equation 6.1.2-5 becomes

$$\begin{aligned}\bar{D}(\tau|\mathbf{e}) &= \int_{\bigcup_J S_J} D_N(\tau|\mathbf{a},\mathbf{e})\, d_A(\mathbf{a}) + \int_{\bigcup_J S_J} D_{EF}(\tau|\mathbf{a},\mathbf{e})\, d_A(\mathbf{a}) \\ &\quad + \int_{\bigcup_J S_J} D_I(\tau|\mathbf{a},\mathbf{e})\, d_A(\mathbf{a}) + \int_{\bigcup_J S_J} D_S(\tau|\mathbf{a},\mathbf{e})\, d_A(\mathbf{a}) \\ &= \int_A D_N(\tau|\mathbf{a},\mathbf{e})\, d_A(\mathbf{a}) + \int_{A_{EF}} D_{EF}(\tau|\mathbf{a},\mathbf{e})\, d_A(\mathbf{a}) \\ &\quad + \int_{A_I} D_I(\tau|\mathbf{a},\mathbf{e})\, d_A(\mathbf{a}) + \int_{A_S} D_S(\tau|\mathbf{a},\mathbf{e})\, d_A(\mathbf{a}) \\ &= \bar{D}_N(\tau|\mathbf{e}) + \bar{D}_{EF}(\tau|\mathbf{e}) + \bar{D}_I(\tau|\mathbf{e}) + \bar{D}_S(\tau|\mathbf{e})\end{aligned} \qquad \text{(Equation 6.1.2-11)}$$

Section 6.1.2.4 describes in further detail the calculation of each term in Equation 6.1.2-11. The results of these calculations are presented in Section 8.

6.1.2.3 Screening of Scenario Classes

As outlined in Section 6.1.2.2, the calculation of total annual dose as the sum of annual dose from each scenario class relies on the simplifying assumption that the occurrence of an early failure or other event has no effect on the consequences of a later event. This simplifying assumption allows the TSPA-LA Model to approximate the dose from a future involving a combination of events, such as a seismic event followed by an igneous intrusion, as the sum of the dose from the seismic event and the dose from the igneous event. In general, this method of approximation affects the TSPA-LA Model results in a conservative way, by overestimating the resulting dose. Table 6.1.2-1 summarizes the effect of each combination of events on the calculation of total mean annual dose; these effects are discussed below.

6.1.2.3.1 Nominal Scenario Class with Other Scenario Classes

During the period before 10,000 years, the corrosion processes included in the Nominal Scenario Class have no consequences that affect the consequences of any early failure or disruptive event. Thus, no combinations of the Nominal Scenario Class with other scenario classes are relevant before 10,000 years.

During the period after 10,000 years, the corrosion processes described by the Nominal Scenario Class affect the consequences of seismic ground motion events, so these processes are included in the Seismic GM Modeling Case. As explained in Section 6.1.2.4.1 and Section 6.1.2.4.3, the inclusion of these processes means that dose due to nominal processes is combined with the additional dose due to seismic ground motion events, and this combined quantity is calculated by the Seismic GM Modeling Case. The corrosion processes are included in the Igneous Intrusion Modeling Case so that the inventory remaining in the WPs at the time of the intrusion is reduced by the radionuclides released due to general corrosion processes prior to the intrusion. In order to avoid double-counting the dose from radionuclides released due to general corrosion processes prior to the intrusion, any observed dose prior to the time of the first intrusion is not included in

the results of the Igneous Intrusion Modeling Case. Nominal corrosion processes are not included in the Seismic FD, Igneous Eruption, or Early Failure Modeling Cases, which results in over counting of radionuclides released in these modeling cases. However, these modeling cases affect only a small fraction of the WPs (at most two percent in the Seismic FD Modeling Case), so the resulting effect on total mean annual dose is minor.

6.1.2.3.2 Early Failure Scenario Class with Other Scenario Classes

In the TSPA-LA Model, early failures are assumed to take place at the time of repository closure. Since an early failure cannot follow any disruptive event, these combinations are not relevant and are not listed in Table 6.1.2-1. In the TSPA-LA, if a disruptive event follows an early failure, the inventory released as a consequence of the disruptive event is estimated without subtracting the inventory that may have been released from the WPs affected by early failure. However, on average less than 2.46/11,629 = 0.02 percent of the WPs are affected by early failure (Output DTN: MO0707WPDRIPSD.000_R0 [DIRS 183005]), so not more than 0.02 percent (on average) of the inventory is counted twice, and the net effect on total mean annual dose of the combination of early failures and disruptive events is negligible.

6.1.2.3.3 Igneous Scenario Class with Other Scenario Classes

The combinations of an igneous intrusion and volcanic eruption with other scenario classes are considered separately.

Igneous Intrusion with Seismic Scenario Class—The TSPA-LA Model assumes that all components of the EBS suffer maximum damage from an igneous intrusion. After the intrusion, the EBS components (DSs and WPs) no longer function as a barrier to advective or diffusive transport of radionuclides. Since the effects of a seismic event (either vibratory ground motion or fault displacement) are damage to components of the EBS, a seismic event following an igneous intrusion should not have any effect on the repository performance.

The TSPA-LA Model overestimates total dose by not excluding the dose resulting from seismic events occurring after an igneous intrusion. However, during 1,000,000 years, the average probability of an igneous intrusion is roughly $\left(1.7\times10^{-8}\ \text{yr}^{-1}\right)\times\left(10^{6}\ \text{yr}\right)=1.7\times10^{-2}$ (Section 6.5.1.1), so the over-estimate of dose affects roughly 2 percent of the realizations of the Seismic GM Modeling Case, and the overall effect on total mean annual dose is minor.

Volcanic Eruption with Seismic Scenario Class—The TSPA-LA Model overestimates total dose by not reducing the inventory that could be released by seismic events, by the amount of inventory released by any volcanic eruptions. However, on average an eruptive event affects less that 0.03 percent of the WPs, so not more than 0.03 percent (on average) of the inventory could be counted twice, and the net effect on total mean annual dose of the combination of volcanic eruptions and seismic events is negligible.

Combinations of Igneous Intrusions with Volcanic Eruptions—The TSPA-LA Model overestimates total dose by not reducing the inventory that could be released by intrusions or eruptions by the amount of inventory released by any preceding igneous event. However, on average an eruptive event affects less that 0.03 percent of the WPs, so the effect on total mean

annual dose of an eruptive event preceding other igneous events is negligible. The TSPA-LA Model accounts for multiple igneous intrusion events and for multiple volcanic eruption events in the calculation of total mean annual dose.

6.1.2.3.4 Seismic Scenario Class with Other Scenario Classes

The TSPA-LA Model overestimates total dose by not subtracting the inventory released due to preceding seismic ground motion events from the inventory available at the time of an igneous event. During 1,000,000 years, essentially all future states of the repository include releases due to seismic ground motion damage; thus, essentially all realizations of the Igneous Modeling Cases overstate releases by the amount of inventory released by seismic ground motion events prior to an intrusion. This interaction is conservative in the sense that the consequences of the Igneous Modeling Cases are always overstated. Additional discussion of the magnitude by which these consequences are overstated is provided in Appendix J, Section J.10.

The inventory released from a fault displacement event is not subtracted from the inventory that could be released by a later disruptive event. In addition, the inventory that could be released from WPs affected by fault displacement is not reduced by releases from any preceding disruptive events. However, a fault displacement affects at most 212/11,629 = 1.8 percent of the WPs, so at most 1.8 percent of the inventory is counted twice, and the net effect on total mean annual dose of the combination of fault displacements, with other disruptive events, is negligible.

6.1.2.4 Calculation of Expected Annual Dose for the Modeling Cases

Equation 6.1.2-11 shows the calculation of total expected annual dose as the sum of expected annual dose for each scenario class. In turn, the expected annual dose for each scenario class is the sum of the expected annual dose for the modeling cases comprising the scenario class. Appendix J presents the formal derivation of expected annual dose for each modeling case. This section summarizes that discussion and gives the equations used to evaluate expected annual dose for each of the modeling cases.

6.1.2.4.1 Nominal Scenario Class

The Nominal Scenario Class includes one modeling case, the Nominal Modeling Case. By definition, the Nominal Scenario Class excludes the occurrence of any early failures or of any events. Thus, there is no aleatory uncertainty in the Nominal Modeling Case related to the occurrence of early failures, igneous or seismic events. Conceptually, the time, location and degree of damage to each WP that fails by nominal corrosion processes are aleatory uncertainties that could be described by appropriate elements of the vector for aleatory uncertainty, $\mathbf{a}$. However, these aleatory quantities are not explicitly represented in the TSPA-LA Model in the same manner as aleatory quantities related to early failures or events. Rather, these aleatory quantities are addressed through a number of averaging operations within submodels that determine time, location and degree of damage occurring by corrosion processes. Section 6.3.5 describes these submodels; Appendix N outlines the averaging operations that account for the aleatory uncertainty in these submodels. Thus, the Nominal Modeling Case computes the expected annual dose $\bar{D}_N(\tau \mid \mathbf{e})$ directly by the models described in Section 6.3.

The expected annual dose for the Nominal Modeling Case, $\bar{D}_N(\tau \mid \mathbf{e}_i)$, is calculated for both 10,000 years and for 1,000,000 years. However, for estimating total expected annual dose for 1,000,000 years, $\bar{D}_N(\tau \mid \mathbf{e}_i)$ is not used directly in Equation 6.1.2-11. Instead, as described in Section 6.1.2.4.4, the dose due to nominal processes is calculated as part of the Seismic GM Modeling Case, and addresses the aleatory uncertainty in corrosion processes using the techniques outlined in Appendix N.

6.1.2.4.2 Early Failure Scenario Class

The Early Failure Scenario Class includes two modeling cases: the Waste Package EF Modeling Case, and the Drip Shield EF Modeling Case. For the Early Failure Scenario Class, expected annual dose at time τ is computed as:

$$\bar{D}_E\left(\tau|\mathbf{e}_i\right) = \bar{D}_{EW}\left(\tau|\mathbf{e}_i\right) + \bar{D}_{ED}\left(\tau|\mathbf{e}_i\right) \quad \text{(Eq. 6.1.2-12)}$$

where $\bar{D}_{EW}\left(\tau|\mathbf{e}_i\right)$ is the expected annual dose from early failed WPs, and $\bar{D}_{ED}\left(\tau|\mathbf{e}_i\right)$ is the expected annual dose from early failed DSs. Equation 6.1.2-12 is justified because early failure is modeled as occurring independently for each WP and DS.

Waste Package EF Modeling Case—The Waste Package EF Modeling Case estimates the dose resulting from the occurrence of early failure of WPs. The aleatory uncertainties in this modeling case include:

- The number of WP early failures
- The type of each WP having early failure
- The location of each WP having early failure, described in terms of the seepage conditions at each location.

For each realization $\mathbf{e}_i$ of epistemically uncertain parameters, the expected dose $\bar{D}_W\left(\tau|\mathbf{e}_i\right)$ is calculated by

$$\bar{D}_{EW}\left(\tau|\mathbf{e}_i\right) = \sum_{r=1}^{2}\sum_{s=1}^{5}\sum_{t=0}^{1} pW_i\, fWT_r\, fBN_s\, pDRP_{rsti}\, nWP\, D_{EW}\left(\tau\left|[1,r,s,t],\mathbf{e}_i\right.\right) \quad \text{(Eq. 6.1.2-13)}$$

where

pW_i is the probability of a randomly chosen WP having early failure (element of $\mathbf{e}_i$)

fWT_r is the fraction of WPs in the repository of type r (co-disposed [CDSP WP] or transportation, aging, and disposal [TAD] canister)

$fDRP_{rsi}$ is the fraction of WPs of type r in percolation bin s (Section 6.3.2) that experience dripping conditions (function of elements of $\mathbf{e}_i$)

$$pDRP_{rsti} = \begin{cases} 1 - fDRP_{rsi} & \text{if } t = 0 \\ fDRP_{rsi} & \text{if } t = 1 \end{cases}$$

fBN_s is the fraction of WPs in the repository that are in percolation bin s

nWP is the number of WPs in the repository

$D_{EW}\left(\tau \middle| [1, r, s, t], \mathbf{e}_i\right)$ is the dose at time τ that results from early failure of one WP of type r in percolation bin s with dripping ($t = 1$) or non-dripping conditions ($t = 2$), and is calculated using the GoldSim component of the TSPA-LA Model.

For derivation of Equation 6.1.2.13, see Appendix J Section J.6.2.

Drip Shield EF Modeling Case—The Drip Shield EF Modeling Case estimates the dose resulting from the occurrence of early failure of DSs. The aleatory uncertainties in this modeling case include:

- The number of DS early failures
- The location of each DS early failure, described in terms of the seepage and conditions at each location
- The type of WP located beneath each DS early failure.

The calculation of expected annual dose for the Drip Shield EF Modeling Case is very similar to Equation 6.1.2-13 for expected annual dose for the Waste Package EF Modeling Case. For each realization $\mathbf{e}_i$ of epistemically uncertain parameters, the expected dose $\overline{D}_D(\tau|\mathbf{e}_i)$ is calculated by

$$\begin{aligned} \overline{D}_{ED}\left(\tau \middle| \mathbf{e}_i\right) &= \sum_{r=1}^{2} \sum_{s=1}^{5} \sum_{t=0}^{1} pD_i \, fWT_r \, fBN_{rs} \, pDRP_{rsti} \, nWP \, D_{ED}\left(\tau \middle| [1, r, s, t], \mathbf{e}_i\right) \\ &= \sum_{r=1}^{2} \sum_{s=1}^{5} pD_i \, fWT_r \, fBN_{rs} \, pDRP_{rs1i} \, nWP \, D_{ED}\left(\tau \middle| [1, r, s, 1], \mathbf{e}_i\right) \end{aligned} \quad \text{(Eq. 6.1.2-14)}$$

where

pD_i is the probability of a randomly chosen DS having early failure (element of $\mathbf{e}_i$)

fWT_r is the fraction of WPs in the repository of type r (CDSP or TAD canister)

nWP is the number of WPs in the repository

$fDRP_{rsi}$ is the fraction of WPs of type r in percolation bin s (Section 6.3.2) that experience dripping conditions (function of elements of $\mathbf{e}_i$)

fBN_{rs} fraction of WPs of type r in percolation bin s

$$pDRP_{rsti} = \begin{cases} 1 - fDRP_{rsi} & \text{if } t = 0 \\ fDRP_{rsi} & \text{if } t = 1 \end{cases}$$

$D_{ED}\left(\tau \middle| [1, r, s, t], \mathbf{e}_i\right)$ is the dose at time τ that results from early failure of one DS over a WP of type r in percolation bin s with dripping ($t = 1$) or non-dripping conditions ($t = 0$), and is calculated using the GoldSim component of the TSPA-LA Model.

The second line in equation 6.1.2-14 results because no WP failure is assumed to occur under an early failed DS unless dripping conditions are present. For derivation of Equation 6.1.2.14, see Appendix J Section J.6.3.

6.1.2.4.3 Igneous Scenario Class

The Igneous Scenario Class includes two modeling cases: the Igneous Intrusion Modeling Case, and the Volcanic Eruption Modeling Case. For the Igneous Scenario Class, expected annual dose at time τ is computed as:

$$\bar{D}_I\left(\tau \middle| \mathbf{e}_i\right) = \bar{D}_{II}\left(\tau \middle| \mathbf{e}_i\right) + \bar{D}_{IE}\left(\tau \middle| \mathbf{e}_i\right) \qquad \text{(Eq. 6.1.2-15)}$$

where $\bar{D}_{II}\left(\tau \middle| \mathbf{e}_i\right)$ is the expected annual dose from igneous intrusions, and $\bar{D}_{IE}\left(\tau \middle| \mathbf{e}_i\right)$ is the expected annual dose from eruptions. Although the occurrence of intrusions and eruptions is not independent, Equation 6.1.2-15 is justified because effects of an intrusion and an eruption are independent.

Igneous Intrusion Modeling Case—The Igneous Intrusion Modeling Case estimates the dose resulting from groundwater transport of radionuclides as a consequence of an igneous intrusion into the repository. The Volcanic Eruption Modeling Case estimates the dose that results from an eruption that occurs during an igneous event. The time of the igneous event is the single aleatory uncertainty in this modeling case. The TSPA-LA conservatively assumes that an igneous intrusion affects all WPs, and that maximum damage occurs to each WP; thus, the extent of damage is not treated as an aleatory uncertainty.

For each realization $\mathbf{e}_i$ of epistemically uncertain parameters, the expected annual dose $\bar{D}_{II}\left(\tau \middle| \mathbf{e}_i\right)$ at time τ is formally calculated by

$$\bar{D}_{II}\left(\tau \middle| \mathbf{e}_i\right) = \int_0^{\tau} D_{II}\left(\tau \middle| [1, t], \mathbf{e}_i\right) \lambda_I\left(\mathbf{e}_i\right) dt \qquad \text{(Eq. 6.1.2-16)}$$

where, $D_{II}\left(\tau \middle| [1, t], \mathbf{e}_i\right)$ is the dose conditional on one intrusion occurring at time t, and $\lambda_I\left(\mathbf{e}_i\right)$ is the frequency of igneous events for realization $\mathbf{e}_i$. Equation 6.1.2-16 accounts for the possibility of more than one igneous intrusion occurring in the future of the repository. Because the first intrusion damages the repository to the maximum extent, subsequent intrusions should not

contribute additional radionuclides to the expected annual dose. However, on average, only 2 percent of realizations include more than one intrusion, so the over-counting of dose is minor.

Nominal corrosion processes are included in the Igneous Intrusion Modeling Case for calculation of dose to 1,000,000 years. However, the calculation of $D_{II}(\tau|[1,t],\mathbf{e}_i)$ does not accumulate the dose from radionuclides released by corrosion processes prior to the intrusion. The dose from the radionuclides released prior to the intrusion is not included in $D_{II}(\tau|[1,t],\mathbf{e}_i)$ to avoid counting these radionuclides twice in the calculation of total annual dose by Equation 6.1.2-1. The dose from radionuclides released prior to the intrusion by corrosion processes is accounted for as part of the Seismic GM Modeling Case, as described in Section 6.1.2.4.3.

The integral in Equation 6.1.2-16 is approximated by employing a quadrature technique to integrate over time t

$$\bar{D}_{II}\left(\tau|\mathbf{e}_i\right) = \sum_{k=0}^{N-1} D_{II}\left(\tau|[1,t_k],\mathbf{e}_i\right)\lambda_I\left(\mathbf{e}_i\right)\Delta t_k \qquad \text{(Eq. 6.1.2-17)}$$

where

T is the time period of interest (10,000 or 1,000,000 years)

$[t_0,t_1,\ldots,t_N]$ is a sequence of times of igneous intrusions occurring in $[0,T]$, for which $D_{II}(\tau|[1,t],\mathbf{e}_i)$ has been computed using GoldSim results

$\Delta t_k = t_{k+1} - t_k$

For derivation of Equation 6.1.2-16 and Equation 6.1.2-17, see Appendix J Section J.7.2.

Volcanic Eruption Modeling Case—The Volcanic Eruption Modeling Case estimates the annual dose resulting from eruptions. The aleatory uncertainties in this modeling case include:

- Number of igneous eruptive events
- Time of each eruptive event
- Eruptive power, eruptive velocity, duration, wind speed, and wind direction for each eruptive event
- Number of WPs affected and fraction of WP content that is ejected into the atmosphere.

For each realization $\mathbf{e}_i$ of epistemically uncertain parameters, the expected annual dose $\overline{D}_{IE}(\tau|\mathbf{e}_i)$ at time τ is formally calculated by

$$\overline{D}_{IE}(\tau|\mathbf{e}_i) = pE\,\lambda_I(\mathbf{e}_i)\,\overline{N}_{IE}\,\overline{F}\int_{U_{IE}}\left[\int_0^{\tau} D_{IE}(\tau|[1,t,1,\mathbf{u}],\mathbf{e}_i)\,dt\right] d_U(\mathbf{u})\,dU \qquad \text{(Eq. 6.1.2-18)}$$

where

pE	is the probability that an igneous event includes one or more eruptive conduits that intercept waste
$\lambda_I(\mathbf{e}_i)$	is the frequency of igneous events for realization $\mathbf{e}_i$
$\overline{N}_{IE}$	is the mean number of WPs affected by an eruptive conduit
$\overline{F}$	is the mean fraction of WP content ejected into the atmosphere
U_{IE}	is the vector space of all values of eruptive power, eruptive velocity, duration, wind speed, and wind direction
$\mathbf{u}$	is a vector of values sampled from the distributions for eruptive power, eruptive velocity, duration, wind speed, and wind direction
$d_U(\mathbf{u})$	is the probability density function (pdf) on U_{IE} formed from the individual probability distributions for eruptive power, eruptive velocity, duration, wind speed, and wind direction
$D_{IE}(\tau\|[1,t,1,\mathbf{u}],\mathbf{e}_i)$	is the dose calculated by GoldSim conditional on one eruption occurring at time t, which affects one WP, with eruptive power, eruptive velocity, duration, wind speed, and wind direction described by $\mathbf{u}$.

The calculation of expected dose in Equation 6.1.2-18 accounts for the possibility that more than one igneous eruption occurs in the future evolution of the repository. The calculation conservatively assumes that each eruption event affects a different set of WPs, thus the consequence of two or more eruption events is the sum of the consequences of each individual event.

Due to the relatively large number of aleatory uncertainties in Equation 6.1.2-18, calculation of expected annual dose employs a Monte Carlo technique. A LHS of size nU is generated from U_{IE}, and the quantities $D_{IE}(\tau|[1,t,1,\mathbf{u}_l],\mathbf{e}_i)$ are computed using GoldSim. The expected dose is calculated using a quadrature technique to integrate over time t

$$\overline{D}_{IE}(\tau|\mathbf{e}_i) = pE\,\lambda_I(\mathbf{e}_i)\,\overline{N}_{IE}\,\overline{F}\sum_{k=0}^{N-1}\left[\sum_{l=1}^{nU} D_{IE}(\tau|[1,t_k,1,\mathbf{u}_l],\mathbf{e}_i)\Big/nU\right]\Delta t_k \qquad \text{(Eq. 6.1.2-19)}$$

where

$\mathbf{u}_l$	are the sampled vectors from U_{IE}
T	is the time period of interest (10,000 or 1,000,000 years)
$[t_0, t_2, \ldots, t_N]$	is a sequence of times of igneous eruptions occurring in $[0,T]$, for which $D_{IE}\left(\tau \middle\| [1,t,1,\mathbf{u}_l], \mathbf{e}_i\right)$ has been computed using GoldSim results

$\Delta t_k = t_{k+1} - t_k$

For derivation of Equation 6.1.2-18 and Equation 6.1.2-19, see Appendix J Section 7.3.

6.1.2.4.4 Seismic Scenario Class

The Seismic Scenario Class includes two modeling cases: the Seismic GM Modeling Case, and the Seismic FD Modeling Case. For the Seismic Scenario Class, expected annual dose at time τ for 10,000 years is computed as:

$$\bar{D}_S\left(\tau \middle| \mathbf{e}_i\right) = \bar{D}_{SG}\left(\tau \middle| \mathbf{e}_i\right) + \bar{D}_{SF}\left(\tau \middle| \mathbf{e}_i\right) \qquad \text{(Eq. 6.1.2-20)}$$

where $\bar{D}_{SG}\left(\tau \middle| \mathbf{e}_i\right)$ is the expected annual dose from seismic ground motion events, and $\bar{D}_{SF}\left(\tau \middle| \mathbf{e}_i\right)$ is the expected annual dose from seismic fault displacement events. Equation 6.1.2-20 is justified because the occurrence of ground motion and fault displacement events is modeled as independent.

For 1,000,000 years, the expected annual dose for the Nominal and the Seismic Scenario Classes are combined, and are computed as:

$$\bar{D}_N\left(\tau \middle| \mathbf{e}_i\right) + \bar{D}_S\left(\tau \middle| \mathbf{e}_i\right) = \bar{D}_{N+G}\left(\tau \middle| \mathbf{e}_i\right) + \bar{D}_{SF}\left(\tau \middle| \mathbf{e}_i\right) \qquad \text{(Eq. 6.1.2-21)}$$

where $\bar{D}_{N+G}\left(\tau \middle| \mathbf{e}_i\right)$ is the expected annual dose resulting from the combination of nominal processes and seismic ground motion events.

Seismic GM Modeling Case—The Seismic GM Modeling Case calculates annual dose from radionuclides released from the EBS due to damage to WPs resulting from vibratory ground motion. In addition, this modeling case accounts for damage to the DS due to vibratory ground motion, and the effects of this damage on radionuclide releases from WPs. The occurrence of seismic events is modeled as a Poisson process with the smallest events of consequence having an annual frequency of 4.287×10^{-4} yr^{-1}. During the first 10,000 years after closure, only a few seismic ground motion events will occur; however, during the 1,000,000-year peak dose period, the TSPA-LA must account for the effects of a sequence of a few hundred seismic events. In addition, because corrosion processes alter the response of the engineered barrier components to seismic events, corrosion processes are included in the Seismic GM Modeling Case calculation for 1,000,000 years, and the dose from radionuclides release due to corrosion processes is

calculated as part of the Seismic GM Modeling Case for 1,000,000 years. Due to these differences, different numerical techniques are used to calculate expected annual dose for 10,000 years and for 1,000,000 years.

The *Seismic Consequence Abstraction* (SNL 2007 [DIRS 176828]) outlines a probabilistic model for effects on the EBS due to seismic ground motion events. The abstraction provides different probability models for:

- the occurrence and extent of SCC damage to CDSP WP and TAD canister WPs
- the occurrence and extent of rupture of CDSP WP and TAD canister WPs
- the occurrence and extent of rockfall in the lithophysal and non-lithophysal zones
- the state of the DS and its supporting framework as a function of time.

The abstraction also accounts for the change in susceptibility of each EBS component to damage, and, if damage occurs, the change in the extent of damage, due to general corrosion taking place.

For 10,000 years, the consequences of seismic ground motion events can be approximated by examining only the occurrence of SCC damage to CDSP WPs with the DS intact and without rockfall, and without considering the effects of corrosion processes. Section 7.3.2 provides justification for the simplifications to the seismic consequences abstraction that lead to this approximation.

The aleatory uncertainties in the Seismic GM Modeling Case for 10,000 years include:

- the number of seismic events that cause SCC damage to CDSP WPs
- the time of each damaging seismic event
- the amount of damage caused by each seismic event.

For each realization $\mathbf{e}_i$ of epistemically uncertain parameters, the expected annual dose $\bar{D}_{SG}\left(\tau\left|\mathbf{e}_i\right.\right)$ at time τ for $\tau < 10{,}000\,\text{yr}$ is formally calculated by

$$\bar{D}_{SG}\left(\tau\left|\mathbf{e}_i\right.\right) = \int_0^{\tau}\left(\lambda_1\left(\mathbf{e}_i\right)e^{-\lambda_1(\mathbf{e}_i)t}\left(\int_{A_{\min}}^{A_{\max}} D_{SG}\left(\tau\left|\left[1,t,A\right],\mathbf{e}_i\right.\right)d_{A1}\left(A\left|\mathbf{e}_i\right.\right)dA\right)\right)dt + \int_0^{\tau}\left(\lambda_1\left(\mathbf{e}_i\right)e^{-\lambda_1(\mathbf{e}_i)t}\left(\int_t^{\tau}\int_{B_{\min}}^{B_{\max}} D_{SG}\left(\tau\left|\left[1,\tilde{t},B\right],\mathbf{e}_i\right.\right)d_{A2}\left(B\left|\mathbf{e}_i\right.\right)\lambda_2\left(\mathbf{e}_i\right)d\tilde{t}\right)\right)dt \quad \text{(Eq. 6.1.2-22)}$$

where

$\lambda_1\left(\mathbf{e}_i\right)$ is the frequency of seismic ground motion events that cause SCC damage to CDSP WPs with intact internals

$\lambda_2\left(\mathbf{e}_i\right)$ is the frequency of seismic ground motion events that cause SCC damage to CDSP WPs with degraded internals

$d_{A1}(A|\mathbf{e}_i)$ is the density function that describes the probability of damage area equal to A occurring on CDSP WPs with intact internals, given that a seismic event that causes damage occurs

$d_{A2}(B|\mathbf{e}_i)$ is the density function that describes the probability of damage area equal to B occurring on CDSP WPs with degraded internals, given that a seismic event that causes damage occurs

$D_{SG}(\tau|[1,t,A],\mathbf{e}_i)$ is the annual dose at time τ resulting from a seismic ground motion event occurring at time t that causes damaged area equal to A.

Two frequencies ($\lambda_1(\mathbf{e}_i)$ and $\lambda_2(\mathbf{e}_i)$) and density functions ($d_{A1}(A|\mathbf{e}_i)$ and $d_{A2}(B|\mathbf{e}_i)$) for damaged area are used in Equation 6.1.2-22 because *Seismic Consequence Abstraction* (SNL 2007 [DIRS 176828]) specifies different probability models for the occurrence and the extent of damage depending on whether the internals of the WP are intact or degraded. The TSPA-LA Model assumes that WP internals degrade rapidly after the first seismic event that damages the WP outer barrier. The calculation of expected annual dose in Equation 6.1.2-22 accounts for the possibility that more than one damaging event occurs in the future of the repository, using the conservative assumption that the annual dose from a sequence of events causing cumulative damage to WPs is reasonably approximated by the sum of the annual dose resulting from the individual events. This assumption of linearity in seismic consequences is justified in Section 7.3.2.

The integral in Equation 6.1.2-22 is approximated by employing quadrature techniques to integrate over time t and damaged areas A and B.

For derivation of Equation 6.1.2-22 and description of its numerical solution, see Appendix J Section J.8.3.

For 1,000,000 years, the full *Seismic Consequences Abstraction* (SNL 2007 [DIRS 176828]) is considered, including both the effects of corrosion processes on EBS components, and the dose resulting from corrosion processes. Because the corrosion processes are included with the Seismic GM Modeling Case for 1,000,000 years, the annual dose calculated by this modeling case is expressed as

$$D_{N+G}(\tau|\mathbf{a},\mathbf{e}) = D_N(\tau|\mathbf{a},\mathbf{e}) + D_{SG}(\tau|\mathbf{a},\mathbf{e}) \quad \text{(Eq. 6.1.2-23)}$$

where $D_N(\tau|\mathbf{a},\mathbf{e})$ represents the dose at time τ resulting from radionuclides released due to corrosion processes, and $D_{SG}(\tau|\mathbf{a},\mathbf{e})$ represents the dose at time τ resulting from radionuclides released due to seismic events. The aleatory uncertainties in corrosion processes is the same as described in the discussion of the Nominal Modeling Case, and is treated by means of the averaging operations described in Appendix N. The aleatory uncertainties in seismic events include:

- The number of seismic events
- The time of each seismic event
- The amount of rockfall in the lithophysal zone caused by each seismic event
- The effect of rockfall on the structure and function of DSs at the time of each seismic event
- The occurrence and extent of damage to each type of WP (CDSP WP and TAD) for each seismic event
- The occurrence and extent of rupture of the outer barrier for each type of WP (CDSP WP and TAD canister) for each seismic event.

Owing to the complexity of the abstraction and numerous seismic events that could occur in the future of the repository, a Monte Carlo technique is used to calculate expected annual dose. Denote by A_G the set of all sequences of seismic events that could occur in the future of the repository. A member $\mathbf{a} \in A_G$ is a vector, the elements of which describe the aleatory quantities listed above that define each seismic event. For each realization $\mathbf{e}_i$ of epistemically uncertain parameters, the expected annual dose $\bar{D}_{SG}\left(\tau \middle| \mathbf{e}_i\right)$ at time τ for $\tau \le 1{,}000{,}000$ yr is formally calculated by

$$\bar{D}_{N+G}\left(\tau \middle| \mathbf{e}_i\right) = \sum_{j=1}^{n} D_{N+G}\left(\tau \middle| \mathbf{a}_{ij}, \mathbf{e}_i\right) \Big/ n \qquad \text{(Eq. 6.1.2-24)}$$

where

$\mathbf{a}_{ij}, j = 1, \ldots, n$ is a random sample from A_G generated in consistency with the distributions that describe each of the elements of a member $\mathbf{a}$ of A_G,

$D_{N+G}\left(\tau \middle| \mathbf{a}_{ij}, \mathbf{e}_i\right)$ is the combined dose from seismic events and corrosion failures described by sample element $\mathbf{a}_{ij}$.

The quantity $\bar{D}_{N+G}\left(\tau \middle| \mathbf{e}_i\right)$ is calculated directly by the GoldSim component of the TSPA-LA Model; results of these calculations are used to compute total expected annual dose, as reported in Chapter 8. It is important to note that the quantities $D_N\left(\tau \middle| \mathbf{a}, \mathbf{e}\right)$ and $D_{SG}\left(\tau \middle| \mathbf{a}, \mathbf{e}\right)$ are not computed separately. The expected dose due to nominal corrosion processes, $\bar{D}_N\left(\tau \middle| \mathbf{e}_i\right)$, is computed separately for the purpose of model validation and analysis and is presented in Section 8.3. For 1,000,000 years, the expected dose due to seismic events only (excluding dose due to nominal corrosion processes) is not calculated separately.

The derivation of Equation 6.1.2-24 is discussed in Appendix J Section J.8.4. For a complete description of A_G and the distributions that describe the elements of a member $\mathbf{a}$, see Appendix J Section J.8.2.

Seismic FD Modeling Case—The Seismic FD Modeling Case calculates annual dose from radionuclides released from the EBS due to damage caused by fault displacements. The aleatory uncertainties in this modeling case include:

- Number of fault displacement events
- Time of each fault displacement event
- Number of WPs of each type (CDSP WP or TAD canister) damaged by each fault displacement event
- The location of each WP damaged by each fault displacement event, described in terms of the seepage conditions at each location
- Area opened in the outer barrier of each WP type by each fault displacement event.

The TSPA-LA Model conservatively assumes that each fault displacement event affects a different set of WPs that have not been damaged by prior fault displacement events. When a fault displacement event occurs, the DS above the affected WPs is assumed to be ruptured by the event.

The calculation of expected annual dose for fault displacements does not explicitly treat the aleatory uncertainty for the location of each affected WP. Instead, to save computational resources, expected annual dose is estimated by modeling 100 WPs of each type, placed proportionally into the percolation bins, and within each bin, into dripping or non-dripping locations. Results are calculated for the set of 100 WPs and then scaled to the expected number of packages affected by a fault displacement event.

For each realization $\mathbf{e}_i$ of epistemically uncertain parameters, the expected annual dose $\overline{D}_{FD}(\tau|\mathbf{e}_i)$ at time τ is calculated by

$$\overline{D}_{SF}\left(\tau|\mathbf{e}_i\right) = \sum_{r=1}^{2}\left[\overline{N}_r \lambda_{Fr}/100\right]\left[\int_0^{\tau}\left(\int_{A_{\min}}^{A_{\max}} D_{SFr}\left(\tau\left|[1,t,100,A_r],\mathbf{e}_i\right.\right) d_{Ar}\left(A_r\right) dA_r\right) dt\right] \quad \text{(Eq. 6.1.2-25)}$$

where

r indicates each type of WP (CDSP WP or TAD canister)

$\overline{N}_r$ is the expected number of WPs of type r damaged by one fault displacement event

λ_{Fr} is the frequency of fault displacement events that cause damage to WPs of type r

$D_{SFr}\left(\tau\left|[1,t,100,A_r],\mathbf{e}_i\right.\right)$ is the annual dose resulting from a fault displacement occurring at time t which damages 100 WPs of type r, causing an opening with an area equal to A_r on each WP

$d_{Ar}(A_r)$ is the density function describing the probability of a fault displacement creating an opening of area A_r on WPs of type r.

The quantity $D_{SFr}\left(\tau\left|[1,t,100,A_r,1],\mathbf{e}_i\right.\right)$ is calculated directly by the GoldSim component of the TSPA-LA Model. The integrals in Equation 6.1.2-25 are approximated using quadrature techniques similar to those employed in Equation 6.1.2-23. For derivation of Equation 6.1.2-25 and the quadrature techniques used in its evaluation, see Appendix J Section J.8.6.

6.1.2.5 Calculation of Expected Annual Dose for the Human Intrusion Modeling Case

The Human Intrusion Modeling Case estimates repository performance in the event that a drilling intrusion intersects the repository. Unlike the other modeling cases, the Human Intrusion Modeling Case is not a component of the calculation of total mean annual dose (Section 6.1.2.2). Rather, the results of the Human Intrusion Modeling Case are compared against the regulations specified in 10 CFR 63.321[DIRS 178394].

Calculation of expected annual dose for the Human Intrusion Modeling Case resembles the calculation in the other modeling cases. The aleatory uncertainty in this modeling case is the type of WP intersected and the location of the drilling intrusion. The time of the intrusion is fixed at 200,000 years (Section 6.7.2), and the Human Intrusion Scenario specifies a single drilling intrusion.

The Human Intrusion Scenario uses a Monte Carlo technique to calculate expected dose. For each realization $\mathbf{e}_i$ of epistemically uncertain parameters, the expected annual dose $\bar{D}_{HI}\left(\tau\left|\mathbf{e}_i\right.\right)$ at time τ is calculated by

$$\bar{D}_{HI}\left(\tau\left|\mathbf{e}_i\right.\right)=\sum_{j=1}^{nA} D_{HI}\left(\tau\left|\left[1,r_j,q_j,SR_j\right],\mathbf{e}_i\right.\right)\Big/nA \qquad \text{(Eq. 6.1.2-26)}$$

where

nA is the number of aleatory realizations

r_j is the type of WP (CDSP WP or TAD canister) intersected in the j^{th} aleatory realization

q_j is the percolation rate in the percolation bin selected in the j^{th} aleatory realization (Section 6.3.2)

SR_j is the SZ source region selected in the j^{th} aleatory realization (Section 6.3.9)

$D_{HI}\left(\tau\left|\left[1, r_j, q_j, SR_j\right], \mathbf{e}_i\right.\right)$ is the annual dose resulting at time τ from a human intrusion that intersects 1 WP of type r_j that experiences percolation rate q_j and intersects the SZ in source region SR_j.

The quantity $D_{HI}\left(\tau\left|\left[1, r_j, q_j, SR_j\right], \mathbf{e}_i\right.\right)$ is calculated directly by the GoldSim component of the TSPA-LA Model.

Table 6.1.2-1. Effect of Combinations of Scenario Classes on Total Mean Annual Dose

Preceding Event	Later Disruptive Event			
	Igneous Intrusion	**Volcanic Eruption**	**Seismic Ground Motion**	**Seismic Fault Displacement**
Early Failure Waste Package	Very minor (~0.02%) overcounting of inventory. Negligible effect on total mean annual dose.	Overcounting of inventory in WPs affected by the eruption event. Negligible effect on total mean annual dose.	Very minor (~0.02%) overcounting of inventory. Negligible effect on total mean annual dose.	Overcounting of inventory in WPs affected by the fault displacement event. Negligible effect on total mean annual dose.
Early Failure Drip Shield	Very minor (~0.01%) overcounting of inventory. Negligible effect on total mean annual dose.	Overcounting of inventory in WPs affected by the eruption event. Negligible effect on total mean annual dose.	Very minor (~0.01%) overcounting of inventory. Negligible effect on total mean annual dose.	Overcounting of inventory in WPs affected by the fault displacement event. Negligible effect on total mean annual dose.
Igneous Intrusion	Included in calculation of Mean Dose for the Igneous Scenario Class $\overline{\overline{D}}_I(\tau)$.	Conservative overstatement of the consequences of the igneous eruption event. Negligible effect on total mean annual dose.	Conservative overstatement of the consequences of the seismic ground motion event. Minor effect on total mean annual dose.	Conservative overstatement of the consequences of the seismic fault displacement event. Negligible effect on total mean annual dose.
Volcanic Eruption	Very minor (~0.03%) overcounting of inventory. Negligible effect on total mean annual dose.	Included in calculation of for the Igneous Scenario Class $\overline{\overline{D}}_I(\tau)$.	Very minor (~0.03%) overcounting of inventory. Negligible effect on total mean annual dose.	Very minor (~0.03%) overcounting of inventory in WPs affected by the fault displacement event. Negligible effect on total mean annual dose.
Seismic Ground Motion	Conservative overcounting of inventory and consequences of an intrusion. Minor effect on total mean annual dose.	Overcounting of inventory in WPs affected by the eruption event. Negligible effect on total mean annual dose.	Included in calculation of mean dose for the Seismic Scenario Class $\overline{\overline{D}}_S(\tau)$.	Overcounting of inventory in WPs affected by the fault displacement event. Negligible effect on total mean annual dose.
Seismic Fault Displacement	Very minor (~2 %) overcounting of inventory. Negligible effect on total mean annual dose.	Overcounting of inventory in WPs affected by the eruption event. Negligible effect on total mean annual dose.	Very minor (~2 %) overcounting of inventory. Negligible effect on total mean annual dose.	Included in calculation of mean dose for the Seismic Scenario Class $\overline{\overline{D}}_S(\tau)$.

INTENTIONALLY LEFT BLANK

6.1.3 Treatment of Uncertainty in the TSPA-LA Model

Sources of Uncertainty—Uncertainties are inherent in projections of the geologic and environmental conditions surrounding the Yucca Mountain repository into the future. Assessment of total system performance over this period must take these uncertainties into account. In addition, the discussion of the quantitative estimates of this performance (e.g., estimates of mean annual dose) will include information regarding the impacts of these uncertainties on those estimates (e.g., uncertainty in the estimate of mean annual dose).

The TSPA-LA Model accounts for uncertainty in two categories: aleatory uncertainty and epistemic uncertainty. Aleatory uncertainty arises from inherent uncertainty about the occurrence of future events that may affect the repository and the effect of these events on repository performance. Because aleatory uncertainty cannot be reduced by the acquisition of additional data or knowledge, this kind of uncertainty is also referred to as irreducible uncertainty. Examples of aleatory uncertainty considered in the TSPA-LA Model include the number and location of early failed WPs, time and amplitude of seismic ground motion events, and occurrence of igneous events. Aleatory uncertainties included in the TSPA-LA Model are listed in Table 6.1.3-1.

The second category is referred to here as epistemic uncertainty. Epistemic uncertainty stems from a lack of knowledge about a quantity that is believed to have a fixed (or deterministic) value. Sources of epistemic uncertainties include incomplete data, measurement errors, and estimates based upon expert judgment. Unlike aleatory uncertainty, epistemic uncertainty is potentially reducible with additional data and knowledge. In the TSPA-LA Model, epistemic quantities are generally inputs to specific submodels, with the submodels having been developed to use single values for these quantities. A particular epistemic quantity can be a parameter for a probability distribution or density function (e.g., adsorption coefficients for transport of radionuclides in the UZ), a field of values selected from alternative sets (e.g., the flow field in the UZ), or a factor added to a parameter to represent the uncertainty (e.g., the uncertainty term added to the model for actinide solubilities). Examples of epistemic uncertainties included in the TSPA-LA Model are indicated in Table 6.1.3-2.

During development of the TSPA-LA Model, a number of technical reviews were conducted to ensure consistent and appropriate treatment of uncertainty and variability for parameters identified as key uncertain inputs to the model (Section 7.5). These technical reviews focused on: (1) confirming that the major sources of uncertainty and/or variability were appropriately represented, (2) verifying that probability distributions were derived using sound statistical methods and interpretations, and (3) ensuring model parameter representations (i.e., probability distributions) are reasonable and defensible, as opposed to depicting extreme variations that could potentially introduce risk dilution (i.e., wider distribution and lower peak mean annual dose).

Probabilistic Framework for Implementing the TSPA-LA Model—Both aleatory and epistemic uncertainties are quantified using probability distributions. However, in the TSPA-LA Model, the numerical treatment of the two categories of uncertainty is different. Because the aleatory uncertainties vary between modeling cases, treatment of aleatory uncertainties also

varies among modeling cases. The subsections of Section 6.1.2 describe the treatment of aleatory uncertainty for each modeling case of the TSPA-LA Model.

In general, epistemic uncertainties are addressed by means of a Monte Carlo technique employing an LHS of the epistemically uncertain quantities. The same LHS is used in each of the modeling cases. This method allows a thorough mapping of the uncertainty in model inputs (parameters) to the corresponding uncertainty in model output (estimates of performance) and also allows results from each modeling case to be combined into an estimate of total mean annual dose. Uncertainty in the model outcome is quantified via multiple model realizations, using LHS to select values for uncertain parameters. The benefits of probabilistic modeling include: (1) obtaining a representative range of possible outcomes (and the likelihood of each outcome) to quantify predictive uncertainty, and (2) analyzing the relationship between the uncertain inputs and uncertain outputs to provide insight into the effect of the uncertainties.

Propagation of Uncertainty—The Monte Carlo analysis for the TSPA-LA Model involves the following four steps (see Appendix J for more detail of each step):

- **Select Imprecisely Known Input Parameters to be Sampled**—The TSPA-LA Model includes several thousand parameters, several hundred of which are treated as uncertain. The magnitude of uncertainty, type of probability distribution used to characterize the uncertainty, and guidance on sampling values for the parameters are developed in the individual process models or abstractions or both, as documented in their respective model reports.

- **Construct Probability Distribution Functions for Each Parameter**—The probabilistic framework employed in Monte Carlo simulations requires that the uncertainty in the TSPA-LA Model inputs be quantified using probability distributions. Examples of such representations can be found in the descriptions of various TSPA-LA submodels in Section 6.3. These distributions are specified in terms of either empirical distribution functions or coefficients of parametric distributions.

- **Generate a Sample Set by Selecting a Parameter Value from Each Distribution**—The next step in the Monte Carlo process requires the generation of a number of parameter distributions that are sampled in the course of an analysis. The TSPA-LA Model uses LHS, where the range of each parameter is divided into intervals of equal probability, and a value is selected at random within each interval. LHS helps achieve a more complete coverage of the range of values of an uncertain parameter than unstratified sampling.

- **Calculate Outcomes for the Sample Set and Aggregate Results for All Samples**—In this step of the Monte Carlo methodology, the modeling case for the scenario class of interest is evaluated for each of the randomly generated parameter sets. This is an operation consisting of multiple model realizations where the outcome (i.e., annual dose as a function of time) is computed for each sampled parameter set. The aggregation of all results produces distributions of system performance measures for the modeling case. After all of the required model realizations have been completed, the overall uncertainty

in the model outcome can be characterized by probability distributions of the system performance measures.

Correlation Methods—The TSPA-LA Model employs several techniques to account for correlations between uncertain input parameters. In some cases, correlations among variables are addressed in the development of the process models and implicitly accounted for in the TSPA-LA Model abstractions. In other cases, correlations among variables are explicitly addressed within the TSPA-LA Model. The GoldSim software provides functionality for correlating pairs of variables when the correlation between each pair is 100 percent. Because GoldSim's stochastic functions only allow correlation between a single pair, Cholesky factorization (Press et al. 1992 [DIRS 103316], Section 2.9) is used to induce the desired rank correlation in sets of three or more random variables while maintaining their marginal distributions. This method is applied to normally distributed variables by using a linear combination of independent normal variables to produce a multivariate normal vector with the correct correlation structure (Iman and Conover 1982 [DIRS 124158], pp. 313 to 320; Anderson 1984 [DIRS 169668], Section 2.4). The random vector is created using a linear combination of independent standard normal random variables. Multiplying this random vector by the lower triangular matrix resulting from the Cholesky factorization of the covariance matrix, results in a vector from a multivariate-normal distribution with mean vector zero and honors the covariance matrix. By extending this method to nonnormal distributions, the marginal distributions are used in a way such that the rank correlation structure is preserved in the transform.

INTENTIONALLY LEFT BLANK

Table 6.1.3-1. Aleatory Uncertainties in the TSPA-LA Model

Scenario Class	Aleatory Uncertainties
Nominal (Section 6.3)	Time and location of general corrosion failures for each type of waste package
Early Failure (Section 6.4)	Number of early failed waste packages
	Type and location of each early failed waste package
	Number of early failed drip shields
	Type of waste package under each early failed drip shield
	Location of each early failed drip shield
Igneous (Section 6.5)	Number of igneous events
	Time of each igneous event
	Number of waste packages affected by eruption
	Eruptive power, height, and duration of each eruption
	Wind speed and wind direction during eruption
Seismic (Section 6.6)	Number of seismic events
	Type of each seismic event: ground motion or fault displacement
	Time of each seismic event
	Peak ground velocity of each ground motion seismic event
	Occurrence and extent of damage to each type of waste package caused by ground motion
	Occurrence and extent of rupture or puncture of each type of waste package caused by ground motion
	Volume of rockfall caused by ground motion for lithophysal and non-lithophysal zones
	Occurrence of failure of drip shield framework caused by ground motion and accumulated rockfall
	Occurrence of failure of drip shield plates caused by ground motion and accumulated rockfall
	Number of waste packages of each type affected by fault displacement
	Failed area on each type of waste package caused by fault displacement

Table 6.1.3-2. Examples of Epistemic Uncertainties in the TSPA-LA Model

Model Component	Epistemic Uncertainties
Unsaturated Zone Flow	Infiltration Submodel (Section 6.3.1): • Infiltration scenario Unsaturated Zone Flow Fields Abstraction (Section 6.3.1): • Hydrologic properties • Ratio of porosity to fracture aperture Drift Seepage Submodel (Section 6.3.3.1): • Permeability and capillary strength parameters • Factor accounting for local heterogeneity in flow-focusing and permeability Drift Wall Condensation Submodel (Section 6.3.3.2): • Correlation parameters for abstraction for fraction of waste package locations with dripping condensation and condensation water flow rate
EBS Environment	EBS Thermal-Hydrologic Environment (Section 6.3.2): • Thermal conductivity of surrounding rock EBS Chemical Environment Submodel (Section 6.3.4): • Ambient waste composition • pCO_2, ionic strength, and pH of in-drift seepage water • Water-rock interaction for seepage water
Waste Package and Drip Shield Degradation	Waste Package and Drip Shield Degradation Submodel (Section 6.3.5.1): • Corrosion rates of Alloy 22 and drip shield components • Temperature and relative humidity at drip shield and waste package • pH, NO_3^-, and Cl^- of crown seepage
Waste Form Degradation and Mobilization	Waste Form Degradation and Mobilization (Section 6.3.7): • Radionuclide inventory for CSNF, DSNF, and HLW • Temperature and relative humidity at waste package • pCO_2, ionic strength, and pH in waste package • Waste form degradation rates • Radionuclide solubility • Colloid concentrations • Mass of Pu and Am embedded in waste form colloids from HLW glass • Forward rate constant for kinetic sorption of radionuclides onto iron oxyhydroxide surfaces • Coefficient for sorption onto colloids for each radionuclide

Table 6.1.3-2. Examples of Epistemic Uncertainties in the TSPA-LA Model (Continued)

Model Component	Epistemic Uncertainties
EBS Flow and Transport	EBS Flow Submodel (Section 6.3.6): • Drip shield and waste package flux splitting factors • Representative subregion typical liquid saturation in invert • Representative subregion typical imbibition flux in invert • Representative subregion typical liquid saturation and flux through the EBS-UZ interface EBS Transport Submodel (Section 6.3.8): • Steel corrosion rates • Specific surface area of steel corrosion products • Adsorption isotherm for water vapor sorption onto degraded waste form and onto steel corrosion products • Density of radionuclide sorption sites in steel corrosion products
Unsaturated Zone Transport	Unsaturated Zone Transport Submodel (Section 6.3.9): • • Fracture aperture • Active Fracture Model gamma parameter • Tortuosity • Rock Matrix K_ds for each radionuclide • Coefficient for sorption onto colloids for each radionuclide • Colloid retardation factors
Saturated Zone Flow and Transport	Saturated Zone Flow and Transport Submodel (Section 6.3.10): • Groundwater specific discharge multiplier • Flowing interval spacing in volcanic units • Colloid retardation in alluvium
Biosphere	Biosphere Submodel (Section 6.3.11): • Biosphere dose conversion factors for groundwater modeling cases • Inhalation biosphere dose conversion factors for Volcanic Eruption Modeling Case
Events	DS Early Failure Submodel (Section 6.4.1): • Probability of early failure for a single drip shield WP Early Failure Submodel (Section 6.4.2) • Probability of early failure for a single waste package Igneous Activity, Igneous Intrusion Submodel (Section 6.5.1): • Igneous event probability (event frequency) Igneous Activity, Volcanic Eruption Submodel (Section 6.5.2): • Igneous event probability (event frequency) • Ash and waste particle size • Radionuclide diffusivity in soils Seismic Activity, GM Damage Submodel (Section 6.6.1.1): • Residual stress threshold for Alloy 22

NOTE: Additional information concerning uncertainty and the distribution of TSPA-LA Model parameters and parameter values can be found in the GoldSim model file.

INTENTIONALLY LEFT BLANK

6.1.4 TSPA-LA Model Structure and Design

This section provides an overview of how model components and submodels are connected within the TSPA-LA Model and how information flows between them. The primary focus of this section is on the description of the TSPA-LA Model for the Nominal Scenario Class. The Nominal Scenario Class reflects the initial starting conditions expected for the proposed repository system and therefore is a natural starting point for presenting the model structure and design. A summary of the TSPA-LA Model structure and information flow for the Early Failure, Igneous, and Seismic Scenario Classes and the Human Intrusion Scenario is presented following the Nominal Scenario Class description.

For all scenario classes, the separation of aleatory and epistemic uncertainty with respect to parameter values was maintained as described in Section 6.1.3. The structure of the model components and submodel reflect this requirement. Connections between the model components and submodels are presented, as well as inputs differentiated between aleatory and epistemic when applicable.

The TSPA-LA Model components and submodels for the following process areas are briefly discussed here and in more detail in Section 6.3:

- Mountain-Scale UZ Flow
- EBS Thermal-Hydrologic (TH) Environment
- Drift-Scale UZ Flow
- EBS Chemical Environment
- WP and DS Degradation
- EBS Flow
- Waste Form Degradation and Mobilization
- EBS Transport
- UZ Transport
- SZ Flow and Transport
- Biosphere.

This list corresponds to model components and submodels previously presented on Figure 6-1 and in Table 6-1. This list is a combination of model components and submodels that represent the order in which these TSPA-LA Model components are discussed in Section 6.3. The intent here is to list the models in the order that information flows within the TSPA-LA Model. Therefore, it is necessary to list the submodels of the EBS Environment and EBS Flow and Transport Model Components separately. For example, as will be described in the next section, the EBS Flow Submodel provides the Waste Form Degradation and Mobilization Model Component with the flow rate of water through a failed WP as a function of time. This information is used by the Waste Form Degradation and Mobilization Model Component to calculate waste form degradation and radionuclide concentrations in WPs. This information in turn is used as input to the EBS Radionuclide Transport Submodel that calculates radionuclide transport through the WP and EBS. Thus, following the flow of information in Section 6.3 requires an expansion of the eight principal model components (and their respective submodels) compared to what is displayed on Figure 6-1. Table 6-1 maps the outline of Section 6.3 to the

eight principal model components depicted on Figure 6-1. The general philosophy used in this document is that the TSPA-LA Model is composed of eight principal model component areas (UZ, SZ, Biosphere, etc.) that represent a part of the natural system or EBS. Each model component area is composed of one or more submodels. A submodel can be either a detailed process model developed, tested, and validated in a supporting document, a simple or detailed abstraction of the process model, an abstraction of the process model results, or direct process model input (e.g., a look-up table or distribution of values). These process models and/or abstractions are defined within the supporting documents. They are developed for use within the TSPA-LA Model to represent the EBS or a natural system process.

Figure 6.1.4-1 schematically depicts the flow of information between the TSPA-LA Model components and submodels for the Nominal Scenario Class. A more detailed representation of information flow within the TSPA-LA Model can be found in Appendix G. TSPA-LA Model components implemented outside of the GoldSim model file are shown outside of the dashed border on Figure 6.1.4-1. The abstraction information provided by external models is input to the TSPA-LA Model GoldSim model file. Information transferred via internally generated outputs that are used as downstream inputs between model components and submodels within the TSPA-LA Model GoldSim model file are shown within the dashed border on Figure 6.1.4-1. The primary output from each submodel and abstraction is denoted by a numerical index and described in the following sections.

6.1.4.1 Mountain-Scale Unsaturated Zone Flow

Mountain-scale UZ flow in the TSPA-LA Model refers to the percolation of groundwater through the unsaturated rocks between the land surface and the water table and includes the future climates, infiltration changes, and site-scale UZ flow. The conceptual model and TSPA-LA Model implementation for these three processes are discussed in detail in Section 6.3.1 and are briefly described in this section. As given in *Future Climate Analysis* (BSC 2004 [DIRS 170002], Table 6-1) and appended by governing regulations, four climates are used in the TSPA-LA Model: (1) present-day climate for the first 550 years after repository closure; 600 years after emplacement, (2) monsoon climate for the period 550 to 1,950 years after repository closure, (3) glacial-transition climate for the period 1,950 to 10,000 years after repository closure, and (4) post-10,000-year climate for the period 10,000 to the modeling time frame of 1,000,000 years after repository closure (Section 1, Governing Regulations). For the present-day, monsoon, and glacial transition climates, a distribution of net infiltration is estimated by the Infiltration Model (SNL 2007 [DIRS 182145]). From this distribution, four infiltration scenarios are selected and provided to the Site-Scale UZ Flow Process Model as the upper boundary condition. These infiltration scenarios correspond to the 10th, 30th, 50th and 90th percentiles of the distribution of spatially-averaged infiltration. For the post-10,000-year period, proposed 10 CFR 63.342(c)(2) [DIRS 178394] specifies that the average percolation flux through the repository follows a log-uniform probability distribution from 13 to 64 mm/yr. Four infiltration rates representing the 31st percentile, 70th percentile, 86th percentile, and 97th percentile values of the distribution are used as target values for the four post-10,000-year period flow fields. The 12 infiltration maps generated for the present-day, monsoon, and glacial transition climates are used as a basis for the spatial variability for the post-10,000-year climate (SNL 2007 [DIRS 184614], Section 6.1.4). For the 12 infiltration maps, the average infiltration through the repository footprint was calculated. The four infiltration maps with average infiltration rates that most closely matched

the chosen average target infiltration rates were used as a basis for generating the flow-fields. The closest infiltration rate maps for the post-10,000-year climate determined by the analysis were the present-day 90th percentile, the 50th percentile glacial transition, the 90th percentile glacial transition, and the 90th percentile monsoon maps. The four infiltration maps were then scaled so that the average infiltration through the repository footprint would match the target values. The Site-Scale UZ Flow Process Model simulates three-dimensional, dual-permeability, steady-state flow conditions, and generates a total of 16 three-dimensional flow fields: 1) four flow fields for each of the 10th percentile, 30th percentile, 50th percentile, and 90th percentile infiltration boundary-condition scenarios, corresponding to the present-day, monsoon, and glacial transition climates within each infiltration scenario, and 2) four flow fields based on the scaled versions of the present-day 90th percentile, the 50th percentile glacial transition, the 90th percentile glacial transition, and the 90th percentile monsoon maps, corresponding to the post-10,000-year period.

Four UZ hydrologic property sets and 16 flow fields generated by the Site-Scale UZ Flow Process Model are used by the Multiscale Thermohydrologic Process Model (MSTHM) (SNL 2007 [DIRS 181383]) for the development of EBS environment TH conditions and are accessed directly by the UZ Transport Submodel (SNL 2008 [DIRS 184748], Sections 6 and 8). In both internal and external applications using the flow fields, the four different infiltration scenarios represent epistemic uncertainty in UZ flow conditions. These scenarios are sampled in the TSPA-LA Model once per realization based on the probability-weighting factors, excluding the contingency area, of 0.62, 0.16, 0.16, and 0.06 for the 10th percentile, 30th percentile, 50th percentile, and 90th percentile infiltration scenarios, respectively. An infiltration index corresponding to the sampled infiltration scenario is applied in the TSPA-LA Model to correlate the sampled infiltration scenario to downstream submodels that are infiltration dependent. The weighting factors are derived from *UZ Flow Models and Submodels* (SNL 2007 [DIRS 184614], Table 6.8-1). Climate change is implemented within the TSPA-LA Model UZ calculations by assuming a series of step changes in boundary conditions for UZ flow and utilizing the flow field corresponding to the selected infiltration scenario and climate. This implementation is based on the assumption that changes in flow fields due to climate apply instantaneously in the MSTHM Process Model and UZ Transport Model Component (see assumption in Section 5.1.1).

Figure 6.1.4-1 shows that 16 flow fields and UZ hydrologic properties generated by the Site-Scale UZ Flow Process Model are also used by the MSTHM Process Model. These flow fields are used to specify the percolation flux, consisting of liquid flux in fracture and matrix continua at the base of the PTn above the repository horizon, as a boundary condition. In addition, these data are used within the TSPA-LA Model for the simulation of the transport of radionuclides in the UZ Transport Submodel, as shown on Figure 6.1.4-1. The description for Output #1, discussed below, pertains to arrow #1 on Figure 6.1.4-1.

Output 1—For each infiltration scenario and climate (Section 6.3.1), the following are outputs from the Site-Scale UZ Flow Process Model (SNL 2007 [DIRS 184614], Section 6.6.3).

The following outputs are passed to the MSTHM Process Model (Section 6.3.2):

- The three-dimensional numerical grid
- The percolation flux at the base of PTn unit above each subdomain location for each infiltration condition and climate period
- UZ hydrologic properties including matrix and fracture properties, such as material type, permeability, porosity, and residual saturation, for the different infiltration property sets, and temperature and gas phase pressures at the lower and/or upper boundary.

The following outputs are passed to the UZ Transport Model Component (Section 6.3.9) of the TSPA-LA Model:

- The three-dimensional numerical grid representing the model domain
- UZ hydrologic properties for each of the four infiltration scenarios (Section 6.3.1) including:
  - The active fracture parameter for each computational cell in the numerical grid
  - Three three-dimensional steady-state flow fields including:
    - Fracture continuum liquid flux
    - Matrix continuum liquid flux
    - Water table levels
    - Fracture continuum liquid saturation
    - Matrix continuum liquid saturation
    - Liquid flux between matrix and fracture continua.

6.1.4.2 Engineered Barrier System Thermal-Hydrologic Environment

The EBS TH Environment Submodel implements the MSTHM Abstraction in the TSPA-LA Model. The MSTHM Abstraction is provided by the MSTHM Process Model, as shown on Figure 6.1.4-1. The MSTHM Abstraction is described in detail in *Multiscale Thermohydrologic Model* (SNL 2007 [DIRS 181383], Section 6.2[a] and Appendix III[a]). The conceptual model and TSPA-LA Model implementation for the EBS TH environment are discussed in detail in Section 6.3.2. The following paragraphs summarize its application for the development of the EBS TH Abstraction and how this abstraction is used in the TSPA-LA Model.

The MSTHM Process Model subdivides the repository footprint into 3,264 equal-area subdomains. Each of the 3,264 MSTHM Process Model subdomains is equally sized in area, 81 m in width by 20 m in length, where the length component is along the waste emplaced drift axis (SNL 2007 [DIRS 181383], Section 6.2.12.1[a]). The MSTHM Process Model performs simulations for the four percolation flux cases and three host-rock thermal conductivity cases (low, mean and high). The four percolation flux cases result from the application of four different infiltration scenarios, termed 10^{th}-, 30^{th}-, 50^{th}-, and 90^{th}-percentile

infiltration scenarios, in the TSPA-LA Model. For the possible combinations of percolation flux case and thermal conductivity case, the MSTHM Process Model calculates time-dependent TH variables, temperature, and relative humidity, for six representative commercial spent nuclear fuel (CSNF) WPs and two representative CDSP WPs, and DS pairs at each subdomain location. In addition, the MSTHM Process Model calculates time-dependent values for average drift-wall temperature, duration of boiling at the drift wall, invert temperature, invert saturation, and invert liquid flux at each of the 3,264 subdomain locations. Before any information is passed to downstream submodels, three sets of analyses are performed. First, the 10th percentile infiltration scenario, glacial-transition values of percolation flux at the base of the PTn at each of the 3,264 MSTHM Process Model subdomain locations are used to group each of the locations into one of five repository percolation subregion quantile ranges of 0.0 to 0.05, 0.05 to 0.3, 0.3 to 0.7, 0.7 to 0.95, and 0.95 to 1.0 (SNL 2007 [DIRS 181383], Section 6.2.12.1[a]). The five repository percolation subregions are shown on Figure 6.1.4-2. In the second analysis, the MSTHM Process Model subdomain locations and associated TH information are designated as belonging to repository percolation subregions one through five, respectively. The third analysis involves determining a single representative CSNF WP and a single representative CDSP WP for each percolation subregion. Representative WPs are selected for each percolation subregion for the purposes of reducing the computational burden of the TSPA-LA Model calculations and adequately representing the spatial variability in repository conditions that control radionuclide release from the repository (Section 7.3.3). The determination of the repository subregions and the selection of the representative WPs are described in Section 6.3.2. The grouping of the repository percolation subregions and the number of subdomain locations in each percolation subregion are summarized in Table 6.1.4-1.

The MSTHM Abstraction produces two sets of outputs that are indexed by fuel type and percolation subregion. Each set contains output for each combination of four infiltration scenarios and three host-rock thermal conductivity conditions. One set contains the comprehensive MSTHM Process Model output (e.g., DS and WP temperature and relative humidity, drift-wall temperature, percolation flux, and fraction of lithophysal unit) at each subdomain location in each percolation subregion for each fuel type. The WP and DS Degradation Model Component and the Drift Seepage Submodel use this information to account for spatial variability in the WP groups. The other set only contains the DS and WP temperature and relative humidity; the drift-wall temperature; and the invert temperature, relative humidity, liquid flux, and saturation for the representative CSNF WP and CDSP WP in each percolation subregion. The data in these two sets are compiled in text files that give parameter values at discrete timesteps. The representative WP data in the text files are read into look-up tables at run time to provide time-dependent parameter values to other submodels within the TSPA-LA Model. The data in representative WP file set are accessed by the EBS TH Environment Submodel to provide representative TH responses for each subregion. These TH responses serve as input to the Drift Wall Condensation Submodel, the EBS Chemical Environment Submodel, the EBS Flow Submodel, the Waste Form Degradation and Mobilization Model Component, and the EBS Transport Submodel. For ease of presentation, the WP and DS Degradation Model Component and the Waste Form Degradation and Mobilization Model Component are shown on Figure 6.1.4-1 rather than the individual submodels that comprise these model components (Sections 6.3.5 and 6.3.7, respectively).

The MSTHM Process Model accounts for the impact of percolation-flux and host-rock thermal conductivity uncertainty on the TH environment conditions, using simulations conducted for the 10th, 30th, 50th, and 90th percentiles of percolation flux with the mean host-rock thermal conductivity values for the host-rock units. Three additional cases are used in conjunction with the four mean host-rock thermal conductivity cases to capture the impact of host-rock thermal conductivity uncertainty: 10th percentile percolation flux with low- and high-thermal conductivity, and 90th percentile percolation flux with high-thermal conductivity. The TH data sets associated with the remaining five of the 12 possible combinations of percolation flux and host-rock thermal conductivity are provided to the TSPA-LA Model as surrogates from the previously identified seven cases. These five cases use their associated values of percolation flux, but refer to one of the other seven cases for the TH data (SNL 2007 [DIRS 181383], Section 6.3.15[a]). Within each realization of the TSPA-LA Model, the infiltration scenario and host-rock thermal conductivity condition are sampled. There are four choices for the infiltration scenario, resulting from the application of four infiltration fields. There are three host-rock thermal conductivity conditions, low, mean and high. These two distributions represent epistemic uncertainty and are sampled once per realization. The resulting values for these two parameters determine which of the 12 TH data sets are applied in downstream calculations of the TSPA-LA Model.

Output 2—The following outputs are passed from the MSTHM Process Model through the MSTHM Abstraction to the EBS TH Environment Submodel (Section 6.3.2):

- Definition of the five repository percolation subregions
- Percolation flux at the base of the PTn
- In-drift TH environment (e.g., DS and WP temperature and relative humidity, drift-wall temperature for each fuel type, CSNF, and CDSP WP).

Output 3—The following outputs are passed from the EBS TH Environment Submodel (Section 6.3.2) to the Drift Seepage and Drift Wall Condensation Submodel (Section 6.3.3):

- For each of the five percolation subregions (Section 6.3.2):
  - The percolation flux at the base of the PTn for each infiltration scenario and climate at each MSTHM subdomain location (Drift Seepage Submodel)
  - The average percolation flux at the base of the PTn for each infiltration scenario and climate (Drift Wall Condensation Submodel)
  - The drift-wall temperature surrounding each of the eight WPs (two CDSP WPs and six CSNF WPs) at each subdomain location (Drift Seepage Submodel)
  - Time-dependent temperature for the drift wall for the representative CDSP WP and the representative CSNF WP (Drift Wall Condensation Submodel)
  - The fraction of lithophysal unit at each location.

Output 4—The following outputs are passed from the EBS TH Environment Submodel (Section 6.3.2) to the WP and DS Degradation Model Components (Section 6.3.5), which then calculates WP and DS failures, including localized corrosion WP failures:

- For each of the five percolation subregions:
  - Time-dependent WP surface temperature on each of the eight WPs (two CDSP WPs and six CSNF WPs) at each subdomain location
  - Time-dependent WP surface relative humidity on each of the eight WPs (two CDSP WPs and six CSNF WPs) at each subdomain location.

Output 5—The following outputs are passed from the EBS TH Environment Submodel (Section 6.3.2) to the EBS Chemical Environment Submodel (Section 6.3.4):

- For each of the five percolation subregions (Section 6.3.2):
  - Time-dependent temperature for the invert for the representative CDSP WP and the representative CSNF WP
  - Time-dependent relative humidity for the invert for the representative CDSP WP and the representative CSNF WP
  - Time-dependent temperature for the drift wall for the representative CDSP WP and the representative CSNF WP
  - Averaged glacial-transition percolation rate for each infiltration scenario for each percolation subregion.
- For the Localized Corrosion Initiation Analysis (Section 6.3.4.3.2):
  - Time-dependent WP surface temperature on each of the eight WPs (two CDSP WPs and six CSNF WPs) at each subdomain location in each percolation subregion
  - Time-dependent WP surface relative humidity on each of the eight WPs (two CDSP WPs and six CSNF WPs) at each subdomain location in each percolation subregion.

Output 6—The following outputs are passed from the EBS TH Environment Submodel (Section 6.3.2) to the EBS Flow Submodel (Section 6.3.6):

- For each of the five percolation subregions (Section 6.3.2):
  - Time-dependent WP surface temperature for the representative CDSP WP and the representative CSNF WP
  - Time-dependent temperature in the invert for the representative CDSP WP and the representative CSNF WP

– Time-dependent liquid flux for the representative CDSP WP and the representative CSNF WP.

Output 7—The following outputs are passed from the EBS TH Environment Submodel (Section 6.3.2) to the Waste Form Degradation and Mobilization Model Component (Section 6.3.7):

- For each of the five percolation subregions (Section 6.3.2):
  - Time-dependent WP surface temperature for the representative CDSP WP and the representative CSNF WP
  - Time-dependent WP surface relative humidity for the representative CDSP WP and the representative CSNF WP.

Output 8—The following outputs are passed from the EBS TH Environment Submodel (Section 6.3.2) to the EBS Transport Submodel (Section 6.3.8):

- For each of the five percolation subregions (see Section 6.3.2):
  - Time-dependent WP surface temperature for the representative CDSP WP and the representative CSNF WP
  - Time-dependent WP surface relative humidity for the representative CDSP WP and the representative CSNF WP
  - Time-dependent temperature in the invert for the representative CDSP WP and the representative CSNF WP
  - Time-dependent saturation in the invert for the representative CDSP WP and the representative CSNF WP.

The TH conditions for each representative WP are identical for dripping and non-dripping environments.

6.1.4.3 Drift Seepage and Drift Wall Condensation

This section describes the implementation of the Drift Seepage and Drift Wall Condensation Submodels. The simulated drift-seepage flux is calculated within the TSPA-LA Model for both ambient and waste-heat-generated thermal periods using responses surfaces abstracted over a heterogeneous fracture-permeability field for a range of representative percolation flux rates, and for ranges of fracture permeability log(k) and fracture capillary-strength parameter (1/α) values (SNL 2007 [DIRS 181244]). The conceptual model and TSPA-LA Model implementation for drift seepage are discussed in detail in Section 6.3.3.1. The drift-seepage analysis performed external to the TSPA-LA Model provides two response surfaces: (1) mean seepage flux into the drift as a function of long-term percolation flux, k, and 1/α, and (2) the standard deviation (SD) of seepage flux into the drift as a function of long-term percolation flux, log(k), and 1/α. Figure 6.1.4-1 shows that drift-scale seepage is modeled externally in the Seepage Process

Model (BSC 2004 [DIRS 167652]). For the TSPA-LA Model, the results are then abstracted as described in *Abstraction of Drift Seepage* (SNL 2007 [DIRS 181244]), and imported into the TSPA-LA Model before performing the PA simulations.

Abstraction of Drift Seepage (SNL 2007 [DIRS 181244], Section 6.7.1.1) also provides spatial variability distributions for both k and 1/α and the flow focusing factor (f_{ff}) for the percolation flux, as well as uncertainty (epistemic) distributions for Δlog(k) and Δ1/α. The TSPA-LA Model samples these uncertainty distributions once per realization to account for parameter uncertainty in both k and 1/α. Using values of percolation flux at the base of the PTn, provided by the MSTHM Abstraction, seepage rates are calculated for each of the 3,264 MSTHM Process Model's subdomain locations. The spatial variability distributions are evaluated for log(k), 1/α, and f_{ff} at each location. The log(k) and 1/α values are adjusted for uncertainty by adding the values of Δlog(k) and Δ1/α, sampled from the uncertainty distributions for each realization. The adjusted log(k) and 1/α values, along with the percolation flux that is adjusted for flow focusing, are used to evaluate the response functions for ambient mean seepage and the SD of ambient seepage. These two quantities are used to form a uniform distribution for ambient seepage that ranges between mean seepage -1.7321 SD and mean seepage + 1.7321 SD (SNL 2007 [DIRS 181244], Section 6.5.1.3). This distribution is sampled to yield the ambient seepage for each WP at each location.

The thermal seepage condition at each WP location (e.g., no seepage when the drift-wall temperature is greater than 100°C, otherwise ambient seepage) is then used to appropriately modify the calculated ambient seepage. This results in a calculated drift-seepage flux for every WP at every subdomain location for the given infiltration scenario and climate. An average seepage flow rate is calculated for the WPs that have seepage, along with the fraction of WPs that have seepage, for each percolation subregion. The details of the seepage submodel calculations for TSPA-LA are discussed in Section 6.3.3.1, and seepage impacts on EBS flow are discussed in Section 6.3.6.

Process modeling (SNL 2007 [DIRS 181648], Section 6.3.7.2.2) has shown that there is a potential for water vapor in the drift atmosphere to condense on cooler portions of the drift walls. Condensation on drift walls and its effects on EBS flow are modeled in the TSPA-LA. The conceptual model and TSPA-LA Model implementation for drift wall condensation are discussed in detail in Section 6.3.3.1. The rate of condensation at a location on the drift wall depends on the availability of water at that location. The rate at which water is available generally increases with an increase in percolation flux, increasing water transport through the invert, and decreasing axial dispersion within the drifts (SNL 2007 [DIRS 181648], Section 8.3.1.1). The TSPA-LA Model's Drift Wall Condensation Submodel calculates the fraction of DS/WP pairs dripped on by drift-wall condensate and the average rate of condensation in each percolation subregion for each WP type. These quantities are determined from two correlations: (1) a correlation for average condensation rate versus average percolation flux, and (2) a correlation for the fraction of DS and WP pairs dripped on by drift-wall condensate versus average percolation flux. The average percolation flux for each of the five repository percolation subregions modeled in the TSPA-LA Model is calculated by averaging the percolation fluxes at the base of the PTn at each MSTHM subdomain location in that percolation subregion using the comprehensive MSTHM Abstraction data (Section 6.3.2). The impact of DS ventilation and axial dispersion uncertainty on condensation are accounted for by selecting between four cases with an equal

probability: (1) ventilated DS-low axial dispersion, (2) ventilated DS-high axial dispersion, (3) unventilated DS-low axial dispersion, and (4) unventilated DS-high axial dispersion. For each TSPA-LA Model realization, the drift-wall condensation case is sampled as an epistemic uncertainty, and the average rate of condensation and fraction of DS/WP pairs dripped on by drift-wall condensate at simulation time *t* is calculated for each percolation subregion and WP type. The average rate of condensation dripping from drift walls is combined with drift seepage to increase the dripping flow rate through the EBS.

Output 9—The following outputs are passed from the Drift Seepage (Section 6.3.3.1) and the Drift Wall Condensation Submodels (Section 6.3.3.2) to the EBS Flow Submodel (Section 6.3.6):

- For each percolation subregion:
  - Time-dependent drift-seepage rate for the DS-representative CDSP WP pairs and DS-CSNF WP pairs
  - The fraction of DS-CDSP WP pairs and DS-CSNF WP pairs in dripping (seepage) environments
  - The average time-dependent condensation rate for the DS-representative CDSP WP pairs and DS-representative CSNF WP pairs
  - The fraction of DS-CDSP WP pairs and DS-CSNF WP pairs in dripping (condensate) environments.

6.1.4.4 Engineered Barrier System Chemical Environment

The time-dependent evolution of the chemical-environment variables, pH and ionic strength, in the invert is determined by the time-dependent composition of water and gas entering the emplacement drift and how these water and gas compositions evolve as the water evaporates under the prevailing TH conditions within the invert. Time histories of seepage water and gas compositions are computed in the TSPA Model in each percolation subregion, based on the EBS P&CE Abstraction response surfaces (SNL 2007 [DIRS 177412]), using temperature, relative humidity, and percolation flux inputs from the EBS TH Environmental model. The evolution of the chemistry of the incoming seepage in the invert in terms of pH and ionic strength is modeled within the TSPA-LA Model using response surfaces in the form of look-up tables for these two variables as a function of percolation rate, the amount of water-rock interaction, temperature, relative humidity, and Pco_2. These response surfaces are provided by the EBS P&CE Abstraction (SNL 2007 [DIRS 177412], Section 6.9.2) and are based on calculations that simulate the evaporation/condensation evolution of each of the four seepage water types and gas compositions for a range of representative EBS TH conditions. The conceptual model and TSPA-LA Model implementation for the chemical environment in the EBS are discussed in detail in Section 6.3.4.

The first step in determining values of pH, ionic strength, chloride concentration, and nitrate concentration is selecting a starting water. In each realization, one of four water types is randomly sampled, and this water type is implemented for each representative WP in each

repository percolation subregion. Once the starting water has been selected, the Pco_2 time history, as a function of the temperature, the water-rock interaction and the selected starting water, is determined. The water-rock interaction is a function of the average percolation rate in each percolation subregion. Once the Pco_2 is determined, the chemical compositions are found in the look-up tables as a function of water-rock interaction, Pco_2, temperature, and relative humidity. For each realization, the TSPA-LA Model determines the pH and ionic strength in the invert for each representative WP at any point in time during the postclosure period. The pH and ionic strength are adjusted for epistemic uncertainty and variability by sampling uncertainty distributions for each parameter once per realization.

The EBS Chemical Environment Submodel also provides look-up tables and implementation instructions to determine abstracted values of time-dependent parameters, chloride and nitrate concentrations, and chloride-to-nitrate ratios. These abstracted variables are used to assess the potential for localized corrosion on the WP outer surface. However, this application of the EBS Chemical Environment Submodel is implemented in the ancillary Localized Corrosion Initiation Analysis for the TSPA-LA Model, as summarized in the next section and described in detail in Section 6.3.5.2.3. This flow of information is shown on Figure 6.1.4-1, but is not captured by an output number in Figure 6.1.4-1.

Output 10—The following outputs are passed from the EBS Chemical Environment Submodel (Section 6.3.4) to the Waste Form Degradation and Mobilization Model Component (Section 6.3.7):

- Outputs from this model component are provided for each percolation subregion and each representative WP, in dripping and non-dripping environments:
  - The time-dependent pH in the invert
  - The time-dependent ionic strength in the invert
  - The time-dependent Pco_2 in the drift.

6.1.4.5 Waste Package and Drip Shield Degradation

Time-dependent WP and DS degradation are implemented within the TSPA-LA Model. For the Nominal Scenario Class, the conceptual model and TSPA-LA Model implementation for the WP and DS degradation in the EBS are discussed in detail in Section 6.3.5. The flow of information between the WP and DS Degradation Model Component and other model components of the TSPA-LA Model are summarized below.

For the Nominal Scenario Class, general corrosion is the only degradation mode modeled for DS degradation. General corrosion rates for the inner and outer surfaces of the DSs are represented by two independent CDFs of the general corrosion rate because the environments above and below the DSs are not expected to be similar (SNL 2007 [DIRS 180778], Section 6.5.2, and 8.1[a]). These distributions represent epistemic uncertainty in DS general corrosion rates. For each realization, a single general corrosion rate is sampled from each distribution of the general corrosion rate and applied to all DSs. In the Nominal Scenario Class, the DSs are failed as a barrier to flow when the corroded thickness equals or exceeds the initial thickness of the DS plates. The status of the DS, intact or damaged, is an input to the EBS Flow submodel that determines the flow rate of water through a damaged DS and then onto a WP.

The TSPA-LA Model for the Nominal Scenario Class includes four WP degradation modes: general corrosion, MIC, and SCC, which are modeled using the Waste Package Degradation Model, and localized corrosion (SNL 2007 [DIRS 178519], Section 6.4.4), which is modeled using the Localized Corrosion Initiation Submodel.

The Nominal Scenario Class is represented by a single modeling case. This modeling case considers those WPs that fail as a result of corrosion processes (e.g., general corrosion, SCC, and/or localized corrosion). The TSPA-LA Model implementation of the WP degradation modes for the Nominal Scenario Class Modeling Case is briefly described as follows.

Nominal Scenario Class Modeling Case: WPs that Degrade by Corrosion—general corrosion rates of the WP outer surface are temperature-dependent and include epistemic uncertainty and variability. The temperature dependence is treated as an epistemic uncertainty that is sampled once per realization. The general corrosion rate, for low, medium, and high uncertainty levels, is sampled for every patch on every WP simulated in a percolation subregion. The uncertain temperature dependence for the realization, and each general corrosion rate on a patch, are used to calculate the temperature-dependent general corrosion rate (as a function of time) for every patch on every selected WP in a percolation subregion.

MIC is represented by an enhancement factor applied to the general corrosion rate of the WP outer surface (i.e., general corrosion rate × enhancement factor). The MIC factor is applied to the general corrosion rate when the relative humidity at the WP outer surface is above a relative humidity threshold. The MIC threshold represents epistemic uncertainty and is sampled once per realization.

Another potential failure mode considered for WPs is SCC in the closure lid. SCC can be initiated on a smooth surface (incipient cracks) or at an existing weld flaw (due to manufacturing defects). Two characteristics of weld flaws are treated as epistemic uncertainties sampled once per realization: flaw-size distribution and flaw-count distribution. SCC is determined by stress and stress intensity factor profiles in the closure-lid weld regions, and subsequent crack growth from the flaw sites. The uncertainty in stress and stress intensity profiles is represented by a scaling factor that is sampled independently, once for each realization. The uncertainty in crack growth rate is a function of the repassivation slope, n, which is also sampled once per realization.

The results for general corrosion, MIC, and SCC are compiled by the WAPDEG DLL (WAPDEG V4.07, STN: 10000-4.07-00 and 10000-4.07-01 [DIRS 181774 and 181064]). In the TSPA-LA Model Nominal Modeling Case, 10 WAPDEG DLL simulations are run per realization, one for each representative WP type (CSNF and CDSP) in each of the five repository percolation subregions. The EBS TH Environment Submodel provides temperature and relative humidity histories for eight WP and DS pairs (six CSNF WPs and two CDSP WPs) at each of the 3,264 subdomain locations. The process begins by randomly sampling a maximum of 500 DS/WP pairs from all of the pairs for a given fuel type in a percolation subregion. If the percolation subregion contains fewer than 500 DS/WP pairs, then all pairs in the percolation subregion are used. At the start of each EBS calculation, the WAPDEG DLL reads in the temperature and relative humidity histories for each selected WP and calculates time-dependent degradation. This information is used by the WAPDEG DLL to calculate the following output: (1) the cumulative number of WP failures as a function of time, (2) the average number

of patches per failed WP as a function of time, and (3) the average number of cracks per failed WP as a function of time.

Localized corrosion on WPs may occur when a WP is contacted by deleterious brine (SNL 2007 [DIRS 178519], Section 8.1, Figure 8-1). Two mechanisms may cause deleterious brine formation on the WP: seepage from dripping at the emplacement drift crown and dust deliquescence. In the TSPA-LA Model, only crown seepage water chemistry has the potential to fail WPs due to localized corrosion (SNL 2007 [DIRS 181267], Section 7.1.5). Only WPs that have DS plate failures coincident with deleterious brine contacting the WP are susceptible to localized corrosion failures. Localized corrosion of the WP is a process that is included in the Nominal Scenario Class. Localized corrosion of the WPs is calculated in the ancillary Localized Corrosion Initiation Analysis for the TSPA-LA Model using a response surface for localized corrosion initiation. The response surface is a function of the pH, chloride concentration, nitrate concentration, and WP temperature. Additionally, the criteria that seepage water must contact the WP for localized corrosion initiation is imposed. Thus, this separate GoldSim model file includes the Drift Seepage submodel, the EBS TH Submodel and EBS Chemical Environment Submodel. In addition, the ancillary model file also includes the general corrosion of the DSs and considers the consequences of seismic activity on the DSs.

Output 11—The following outputs are passed from the WP and DS Degradation Model Component (Section 6.3.5) to the EBS Flow Submodel (Section 6.3.6) for the Nominal Modeling Case:

- For each percolation subregion and each WP type (CDSP WPs and CSNF WPs):
  - The time-dependent average number of patch penetrations per failed DS
  - The time-dependent average number of patch penetrations per failed WP.

Output 12—The following outputs are passed from the WP and DS Degradation Model Component (Section 6.3.5) to the Waste Form Degradation and Mobilization Model Component (Section 6.3.7):

Nominal Modeling Case:

- For each percolation subregion and each fuel type (CSNF WPs):
  - The time-dependent fraction of WPs failed.

Output 13—The following outputs are passed from the WP and DS Degradation Model Component (Sections 6.3.5) to the EBS Transport Submodel (Section 6.3.8) for the Nominal Modeling Case:

- For each percolation subregion and each fuel type (CDSP WPs and CSNF WPs):
  - The time-dependent fraction of WPs failed

– The time-dependent average number of crack penetrations per failed WP
– The time-dependent average number of patch penetrations per failed WP.

6.1.4.6 Engineered Barrier System Flow

The following discusses the implementation of the EBS Flow Submodel (SNL 2007 [DIRS 177407], Section 6). The EBS Flow Submodel is implemented within the TSPA-LA Model and determines the volumetric flow rate of seepage water (including seepage into the drifts and drift-wall condensation) at different locations as seepage water moves through breached DSs, breached WPs, and the invert. In addition, the EBS Flow Submodel determines the fraction of WPs that are dripped upon, either by drift seepage and/or drift-wall condensation. The conceptual model and TSPA-LA Model implementation for flow in the EBS are discussed in detail in Section 6.3.6.

The TSPA-LA Model includes two dripping environments for each percolation subregion: (1) the seeping environment, which includes dripping above the WP from drift seepage and may also include drift-wall condensation; and (2) the non-seeping environment, which includes the WPs that are not exposed to drift seepage, but may or may not be exposed to drift-wall condensation. Inputs to the EBS Flow Submodel include the drift-seepage rate and the drift-wall condensation rate and the fraction of WPs exposed to drift-seepage and the drift-wall condensation from the UZ Flow Model Component. Both rates are combined to yield a total dripping rate. The flow rate of water through each breached DS or WP is proportional to the total dripping rate and the average number of patch penetrations on each DS or WP from the WP and DS Degradation Model Component. EBS flow is calculated for WPs of each type located in seeping and non-seeping environments. Flow in the seeping environments combines drift seepage and drift-wall condensation above and below the WP and includes the imbibition flux in the invert. Flow in the non-seeping environments includes drift wall condensation above and below the WP and includes the imbibition flux in the invert. Inputs to the EBS Flow Submodel for each WP type and repository percolation subregion include:

- The average total dripping rates due to seepage and drift-wall condensation
- The fraction of WPs dripped upon due to seepage and drift-wall condensation drift-wall condensation
- The average number of patch penetrations per failed CSNF DS and CDSP DS
- The average number of patch penetrations per failed CSNF WP and CDSP WP.

The EBS Flow Submodel does not use the average number of crack penetrations per failed WP because stress corrosion cracks are too small to allow advective water flow through these cracks (DTN: MO0706SPAFEPLA.001_R0 [DIRS 181613], FEP Number 2.1.03.10.0A).

The EBS Flow Submodel introduces two uncertain (epistemic) flux-splitting parameters to characterize the fraction of flow that enters breaches on DSs and on the WPs. These two parameters are sampled once per realization and are applied to all representative DS and WP pairs located in the dripping environments. Outputs from the EBS Flow Submodel are used

by: (1) the Waste Form Degradation and Mobilization Model Component, which uses the flow rate through a failed WP to calculate pH and ionic strength in the WP; and (2) the EBS Transport Submodel, which uses the flow rate through a failed WP and volumetric flow rate through the invert to calculate advective transport of radionuclides through a failed WP and through the invert to the host rock.

Output 14—The following output is passed from the EBS Flow Submodel (Section 6.3.6) to the Waste Form Degradation and Mobilization Model Component (Section 6.3.7):

- For each representative WP group, as applicable, in a seeping and non-seeping environment, in each percolation subregion:
  - The volumetric flow rate of water through the WP as a function of time.

Output 15—The following outputs are passed from the EBS Flow Submodel (Section 6.3.6) to the EBS Transport Submodel (Section 6.3.8):

- These outputs are provided for each representative WP in a seeping and non-seeping environment, in each percolation subregion:
  - The flux through the invert pore space as a function of time
  - The flow rate of water through the WP as a function of time
  - The fraction of WPs in a seeping environment
  - The fraction of WPs in a non-seeping environment.

6.1.4.7 Waste Form Degradation and Mobilization

The Waste Form Degradation and Mobilization Model Component, shown on Figure 6.1.4-1, includes submodels for radionuclide inventory, in-package chemistry, cladding failure, waste form degradation, dissolved concentration limits of radioactive elements, and EBS colloids. The conceptual models and TSPA-LA Model implementations for the submodels of the Waste Form Degradation and Mobilization Model Component are discussed in detail in separate subsections of Section 6.3.7. The flow of information between submodels of the Waste Form Degradation and Mobilization Model Component and other submodels of the TSPA-LA model are described below.

In-package chemistry is modeled within the TSPA-LA Model using simplified expressions to define the bulk chemistry consisting of pH, ionic strength, and total carbonate concentration ($\sum CO_3$) as a function of time inside a WP. Chemistry outputs are used to set conditions for waste form degradation, colloid stability, and to determine dissolved concentration limits inside the WPs. Within the TSPA-LA Model, no performance credit is taken for zircaloy or stainless steel cladding as a mechanism to prevent radionuclide release or inhibit CSNF waste form degradation (SNL 2007 [DIRS 180616], Section 6.2[a]). Waste form degradation is modeled within the TSPA-LA Model using empirical degradation rate formulas developed for the three different waste form types: CSNF, DOE spent nuclear fuel (DSNF), and HLW. DSNF and HLW glass are combined and disposed in CDSP WPs. Dissolved concentration limits of radionuclides (i.e., solubility limits for radioactive elements in the TSPA-LA Model) are

modeled using look-up tables, distributions, or single values. The formation, stability, and concentration of radionuclide-bearing colloids in the WP and EBS, as well as reversible and irreversible sorption of dissolved radionuclides, are modeled using empirical relationships and uncertainty distributions for sorption coefficients.

The three waste form categories (CSNF, DSNF, and HLW glass) are contained and disposed in two types of WPs: CSNF WPs and CDSP WPs. The CDSP WPs will contain both DSNF and HLW glass. The inclusion of mixed oxide SNF and lanthanide borosilicate (LaBS) glass HLW in the TSPA-LA Model is accomplished by adding radionuclide-specific inventories to the GoldSim source term (SNL 2007 [DIRS 180472]). WPs containing naval SNF WPs are conservatively represented as CSNF WPs containing CSNF inventory (see discussion in Section 6.3.7.1). Each percolation subregion environment represents a group of WPs in that subregion of the same type and in the same environment. Assigning individual WPs into WPs groups is discussed in detail in Section 6.1.5. The total radionuclide inventory (Section 6.3.7.1) in each WP group available for degradation and transport is calculated for each percolation subregion by taking into account the number and type of failed WPs.

The In-Package Chemistry Submodel is implemented using response surfaces and parameter distributions for four different abstraction conditions: CSNF and CDSP WPs that are dripped on, and CSNF and CDSP WPs that are not dripped on. Due to the contribution of drift-wall condensation, a WP can be dripped on if it is in a seeping or non-seeping environment, but only if its DS has failed. The In-Package Chemistry Submodel is implemented by sampling seepage rate-dependent uncertainty distributions and P_{CO_2}-dependent response surfaces for pH. Ionic strength is determined by sampling uncertainty distributions whose range is a function of the relative humidity within the breached WP for non-dripping conditions and by sampling uncertainty distributions whose range is a function of the seepage rate through a breached WP for dripping conditions. The sampled values of pH and ionic strength represent epistemic uncertainty and are sampled once per realization. The $\sum CO_3$ for each abstraction condition is calculated using a temperature, P_{CO_2}, and pH-dependent equation. This calculated value includes no additional uncertainty. Inputs to the In-Package Chemistry Submodel include volumetric flow rates of seepage into a failed WP as provided by the EBS Flow Submodel, the P_{CO_2} provided by the EBS Chemical Environment Submodel, and the temperature and relative humidity provided by the EBS TH Environment Submodel.

Outputs from the In-Package Chemistry Submodel are provided for each representative WP and each representative early-failed WP, if available, in dripping and non-dripping environments in each percolation subregion and consist of:

- The pH as a function of time
- The ionic strength as a function of time
- The $\sum CO_3$ as a function of time.

These outputs are used internally in the TSPA-LA Model by the Waste Form Degradation and Mobilization Model Component as inputs to the rate equations for the Waste Form Degradation Submodels, the dissolved concentration limits look-up tables, and EBS colloids stability criteria.

Most of the CSNF is encased in zirconium-alloy cladding, with only 1 percent of CSNF encased in stainless-steel cladding (DTN: MO0411SPACLDDG.003_R1 [DIRS 180755]). No performance credit is taken for zirconium-alloy cladding or stainless-steel cladding in the CSNF WP. The cladding does not reduce the amount of water that can contact the spent fuel in the CSNF WP nor does it reduce the release rate of the inventory when the waste form degrades. Both zirconium-alloy cladding and stainless-steel cladding are modeled as being perforated upon emplacement of the WPs in the repository. Perforated rods are modeled as instantly split down the rod length after the WP has failed (SNL 2007 [DIRS 180616], Section 6.2.4[a]).

No performance credit is taken for CSNF cladding; therefore, all of the CSNF inside a failed CSNF WP is exposed and available for degradation. Waste form degradation is modeled within the TSPA-LA Model using empirical formulas for the degradation rate developed for the three different waste form types: CSNF, DSNF, and HLW.

CSNF is isolated from repository environmental conditions until the WP is breached. Since no performance credit is taken for CSNF cladding, after the WP is breached, the CSNF may be exposed to humid air or dripping water. Upon exposure to moisture, radionuclides can be released by two mechanisms: (1) instantaneous release of the gap fraction and grain boundary inventory, and (2) matrix dissolution under alkaline or acidic conditions (BSC 2004 [DIRS 169987], Section 6). The fraction of the inventory emplaced in the repository that makes up the initial release inventory is determined by sampling distributions representing epistemic uncertainty. These distributions are sampled once per realization. For the CSNF inventory that is not part of the initial release inventory, matrix dissolution is modeled using two rate formulas, one for $pH < 6.8$ and one for $pH \geq 6.8$ (BSC 2004 [DIRS 169987], Section 8.1). Both CSNF degradation rate formulas are a function of specific surface area of exposed fuel, temperature, $\sum CO_3$, Po_2, and in-package pH. Epistemic uncertainty in a specific surface area of exposed fuel is sampled once per realization. The CSNF degradation rate is calculated using input provided by two submodels: the EBS TH Environment Submodel provides the time-dependent temperature of the CSNF, and the In-Package Chemistry Submodel provides time-dependent pH and total carbonate concentration inside the failed WP. As the CSNF waste form degrades, the EBS Transport Submodel calculates the mass and saturated volume for the degraded CSNF rind and a rind thickness. These parameters are used to determine radionuclide concentrations in the fuel rind and to model transport from the CSNF rind into the WP.

The DSNF is modeled as being immediately available for dissolution and mobilization after a WP containing DSNF is breached. Because of this simplification, no rate equation or rate parameters are necessary to implement the DSNF Waste Form Degradation Abstraction for DSNF in the TSPA-LA Model (BSC 2004 [DIRS 172453], Sections 6.2 and 8.1). Each time a CDSP WP fails, the DSNF inventory associated with the failed WP, after accounting for decay and ingrowth, is made immediately available for transport (subject to solubility constraints) in the volume of water associated with the degraded DSNF and WP corrosion products (see Section 6.3.8.2). Once released, radionuclides are available for transport through the WPs to the EBS.

Degradation of HLW glass inside a damaged CDSP WP is included in the TSPA-LA Model. The rate equation is a function of an effective rate constant, temperature, pH, and the exposed surface area of the HLW glass (BSC 2004 [DIRS 169988], Section 8.1). The effective rate

constant is treated as an epistemic uncertainty, and is represented by two distributions, one for acidic conditions and one for alkaline conditions. These distributions are sampled once per realization. The exposed surface area of the glass is calculated as the product of the specific surface area of the glass and the glass exposure factor. The exposure factor is treated as an epistemic uncertainty and is sampled once per realization. The HLW Glass degradation rate is calculated using input provided by two submodels: the EBS TH Environment Submodel provides the time-dependent temperature of the CDSP WP, and the In-Package Chemistry Submodel provides time-dependent pH inside the failed WP. As the HLW glass degrades, the EBS Transport Submodel calculates the mass and saturated volume for the degraded HLW rind and a rind thickness. These parameters are used to determine radionuclide concentrations in the HLW rind and to model transport from the rind into the WP.

Outputs from the Waste Form Degradation Submodel for HLW glass, CSNF, and DSNF degradation are provided for each representative WP and each representative early-failed WP, as applicable in seeping and non-seeping environments, and in each percolation subregion, as follows:

- The degradation rate of HLW glass
- The degradation rate of CSNF fuel
- The instantaneous degradation of DSNF fuel.

These outputs are used internally in the Waste Form Degradation and Mobilization Model Components to determine the concentration of radionuclides in water in the associated degraded fuel rind.

The Dissolved Concentration Limits Submodel determines radionuclide concentration limits. The Dissolved Concentration Limits Submodel is used to calculate the solubility of certain radionuclides in the WP and in the invert that are potentially important to dose. The Dissolved Concentration Limits Submodel is implemented in the TSPA-LA Model in the form of: (l) look-up tables for plutonium, neptunium, uranium, thorium, americium, and protactinium, plus one or more epistemic uncertainty terms; (2) constant values over two pH intervals for radium; or (3) undefined values for technetium, carbon, iodine, cesium, and strontium (SNL 2007 [DIRS 177418], Sections 6 and 8.1). The look-up tables provide radioelement solubility as a function of pH and CO_2 fugacity (fco_2). Solubilities are evaluated as a function of time to account for the evolution of pH and fco_2 during the postclosure period. One or more epistemic uncertainty terms are evaluated by sampling their respective distributions once per realization and are added to each tabulated solubility value. These uncertainty terms represent uncertainty in the solubility constants of phases that control the solubility of plutonium, neptunium, uranium, thorium, and americium; uncertainty of the fluoride concentration in water that controls the solubilities of neptunium, uranium, thorium, americium, and protactinium; and uncertainty in the chemical analogy in the case of protactinium. The In-Package Chemistry Submodel and the EBS Chemical Environment Submodel provide the pH, ionic strength, and fco_2 inputs to the Dissolved Concentration Limits Submodel when the Dissolved Concentration Limits Submodel is implemented in the WPs and in the invert, respectively (SNL 2007 [DIRS 177418], Executive Summary, Sections 1 and 6.4).

Outputs from the Dissolved Concentration Limits Submodel are provided for each representative WP, as applicable in seeping and non-seeping environments, and for each percolation subregion, as follows:

- The time-dependent solubilities for plutonium, neptunium, uranium, thorium, americium, and protactinium
- The time-dependent value of radium solubility, which can be one of two values depending on pH.

These outputs are used by the EBS Transport Submodel to calculate radionuclide concentration limits that are in the volumes of water associated with the CSNF rind, in the DSNF rind, in the HLW glass rind, in the in-package corrosion products, and in the invert.

The TSPA-LA Model's EBS Colloids Submodel calculates the types and concentrations of colloids potentially generated after WP failure. Three types of colloids are considered: (1) waste form degradation colloids, which are generated from degradation of the glass waste form and SNF waste forms; (2) colloids produced from the steel components of the WPs and invert; and (3) colloids present in natural seepage water entering the EBS. Nine radionuclides can potentially sorb on the colloids: plutonium, americium, cesium, protactinium, thorium, tin, radium, uranium, and neptunium. Inputs to the colloid-associated EBS Colloids Submodel include pH and ionic strength in the WP provided by the In-Package Chemistry Submodel, dissolved radionuclide concentrations in the WP and invert from the EBS Transport Submodel, and pH and ionic strength in the invert provided by the EBS Chemical Environment Submodel.

At each timestep in the TSPA-LA Model calculations, the EBS Colloids Submodel uses in-package ionic strength, pH, and dissolved radionuclide concentrations to evaluate the formation and stability of colloids in the WP. Besides reversible sorption, irreversible (kinetic) sorption of plutonium and americium onto iron oxyhydroxide colloids and waste form colloids derived from HLW glass and CSNF is also considered. A competitive sorption model with a sorption capacity is implemented for the reversible sorption onto the three colloid types.

The EBS Chemical Environment Submodel (Section 6.3.4) calculates the ionic strength and pH of the invert water. Based on the values of ionic strength and pH in the invert, the EBS Colloids Submodel determines colloid stabilities and concentrations for the invert conditions and redistributes available radionuclide mass based on the distribution coefficients and the total mass of each type of colloid. These colloids and associated radionuclides are then subject to transport through the invert and into the UZ.

Several epistemic uncertainties, related to colloid stability and colloid-associated radionuclide concentrations, are represented by distributions that are sampled once per TSPA-LA Model realization. These uncertain parameters include the equilibrium sorption distribution coefficients, the specific surface area of corrosion-generated colloids, the groundwater colloid concentration, and the forward rate constant for irreversible (kinetic) sorption.

Output 16—The following outputs are passed from the Waste Form Degradation and Mobilization Model Components (Section 6.3.7) to the EBS Transport Submodel (Section 6.3.8):

- Outputs from the Waste Form Degradation and Mobilization Model Component are provided for each representative WP in seeping and non-seeping environments. For each percolation subregion, they provide:
  - The mass of radionuclides available for transport through the EBS
  - The concentrations limits of radionuclides inside a failed WP and in the invert
  - The concentrations of radionuclides, plutonium and americium, irreversibly attached (embedded in) waste form colloids
  - The concentrations of radionuclides, americium and plutonium, which are irreversibly attached to iron oxyhydroxide colloids
  - The concentrations of radionuclides: americium, plutonium, protactinium, cesium, thorium, tin, radium, uranium, and neptunium, which are reversibly attached to colloids.

6.1.4.8 Engineered Barrier System Transport

The EBS Transport Submodel is described in *EBS Radionuclide Transport Abstraction* (SNL 2007 [DIRS 177407], Section 6). The conceptual models and TSPA-LA Model implementations for the EBS Transport submodel are discussed in detail in Section 6.3.8 and are summarized below.

EBS transport is modeled directly within the TSPA-LA Model at run time, using a one-dimensional, finite-difference numerical solution algorithm that is embedded in the GoldSim operating software (GoldSim V9.60.100, STN: 10344-9.60-01 [DIRS 181903]) of the TSPA-LA Model. Each representative WP group in each repository percolation subregion is modeled. The modeled system uses a linked series of mixing cells that represent the waste form as the source of radionuclides and colloids, corrosion products as a source of iron oxyhydroxide colloids and stationary corrosion products in the WP that sorb radionuclides, and the invert crushed tuff as a sorbing medium. The EBS Transport Submodel describes the transport of both dissolved radionuclides and radionuclides sorbed onto colloids through the TSPA-LA Model's mixing cells via diffusion and advection. The outputs from the EBS Transport Submodel are mass flux of dissolved radionuclides and mass flux of colloid-associated radionuclides into the host-rock fractures and host-rock matrix below the repository. The total mass flux into the UZ host rock and the fraction going into the fractures and the matrix in the UZ is computed based on modeling approximately 18 m of dual continuum below the repository as part of the EBS Transport Submodel. The calculated radionuclide mass flux as a function of time at the EBS-UZ interface is passed to the UZ Transport Model Component of the TSPA-LA Model. The UZ Transport Model Component applies a three-dimensional, dual-permeability UZ Transport model that uses a finite element, heat and mass (FEHM) software code (FEHM V2.24, STN: 10086-2.24-01-00 [DIRS 179419]).

Several epistemic uncertainties related to transport in WPs and the invert are represented by distributions that are sampled once per realization. In the WPs these include: (1) the water adsorption isotherm parameters, (2) the surface properties such as specific surface area and sorption site density of the stationary corrosion products, (3) the corrosion rate of in-package stainless-steel and carbon-steel components, (4) diffusive path length from a WP to the invert, and (5) the uncertainty in pH from surface complexation calculations. In the invert, these include radionuclide reversible sorption coefficients and an invert diffusion coefficient for radionuclide diffusion.

Implementation of the EBS Radionuclide Transport Submodel requires transport connections between the single-continuum invert and the dual-continuum host rock. For each representative waste-emplacement drift, these connections determine the fraction of radionuclide mass flux transported into the host-rock matrix continuum, and the fraction transported into the host-rock fracture continuum after release from the EBS. The diffusive transport connections are derived by enforcing mass flux continuity between the invert and the host rock, which determines the split of invert diffusive releases between the UZ fracture and matrix continua. However, the split for advective mass flux is imposed. The total advective mass flux leaving the invert is based on the combined fluid flux in the invert (a combination of seepage, condensation, and imbibition flux), but when the advective mass flux is passed to the UZ, it is partitioned such that the advective fraction carried by the imbibition flux is sent to the UZ matrix, while the remainder is sent to the UZ fractures. Mass partitioning fractions are also passed from the EBS Transport submodel to the UZ Transport Model Component.

The following time-dependent outputs are calculated for each WP group in each percolation subregion.

Output 17—The following outputs are passed from the EBS Transport Submodel (Section 6.3.8) to the UZ Transport Submodel (Section 6.3.9):

- Outputs from the EBS Transport Submodel are provided for each representative WP and each representative early-failed WP, as applicable, in seeping and non-seeping environments, for each percolation subregion, as follows:
  - The radionuclide mass release rate to the UZ.
  - The diffusive and advective release fractions from the EBS into the UZ below the repository.

6.1.4.9 Unsaturated Zone Transport

UZ transport is modeled within the TSPA-LA Model by the UZ Transport Submodel. The conceptual models and TSPA-LA Model implementations for the UZ Transport Submodel are discussed in detail in Section 6.3.9 and are summarized below.

The UZ Transport Submodel implements the three-dimensional, dual-permeability, finite-element software code FEHM (FEHM V2.24, STN: 10086-2.24-01-00 [DIRS 179419]) particle tracker (SNL 2008 [DIRS 184748], Sections 6 and 8). The UZ flow fields for each combination of infiltration scenario and climate change are accessed directly by the UZ

Transport Submodel. The FEHM particle tracker transports particles with the same dual-permeability spatial grid as used in the Site-Scale UZ Flow Process Model (SNL 2007 [DIRS 184614]), including the same water flux and liquid saturation values. When climate changes, the TSPA-LA Model uses the UZ flow fields associated with the new climate for the given infiltration scenario.

As noted in Section 6.1.4.8, Output 17, the mass of dissolved radionuclides and reversibly sorbed radionuclide mass on colloids from the EBS are combined and released to the UZ as a total radionuclide mass. This mass is equilibrated within the UZ between the aqueous phase and the groundwater colloids present in the UZ. Americium and plutonium isotopes that are irreversibly sorbed onto colloids are transported separately as fast and slow fractions. The following UZ transport processes are simulated:

- Advective and diffusive transport of dissolved and colloid bound radionuclides in the fractures and rock matrix
- Fracture-matrix interaction and matrix diffusion
- Sorption of dissolved radionuclides in the matrix continuum
- Retardation of colloids, on which radionuclides are irreversibly sorbed, in the fracture continuum
- Colloid filtration at interfaces between matrix units
- Colloid size exclusion at fracture-matrix continua interfaces
- Radioactive decay and ingrowth.

The release of radionuclides from the EBS to the UZ is calculated as follows: The radionuclide mass flux, calculated by the EBS Transport Submodel and released from the five repository percolation subregions, enters the FEHM grid nodes that reside within the subregions. The number of FEHM grid nodes receiving released radionuclides depends on the number of WPs that have failed. At each timestep, there are a number of failed WPs from each representative group in each repository percolation subregion. The radionuclide mass flux released from each failed WP in a group is equal to the mass flux from the representative WP group divided by the number of failed WPs in that group. To simulate WPs failing at different locations, the FEHM release nodes in the UZ are randomly selected for each group, without replacement (to prevent a node from being selected more than once), from the available UZ FEHM grid nodes within each percolation subregion. If the number of failed WPs in a group exceeds the number of FEHM grid nodes in a percolation subregion, releases are allocated evenly to all FEHM grid nodes in the percolation subregion.

For each realization, a set of uncertain material properties for UZ transport is sampled and the values or parameters generated from the sampled values are used in the UZ transport particle tracking analysis. These epistemic uncertainties are represented by distributions and include matrix adsorption coefficients, matrix diffusion coefficients (as generated from sampled values

of tortuosities and species-dependent values of free-water diffusion coefficients), fracture apertures (as generated from sampled values of fracture porosity and fracture frequency), active fracture model gamma parameters, colloid equilibrium sorption parameters (as generated from sampled values of sorption coefficients onto colloids and colloid concentrations), and colloid retardation factors for UZ transport. In addition, colloid filtration sizes for rock units are sampled and compared to sampled values of colloid size for each particle during the particle tracking process. This information is accessed by the UZ Transport Submodel during TSPA-LA Model simulations. Note that because UZ transport processes tend to be more sensitive to rock property uncertainties, some UZ rock properties (e.g., the AFM gamma) are sampled for the UZ Transport Submodel, whereas they are not sampled for the Site-Scale UZ Flow Process Model. Outputs from the UZ Transport Submodel at each timestep are radionuclide mass release rates from the fractures and matrix to four UZ collector regions at the water table. When the climate changes, the elevation of the water table is instantaneously set to the elevation associated with the new flow field. Any radionuclides in the UZ below the new and higher water table elevation at the time the climate changes are immediately removed from the UZ and provided as inputs to the SZ Flow and Transport Submodel. The immediate change in the water table which decreases the transport length to the SZ and the immediate application of mass residing between the old and new water table to the SZ, represents a reasonable, technically defensible conservative implementation (SNL 2008 [DIRS 184748], Section 6.4.8).

Output 18—The following outputs are passed from the UZ Transport Model Component (Section 6.3.9) to the SZ Flow and Transport Submodel (Section 6.3.10):

- The mass release rate of dissolved radionuclides (or, where applicable, combined dissolved radionuclides and radionuclides reversibly sorbed onto colloids) from each collector region to the SZ

- The mass release rate of radionuclides irreversibly sorbed onto retarded (slow) and unretarded (fast) colloids from each collector region to the SZ

- The cumulative potential mass release of ingrowth products associated with inventory boosting (see Section 6.3.10.3).

6.1.4.10 Saturated Zone Flow and Transport

The SZ Flow and Transport Submodel is described in *Saturated Zone Flow and Transport Model Abstraction* (SNL 2008 [DIRS 183750]). The conceptual models and TSPA-LA Model implementations for the SZ Transport Submodel are discussed in detail in Section 6.3.10 and are summarized below.

The SZ Flow and Transport Submodel of the TSPA-LA Model evaluates the transport of radionuclides, from their introduction at the water table below the repository, to the accessible environment 18-km downstream from the repository (66 FR 55732 [DIRS 156671], p. 55753). The groundwater used by the hypothetical farming community is conservatively assumed to contain all radionuclide mass in the SZ that crosses the boundary of the accessible environment. The captured radionuclide mass is homogeneously distributed in 3,000 acre-ft/yr of groundwater (10 CFR 63.312(c) [DIRS 180319]). The TSPA-LA SZ Flow and Transport Submodel uses two

abstractions to describe SZ flow and transport: (1) a 3-D SZ Flow and Transport Abstraction of individual radionuclides that are important to dose and (2) a 1-D SZ Flow and Transport Abstraction that calculates the transport of second-generation daughter radionuclides (Figure 6.3.10-8).

The 3-D SZ Flow and Transport Abstraction and the 1-D SZ Flow and Transport Abstraction receive inputs from two other sources. The Climate Analysis (BSC 2004 [DIRS 170002]) provides the duration of climates. The Infiltration Model (SNL 2007 [DIRS 182145]) provides the net infiltration flux (Section 6.3.1) to scale groundwater flux for the future climates considered for the TSPA-LA Model. Changes in recharge and groundwater flux in the SZ, associated with climate variations, are approximated as step changes from one steady-state flow condition to the next. Note although the data from the new Infiltration Model described in SNL 2007 [DIRS 182145] is reflected in the groundwater flux scaling factors, the new infiltration rates were not used to update the recharge in the repository area. The use of the old recharge data is not expected to make a marked difference since even though the weighted flow through the UZ Flow Model footprint has increased 49 percent over the previous net infiltration, the recharge is a small portion (13 percent) of the infiltration budget and the flow budget (1 percent) (SNL 2007 [DIRS 177391], Section 6.4.3.9).

Using 12 representative radionuclide groups, the 3-D SZ Flow and Transport Process Model (SNL 2008 [DIRS 183750]) is run outside the TSPA-LA Model. It is used to perform a series of probabilistic transport simulations for a unit mass source rate to obtain unit mass breakthrough curves at the 18-km boundary of the accessible environment, for each of the 12 representative radionuclide groups. For each realization, parameters containing epistemic uncertainty are sampled and used in the three-dimensional and one-dimensional SZ Flow and Transport Models (SNL 2008 [DIRS 183750], Table A-1[a]). The uncertain parameters include: (1) effective porosity in the alluvium; (2) values of the distribution coefficient, K_d, in the tuff and alluvium; (3) parameters used for irreversible and reversible sorption onto colloids; (4) longitudinal dispersivity; (5) transverse dispersivity; (6) coordinate offsets for the point source locations within each of the four SZ capture regions; (7) horizontal permeability anisotropy; (8) fraction of the groundwater flow path within the alluvium; and (9) parameters related to matrix diffusion in the tuff (SNL 2008 [DIRS 183750], Table 7.1[a]).

The unit mass breakthrough curves generated by the 3-D SZ Flow and Transport Process Model, in combination with the convolution integral method, are used by the 3-D SZ Flow and Transport Abstraction in the TSPA-LA Model to calculate transport in the SZ to the accessible environment. For a given timestep, the convolution integral method takes a point-source radionuclide mass from the bottom of the UZ Transport Submodel from four capture regions (SNL 2008 [DIRS 183750], Section 6.5.2.13). The total radionuclide mass release rate, for both matrix and fracture continua in each of these four capture regions, is released to a single location that is randomly selected in each capture region. The location of the random release point in each SZ capture region was selected during the generation of the SZ Convolute Abstraction breakthrough curves for each realization. The location of the UZ release point (Figure 6.3.9-6) used in each realization is, therefore, implicit to the sampled breakthrough curve used in the SZ convolution integral approach. The randomly selected point source location is determined by applying sampled offset values to known coordinates within each of the four SZ capture region. The sum of the fracture and matrix radionuclide mass release rates is released to

four SZ capture regions (Figure 6.3.10-6) and then fed to the SZ convolution integral model, SZ_Convolute (SZ_Convolute V3.10.01, STN: 10207-3.10.01-00 [DIRS 181060]), and to the one-dimensional SZ pipe model (SNL 2008 [DIRS 183750], Section 6.3) at each TSPA-LA Model timestep. The 3-D SZ Flow and Transport Abstraction combines this source with the appropriate unit mass breakthrough curve for that radionuclide to determine the mass flux of radionuclides across the 18-km boundary. The breakthrough curves reside in files in the GoldSim software run-time directory and are accessed when needed by the SZ_Convolute DLL. The SZ_Convolute method convolves the source term with the SZ_Convolute library of unit breakthrough curves.

For some of the daughter radionuclides that are considered in the TSPA-LA Model, a 1-D SZ Flow and Transport Abstraction is used to account for decay and ingrowth during transport for four decay chains. The 1-D SZ Flow and Transport Abstraction is incorporated directly in the TSPA-LA Model as three one-dimensional pipe segments for each SZ source region using GoldSim pipe pathway elements. The simplified 1-D SZ Flow and Transport Abstraction is required because the radionuclide transport methodology used in the 3-D SZ Flow and Transport Abstraction does not calculate ingrowth by radioactive decay. The rates of groundwater flow within individual pipe segments are adjusted to match the flow rates in the 3-D SZ Flow and Transport Abstraction. The flow path length of the first segment is constant and represents a distance for which the properties of the volcanic medium and gradient are relatively uniform. The flow path lengths of the second and third segments are a function of two uncertain parameters: the first represents uncertainty in the horizontal permeability anisotropy, and the second represents uncertainty in the northwestern boundary of the alluvium. These two parameters are sampled once per SZ realization. Values of transport parameters in the one-dimensional SZ pipe segments correspond to the values used in the 3-D SZ Flow and Transport Abstraction on a realization-by-realization basis.

Results from the 3-D SZ Flow and Transport Abstraction are combined with the results of the 1-D SZ Flow and Transport Abstraction to produce a radionuclide mass release rate at the boundary of the accessible environment. The TSPA-LA Model coordinates the consistent, random selection of radionuclide breakthrough curves and properties for the one-dimensional transport calculation for each realization.

Output 19—The output passed from the SZ Flow and Transport Submodel (Section 6.3.10) to the Biosphere Submodel (Section 6.3.11) is the mass flux of radionuclides (in 3,000 acre-ft of water) at the 18 km boundary of the accessible environment (66 FR 55732 [DIRS 156671], p. 55753).

6.1.4.11 Biosphere

The annual dose to the RMEI is modeled using BDCFs that convert radionuclide concentrations in groundwater, or in volcanic ash to dose. The two exposure cases considered in the TSPA-LA Model are the groundwater exposure case and the volcanic ash exposure case. For the groundwater exposure case, radionuclides enter the accessible environment from wells that extract contaminated groundwater from the SZ aquifer. Human exposure arises from using the contaminated water for domestic and agricultural purposes. Groundwater BDCFs apply to the Nominal Scenario Class, the Early Failure Scenario Class, the Seismic Scenario Class, the

Igneous Intrusion Modeling Case of the Igneous Scenario Class, and the Human Intrusion Scenario. In the volcanic ash exposure case, radionuclides are released as contamination in volcanic ash that is dispersed into the atmosphere with possible redistribution by fluvial processes leaving a contaminated layer on surface soil. Human exposure occurs in the accessible environment with the transport of radionuclides from surface soil to other environmental media such as foodstuffs, inhalable contaminated atmospheric particulate matter, and groundshine. Volcanic Ash BDCFs apply to the Volcanic Eruption Modeling Case of the Igneous Scenario Class. The BDCFs are developed outside the TSPA-LA Model, using the Biosphere Process Model (SNL 2007 [DIRS 177399]).

Using the methods developed in *Biosphere Model Report* (SNL 2007 [DIRS 177399]), BDCFs for the groundwater exposure cases and the volcanic ash exposure cases were calculated, using probabilistic analysis, in a series of simulations for each of the primary radionuclides tracked in the TSPA-LA Model (DTN: MO0702PAGBDCFS.001_R0 [DIRS 179327], DTN: MO0702PAVBPDCF.000_R0 [DIRS 179330]). In the case of the Volcanic BDCFs, the results were insensitive to climate change and were provided for only the present-day climate. For the Groundwater BDCFs, climate has an influence on the BDCFs as a result of changes in agricultural practices and swamp cooler usage. For each primary radionuclide, one thousand stochastic BDCFs were developed for each of the three climates (present-day, monsoon, and glacial transition) anticipated to occur over the next 10,000 years (SNL 2007 [DIRS 177399]). The present-day accessible environment, being the warmest and driest, uses the largest volume of contaminated groundwater and generates higher BDCFs than the other climates. To prevent speculation about climate changes over the 1,000,000-year period, TSPA used these conservative, present-day BDCFs for all simulation time periods. In a similar vein, the BDCFs for the Volcanic Eruption Modeling Case were generated stochastically using 1,000 realizations. In the TSPA-LA Model, a discrete distribution whose output is an integer from 1 to 1,000, inclusive, is used to randomly select a particular set of values from these BDCF tables. The selected BDCFs for each radionuclide are then multiplied by the appropriate radionuclide concentrations and summed over all radionuclides to compute annual dose to the RMEI. In the SZ, radionuclide concentrations are calculated from the annual radionuclide mass flux provided by the SZ Flow and Transport Model Component uniformly dispersed in the 3,000 acre-feet of water. For the Volcanic Eruption Modeling Case, the BDCFs are multiplied by the appropriate concentrations, one concentration is that in the resuspendible soil layer, and the other is the concentration appropriate for crop uptake (i.e., averaged over the tillage depth).

In addition to the annual dose calculation, the Biosphere Model Component also includes the calculations of activity concentration in groundwater and beta-photon doses for evaluating compliance with the groundwater protection limits (SNL 2007 [DIRS 177399]; DTN: MO0702PAGWPROS.001_R0 [DIRS 179328]). Three items, including the gross alpha concentration in groundwater, the radium concentration in groundwater, and the annual dose from beta- and photon-emitting radionuclides ingested by daily consumption of two liters of groundwater are evaluated for compliance. These calculations are based on the activity concentration of each primary radionuclide in groundwater, as calculated from radionuclide concentrations that are provided by the SZ Flow and Transport Model Component. They use the conversion factors (DTN: MO0702PAGWPROS.001_R0 [DIRS 179328]) for calculating the annual beta and photon dose, and the number of alpha particles as per the requirement in

10 CFR 63.331 [DIRS 180319], emitted per decay of the primary radionuclides, as TSPA-LA Model inputs provided by the Biosphere Model Component.

The Biosphere is the last component in the chain of TSPA-LA Model components and, thus, has no output coupling; rather, the Biosphere component outputs are the time evolution of stochastic dose histories and other parameters (alpha activity and organ/whole body doses) required by 10 CFR 63.331 ([DIRS 180319], Table 1) to evaluate repository system performance.

Output 20—The following outputs are passed from the Biosphere Model Component at each timestep (Section 6.3.11):

- The annual dose incurred by the RMEI for every radionuclide under consideration for both groundwater exposure and volcanic ash exposure cases
- The gross alpha concentration in groundwater
- The radium concentration in groundwater
- The annual whole body and individual organ doses from beta- and photon-emitting radionuclides by daily consumption of two liters of groundwater.

6.1.4.12 Events

In addition to the analysis of the Nominal Scenario Class described in Sections 6.1.4.1 through 6.1.4.11, the TSPA-LA Model is used to analyze early failure events and other disruptive events. The early failure events analyses consider early failure of WPs and DSs. The early failure events are captured in two separate modeling cases: (1) Waste Package EF Modeling Case, and (2) Drip Shield EF Modeling Case. The disruptive events analyses consider igneous events, including an igneous intrusion into the repository and a volcanic eruption through the repository, seismic events, with either ground motion affecting the repository or fault ruptures intersecting the repository, and a human intrusion. The Igneous Scenario Class includes two modeling cases: (1) Igneous Intrusion Modeling Case, with groundwater transport; and (2) Volcanic Eruption Modeling Case, with atmospheric transport. The Seismic Scenario Class includes two modeling cases: (1) Seismic GM Modeling Case, and (2) Seismic FD Modeling Case. The Human Intrusion Scenario includes one stylized Human Intrusion Modeling Case.

6.1.4.12.1 Early Failure Scenario Class

The two early failure Scenario Class modeling cases, mentioned above and considered for the TSPA-LA Model, are discussed below.

The Waste Package EF Modeling Case considers all WPs that fail early due to manufacturing or material defects, including improper pre-emplacement operations. The implementation of early WP failures in the TSPA-LA Model consists of sampling or specifying aleatory quantities associated with the early failure events. These include: the number of WPs that fail early in a realization and how these WPs are distributed among the different WP types (Section 6.4), and the percolation subregion and dripping environment type containing the EF WPs. Like the Nominal Scenario Class, in the TSPA-LA Model's early failure WP analysis, two types of WPs

are considered: (1) CDSP WPs, and (2) CSNF WPs; five percolation subregions are considered; and two dripping environments, seeping and non-seeping are considered. Localized corrosion and general corrosion of the WPs are considered in the Waste Package EF Modeling Case; however, these two mechanisms would not introduce any additional damage to the early-failed WPs because the entire surface area of the early failure WP is damaged at the time of the early failure. General corrosion of the DS is included in the Waste Package EF Modeling Case. Other than the Waste Package Degradation Model Component, the Waste Package EF Modeling Case invokes the same modeling components and submodels used in the Nominal Scenario Class.

The Drip Shield EF Modeling Case considers all DSs that fail early due to manufacturing or material defects including improper pre-emplacement operations. The implementation of early DS failures in the TSPA-LA Model consists of sampling or specifying aleatory quantities associated with the early failure events. These include: the number of DSs that fail early in a realization and how these DSs are distributed among the different WP types (Section 6.4), and the percolation subregion and dripping environment type containing the EF DSs. Like the Nominal Scenario Class, in the TSPA-LA Model's early failure DS analysis, two types of WPs are considered: (1) CDSP WPs and (2) CSNF WPs; five percolation subregions are considered; and two dripping environments, seeping and non-seeping are considered. In order for WP releases to occur under an early-failed DS, a WP beneath the early-failed DS is modeled as a WP in a seeping environment that fails immediately by localized corrosion once seepage contacts the WP. In the absence of localized corrosion, the WP under an early-failed DS would not be subject to releases before nominal processes result in WP failures. The implementation of placing the early- failed DS in a seeping environment requires that the resulting dose be weighted by the probability of at least one early-failed DS occurring in a seeping environment. Localized corrosion of a WP under an early-failed DS is assumed to be instantaneous once seepage contacts the WP. As a result of localized corrosion, general corrosion of a WP is considered in the Drip Shield EF Modeling Case; however, this mechanism would not introduce any additional damage to a WP beneath an early-failed DS because localized corrosion damages the entire surface area of the WP. General corrosion of the DS is excluded in the Drip Shield EF Modeling Case. Other than the WP and DS Degradation Model Component, the Drip Shield EF Modeling Case invokes the same modeling components and submodels used in the Nominal Scenario Class.

Figure 6.1.4-3 schematically depicts the flow of information between the principal TSPA-LA Model components and submodels for the early failure modeling cases. The flow of information between submodels in these two modeling cases is similar to the Nominal Scenario Class Modeling Case depicted on Figure 6.1.4-1 with some exceptions that are described below and described in detail in Section 6.4.

The WP and DS Degradation Model Component, which combines the localized corrosion and general corrosion processes in the Nominal Scenario Class, is replaced with early failure degradation modes for the WPs and/or DSs. As discussed above, localized corrosion and general corrosion of WPs provide no additional damage to the early-failed WP, and therefore the WP damage and failure areas calculated by the WP and DS Degradation model component are not applicable in the Waste Package EF Modeling Case. DS degradation by general corrosion is still applicable in the Waste Package EF Modeling Case. As discussed above, general corrosion of DSs provides no additional damage to early-failed DSs, and therefore the DS damage and failure

areas calculated by the WP and DS Degradation model component are not applicable in the Drip Shield EF Modeling Case. WP degradation by localized corrosion is assumed to occur instantly once a WP beneath an early-failed DS is contacted by seepage water.

6.1.4.12.2 Igneous Scenario Class

The two Igneous Scenario Class modeling cases, mentioned above and considered for the TSPA-LA Model, are discussed below (Section 1.5.3).

The following events occur in the Igneous Intrusion Modeling Case, as described in *Dike/Drift Interactions* (SNL 2007 [DIRS 177430], Section 6). The Igneous Intrusion Modeling Case considers an igneous event in which a fracture with magma rising in it (dike) intersects the repository drifts. The magma flows into and fills the drifts, cooling in place with no eruption to the surface unless the magma is within an eruptive conduit. The intruding magma engulfs all WPs and DSs in those repository drifts that are intersected by the dike. In response to the heat and corrosive gases, the WPs and fuel cladding fail, exposing the radioactive waste to the magma. After the magma-filled drifts cool to ambient conditions (i.e., temperatures prior to magma emplacement), the water moving into the intruded drifts is altered by the chemistry of the basaltic rock. This affects the mobility (solubility) of the radionuclides in the exposed waste. Radionuclides exposed to water moving into the magma-intruded drifts are transported by the groundwater downward through the UZ to the water table and then out to the accessible environment by flow and transport processes in the SZ.

Figure 6.1.4-4 schematically depicts the flow of information between the principal TSPA-LA Model components and submodels for the Igneous Intrusion Modeling Case. The flow of information between submodels in this modeling case is similar to the Nominal Scenario Class Modeling Case depicted on Figure 6.1.4-1 with some exceptions that are applied after the igneous intrusion occurs. These exceptions are described below and described in detail in Section 6.5.

- The Igneous Intrusion Modeling Case allows for all nominal processes to occur before the igneous intrusion occurs.
- As a result of the igneous intrusion, the Igneous Intrusion Modeling Case fails all WPs and DSs in the repository.
- The Igneous Intrusion Modeling Case does not include drift-wall condensation after the igneous intrusion.
- The TSPA-LA Model uses a seepage flux equal to the local percolation flux and neglects capillary diversion at the drift wall after the igneous intrusion. Therefore, the Drift Seepage Submodel response surfaces for seepage are not implemented after the igneous intrusion. The seepage response surfaces provide the seepage flow rates and seepage fractions applicable for the nominal conditions, which prevail prior to the igneous intrusion.

- For approximately the first 100 years after intrusion, waste form temperatures are perturbed by the hot intruded magma. A temperature abstraction is applied, as described in *Dike/Drift Interactions* (SNL 2007 [DIRS 177430], Section 6.7). This abstraction is used to specify waste form and invert temperatures during this period.

In addition to the changes affecting the information flow noted above, the following submodel changes are also implemented:

- In the Igneous Intrusion Modeling Case, the DSs and WPs in intruded drifts provide no further protection; therefore, DS and WP degradation, as calculated by the WP and DS Degradation model component, are no longer applicable in the intruded drifts.

- The TSPA-LA Model exposes waste that is contained in the failed WPs directly to the intruding magma. Radionuclides are then transported through the failed WPs and released to the invert where they are transported to the EBS-UZ interface.

Additional information developed to support the TSPA-LA Model in igneous intrusion groundwater transport includes the following:

- Mean annual frequency of a dike intersecting the repository.

The Volcanic Eruption Modeling Case models: (1) damage to the EBS and the amount of waste erupted to the surface, (2) the atmospheric transport and eventual deposition of the waste-contaminated ash on the land surface, (3) redistribution of the contaminated tephra, and (4) the estimate of dose to the RMEI in the Biosphere Model Component. Figure 6.1.4-5 schematically depicts the flow of information for the Volcanic Eruption Modeling Case. The volcanic eruption is modeled using the numerical code ASHPLUME (SNL 2007 [DIRS 177431]), via the ASHPLUME DLL (ASHPLUME_DLL_LA V2.1, STN: 11117-2.1-01 [DIRS 181035]) that is dynamically linked to the TSPA-LA Volcanic Eruption Model at run time. The consequences of a volcanic eruption also include the change in dose at the location of the RMEI from the transport of radioactive waste-contaminated ash through sedimentary processes that include both eolian and fluvial transport mechanisms. The Redistributed Tephra Abstraction calculates source term multipliers that are used to account for this effect at the location of the RMEI, for both interstream divide areas and distributary channels. The tephra redistribution calculations for a probability-weighted volcanic event are performed using the FAR (FAR V1.2, STN: 11190-1.2-00 [DIRS 182225]).

6.1.4.12.3 Seismic Scenario Class

This Seismic Scenario Class considers seismic disruptions (i.e., fault displacement and ground motion) as additional events that occur during the time period of evaluation. This scenario class includes two modeling cases: (1) a ground motion case for the vibratory ground motion damage to the WPs, and (2) a fault displacement case for the fault displacement damage to the WPs and DSs.

The Seismic Scenario Class describes the performance of the repository system in response to seismic events with a mean annual exceedance frequency in the range of 4.287×10^{-4} to 1×10^{-8}

per year (SNL 2007 [DIRS 176828], Table 6-88). This modeling case includes the effects of ground motion and fault displacement on the host rock, DSs, and WPs. The Seismic Scenario Class takes into account changes in seepage flux and TH on the WP surface that might occur as a result of emplacement drift degradation in the lithophysal region due to seismic events. Figure 6.1.4-6 schematically depicts the flow of information between principal TSPA-LA submodels for the Seismic Scenario Class. The flow of information between submodels in the Seismic Scenario Class is very similar to the Nominal Scenario Class, as depicted on Figure 6.1.4-1.

The majority of the submodels for the Seismic Scenario Class are the same as those implemented for the Nominal Scenario Class, with two exceptions:

- Ground motion and fault displacement damage to DSs and WPs is calculated as a function of the seismic events, in addition to the damage determined by calculations with the WAPDEG DLL for expected degradation and corrosion processes. This information is provided by *Seismic Consequence Abstraction* (SNL 2007 [DIRS 176828]).

- Drift seepage in the lithophysal and non-lithophysal units is calculated for degraded drifts. Therefore, the Drift Seepage Abstraction, including drift collapse, is implemented. In addition, drift-wall condensation ceases once the drift is fully collapsed.

Additional information that is developed to support the TSPA-LA Model for seismic damage to the DSs and WPs includes an annual frequency of occurrence for seismic events, the hazard curve for mean ground motion at a depth of 300 m beneath the surface of Yucca Mountain, and the mean hazard curves for fault displacement. Multiple seismic events over the modeled duration are included, with the impacts of each event being additive to previous events.

6.1.4.12.4 Human Intrusion Scenario

The Human Intrusion Scenario includes one Human Intrusion Modeling Case. The Human Intrusion Scenario considers the intrusion of a single water or exploratory well into the repository, through a DS and WP, and into the underlying SZ as required by 10 CFR 63.322 (DIRS 180319).

Figure 6.1.4-7 schematically depicts the flow of information between principal TSPA-LA submodels needed to calculate total system performance for the Human Intrusion Modeling Case. The flow of information between submodels in the Seismic Scenario Class is very similar to the Nominal Scenario Class, as depicted on Figure 6.1.4-1.

The majority of the submodels for the Human Intrusion Scenario are the same as those implemented for the Nominal Scenario Class (described in Section 6.3), with four exceptions:

- Mechanical damage to WPs, DSs, and cladding
- Drift seepage for the Human Intrusion Scenario
- UZ Transport for the Human Intrusion Scenario

- EBS flow for the Human Intrusion Scenario.

At the time of the human intrusion, mechanical damage to the single WP and DS is conceptualized as a patch opening the size of the drill bit. DS and WP openings due to general corrosion, MIC, SCC, and localized corrosion are not included in the Human Intrusion Scenario, instead outputs calculated by the WP and DS Degradation Model Component are replaced with a patch opening the size of the drill bit once the human intrusion has occurred. Seepage and water flow through the borehole and into the WP occurs at the percolation rate at the base of the PTn, without consideration of flow focusing. The Drift Seepage Submodel is used to calculate the seepage flux down the borehole. The EBS Flow submodel calculations that determine how much seepage penetrates the DS and WP is replaced with the assumption that all the water that flows down the borehole also flows into the WP. UZ Transport through the borehole from the WP boundary down to the water table occurs using a GoldSim pipe pathway element. The water flux through the UZ is the same as that through the EBS. UZ releases are randomly assigned to one SZ capture region. Once assigned to a capture region, the SZ and Biosphere Model Components treat the UZ releases from the borehole like UZ releases from the UZ Transport Model Component of the Nominal Scenario Class.

Additional information that is developed to support the TSPA-LA Model for inadvertent Human Intrusion through a DS and a WP includes probability of occurrence for earliest time a WP could be penetrated by drilling.

Table 6.1.4-1. Percolation Subregion Information

Percolation Subregion Number	Percolation Subregion Quantile	Number of Locations in Percolation Subregion
1	0 – 0.05	163
2	0.05 – 0.3	816
3	0.3 – 0.7	1306
4	0.7 – 0.95	816
5	0.95 – 1.0	163

Source: SNL 2007 [DIRS 181383], Section 6.2.12.1[a]

NOTE: The number of locations in each percolation subregion is calculated by multiplying the total number of locations, 3,264 (SNL 2007 [DIRS 181383], Section 6.2.12[a]), by the quantile range. Percolation subregions 1 and 5 are rounded down, while percolation subregion 3 is rounded up.

INTENTIONALLY LEFT BLANK

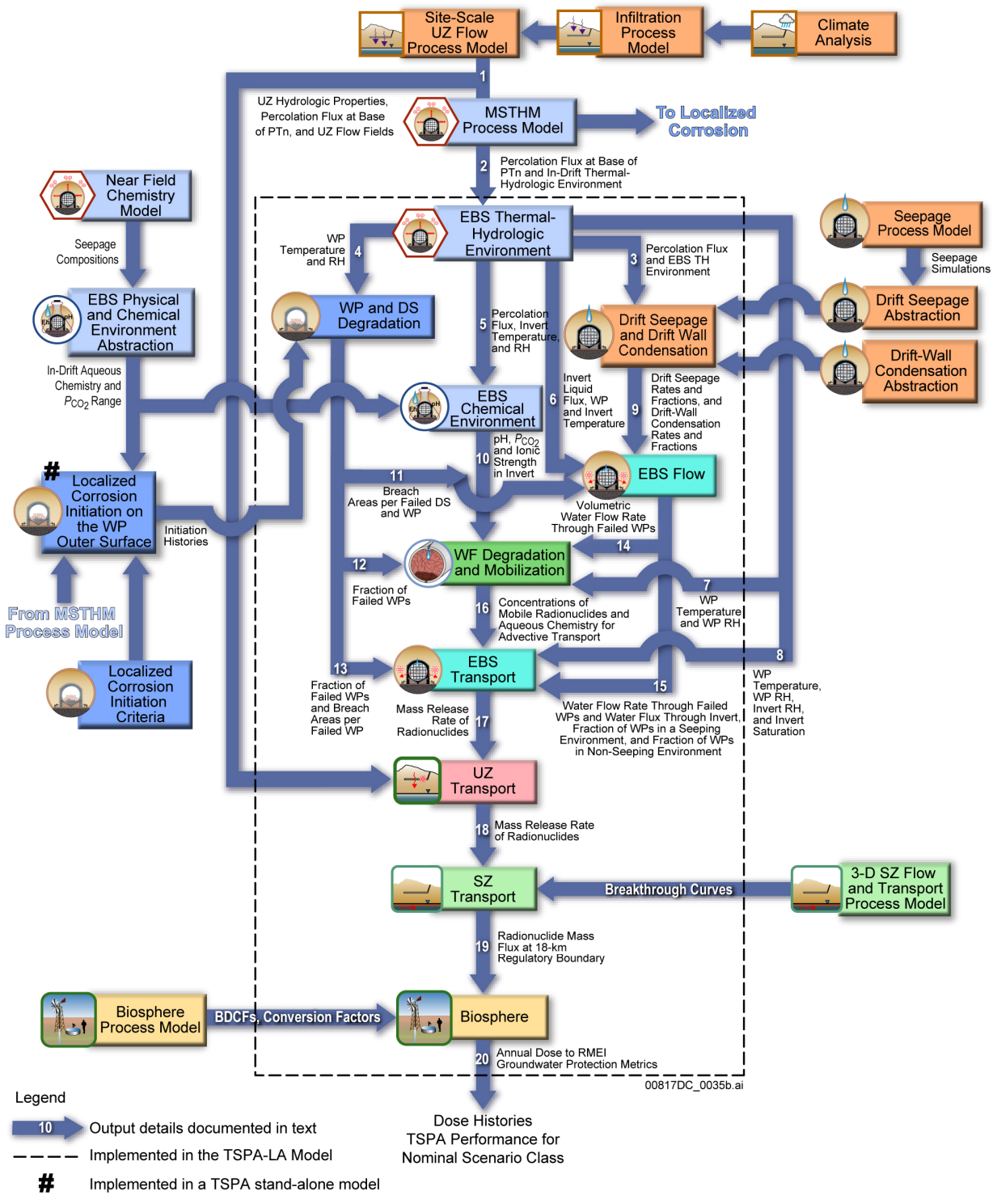

Figure 6.1.4-1. Information Transfer Between the Model Components and Submodels of the TSPA-LA Nominal Scenario Class

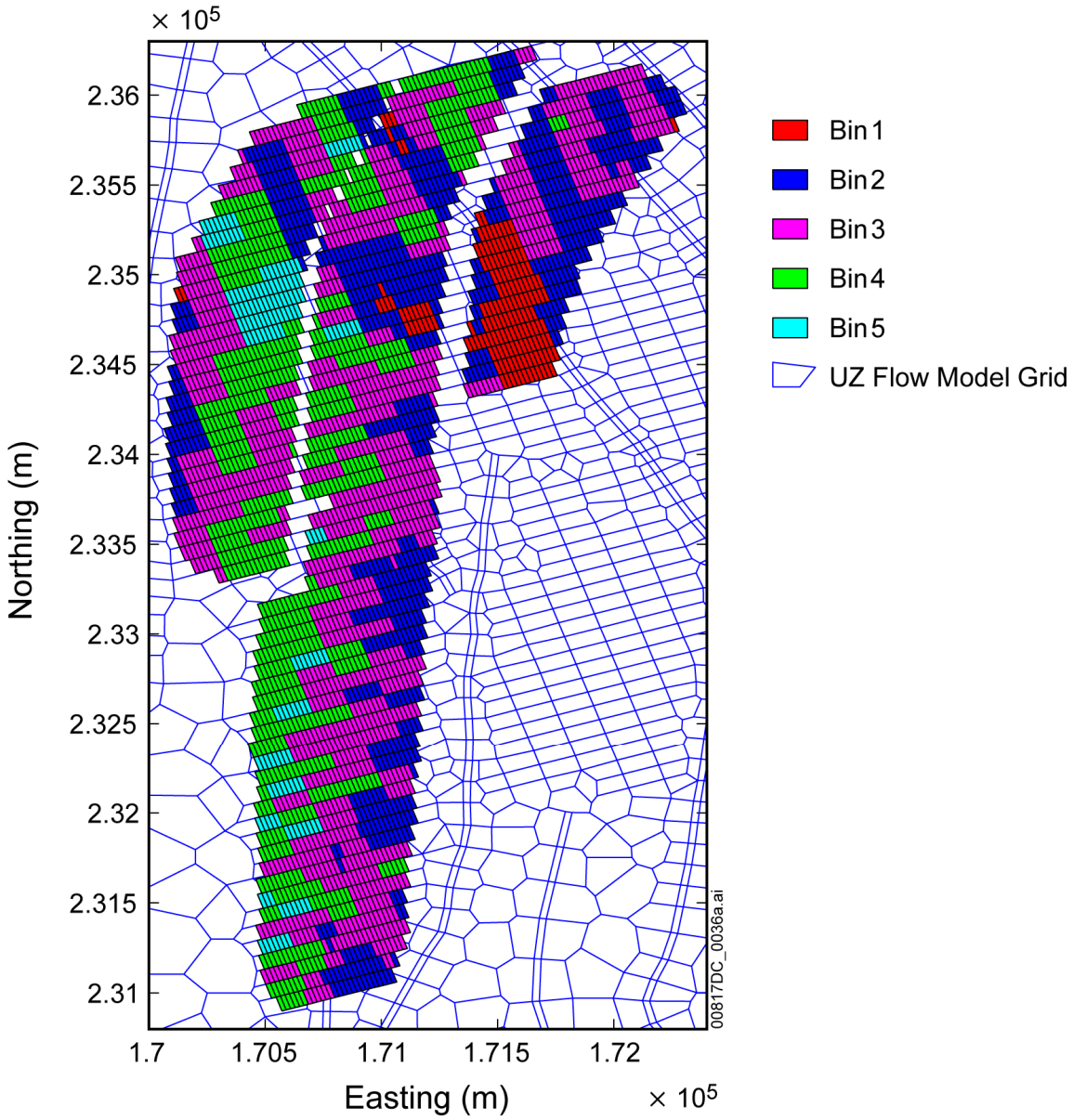

Sources: SNL 2007 [DIRS 181383], Figure VIII-1[a].

Figure 6.1.4-2. Repository Percolation Subregions Used in the TSPA-LA Model (based upon the 10th percentile percolation flux case, glacial-transition climate)

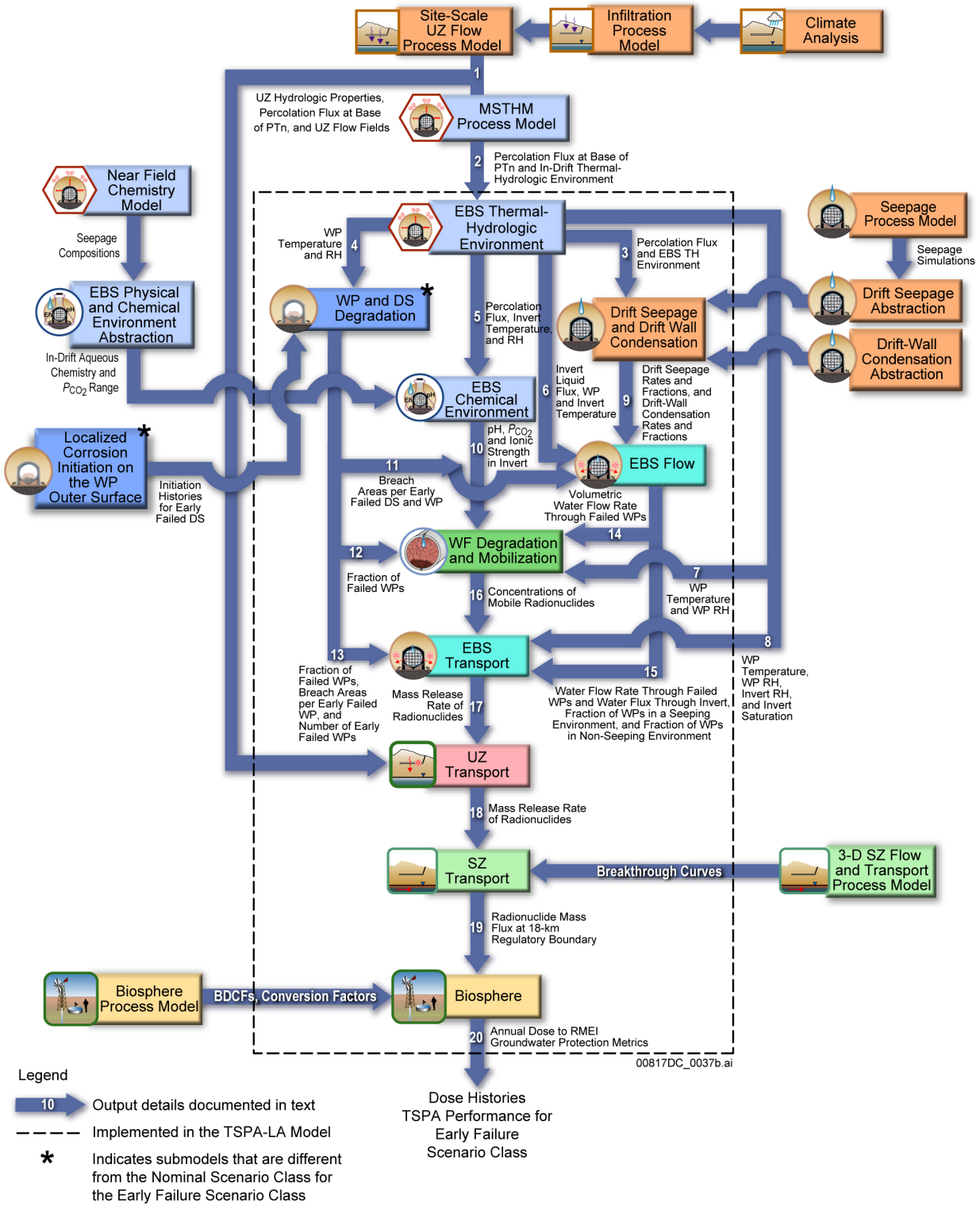

Figure 6.1.4-3. Information Transfer Between the Model Components and Submodels of the TSPA-LA Early Failure Scenario Class

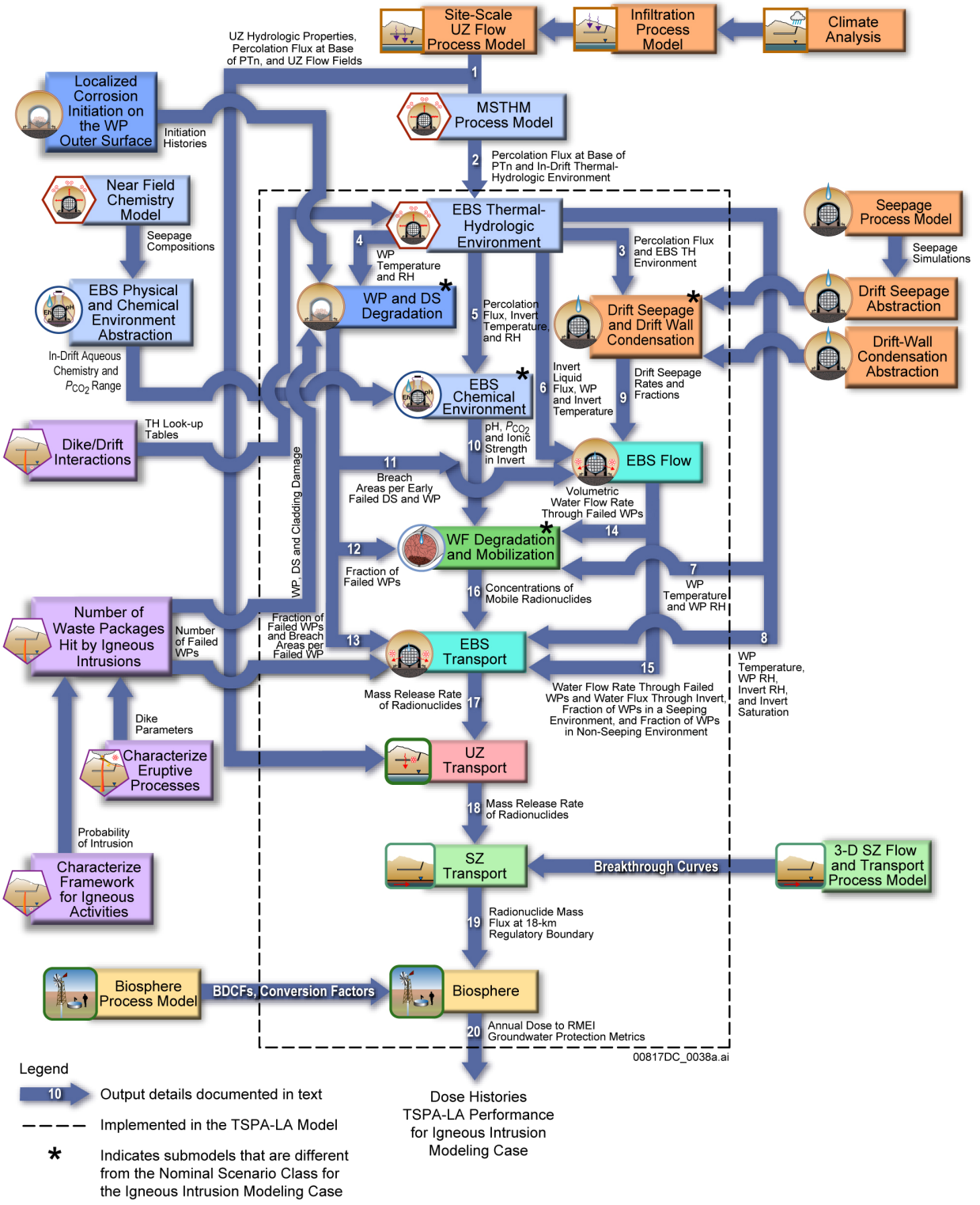

Figure 6.1.4-4. Information Transfer Between the Model Components and Submodels of the TSPA-LA Igneous Intrusion Modeling Case

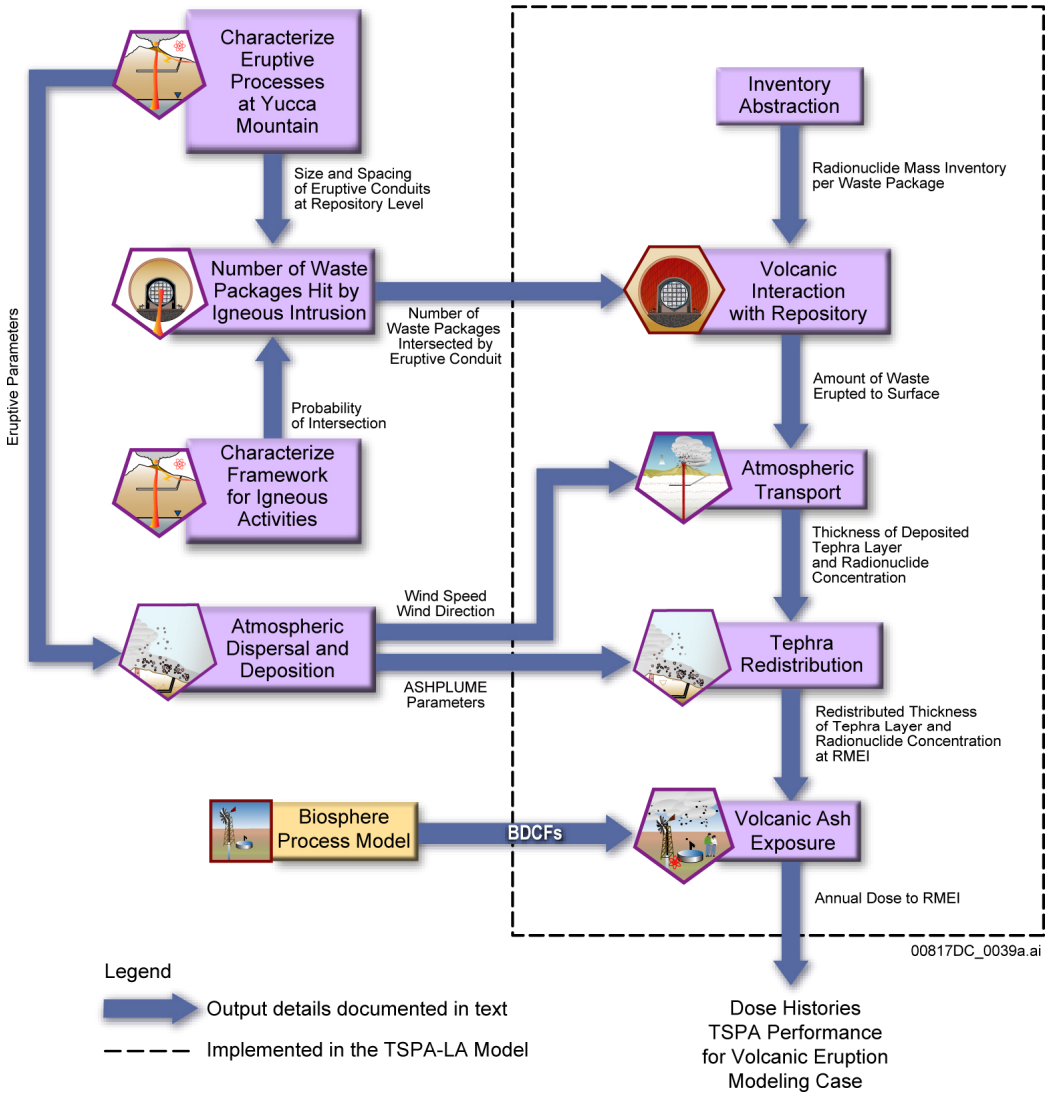

Figure 6.1.4-5. Information Transfer Between the Submodels of the TSPA-LA Volcanic Eruption Modeling Case

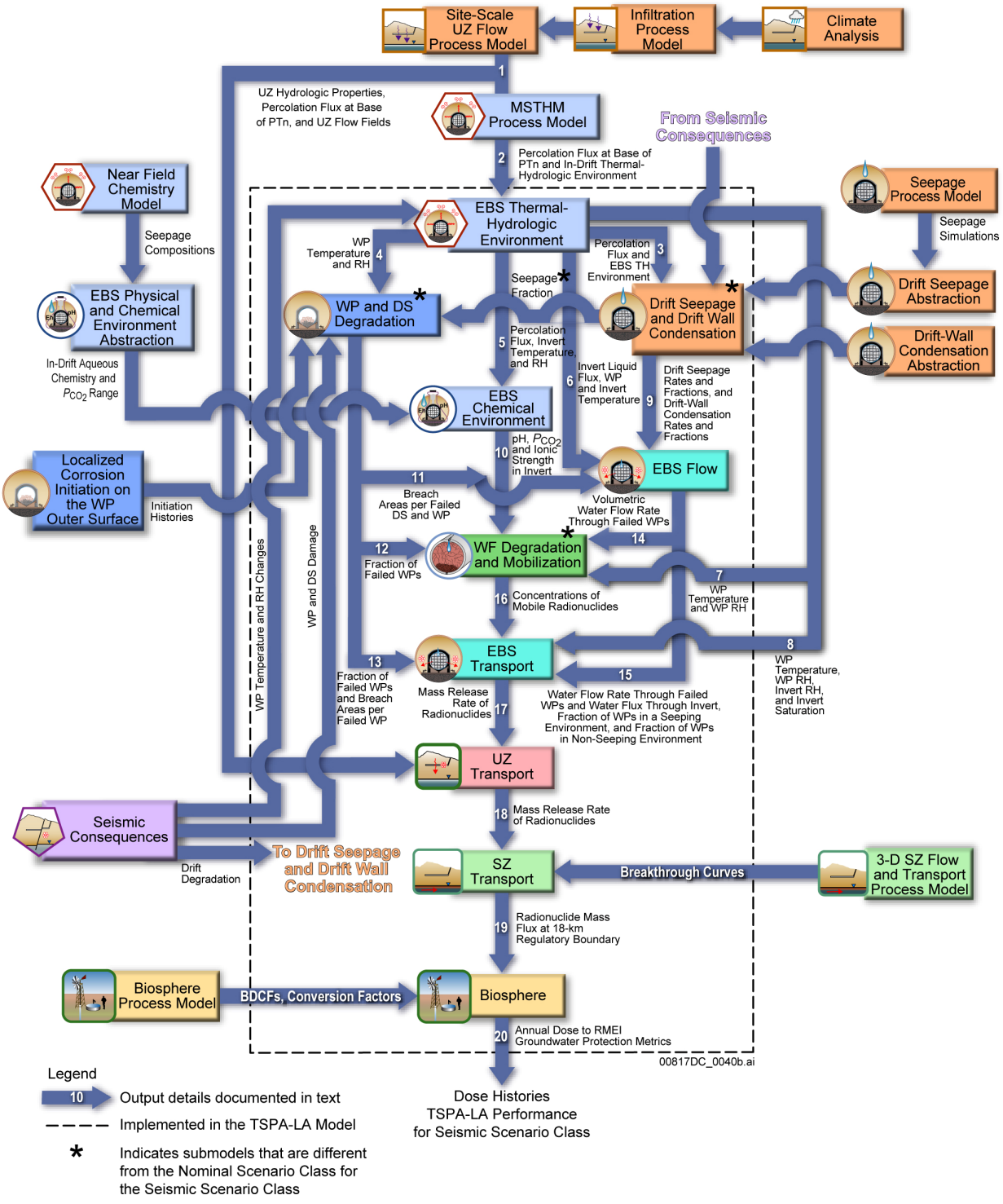

Figure 6.1.4-6. Information Transfer Between the Model Components and Submodels of the TSPA-LA Seismic Scenario Class

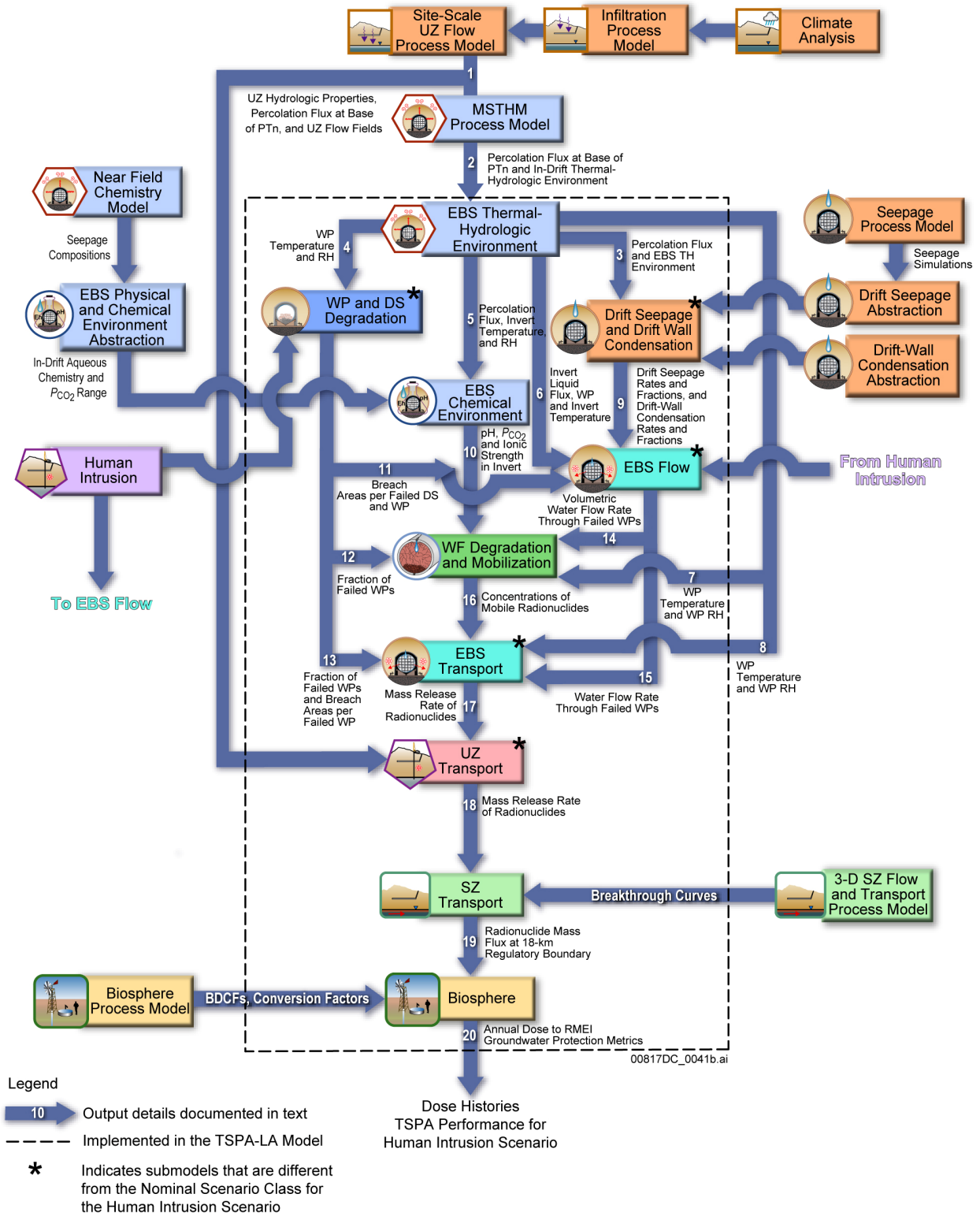

Figure 6.1.4-7. Information Transfer Between the Model Components and Submodels of the TSPA-LA Human Intrusion Scenario

INTENTIONALLY LEFT BLANK

6.1.5 TSPA-LA Model File Architecture

The overall information flow discussed above forms the basis for the TSPA-LA computational model architecture. GoldSim V9.60.100 (STN: 10344-9.60-01 [DIRS 181903]) simulation software serves as the integrating shell that links various submodels and codes that comprise the TSPA-LA Model. For many modeling cases, the TSPA-LA Model GoldSim output is further processed with EXDOC_LA V2.0 (STN: 11193-2.0-00 [DIRS 182102]) to determine the expected dose for each modeling case and a total expected dose combining all of the modeling cases.

GoldSim is a stochastic sampling program that integrates all the submodels, codes, and response surfaces together into a coherent structure that allows for consistent sampling of parameter values among the submodels. The GoldSim program is used to conduct multi-realization simulations of the entire repository system. Values of stochastic parameters for each realization are sampled from uncertainty distributions. Thus, each realization of the total system has a unique set of the values of the input parameters. In addition, each realization is considered to be equally likely, unless importance sampling is used to emphasize some realizations (usually to increase the likelihood of sampling an unlikely event or parameter value). Multiple realizations of the TSPA-LA Model yield a probability distribution of dose rate in the biosphere that shows uncertainty in dose rate based on uncertainty in all of the submodels. When an uncertain parameter appears in more than one GoldSim file (e.g., the sampled infiltration scenario is used in both the Localized Corrosion Initiation Analysis model file and the TSPA-LA Model file), replicate sampling in the two GoldSim files can be achieved by copying the distribution from one model file into the other. This feature allows for different model files to share the exact same sampling for common parameters.

GoldSim was used for five work products: (1) the TSPA-LA Model, (2) the Localized Corrosion Initiation Analysis, (3) waste form inventory decay calculation, (4) eruptive phase dose calculation, and (5) TSPA-LA Model post-implementation verification tests. Different qualified versions of GoldSim were used over the two-year period when these work products were under development.

Much of the computational work for the TSPA-LA Model is done a priori using separate software codes whose results are integrated within the GoldSim software as response surfaces, DLLs, look-up tables, and inputs. For example, the UZ flow fields are computed using the software code Transport of Unsaturated Groundwater and Heat V1.6 (TOUGH2 V1.6 (STN: 10007-1.6-01 [DIRS 161491])). This is a three-dimensional, finite-volume numerical simulator, representing the entire UZ model domain for the dual-permeability Site-Scale UZ Flow Process Model. Details of the calculation results using detailed process models are presented in analysis model reports that support the TSPA-LA Model and are described in Section 6.3. Many of the results of these detailed process-level calculations are provided to the TSPA-LA Model as multidimensional tables that are read into GoldSim at run time. Examples of these multidimensional tables include: (1) liquid flux and velocity fields for the UZ as a function of x, y, z, t, and infiltration flux, as well as other uncertain UZ rock property parameters; and (2) temperature and relative humidity as a function of time and location within the repository.

Once the GoldSim runs are completed and the modeling case dose results are exported to text files, additional software is required to calculate the expected dose for a subset of the modeling cases. The GoldSim runs provide the inputs into these additional dose calculations, which are performed by EXDOC_LA V2.0. The EXDOC_LA V2.0 code calculates the expected dose, conditional on an event occurring. The overall purpose is to separate aleatory and epistemic uncertainty. The solution is integrated over the aleatory uncertainty, for fixed values of the epistemic parameters, to calculate an expected value, conditional on one epistemic element. This operation is repeated for each sample element, to obtain a group of expected results. Statistics (i.e., mean and percentiles) are calculated for these results. The treatment of aleatory uncertainty can be thought of as an inner loop in the calculation and the treatment of epistemic uncertainty as an outer loop. Moreover, EXDOC_LA V2.0 calculates the related complementary cumulative density functions (CDFs) (and associated statistics) for a selected timestep, to allow presentation of both aleatory and epistemic uncertainty on the same graph. In order to produce representative output to be used as input to the EXDOC_LA V2.0 calculations, the TSPA-LA Model in GoldSim is configured with separate sampling of epistemic and aleatory quantities. For computing efficiency, the TSPA-LA GoldSim model is performed with specified aleatory quantities and EXDOC_LA V2.0 is used to calculate the expected dose from these GoldSim runs. As an example, the GoldSim calculations for the Igneous Intrusion Modeling Case are performed for 10 specified event times and EXDOC_LA V2.0 is used to determine the expected dose accounting for event times between these specified values. Thus, GoldSim and EXDOC_LA V2.0 are both required to generate the expected dose.

6.1.5.1 TSPA-LA Model Implementation in GoldSim

The GoldSim V9.60.100 software program is flexible in representing the various component processes in the TSPA-LA Model. The four ways that submodels may be coupled into GoldSim, from most complex to least complex, include the following:

- External function calls to detailed process software codes, such as the UZ transport software, FEHM V2.24 (STN: 10086-2.24-01-00 [DIRS 179419]), or the WP degradation software, WAPDEG V4.07 (STN: 10000-4.07-00 [DIRS 181774] and STN: 10000-4.07-01 [DIRS 181064])

- Cell or Pipe Pathway Elements in GoldSim, which are basically equilibrium batch reactors, which when linked in series, provide a description of transport through selected parts of the repository system, such as in EBS transport

- Response surfaces, which take the form of multidimensional tables, representing the results of modeling with detailed process models that are run before running the TSPA-LA Model (e.g., inputs to the EBS TH Environment, such as temperature and relative humidity in the invert)

- Functional or stochastic representations of a submodel directly built into the GoldSim code, such as seismic ground motion damage or BDCFs.

The details of implementation for specific submodels are best understood by direct review of the TSPA-LA Model implementation within GoldSim, also known as a GoldSim model file. The

text within the GoldSim model files described in this report was updated after the models were run. The updated GoldSim models with the descriptive text are part of output DTN: MO0708GWEFINAL.000_R0 [DIRS 182977].

While Sections 6.3.1 to 6.3.9 include a detailed conceptual description of the submodels included in the TSPA-LA Model, each subsection also includes a discussion of TSPA-LA Model implementation of the submodel discussed in that section with a model pathway to the appropriate location in the GoldSim model file, allowing a detailed review of the implementation. In addition, the GoldSim model file includes a description of the inputs and calculations being performed within each submodel. A summary of the locations of submodel documentation within the GoldSim model file is provided in Table 6.1.5-1.

6.1.5.2 Controlled Data: TSPA Input Database and Data Control Processes

The TSPA Input Database provides all inputs to the TSPA-LA Model. The input database captures values for fixed and uncertain parameters, coefficients in response surface equations, look-up tables, time series data, stochastic distributions, and external files used by TSPA-LA software. To ensure direct inputs to the TSPA-LA Model file are documented, they were also captured on PEFs. Inputs captured by the TSPA Input Database and PEFs consist of three general types and are documented in output DTNs (i.e., output DTN: MO0709TSPAREGS.000_R0 [DIRS 182976]). The three types of inputs are:

1. Direct inputs from controlled sources used directly in the TSPA-LA Model
2. Inputs from controlled sources, but adapted for use in the TSPA-LA Model
3. Inputs generated and used by TSPA in the TSPA-LA Model.

Inputs of the first type are acquired by TSPA analysts from the Yucca Mountain Project Technical Data Management System (TDMS) or from the analysis model reports that provide input to the TSPA-LA Model. These inputs are used directly in the TSPA-LA Model without modification. These parameter values are entered in the TSPA Input Database and captured on a PEF.

Inputs of the second type are also acquired by TSPA analysts from the Yucca Mountain Project TDMS or from the analysis model reports that provide input to the TSPA-LA Model. These inputs are used directly in the TSPA-LA Model with minor formatting. In some instances, prior to entering inputs into the TSPA Input Database, input values are modified by a TSPA analyst to be compatible with the form required by TSPA-LA software or applicable submodels. Such modifications are simple modifications and may include rounding to a specified number of significant digits, removing duplicate input values in defined look-up tables, sorting input values numerically, or converting inputs to units required by the appropriate TSPA-LA submodel or analysis. The changes made by the TSPA analyst are captured on PEFs.

Inputs of the third type are acquired by TSPA analysts from the Yucca Mountain Project TDMS or from the analysis model reports that provide input to the TSPA-LA Model and are processed by TSPA analysts before being captured in the TSPA Input Database and on a PEF. Inputs of the third type include formatting direct inputs through the use of TSPA Department-generated software, manipulating inputs from controlled sources to be consistent with TSPA-LA

conceptual models, and correlating and sampling of the values of the uncertain parameters used both internally by the TSPA-LA Model and TSPA-LA Localized Corrosion Initiation Analysis GoldSim files, and externally by TSPA-LA Model and TSPA-LA Localized Corrosion Initiation Analysis DLLs. In addition, TSPA analysts generate input files used external to the TSPA-LA Model and TSPA-LA Localized Corrosion Initiation Analysis GoldSim files by other qualified software. Like inputs of the first and second type, the changes made by TSPA are captured on PEFs. In the event that substantial preprocessing is required by the TSPA Department, a TSPA analyst performs the preprocessing calculations, submits the information to the Yucca Mountain Project TDMS, including all pertinent documentation, and retrieves the information from the TDMS or a controlled source for use in the TSPA-LA Model.

Figures 6.1.5-1 through 6.1.5-6 depict a sequence of process steps that take place in order to initialize and run the TSPA-LA Model. The initial figure (Figure 6.1.5-1) provides an illustrated overview of all the various elements that make up the framework required for initializing and running the TSPA-LA Model. The framework includes project documents and databases (i.e., analysis model reports and TDMS), as well as elements that are specific to the TSPA-LA Model (i.e., controlled files on the TSPA-LA Model file server and in the TSPA Input Database). PEFs are the most important documents for ensuring traceability of information for all inputs, whether from sources supporting TSPA or intermediate inputs produced during the execution of the TSPA-LA Model. A full discussion of PEFs can be found in Section 4.3. The arrows on the figure illustrate the transfer of information or software. Information transfers include input parameter values and files generated as part of a preprocessing step. Figures 6.1.5-2 through 6.1.5-6 describe the succeeding steps in the processing input data to the TSPA-LA Model. For each figure, the elements in use for the step being discussed will be shown in the lighter of the two colors. The dashed lines on the figure indicate cases where the location of files and software are stored in the TSPA Input Database, but the information or software are actually accessed from the TSPA-LA Model file server.

Input parameter values are loaded into the TSPA Input Database (Figure 6.1.5-2). Parameter values that are in files (e.g., UZ flow fields) are placed in a controlled directory on the TSPA-LA Model file server. The locations of those files are stored in the TSPA Input Database, along with the MD5 digital signature identifying the file. The majority of the input parameters are taken from analysis model reports and the TDMS. Inputs are also taken from other sources (e.g., NRC Proposed Rule 10 CFR Part 63 [DIRS 178394] and [DIRS 180319]) or are generated by the TSPA Department. DLLs are obtained from Software Configuration Management and are installed in a controlled directory on the TSPA-LA Model file server. The locations of those DLLs are stored in the TSPA Input Database, along with the MD5 digital signature identifying the DLL. The traceability of the values of the input parameters and DLLs is documented on PEFs. Any modifications to the original source input (e.g., a change in significant figures, unit conversion) are documented as part of the PEF.

The TH information provided by the MSTHM Abstraction is preprocessed by the PREWAP_LA V1.1 code (STN: 10939-1.1-00 [DIRS 181053]) and the resultant preprocessed PREWAP TH files are documented by a PEF (Figure 6.1.5-3). The set of PREWAP TH files are placed in the TDMS and also placed in a controlled directory on the TSPA-LA Model file server and the location of the files is stored in the TSPA Input Database.

Input parameters values are downloaded from the TSPA Input Database to the localized corrosion analysis in the GoldSim model file (Figure 6.1.5-4). The file is then run for the same number of realizations as the TSPA-LA Model to generate localized corrosion failure histories for each modeling case that includes localized corrosion. A database download is performed to transfer input files (e.g., PREWAP TH files) and the DLLs (i.e., PassTable3D_LA V2.0 (STN: 11143-2.0-00 [DIRS 182556])) associated with the files to the directory where the localized corrosion analysis file runs. The file is run three times, once for the Nominal Modeling Case, once for the Seismic GM Modeling Case, and once for the Seismic FD Modeling Case (Section 6.3.5.2.3). The values of uncertain parameters sampled in the Localized Corrosion Initiation Analysis model file are perfectly correlated to the same distributions sampled within the TSPA-LA Model file. Therefore, each realization of the Localized Corrosion Initiation analysis matches up to the same realization of the TSPA-LA Model GoldSim file. The information for the localized corrosion initiation files is extracted from the localized corrosion analysis file. A PEF is generated to document the production of the localized corrosion initiation files. Then, the localized corrosion analysis files are placed in the TDMS and also placed in a controlled directory on the TSPA-LA Model file server. The locations of the files are stored in the TSPA Input Database.

UZ_PARAMS_MULTI_LA_COMPLIANCE files contain samples of the values of uncertain parameters used in the UZ Transport Model Component (Section 6.3.9) and are generated by running the TSPA-LA Model GoldSim model file (Figure 6.1.5-5). Input parameters values are downloaded from the TSPA Input Database to the TSPA-LA Model GoldSim model file. The database download also transfers input files and the DLLs associated with the file to the directory from which the TSPA-LA Model GoldSim model file is run. Because the TSPA-LA Model is run only to sample the values of uncertain UZ parameters needed for the UZ_PARAMS_MULTI_LA_COMPLIANCE file, it can be configured to run for only the first two timesteps. TSPA-LA Model runs are made for the number of epistemic realizations that the TSPA-LA Model is configured to run (i.e., 300 and 1,000 realizations) (Section 6.3.9.3). The values of the UZ uncertain parameters required for a UZ_PARAMS_MULTI_LA_COMPLIANCE file are extracted and put into the UZ_PARAMS_MULTI_LA_COMPLIANCE files. A PEF is generated to document the production of the UZ_PARAMS_MULTI_LA_COMPLIANCE files. Those files are then placed in a controlled directory on the TSPA-LA Model file server. The locations of those files are stored in the TSPA Input Database. Once all the input parameters to the TSPA-LA Model are pre-processed for use by the TSPA-LA Model, the input parameter values are downloaded from the TSPA Input Database to the TSPA-LA Model (Figure 6.1.5-6). The database download also transfers input files, and the DLLs associated with the files, to the directory from which the TSPA-LA Model GoldSim model file is run.

Figure 6.1.5-7 illustrates the linkages between the software that supports the execution of the TSPA-LA GoldSim model file and the separate GoldSim model file for the Volcanic Eruption Modeling Case. Most of the software consists of DLLs that are called by GoldSim at run time. The software and their functions are described in Section 3. The Localized Corrosion Initiation Analysis is a separate GoldSim model file (Figure 6.1.5-8). This figure illustrates the linkages between the software and the relation of the software to the TSPA-LA Model components discussed in Section 6. The submodels for EBS thermal-hydrology, EBS chemistry, drift seepage, DS degradation, and seismic consequences for the Seismic GM and FD Modeling Cases

and the associated DLLs are implemented in both the GoldSim model file and in the GoldSim model file for the Localized Corrosion Initiation Analysis.

6.1.5.3 Implementation File Structure for the TSPA-LA Model

The layout of calculation containers in GoldSim provides a framework for discussing the implementation of the TSPA-LA Model in GoldSim. Understanding the roles of the containers and their contents is essential for navigating through the TSPA-LA Model files. The layout of containers in the GoldSim software generally follows the Section 6.3 discussion of the model components and submodels, but there are differences at the detail level.

The container structure represents the end result of the construction and evolution of the GoldSim model file developed by TSPA analysts. The end result is a complex file structure that meets the requirements of the TSPA-LA Model. This section is designed to provide information that will facilitate investigation of the TSPA-LA Model and the associated GoldSim model file.

GoldSim Submodels—The TSPA-LA Model implemented in GoldSim contains three GoldSim submodels embedded in one main GoldSim model. Each GoldSim submodel is a completely separate model within the main model and each has it own simulation settings. A GoldSim submodel is a special GoldSim element that performs a complete simulation and passes calculated results to the main model. The three GoldSim submodels in the TSPA-LA Model are: (1) the Epistemic Parameters GoldSim Submodel, (2) the Aleatory Parameters and Dynamic Calculations GoldSim Submodel, and (3) the EBS GoldSim Submodel. A description of each GoldSim Submodel is presented below. The main model sets the simulation settings for these three embedded models and then calls upon each model to perform its simulation. Once all three embedded models have performed their simulation, the main model receives the results and then performs the calculations for the UZ Transport, SZ Flow and Transport, and Biosphere Model Components using these results.

The Epistemic Parameters GoldSim Submodel is a static model that samples distributions of the values of parameters that characterize epistemic uncertainty. The Epistemic Parameters GoldSim Submodel (GoldSim element name: Epistemic_Params) is located in the Epistemic_Uncertainty container shown on Figure 6.1.5-9 and is one containment level below the Epistemic_Uncertainty container level inside the GoldSim model file. Table 6.1.5-1 provides the GoldSim model file pathway to the Epistemic Parameters GoldSim Submodel. The output of the Epistemic Parameters GoldSim Submodel is a suite of values for all parameters that are characterized by epistemic uncertainty. No additional distributions characterize epistemic uncertainty within the TSPA-LA Model or any of the other two GoldSim submodels. These values may be determined by sampling uncertain distributions or may be determined by the evaluation of time-independent calculations that include values sampled from uncertain distributions. The Epistemic Parameters GoldSim Submodel is a small GoldSim model embedded in a larger model and hence it has its own Monte Carlo simulation settings. Because it has its own Monte Carlo simulation settings, the Epistemic Parameters GoldSim Submodel can perform a unique Latin Hypercube Sampling for all realizations performed by the TSPA-LA Model, or it can repeat sequences of sampled values. Within the suite of modeling cases that are performed, the TSPA-LA Model invokes both sampling options within the Epistemic Parameters GoldSim Submodel. In order of calculation hierarchy, the Epistemic Parameters GoldSim

Submodel provides values to both the Aleatory Parameters and Dynamic Calculations GoldSim Submodel and the EBS GoldSim Submodel, as well as to the calculations for the UZ Transport, SZ Flow and Transport, and Biosphere Model Components performed in the main model.

The Aleatory Parameters and Dynamic Calculations GoldSim Submodel is a dynamic model that samples distributions of the values of parameters that characterize aleatory uncertainty and performs additional dynamic calculations utilizing these sampled values. The Aleatory Parameters and Dynamic Calculations GoldSim Submodel (GoldSim element name: Aleatory_Params) is located in the Time_Zero container shown on Figure 6.1.5-9 and is one containment level below the Time_Zero container level inside the GoldSim model file. Table 6.1.5-1 provides the GoldSim model file pathway to the Aleatory Parameters and Dynamic Calculations GoldSim Submodel. The output of the Aleatory Parameters and Dynamic Calculations GoldSim Submodel is a suite of calculated values and time histories for all of the parameters that are characterized by aleatory uncertainty. No additional distributions characterize aleatory uncertainty within the TSPA-LA Model or any of the other two GoldSim submodels. These values may be determined by sampling uncertain distributions or by calculations that include values sampled from uncertain distributions. Because the Aleatory Parameters and Dynamic Calculations GoldSim Submodel is a dynamic model, it has a simulation clock and can perform time-dependent calculations. If a calculation includes an epistemic quantity, the value of the epistemic quantity is first determined in the Epistemic Parameters GoldSim Submodel and then passed into the Aleatory Parameters and Dynamic Calculations GoldSim Submodel. The Aleatory Parameters and Dynamic Calculations GoldSim Submodel is a small GoldSim model embedded in a larger model and hence it has its own Monte Carlo simulation settings. Because it has its own Monte Carlo simulation settings, the Aleatory Parameters and Dynamic Calculations GoldSim Submodel can perform a unique Latin Hypercube Sampling for all realizations performed by the TSPA-LA Model, or it can repeat sequences of sampled values. Within the suite of modeling cases that are performed, the TSPA-LA Model invokes both sampling options within the Aleatory Parameters and Dynamic Calculations GoldSim Submodel. The Aleatory Parameters and Dynamic Calculations GoldSim Submodel provides calculated values to the EBS GoldSim Submodel, discussed next, but does not provide values to the Epistemic Parameters GoldSim Submodel and does not directly provide any transport-related values to the UZ Transport, the SZ Flow and Transport, or the Biosphere Model Components performed in the main model. In order of calculation hierarchy, the Aleatory Parameters and Dynamic Calculations GoldSim Submodel receive values from the Epistemic Parameters GoldSim Submodel and provide values to the EBS GoldSim Submodel.

The EBS GoldSim Submodel is also a dynamic model. With the exception of some static calculations that determine the size of the WP groups modeled by the GoldSim source term elements and the fractional failure history of each WP group, this embedded model performs all of the EBS-related calculations that support the UZ Flow, EBS Environment, WP and DS Degradation, Waste Form Degradation and Mobilization, and EBS Flow and Transport Model Components. The EBS GoldSim Submodel (GoldSim element name: EBS_Submodel) is located in the Time_Zero container shown on Figure 6.1.5-9 and is three containment levels below the Time_Zero container level inside the GoldSim model file. Table 6.1.5-1 provides the GoldSim model file pathway to the EBS GoldSim Submodel. The output of the EBS GoldSim Submodel provides the time histories of radionuclide flux from the bottom of the invert into the UZ beneath the repository, taking into account all repository-related processes. The EBS

GoldSim Submodel does not sample any uncertain distributions. Inputs to the EBS GoldSim Submodel include sampled values of epistemic parameters from the Epistemic GoldSim Submodel and all of the values of the aleatory parameters and associated time history results from the Aleatory Parameters and Dynamic Calculations GoldSim Submodel. In addition, the TSPA-LA Model performs additional calculations between performing the calculations of the Aleatory Parameters and Dynamic Calculations GoldSim Submodel and the EBS GoldSim Submodel. These calculations are static calculations that populate the number of WPs in each GoldSim source term within the EBS GoldSim Submodel and also determine the fraction of WPs that are exposed to drift seepage and the time history of WP failures from general and localized corrosion. These static calculations involve external DLLs that perform the related calculations necessary to model the EBS.

Looping Containers—Unlike the Epistemic GoldSim Submodel and the Aleatory Parameters and Dynamic Calculations GoldSim Submodel, the EBS GoldSim Submodel is placed within looping containers. A looping container is another special GoldSim element that allows the calculations within the container to be repeated in a DO-WHILE loop. The EBS GoldSim Submodel simulation is performed in 15 loops within one realization of the TSPA-LA Model, one loop for each of 15 WP groups. Each of the 15 WP groups is described by a set of average properties for the entire group. Combining groups of WPs that have similar properties results in average properties that are derived from a subset of WPs that have less variation. For the TSPA-LA Model, the WP properties that define the different WP groups are: (1) the percolation flux rate above the WP location, (2) the occurrence of drift seepage above the WP location, and (3) whether or not drift seepage-induced localized corrosion damages the WPs at a WP location. Choosing the number of WP groups to model balances computational efficiency against the most important processes that govern releases from the EBS. Using a looping container over each WP group ensures that the calculations that are performed for each WP group are consistent with the calculations performed for the other groups. Therefore, the TSPA-LA Model models the EBS GoldSim Submodel in 15 different loops, each loop models a different WP group. The 15 loops are actually performed in two loops, an outer loop (called EBS_PS_Loop in the GoldSim model file), referred to as the percolation subregion loop, and an inner loop (EBS_PSE_Loop in the GoldSim model file), referred to as the percolation subregion environment loop. The outer loop is performed five times, once for each percolation subregion. These five loops account for spatial variability in the percolation flux above the repository. This discretization is described in detail in Section 6.3.2 of this report. Within each of these five percolation subregion loops, the EBS GoldSim Submodel performs calculations for three additional loops, bringing the total number of loops to 15. These three loops consider two different drift seepage conditions above each WP location and two different damage mechanisms to the WP. The first loop considers all the WPs in a percolation subregion that are not exposed to drift seepage. The fraction of WPs that are exposed to drift seepage is determined by the Drift Seepage Submodel of the UZ Flow Model Component. The second loop models all WPs that are exposed to drift seepage and do not experience localized corrosion in the modeled duration. The third loop models all WPs that are exposed to drift seepage and experience localized corrosion in the modeled duration. The distinction between seepage locations and non-seepage locations is important because advection and diffusion from a failed WP can result in greater mass release than for diffusion release alone. Advection from the WP can only occur if there is a water source dripping onto a failed WP. The distinction between localized corrosion packages and non- localized corrosion packages is important when considering the opening area on the WP. The rate of advection and diffusion

from a failed WP is proportional to the opening area on the failed WP. In the absence of localized corrosion, crack damage from SCC (Section 6.3.5) and/or seismic ground motion (Section 6.6.1) has a different release rate than a WP with localized corrosion patch openings that completely penetrate the WP. Appendix N presents the derivation of the equations used to calculate the number of WPs (referred to as WP parsing) modeled by each WP group.

High Level Containers—The highest level of the GoldSim model file is a set of containers that define the overall organization of the GoldSim model file (Figure 6.1.5-9). These containers are not all of the same type or size. Global_Model_Input (Figure 6.1.5-9) stores the configuration properties for the TSPA-LA Model and other inputs referenced throughout the TSPA-LA Model. Epistemic_Uncertainty (Figure 6.1.5-9) contains the Epistemic Parameters GoldSim Submodel. Time_Zero (Figure 6.1.5-9) contains both the Aleatory Parameters and Dynamic Calculations GoldSim Submodel and the EBS GoldSim Submodel. This container is a conditional container that performs dynamic calculations prior to advancing the simulation clock controlling the calculations performed for the UZ Transport, SZ Flow and Transport, and Biosphere Model Components in the main model. The calculations for these model components are captured within the TSPA_Model (Figure 6.1.5-9) container. In general, within these high-level containers or the GoldSim Submodels embedded directly beneath them, the model elements that define the input parameters and perform calculations are grouped into nine containers, one for each of the eight principal model components, shown on Figure 6-1, and one for events. Understanding the containers and their organization is important for navigating through the GoldSim model file and finding information, but they do not always correspond to the conceptual organization of the TSPA-LA Model discussed elsewhere in this report. For instance, within the Aleatory Parameters and Dynamic Calculations GoldSim Submodel, the Aleatory_Calcs_Seismic container contains information related to the Seismic Scenario Class, discussed in Sections 6.1.4.12.2 and 6.5, but does not contain all of the submodels involved in representing the Seismic Scenario Class. Additional inputs and calculations are defined in the Epistemic Parameters GoldSim Submodel and within the EBS GoldSim Submodel where radionuclide releases from seismic-damaged WPs are modeled.

The conceptual TSPA-LA Model discussion focuses on model components and submodels that can be divided, at the highest level, between natural system models and engineered system models. The following discussion will define, at a high level, the implementation of these models in the GoldSim model file.

Submodel Organization—The TSPA-LA Model is a system of scientific models and abstractions sharing numeric information and linked together in the GoldSim software. In general, the TSPA-LA Model is composed of eight principal model components and an event scenarios component. Each model component is itself a system of dynamic calculations performed by one or more submodels. Within a model component container, the submodels that comprise the model component are organized into separate containers. Each submodel may be a function of the calculated values from other submodels within the same model component or another model component. To enhance transparency, each submodel is further organized into separate containers for inputs, calculations, and outputs. The inputs to a submodel may include parameter definitions and results from other submodels. These two types of inputs are segregated into Model_Input and Model_Feed containers, respectively. The calculations for each submodel are performed in a Model_Calcs container. The outputs of the submodel that are

passed to other submodels are captured in a Model_Output container. The elements within the Model_Feeds container of one submodel are linked to the elements within the Model_Output container of another.

Representation of the Natural System above the Repository—The natural system above the repository includes the land surface, the soil and rock near the land surface, and the UZ above the repository. The information pertaining to this part of the repository system is located in three locations in the TSPA-LA Model. Uncertain inputs are captured in the Epistemic_Params_UZ_Flow and Epistemic_Calcs_UZ_Flow containers within the Epistemic Parameters GoldSim Submodel. Additional input parameters and UZ flow calculations are located in the Time_Zero container. Static calculations to obtain the fraction of WPs that are exposed to drift seepage, which is used to determine the number of WPs to model in each WP group, are located in the Static_Calcs_UZ_Flow container. These static calculations are located in the percolation subregion (outer) loop of the EBS calculations. Therefore, the UZ Flow calculations in the Static_Clacs_UZ_Flow container are performed five times, once in each percolation subregion loop. Within each percolation subregion loop, the inputs to the UZ Flow calculations are appropriate for the active percolation subregion and thus the calculated values of the UZ Flow Model Component will vary in each percolation subregion loop. The rest of the calculations that are part of the UZ Flow Model Component are found within the Global_UZ_Flow, Seep_Params and Condensation_Model containers within the EBS GoldSim Submodel. The calculations inside these three containers are performed 15 times, once for each outer loop and inner loop pair of the EBS GoldSim Submodel. For each loop, implementation using IF…THEN…ELSE functions allows the inputs to the UZ Flow calculations to change to the appropriate values for the active percolation subregion and seeping environment type. However, because WP damage by localized corrosion does not affect UZ Flow properties, the calculated values of the UZ Flow Model Component within one percolation subregion loop will be the same in the second and third percolation subregion environment loops. Combining all of this information, the UZ Flow Model Component includes information on climate state, infiltration, seepage into drifts, and drift-wall condensation.

Representation of the Engineered System—The calculations that model the performance of the Engineered_System are located in four locations in the TSPA-LA Model. Uncertain inputs are captured in the Input_Params_Epistemic container within the Epistemic Parameters GoldSim Submodel. Within this container, the input parameters are further organized into containers defined for each EBS Model Component, EBS Environment, WP and DS Degradation, Waste Form Degradation and Mobilization, and EBS Flow and Transport. Within each of these model component containers, the uncertain inputs may be further organized into separate containers for each submodel of the model component. The level of discretization within the Epistemic Parameters GoldSim Submodel increases with increasing complexity of the model component. Additional input parameters and EBS calculations are located in the Time_Zero container. Dynamic calculations related to the chemical interaction between seepage water and the host rock and the integrity of the DS under nominal conditions are performed in the Aleatory Parameters and Dynamic Calculations GoldSim Submodel. The water-rock interaction calculation is discussed in detail in Section 6.3.4. The nominal corrosion of the DS is discussed in Section 6.3.5. Static calculations that are used to determine the number of WPs to model in each WP group, the WP Parsing Submodel, and localized corrosion and general corrosion failures of the WP are located in the Static_Calcs_PS_Loop container. Two of the four EBS-

related model components have calculations within this container, WP and DS Degradation and EBS Flow and Transport. These calculations are located in the percolation subregion (outer) loop of the EBS calculations. Therefore, the EBS calculations in the Static_Calcs_PS_Loop container are performed five times. Each time the inputs to the calculations are appropriate for the active percolation subregion and thus the calculated values will vary in each loop. The rest of the calculations that model the EBS are found within the EBS GoldSim Submodel. The EBS GoldSim Submodel container includes a greater variety of information than any of the other containers. The overall discretization of WP groups and the structure of the container are shown on Figure 6.1.5-10. Some aspects of the implementation of the EBS submodels can be characterized as global and are independent of details such as fuel type or location within the repository. Much of the implementation, however, is dependent on the discretization of the submodel by waste type, percolation flux subregion or bin, and seepage environment.

The first level of discretization is by waste type. The TSPA-LA Model considers two types of WPs: CSNF and CDSP WPs. These WPs represent all of the WP types considered in the TSPA-LA Model. Details of how this representation is developed are found in Section 6.3.2.2.2. Within the TSPA-LA Model, discretization by waste type is handled explicitly by implementing different GoldSim elements to perform the fuel type-specific calculations.

The second level of discretization is by percolation subregion. The magnitude of infiltration varies spatially across the land surface above the repository footprint and percolation flux varies spatially at the repository level. This spatial variability is captured in a CDF of percolation flux values that are calculated for 3,264 locations (SNL 2007 [DIRS 181383], Section 6.2.12.1[a]). This CDF provides the basis for the TSPA-LA Model representation by percolation subregions, as described in Section 6.3.2. Percolation subregion locations are shown on Figure 6.1.4-2.

The third level of discretization is by seeping environment (i.e., seepage with or without drift-wall condensate) and localized corrosion failure mode. The CSNF and CDSP WPs that are in each percolation subregion are identified as either having seepage above each WP location or not. Those that have seepage are further discretized into two groups, those that experience localized corrosion damage and those that do not experience localized corrosion damage.

The three levels of discretization result in the 30 environments in the TSPA-LA Model (two fuel types × five percolation flux subregions × three seepage/ localized corrosion states) that are used to represent all of the WPs in the repository.

Figure 6.1.5-11 illustrates how the repository is conceptualized with the three levels of discretization discussed above. The representation is purposely a schematic to emphasize the conceptually important aspects of the discretization. The left portion of the figure shows the percolation flux subregions, as defined in Section 6.1.4.2, superimposed on the repository footprint. The rest of the figure shows a schematic representation of these subregions (the boxes) and illustrates the discretization by waste type and seeping/localized corrosion conditions. The levels of discretization shown on Figure 6.1.5-10 together with the repository conceptualization shown on Figure 6.1.5-11 lead to the implementation found in the GoldSim model file.

The discretization structure determines the type of information that is included in the containers at each level. Containers at the highest level of Global_Inputs_and_Calcs in the EBS GoldSim

Submodel, the Global_WP_DS_Deg, Global_EBS_Environ, Global_WF_Deg_Mob, and Global_EBS_F_and_T containers, include global inputs, such as the corrosion rate for Alloy 22, the chemistry inside a failed WP under seeping or non-seeping conditions, and the regression coefficients in the waste form degradation rate equations. This is information used for all percolation flux subregion environments.

At the level of discretization by waste type, the CSNF_Packages and CDSP_Packages containers within the EBS GoldSim Submodel, GoldSim containers include information needed to evaluate processes that are specific for each fuel type.

The next level of discretization is by percolation subregion environment and refers to the 30 environments defined on Figure 6.1.5-10. As stated earlier, the TSPA-LA Model captures the required EBS calculations for all 15 CSNF environments in one container and for all 15 CDSP WP environments in another container. These two calculation containers accommodate the 30 environments by using IF…THEN…ELSE functions to vary the calculation inputs to those specific for each of the 30 environments. The detailed source term calculations are performed within each of these two percolation subregion environment containers. Parameter values identified here include the temperature and relative humidity of the invert and WP surface, reading WAPDEG V4.07 DLL output to determine crack and patch failures, and chemical parameters for the WP and invert for dripping and non-dripping conditions, solubilities of radionuclides in the invert and in the WPs, which are values that are determined from look-up tables that are defined elsewhere. At this level, the TSPA-LA Model also calculates the mass flux of radionuclides at the base of the invert.

Once calculated, results of EBS conditions and radionuclide mass flux rates are passed from each loop to TS_PROC.DLL. This is a specialized GoldSim DLL that stores and segregates results for each outer loop of a GoldSim submodel. For results that differ for each inner loop, the DLL can be configured to add or average the results of each inner loop. The model components that comprise the EBS are discussed in additional detail in Sections 6.3.2 through 6.3.8.

Representation of the Natural System Below the Repository—The natural system below the repository includes the UZ, the SZ, and the biosphere. Related model components are shown on Figure 6-1 and are present in the TSPA_Model container at the highest level of the GoldSim model file. Within the TSPA_Model container there are six high level containers. The UZ_Flow container is a repeat implementation of the Climate Submodel of the UZ Flow Model Component. This information is used by the UZ Transport and SZ Flow and Transport Model Components. The Engineered_System container captures the radionuclide mass flux from the bottom of the invert into the UZ beneath the repository and the number of failed WPs. This information is fed directly into the UZ Transport Model Component from within this container. In addition, this container also captures EBS-related results that are useful for model analysis. The calculations for the model components representing the natural system below the repository are captured in the UZ_Transport, SZ_Transport, and Biosphere containers. Each of these containers is briefly discussed below. Finally, all model results that are useful for model analysis are captured within the results container.

Similar to the organization discussed previously, the uncertain parameters that characterize epistemic uncertainty for the UZ Transport, SZ Flow and Transport, and Biosphere Model

Components are captured in separate containers within the Epistemic Parameters GoldSim Submodel. Many of the uncertain parameters used in the UZ Transport Model Component are shared by the EBS Flow and Transport Model Component. The uncertain parameters used by both models are sampled within the EBS Flow and Transport Model Component. Additionally, all uncertain parameters used in the UZ Transport Model Component are pre-sampled and written to an external file accessed by the FEHM V2.24 DLL during UZ transport calculations. Because a large number of uncertain parameters are shared between the EBS and UZ transport Submodels, all uncertain parameters used in UZ transport calculations have been co-located with parameters of the EBS Flow and Transport Model Component so that the elements that generate the UZ external file are co-located. Similarly, the epistemic uncertainties in the SZ Flow and Transport Model Component are correlated to input files accessed by the SZ_Convolute V3.10 DLL (STN: 10207-3.10.01-00 [DIRS 181060]). Thus, these parameter values are pre-sampled and stored in look-up tables. The pre-sampled values in the look-up tables share an index value with the external files. The index is randomly sampled in the Epistemic Parameters GoldSim Submodel, ensuring consistency between the calculations performed inside the GoldSim model and those performed by the SZ_Convolute V3.10 DLL. The epistemic uncertainties in the Biosphere Model Component are reflected in BDCFs. The BDCFs for different radionuclides may be highly correlated and are provided to TSPA as look-up tables of correlated values. Each look-up table shares a common index variable. The index is randomly sampled in the Epistemic Parameters GoldSim Submodel, ensuring that the desired correlation among BDCFs is applied.

The model calculations addressing the performance of the Natural System below the Repository are calculated in the TSPA_Model container of the TSPA-LA Model. Within this container, separate containers exist for the three model components comprising the natural system below the repository. The UZ Transport Model Component receives the radionuclide mass flux from the bottom of the invert. Time histories of releases from the bottom of the invert into the fractures and matrix beneath the repository are captured in the Engineered_System container. Additional EBS outputs are also captured within this container. These results are used by the TSPA analysts to analyze the performance of the EBS.

The UZ_Transport container includes a call to the FEHM V2.24 DLL, as well as input parameters needed by the FEHM V2.24 DLL and outputs from the calculations done by the FEHM V2.24 DLL. 16 flow fields are calculated using TOUGH2 V1.6. These flow fields represent four infiltration scenarios for each of four climate states. These 16 flow fields are used for calculations made in the UZ_Transport container. The UZ_Transport container contains input parameters such as fracture porosity and matrix diffusion coefficients. The FEHM V2.24 DLL calculates radionuclide release rates from the UZ fractures and matrix to the SZ. The UZ Transport Model Component is discussed in additional detail in Section 6.3.9.

The SZ_Transport container includes outputs from the 3-D SZ Flow and Transport Model Component, consisting of radionuclide breakthrough curves that provide the information needed to perform one-dimensional calculations that account for radionuclide decay and the growth of radionuclide daughter products during transport through the SZ. The SZ_Transport container includes parameter values needed for the three-dimensional and one-dimensional calculations, inputs of radionuclide mass from the UZ, the calculations of radionuclide transport through the SZ, and outputs of radionuclide mass to the biosphere. The 3-D SZ Flow and Transport Model

Component is performed using the SZ_Convolute V3.10 DLL. The SZ Flow and Transport Model Component is discussed in additional detail in Section 6.3.10.

The Biosphere container includes information needed to calculate dose to the RMEI, due to the radionuclides released from the repository and transported through the UZ and SZ. The Biosphere container includes BDCFs, groundwater protection conversion factors, and radionuclide mass flux inputs from the SZ. The Biosphere Model Component is discussed in additional detail in Section 6.3.11.

Events—Early failures of the WP and DS and other disruptive event scenarios are addressed in the TSPA-LA Model using distinct scenario classes. The implementation of these scenario classes is integrated into the TSPA-LA Model's GoldSim model file, along with the implementation of the Nominal Scenario Class. In general, parameters relating to the event scenarios use separate containers to segregate the Nominal Scenario Class calculations from the Early Failure Scenario Class, the Seismic Scenario Class, the Igneous Scenario Class, and the Human Intrusion Scenario. Similar to the calculations supporting the Nominal Scenario Class, much of the information used for the events scenario classes can be found throughout the TSPA-LA Model's GoldSim model file in containers used for calculations for the Nominal Scenario Class.

Within the Epistemic Parameters GoldSim Submodel, the Aleatory Parameters and Dynamic Calculations GoldSim Submodel, and the EBS GoldSim Submodel, separate containers hold the input parameter definitions and calculations that are applicable in the event scenarios. An events container is placed alongside the other model component containers in each of these locations. Within this container, inputs and calculations are further segregated into containers for each event type. Performing a GoldSim model run for an event scenario is similar to running the Nominal Scenario Class model file. The TSPA-LA Model has been built using GoldSim selector elements to pass submodel outputs from one submodel to another. The default result for these output elements is the sampled or calculated value for the Nominal Scenario Class. When configured to run an event scenario, these submodel output elements use IF…THEN…ELSE functions to replace or augment a Nominal Scenario Class result with the event-specific calculation result (if appropriate).

Modeling early failure event scenarios includes the conditions of early failures of the DSs or WPs. The Early Failure Scenario Class is discussed in detail in Section 6.4. The Drip Shield EF and Waste Package EF Modeling Cases model the performance of the repository following an early failure event. Submodels of the WP and DS Degradation Model Component from the Nominal Scenario Class are augmented with additional processes that are applicable for an early failure event. The Drip Shield EF Modeling Case is discussed in greater detail in Section 6.4.1. The Waste Package EF Modeling Case is discussed in greater detail in Section 6.4.2.

Modeling seismic events includes conditions resulting from seismic ground motion activity and fault displacement. The Seismic Scenario Class modeling cases model the performance of the repository following one or more seismic events. Consequences to the drift, DS, and WP from seismic activity are included. Submodels of the UZ Flow, EBS Environment, WP and DS Degradation Model Components from the Nominal Scenario Class are augmented with additional processes that are applicable for the repository following seismic activity. The

Seismic GM Modeling Case and the Seismic FD Modeling Case are discussed in detail in Section 6.6.1. The Seismic Scenario-related containers include the parameters needed to characterize a potential seismic event, and the potential consequences to the drift, WPs, and DSs, including levels of ground motion, rockfall potential, and the potential for fault displacement.

The Igneous Scenario-related containers include information for the Igneous Intrusion Modeling Case. The Igneous Intrusion Modeling Case models the performance of the repository following an igneous intrusion. Submodels of the UZ Flow, EBS Environment, WP and DS Degradation, and Waste Form Degradation and Mobilization Model Components from the Nominal Scenario Class are augmented with additional processes that are applicable after the igneous intrusion. The Igneous Intrusion Modeling Case is discussed in greater detail in Section 6.5.1. The Volcanic Eruption Modeling Case is performed in a separate GoldSim model file and is discussed in detail in Section 6.5.2. However, in general, this model file is organized similar to the TSPA-LA Model, but with less complexity because the modeling case excludes a number of the EBS and groundwater-related model components. The information in this model file includes parameter inputs for ASHPLUME, as well as the call to the ASHPLUME_DLL_LA V2.1 DLL (STN: 11117-2.1-00 [DIRS 181035] and STN: 11117-2.1-01 [DIRS 180147]), and the calculations for tephra redistribution and the probabilistic weighting of the source term used to determine dose.

Modeling a human intrusion event includes groundwater drilling operations that intersect the repository, resulting in a breach to a DS and a WP, followed by subsequent radionuclide transport down the borehole and into the SZ. Submodels of the UZ Flow, WP and DS Degradation, EBS Flow and Transport, and UZ Transport Model Components from the Nominal Scenario Class are augmented with additional processes that are applicable for a human intrusion event. The Human Intrusion Modeling Case is discussed in greater detail in Section 6.7.1.

INTENTIONALLY LEFT BLANK

Table 6.1.5-1. Location of Implementation Description in the GoldSim TSPA Model File

Submodel	Documentation Location(s)
Epistemic Parameters GoldSim Submodel	\Epistemic_Uncertainty\Epistemic_Params
Aleatory Parameters and Dynamic Calculations GoldSim Submodel	\Time_Zero\Aleatory_Params
EBS GoldSim Submodel	\Time_Zero\EBS_PS_Loop\EBS_PSE_Loop\EBS_Submodel
Natural System below the Repository	\TSPA_Model
Climate	Epistemic: NA Aleatory: NA EBS: \Global_Inputs_and_Calcs\Global_UZ_Flow\Climate Other: \TSPA_Model\UZ_Flow\Climate
Infiltration	Epistemic: \Input_Params_Epistemic\Epistemic_Params_UZ_Flow\Uncertain_Params_Infiltration Aleatory: NA EBS: \Time_Zero\EBS_PS_Loop\Static_Calcs_PS_Loop\Static_Calcs_UZ_Flow\Infiltration \Global_Inputs_and_Calcs\Global_UZ_Flow\Infiltration
Drift Seepage	Epistemic: \Input_Params_Epistemic\Epistemic_Params_UZ_Flow\Input_Params_Seepage_Uncert \Input_Params_Epistemic\Epistemic_Params_UZ_Flow\Uncertain_Params_Seepage Aleatory: NA EBS: \Time_Zero\EBS_PS_Loop\Static_Calcs_PS_Loop\Static_Calcs_UZ_Flow\Drift_Seepage \Global_Inputs_and_Calcs\Global_UZ_Flow\Drift_Seepage
Drift Wall Condensation	Epistemic: \Input_Params_Epistemic\Epistemic_Params_UZ_Flow\Uncertain_Params_DWC Aleatory: NA EBS: \Global_Inputs_and_Calcs\Global_UZ_Flow\Drift_Wall_Condensation
EBS TH Environment	Epistemic: \Input_Params_Epistemic\Epistemic_Params_EBS_Environ\Uncertain_Params_TH Aleatory: NA EBS: \Global_Inputs_and_Calcs\Global_EBS_Environ\EBS_Environment\ThermoHydrology

Table 6.1.5-1. Location of Implementation Description in the GoldSim TSPA Model File (Continued)

Submodel	Documentation Location(s)
WP and DS Degradation	Epistemic: \Input_Params_Epistemic\Epistemic_Params_WP_DS_Deg\ Aleatory: \Model_Calcs_Aleatory\Aleatory_Calcs_WP_DS_Deg EBS: \Time_Zero\EBS_PS_Loop\Static_Calcs_PS_Loop\Static_Calcs_WP_DS_Deg \Global_Inputs_and_Calcs\Global_WP_DS_Deg\Global_IWPD
Localized Corrosion	Epistemic: \Input_Params_Epistemic\Epistemic_Params_WP_DS_Deg\ Aleatory: NA EBS: \Time_Zero\EBS_PS_Loop\Static_Calcs_PS_Loop\Static_Calcs_WP_DS_Deg \Global_Inputs_and_Calcs\Global_WP_DS_Deg\Global_LC
Radionuclide Inventory	Epistemic: \Input_Params_Epistemic\Epistemic_Params_WF_Deg_Mob\Uncertain_Params_RN_Inventory Aleatory: NA EBS: \Global_Inputs_and_Calcs\Global_WF_Deg_Mob\RN_Inventory
In-Package Chemistry	Epistemic: \Input_Params_Epistemic\Epistemic_Params_WF_Deg_Mob\Uncertain_Params_InPkg_Chem Aleatory: NA EBS: \Global_Inputs_and_Calcs\Global_WF_Deg_Mob\In_Package_Chemistry
Waste Form Degradation	Epistemic: \Input_Params_Epistemic\Epistemic_Params_WF_Deg_Mob\Uncertain_Params_CSNF_WF Aleatory: NA EBS: \Global_Inputs_and_Calcs\Global_WF_Deg_Mob\WF_Degradation\CSNF_WF_Dissolution
	Epistemic: \Input_Params_Epistemic\Epistemic_Params_WF_Deg_Mob\Uncertain_Params_HLW_WF Aleatory: NA EBS: \Global_Inputs_and_Calcs\Global_WF_Deg_Mob\WF_Degradation\Input_Params_HLW_WF
	Epistemic: NA Aleatory: NA EBS: \Global_Inputs_and_Calcs\Global_WF_Deg_Mob\WF_Degradation\Input_Params_DSNF_WF

Table 6.1.5-1. Location of Implementation Description in the GoldSim TSPA Model File (Continued)

Submodel	Documentation Location(s)
Cladding Degradation	Epistemic: NA Aleatory: NA EBS: \Global_Inputs_and_Calcs\Global_WF_Deg_Mob\Clad_Degradation
EBS Chemical Environment	Epistemic: \Input_Params_Epistemic\Epistemic_Params_EBS_Environ\Uncertain_Params_EBS_CE Aleatory: \Input_Params_Aleatory\Input_Params_EBS_Environ\Input_Params_EBS_CE EBS: \Global_Inputs_and_Calcs\Global_EBS_Environ\EBS_Environment\EBS_Chemical_Environment
Dissolved Concentration Limits	Epistemic: \Input_Params_Epistemic\Epistemic_Params_WF_Deg_Mob\Uncertain_Params_Solubility Aleatory: NA EBS: \Global_Inputs_and_Calcs\Global_WF_Deg_Mob\Global_Solubility
EBS Colloids	Epistemic: \Input_Params_Epistemic\Epistemic_Params_EBS_F_and_T\Uncertain_Params_Colloids Aleatory: NA EBS: \Global_Inputs_and_Calcs\Global_EBS_F_and_T\Model_Input_EBS_Transport\Input_Params_Colloids
EBS Flow	Epistemic: \Input_Params_Epistemic\Epistemic_Params_EBS_F_and_T\Uncertain_Params_Flux_Split Aleatory: NA EBS: \Time_Zero\EBS_PS_Loop\Static_Calcs_PS_Loop\Static_Calcs_EBS_F_and_T\EBS_Flow \Global_Inputs_and_Calcs\Global_EBS_F_and_T\Model_Feeds_EBS_Flow
EBS Transport	Epistemic: \Input_Params_Epistemic\Epistemic_Params_EBS_F_and_T Aleatory: NA EBS: \Global_Inputs_and_Calcs\Global_EBS_F_and_T\Model_Input_EBS_Transport
EBS-UZ Interface	Epistemic: \Input_Params_Epistemic\Epistemic_Params_EBS_F_and_T\Uncertain_Params_EBS_UZ_Trans Aleatory: NA EBS: \Global_Inputs_and_Calcs\Global_EBS_F_and_T\EBS_UZ_Transport_Inputs
UZ Transport	Epistemic: \Input_Params_Epistemic\Epistemic_Params_UZ_Transport Aleatory: NA Other: \TSPA_Model\UZ_Transport
SZ Flow and Transport	Epistemic: \Input_Params_Epistemic\Epistemic_Params_SZ_Transport Aleatory: NA Other: \TSPA_Model\SZ_Transport

Table 6.1.5-1. Location of Implementation Description in the GoldSim TSPA Model File (Continued)

Submodel	Documentation Location(s)
Biosphere	Epistemic: \Input_Params_Epistemic\Epistemic_Params_Biosphere Aleatory: NA Other: \TSPA_Model\Biosphere
Early Failure Scenario Class	Epistemic: \Input_Params_Epistemic\Epistemic_Params_Events\Epistemic_Parameters_EF Aleatory: \Input_Params_Aleatory\Aleatory_Params_Events\Aleatory_Params_EF EBS: \Time_Zero\EBS_PS_Loop\Static_Calcs_PS_Loop\Static_Calcs_Events\Static_Calcs_EF \Global_Inputs_and_Calcs\Global_Events\Global_EF
Igneous Scenario Class	Epistemic: \Input_Params_Epistemic\Epistemic_Params_Events\Epistemic_Params_Igneous_Intr Aleatory: \Input_Params_Aleatory\Aleatory_Params_Events\Aleatory_Params_Igneous_Intr EBS: \Time_Zero\EBS_PS_Loop\Static_Calcs_PS_Loop\Static_Calcs_Events\Igneous_Intrusion \Global_Inputs_and_Calcs\Global_Events\Igneous_Scenario
	Epistemic: \Model_Uncertainties\EU Aleatory: \Model_Uncertainties\AU EBS: \Eruptive_Model
Seismic Scenario Class	Epistemic: \Input_Params_Epistemic\Epistemic_Params_Events\Epistemic_Params_Seismic Aleatory: \Input_Params_Aleatory\Aleatory_Params_Events\Input_Params_Seismic_Uncert \Input_Params_Aleatory\Aleatory_Params_Events\Input_Params_Seismic_FD_Uncert EBS: \Time_Zero\EBS_PS_Loop\Static_Calcs_PS_Loop\Static_Calcs_Events\Seismic_Fault_Displacement \Global_Inputs_and_Calcs\Global_Events\Seismic_Scenario
Human Intrusion Scenario	Epistemic: NA Aleatory: \Input_Params_Aleatory\Aleatory_Params_Events\Aleatory_Params_HI EBS: \Time_Zero\EBS_PS_Loop\Static_Calcs_PS_Loop\Static_Calcs_Events\Human_Intrusion_Events \Global_Inputs_and_Calcs\Global_Events\Human_Intrusion Other: \TSPA_Model\UZ_Transport\UZ_Transport_Calculations\HI_Borehole_Transport

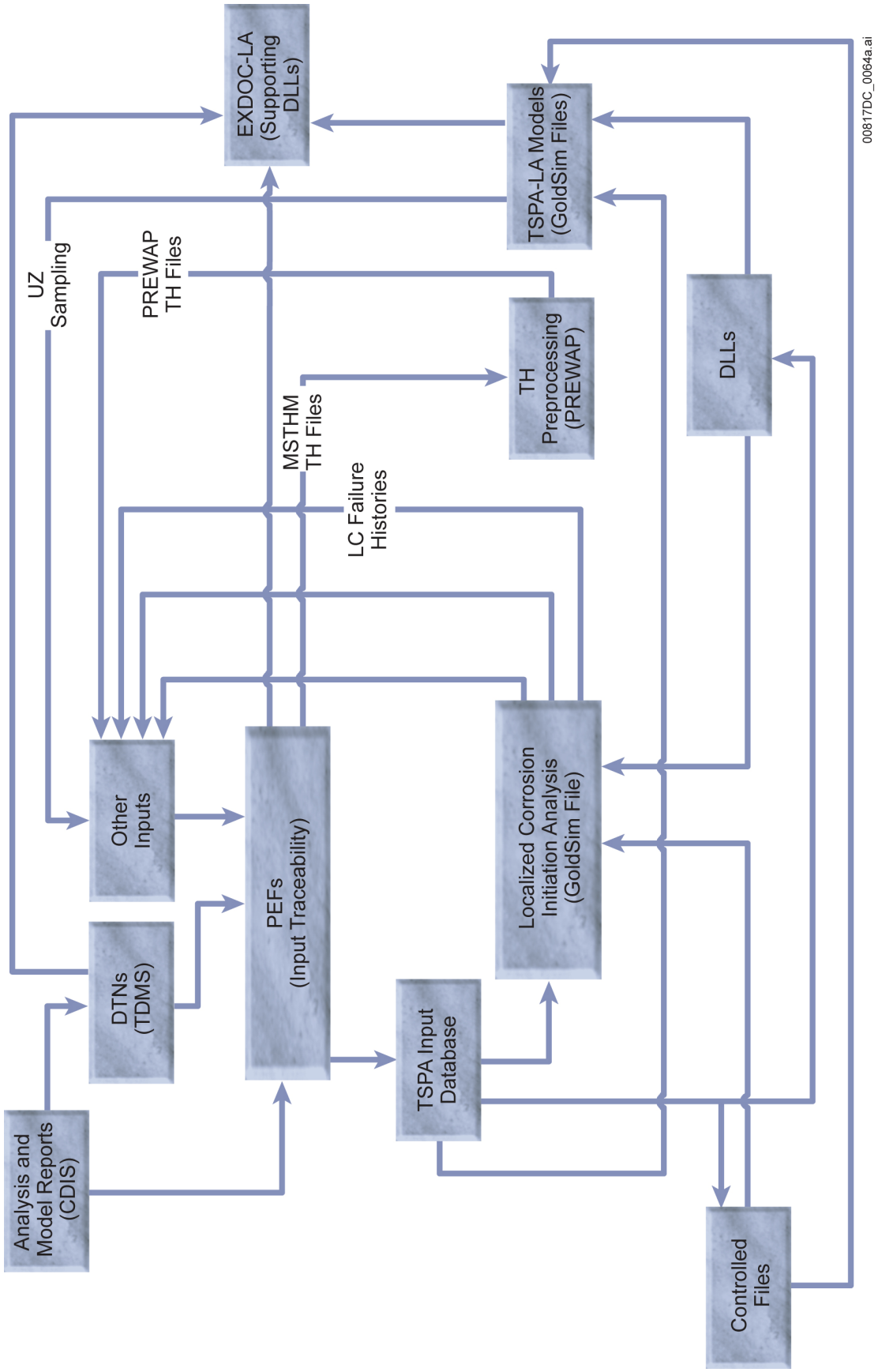

Figure 6.1.5-1. Illustrated Overview of all the Various Elements that Make Up the Framework for Initializing and Running the TSPA-LA Model

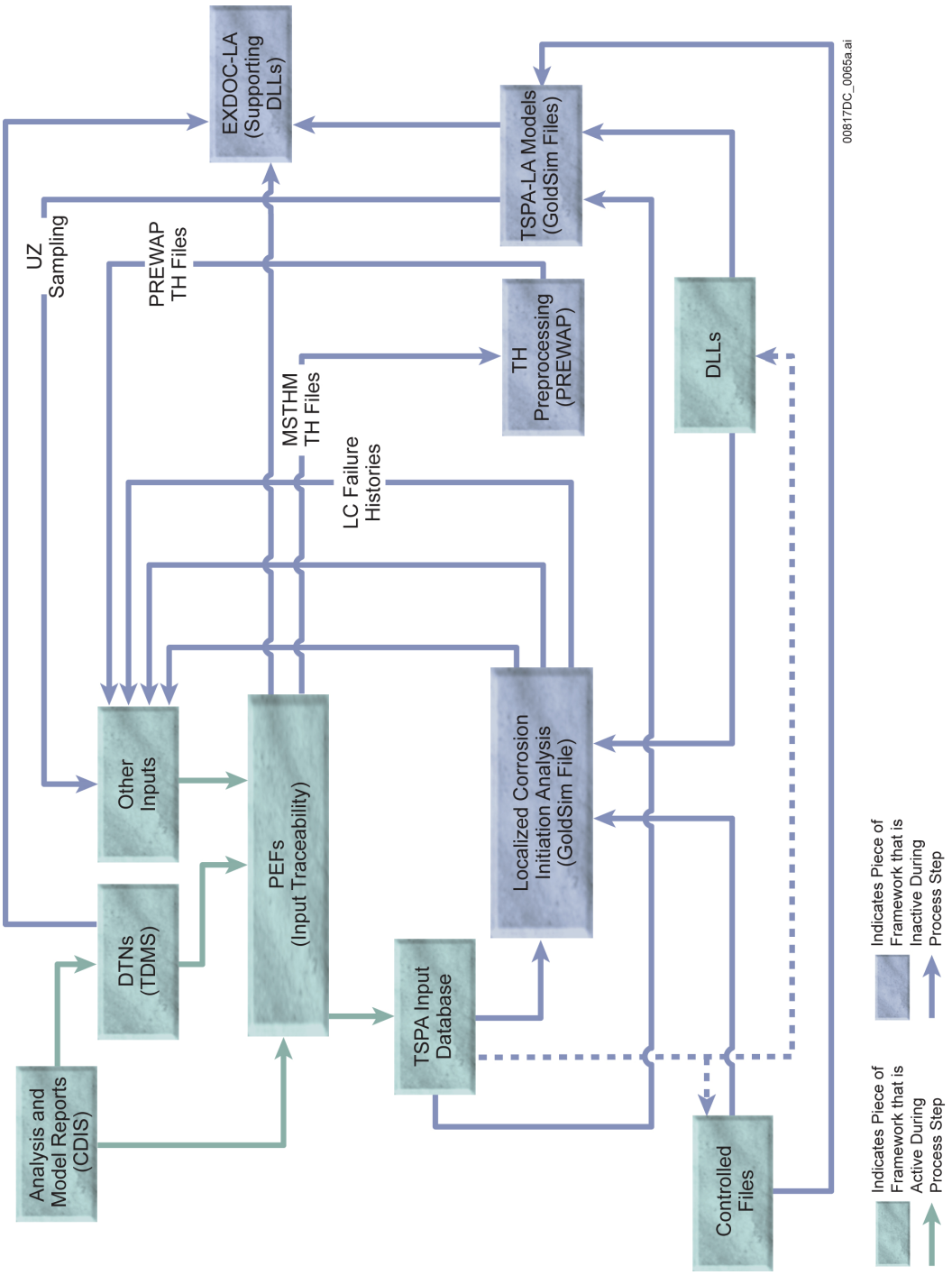

NOTE: Dashed lines indicate cases where location of files and software are stored in the TSPA Input Database, but the information is actually accessed from the TSPA-LA Model file server.

Figure 6.1.5-2. Illustration Depicting Elements Required for Loading of Initial Parameter Values and Dynamically Linked Libraries for the TSPA-LA Model

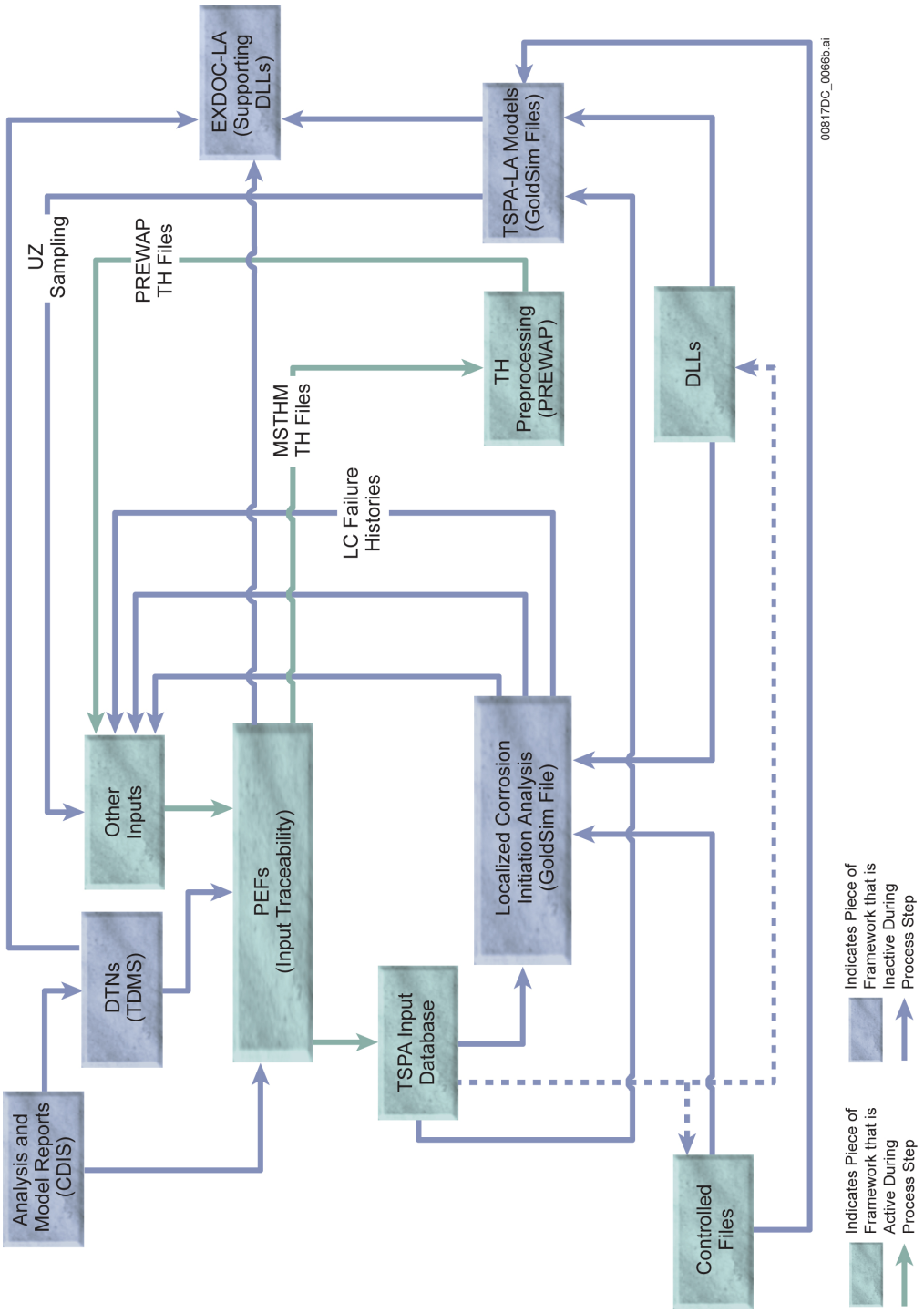

NOTE: Dashed lines indicate cases where location of files and software are stored in the TSPA Input Database, but the information is actually accessed from the TSPA-LA Model file server.

Figure 6.1.5-3. Illustration Depicting Elements Active When Information from the Multiscale Thermohydrologic Model is Preprocessed by PREWAP_LA

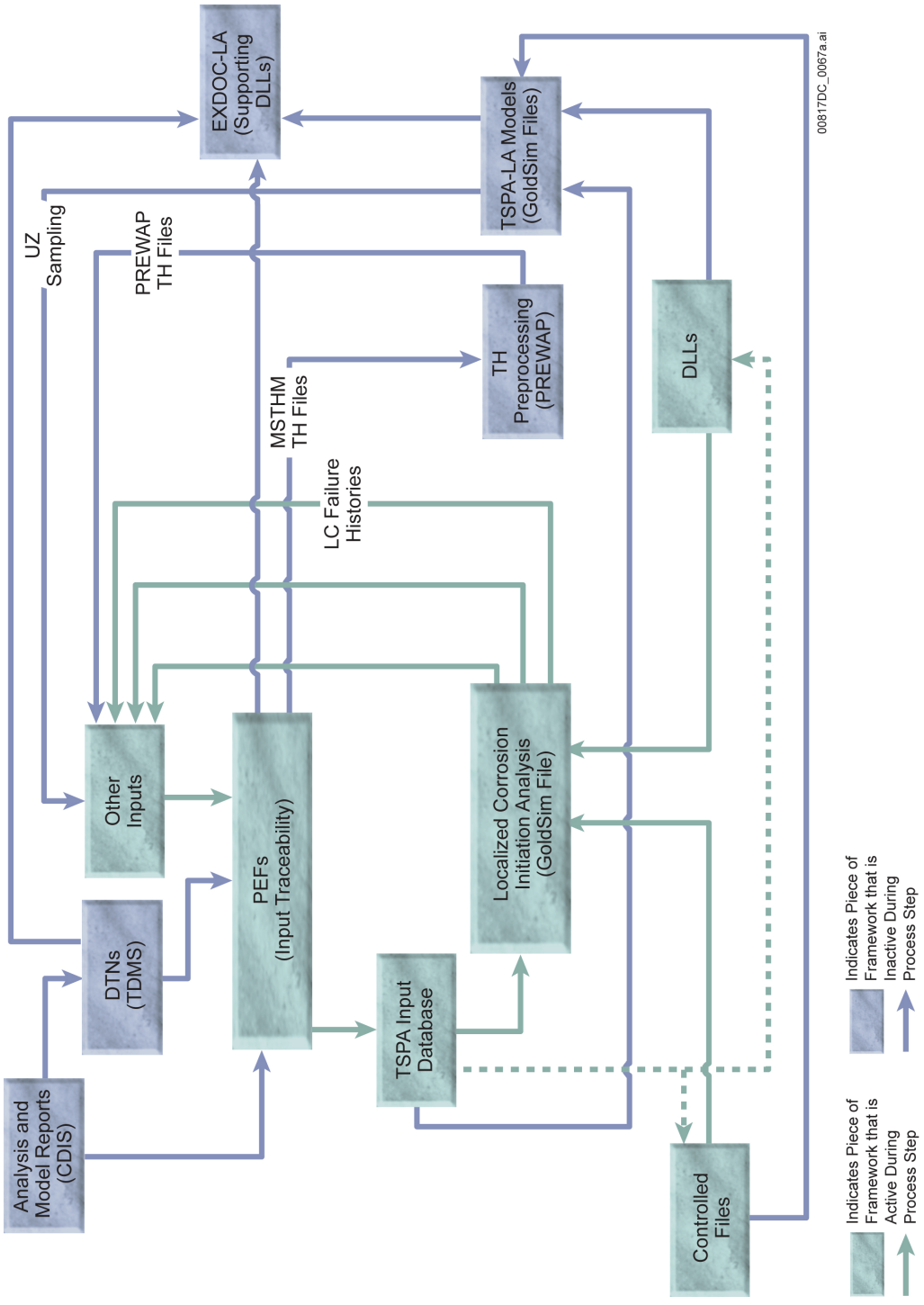

NOTE: Dashed lines indicate cases where location of files and software are stored in the TSPA Input Database, but the information is actually accessed from the TSPA-LA Model file server.

Figure 6.1.5-4. Illustration Depicting Elements Active When Preprocessing for the Localized Corrosion Initiation Analysis

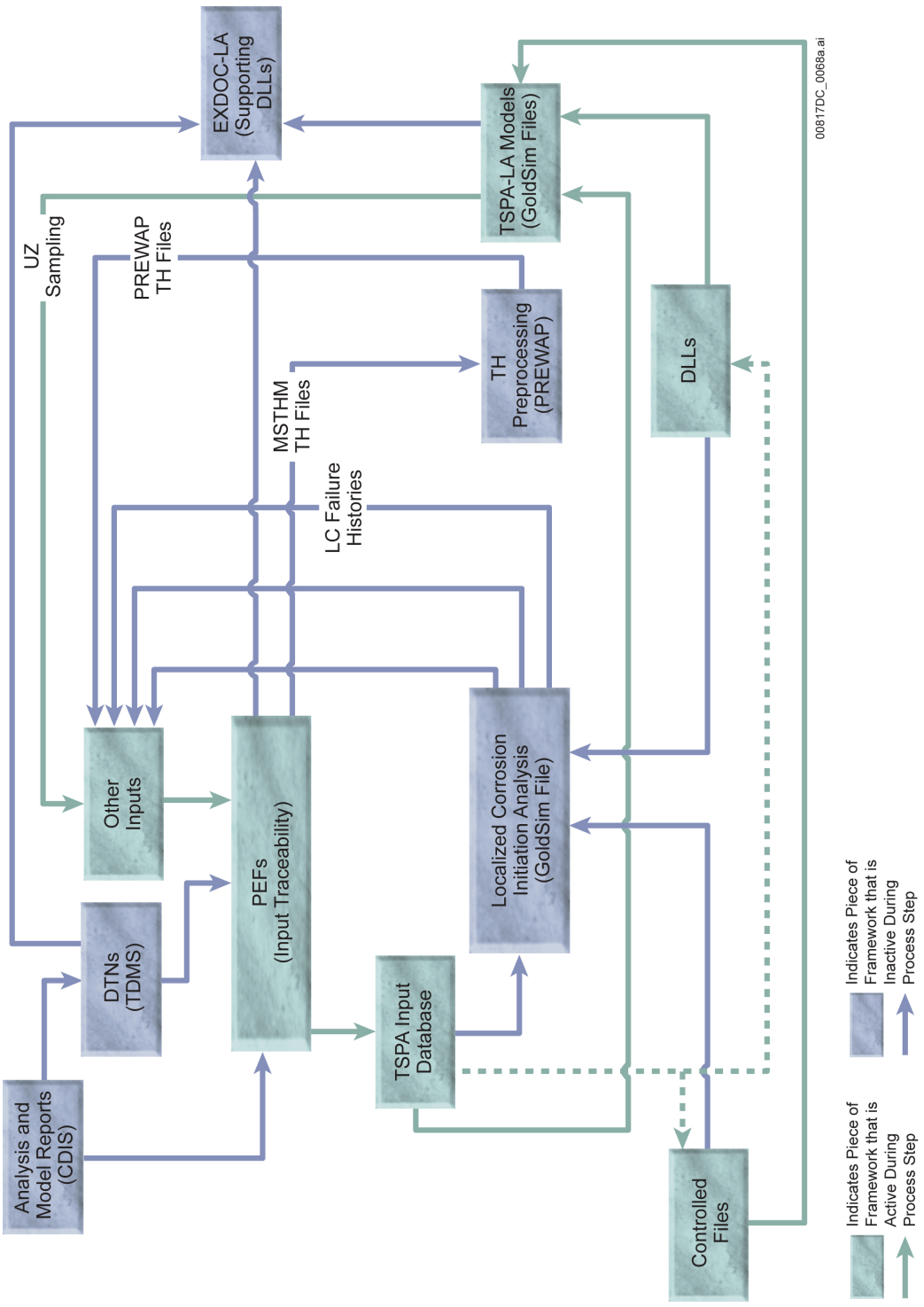

NOTE: Dashed lines indicate cases where location of files and software are stored in the TSPA Input Database, but the information is actually accessed from the TSPA-LA Model file server.

Figure 6.1.5-5. Illustration Depicting Elements Active when Sampling of Uncertain Unsaturated Zone Parameters and Generation of Input Files

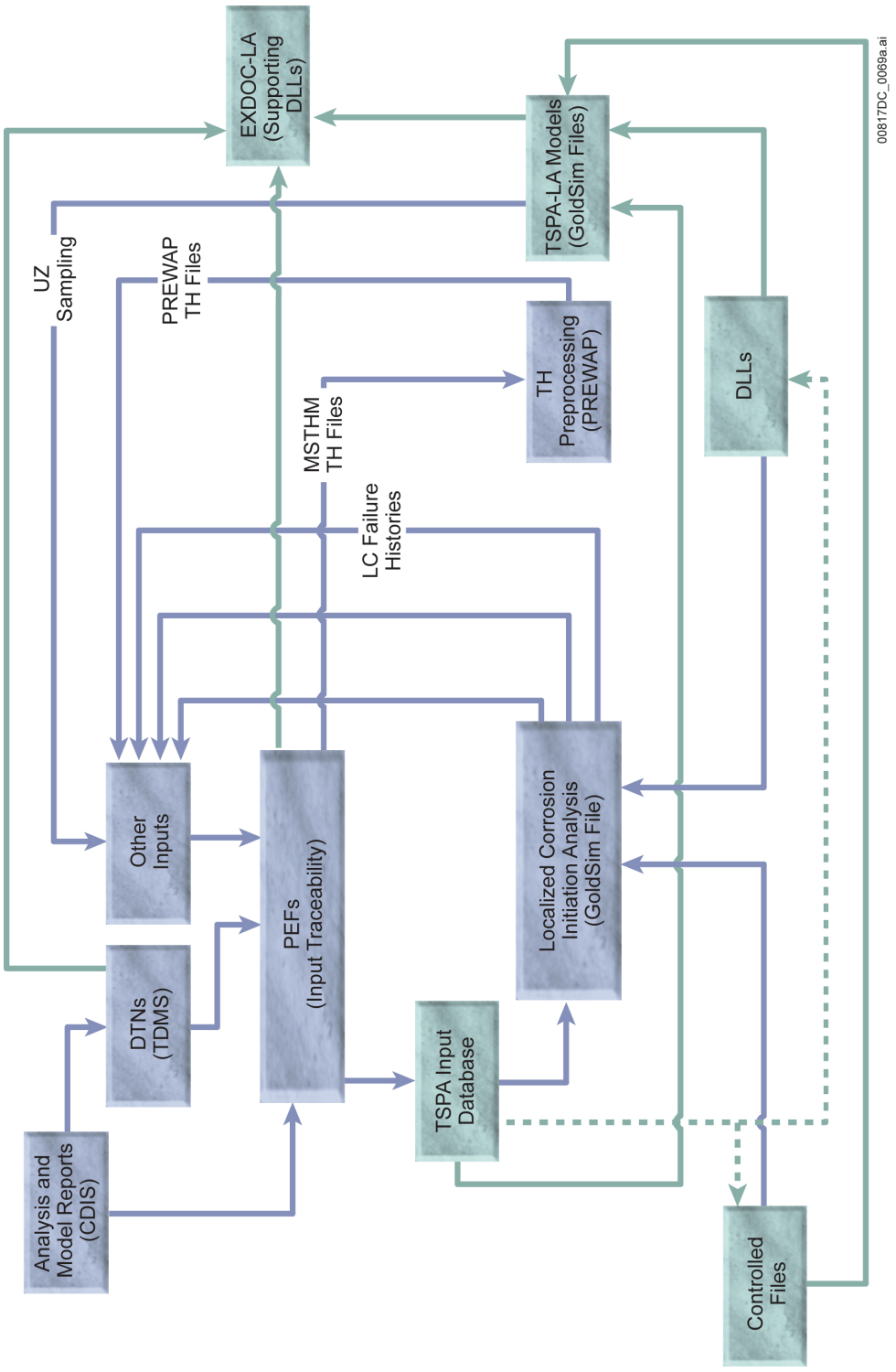

NOTE: Dashed lines indicate cases where location of files and software are stored in the TSPA Input Database, but the information is actually accessed from the TSPA-LA Model file server.

Figure 6.1.5-6. Illustration Depicting Elements Active in the Execution of the TSPA-LA GoldSim Model File and the TSPA-LA Volcanic Eruption GoldSim Model File

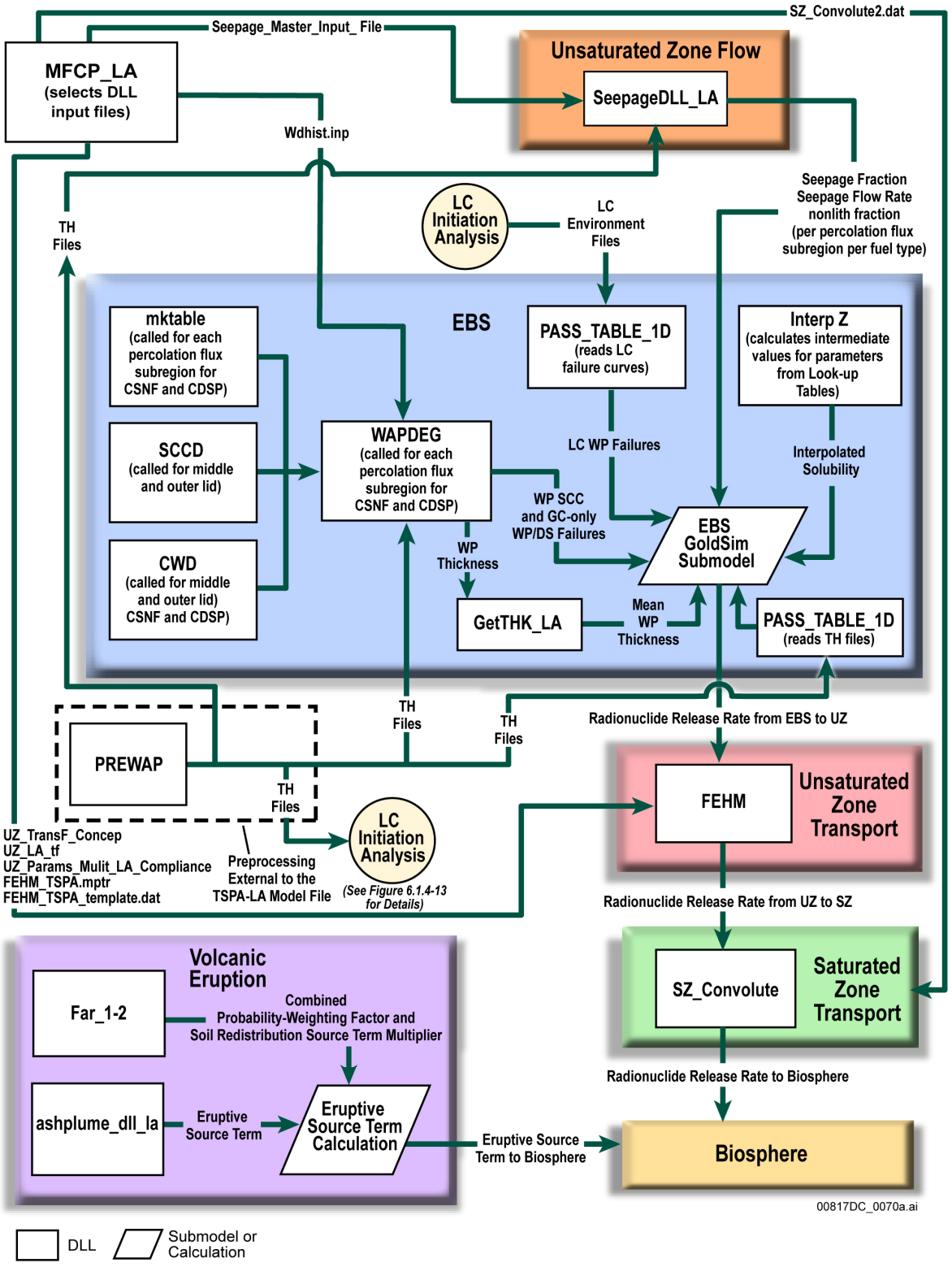

Figure 6.1.5-7. TSPA-LA Software Configuration Illustrating Software Run with GoldSim

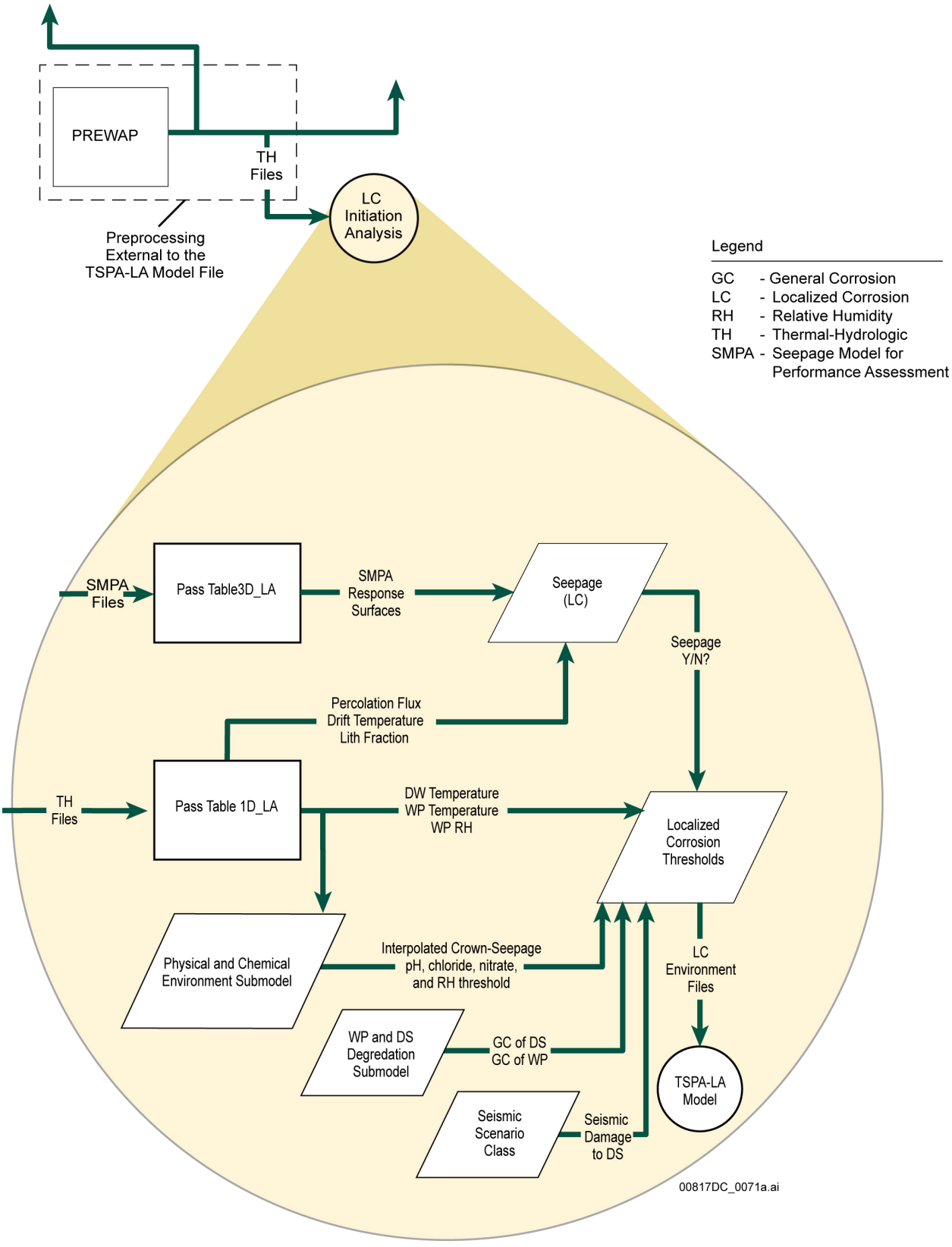

Figure 6.1.5-8. Details of the Software Configuration for the Localized Corrosion Initiation Analysis

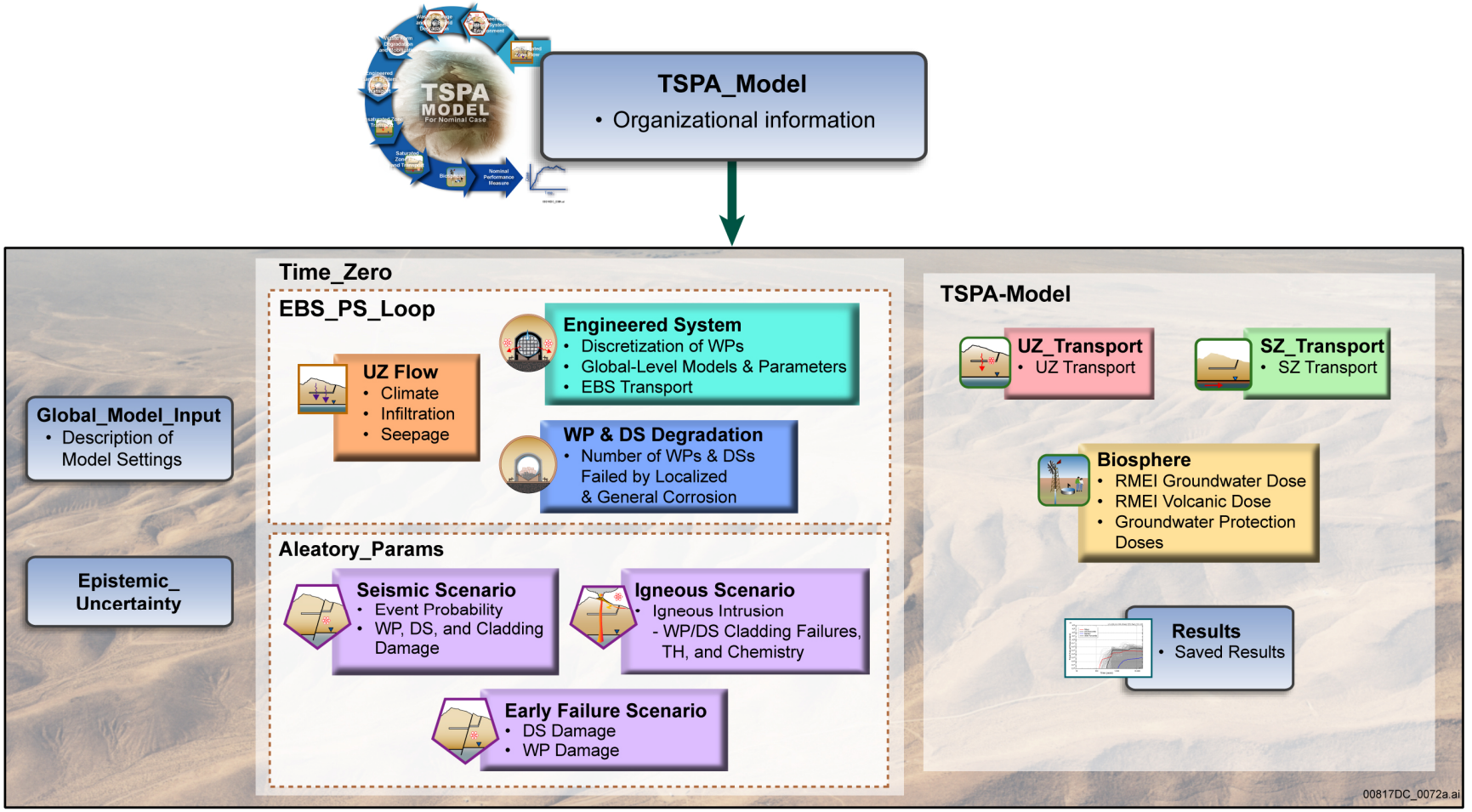

Figure 6.1.5-9. Layout of Calculation Containers that Define the Highest Level of Organization of the TSPA-LA Model File

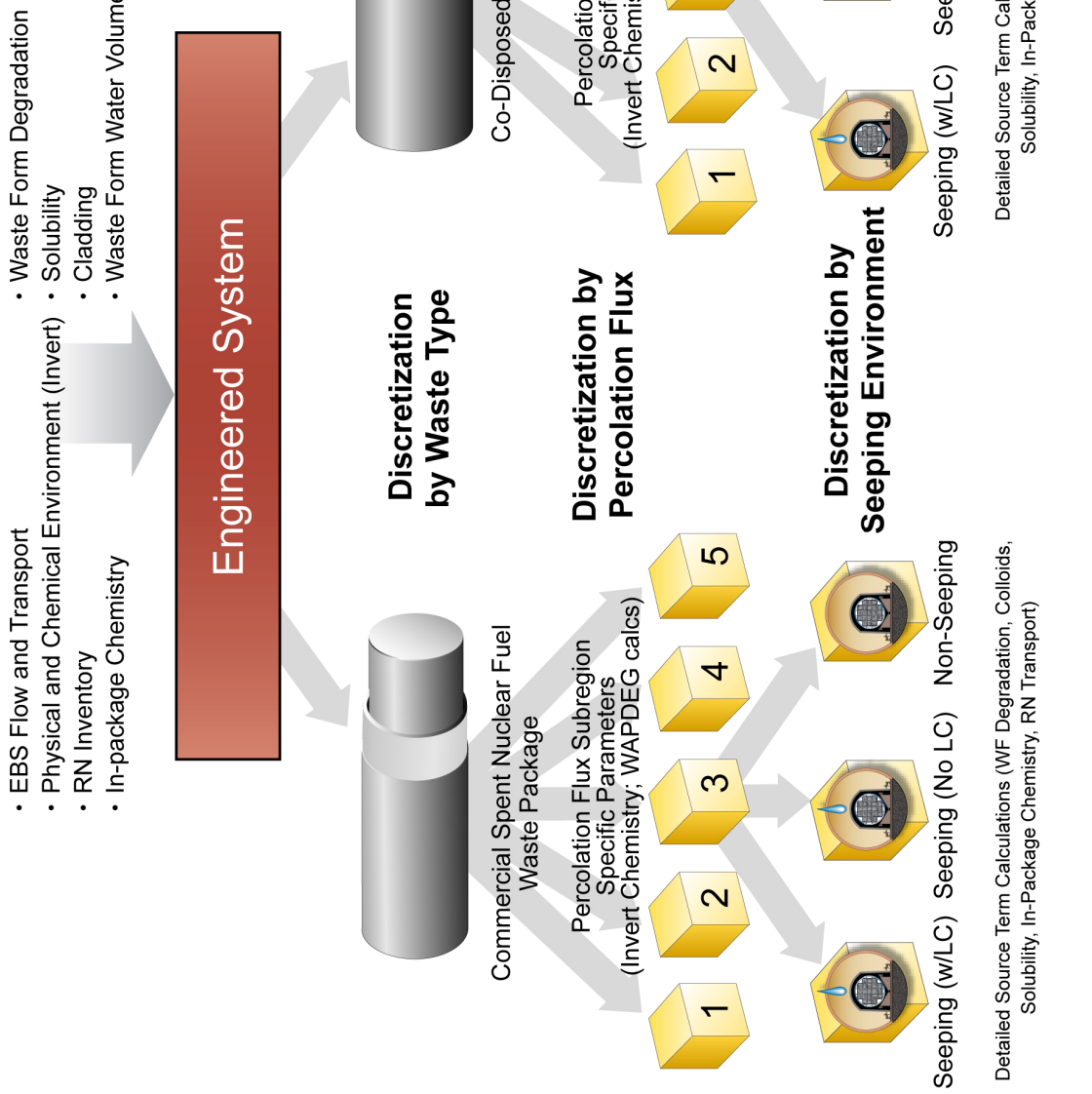

Figure 6.1.5-10. Levels of Discretization of Engineered System Representation in the TSPA-LA Model File

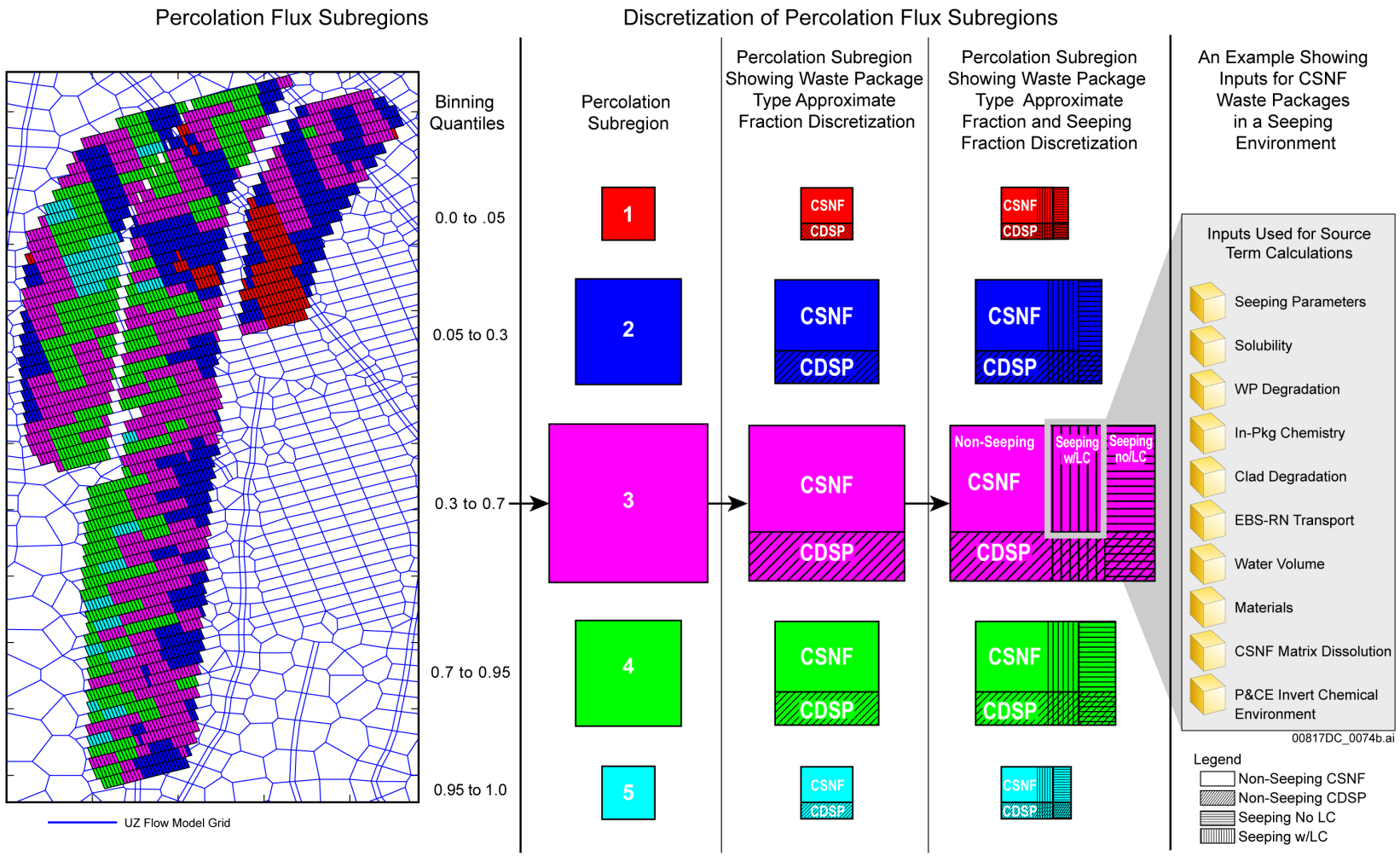

Source: Percolation Flux Map from SNL 2007 [DIRS 181383], Figure VIII-1[a].

NOTE: The early failure packages are randomly set in one of the five repository percolation subregions at the start of a realization.

Figure 6.1.5-11. Schematic of the Five Repository Percolation Subregions Showing the Implementation of the Levels of Discretization Shown on Figure 6.1.5-10

INTENTIONALLY LEFT BLANK

6.2 ALTERNATIVE CONCEPTUAL MODELS

Alternative conceptual models (ACMs) are a means to specifically acknowledge model form uncertainty. A model is a set of working hypotheses and assumptions that provide an acceptable description of a system for the intended purpose. The hypotheses and assumptions must be logically consistent with one another, in agreement with existing information, able to predict system behavior, and able to be tested. In 10 CFR 63.114(c) [DIRS 178394], the NRC specifically requires the DOE to, "Consider alternative conceptual models of features and processes that are consistent with available data and current scientific understanding and evaluate the effects that alternative conceptual models have on the performance of the geologic repository."

A model that is evaluated and chosen to represent a system is called the base-case model. Any remaining models that meet the above criteria are then designated ACMs for the system. In addition to ACMs, the TSPA-LA Model contains various conservative assumptions that played an important role in enhancing the confidence and defensibility of the model. These conservatisms and their impact on the TSPA-LA Model are documented in Appendix C.

General Consideration of Alternative Conceptual Models

As suggested by the statements in 10 CFR 63.114(c) [DIRS 178394], a conceptual model can be truly alternative only if it meets the following criteria:

- It must differ significantly from the initial (or base-case) conceptual model.
- It must be consistent with available data and current scientific understanding.
- It must be reasonable (i.e., there is a reasonable physical basis for the alternative).

The ACMs in all model components, submodels, and process models that provide inputs to the TSPA-LA Model were considered according to a process that included the identification, screening, and evaluation of potential ACMs as part of the analysis documented in the model reports that feed the TSPA-LA Model. Reasonable and technically defensible conservatism at the subsystem level has been used to select the best ACM to use rather than quantitatively propagate multiple ACMs to the TSPA-LA Model. Generally, additional uncertainty is incorporated into the selected conceptual model if more than one ACM is deemed appropriate for use rather than considering multiple ACMs in the TSPA-LA Model. If an ACM appears to be significant at the subsystem level, an appropriate abstraction is developed for that ACM for consideration within the TSPA-LA Model. The result of the process is documented within the individual model reports. It is important to note that treatment of ACMs within the individual model reports may differ significantly to be consistent with available data and current scientific understanding. For instance, some ACMs may be assessed qualitatively with the conclusion that the ACM is captured by the selected conceptual model abstraction recommended for use in the TSPA-LA Model. Whereas, in another case, a more detailed computational analysis may be needed to assess the ACM, resulting in additional uncertainty or other modification to the selected conceptual model abstraction used in the TSPA-LA Model. ACMs that were identified and evaluated in model components, submodels, process models, and model reports supporting the TSPA-LA Model are summarized in Table 6.2-1 and Sections 6.3, 6.4, 6.5, 6.6, and 6.7. Each model component and submodel discussion includes a summary evaluation of ACMs.

An important reason for considering ACMs at the subsystem level is to help build confidence that plausible changes in modeling assumptions or simplifications will not change conclusions regarding the subsystem and subsequently the total system performance. Consideration and treatment of ACMs used to support the TSPA-LA Model is demonstrated through a stepwise process including subsystem-level impact evaluations and analyses presented in the process level model reports. Important differences demonstrated at the subsystem level are evaluated through TSPA-LA Model sensitivity and regression analyses. Section 6.3 summarizes the general consideration and treatment of ACMs used to support the TSPA-LA Model in each submodel area.

Table 6.2-1. Table of Alternative Conceptual Models

Alternative Conceptual Models	Key Assumptions	Assessment and Basis
Unsaturated Zone Flow Model Component (Section 6.3.1 and Section 6.3.3)		
UZ Flow: Lateral flow in the PTn	The ACM employs a different hydrogeologic property set for the PTn unit that does not favor large-scale lateral diversion of flow in the PTn (BSC 2004 [DIRS 169861], Section 6.5.2.2).	Modeling results show that the base-case model generally provides slightly more conservative transport time estimates than the ACM (BSC 2004 [DIRS 169861], Section 6.9.2). Comparative studies of chloride distributions within the UZ, simulated using the base case and ACM flow fields, indicate consistently that the base-case flow fields provide an overall better match with the observed chloride data (BSC 2004 [DIRS 169861], Section 6.5.2.2). Note that this study was performed with flow models based on the original infiltration model, but the implications of the study are not expected to change.
UZ Flow: Transient infiltration pulse	The ACM assumes that episodic variations in surface infiltration rates may not be effectively dampened by the PTn and may still affect radionuclide transport initialized at the repository level.	Modeling studies show that episodic variations in infiltration in areas where the PTn is thick are largely dampened by the time they reach the repository level. In addition, since the episodic variations at the repository level for thin PTn sections are small relative to other uncertainties in percolation fluxes, the assumption of steady-state flow, as used in the TSPA-LA Model, is considered to be valid (SNL 2008 [DIRS 184614], Section 6.9).
UZ Flow: Film Flow	Film flow may occur between cavities and fractures (SNL 2008 [DIRS 184614], Section 7.8.3.3). Film flow may also be a process by which fast flow occurs in the fractures (BSC 2004 [170035] Section 7.3).	Film flow may occur between cavities and fractures as indicated by coatings and water release tests. Not considering the explicit influence of cavities is a conservative approach since the cavities would retard the transport of water (SNL 2008 [DIRS 184614], Section 7.8.3.3). Although the importance of film flow in the fractures is a matter of debate (BSC 2004 [170035] and Preuss 1999 [DIRS 104250]), a comparison between the AFM and a film-flow model has been performed (BSC 2004 [DIRS 170035] Section 7.3). The analysis, comparing the AFM and the film-flow model, showed that the AFM would capture the fast flow behavior of water film if film flow was the major fracture flow mechanism (BSC 2004 [170035] Section 7.3.1 and Section 8.2).

Table 6.2-1. Table of Alternative Conceptual Models (Continued)

Alternative Conceptual Models	Key Assumptions	Assessment and Basis
UZ Flow: Discrete Fracture Flow	The discrete-fracture or "weeps" type model is an alternative model that explicitly defines the fractures in a fracture-flow system.	The discrete-fracture or "weeps" type model is subject to extremely high uncertainties with respect to the fracture data needed to describe the system. In addition, the computational burden associated with this type model is beyond present or near future resources. Therefore, this type model is not considered (SNL 2008 [DIRS 184614], Section 6.1.2).
UZ Flow: Inclusion of TH, THC, and Thermal-Hydrologic-Mechanical Effects on UZ Flow	Vaporization due to repository heat will keep the drift dry for several hundred to a few thousand years. Thermal (TH), Thermal Hydrologic Chemical (THC), and thermal-hydrologic-mechanical (THM) effects may influence the flow fields used to describe flow in the UZ.	TH, THC, and thermal-hydrologic-mechanical effects are insignificant after the change to glacial-transition climate, the period when most radionuclide transport would take place (SNL 2008 [DIRS 184748], Section 6.7). Additional conclusions with respect to TH, THC, and thermal-hydrologic-mechanical effects on UZ Flow and Transport presented in *Mountain-Scale Coupled Processes (TH/THC/THM)* include: (1) mountain-scale TH will have a large impact on fluid flow near the repository at early times but insignificant impact on UZ flow fields (BSC 2005 [DIRS 174101], Section 8.1); (2) changes in water chemistry, mineralogy, and hydrologic properties in the ambient temperature regions are minimal over the 7,000 years the THC model was simulated (BSC 2005 [DIRS 174101], Section 8.2); and (3) thermal-hydrologic-mechanical induced changes in mountain-scale hydrologic properties have no significant impact on vertical percolation through the repository horizon (BSC 2005 [DIRS 174101], Section 8.3).
Drift Seepage: Flow Through Discrete Fractures	ACM that simulates flow through discrete fractures rather than through a stochastic continuum (SNL 2007 [DIRS 181244], Section 6.4).	It was concluded that conceptual model uncertainty is small compared to other sources of uncertainty that are explicitly accounted for by the base case conceptual model, its numerical implementation, and the associated uncertainty estimates that are propagated through the TSPA-LA Model (SNL 2007 [DIRS 181244], Section 6.4.1.2).

Table 6.2-1. Table of Alternative Conceptual Models (Continued)

Alternative Conceptual Models	Key Assumptions	Assessment and Basis
Drift Seepage: Episodic-Preferential Flow in Superheated Rock	The effectiveness of the vaporization barrier was examined with an ACM representing water flow into a superheated rock environment (SNL 2007 [DIRS 181244], Section 6.4.3.2). In this ACM, the thermally perturbed downward flux from the condensation zone toward the superheated rock zone is conceptualized to form episodic preferential-flow patterns.	It was concluded that results of the ACM are reasonably consistent with the thermal seepage process-model results used for the seepage abstraction used for TSPA-LA (SNL 2007 [DIRS 181244], Section 6.4.3.2).
Drift Seepage: Flow-focusing factor based on a coarser resolution of scale	This ACM flow-focusing factor was based on a coarser resolution of scale at which the flow-focusing factors were averaged over 5-meter long sections along the bottom of the model (SNL 2007 [DIRS 181244], Section 6.6.5.2.2).	Since no quantitative observation of flow focusing is available for a direct comparison of conceptual models model (SNL 2007 [DIRS 181244], Section 6.6.5.2.3), since this ACM would give less conservative (much lower seepage rates with only a slight increase in seepage fraction) results the base conceptual model should be used.
Drift Seepage: Igneous seepage model that considers a capillary barrier and flow diversion	The two ACMs for evaluating drift seepage after an igneous event are based on a conceptual model where thermal contraction gives rise to numerous fractures and joints in the cooling process filling the drift with fractured magma of relatively high permeability and low capillary strength (SNL 2007 [DIRS 181244], Section 6.5.1.7). This conceptualization gives rise to a capillary barrier and flow diversion. The two ACMs are based on whether the non-collapsed seepage lookup table or the collapsed seepage lookup table is used.	Since information on which one of the possible in-drift conditions after an igneous event is not available (SNL 2007 [DIRS 181244], Section 6.5.1.7), the conceptual model with the greatest seepage rates was chosen.
Drift-Wall Condensation: Thermal Conductivity/Heat Transfer	In the Thermal Conductivity/Heat Transfer ACM, the air phase is treated as a solid material (SNL 2007 [DIRS 181648], Section 6.1.4).	This ACM is essentially accounted for in the MSTHM Abstraction (SNL 2007 [DIRS 181648] Sections 6.1.4 and 6.4).
Drift-Wall Condensation: CFD Simulation for Drift Condensation Processes	ACM simulates the drift with a CFD code and the surrounding rock with porous media code. The CFD code FLUENT (Software Code: FLUENT. V6.0.12 (Fluent, Inc. [DIRS 164315]), contains limited porous media capabilities that only considers single-phase flow (SNL 2007 [DIRS 181648], Section 6.1.4).	Conduction-only heat transfer in the surrounding rock and the invert is acceptable, and this ACM is not considered further (SNL 2007 [DIRS 181648], Section 6.1.4).

Table 6.2-1. Table of Alternative Conceptual Models (Continued)

Alternative Conceptual Models	Key Assumptions	Assessment and Basis
EBS Environment Model Component (Section 6.3.2 and 6.3.4)		
EBS TH Environment: Mountain-Scale TH Model	An ACM to the MSTHM Process Model is a Mountain-Scale Thermal Hydrologic model developed by Lawrence Berkeley National Laboratory (Haukwa et al. 1998 [DIRS 117826]). The Lawrence Berkeley National Laboratory model is a monolithic TH model. The Mountain-Scale TH Model used: (1) coarser grid discretization at the drift scale than the MSTHM Process Model; (2) a line-averaged approximation of the heat-generation-rate-versus-time table (whereas the MSTHM Process Model represented the WPs as discrete heat sources); and (3) a lumped heat source that filled the entire cross section of the emplacement drift (SNL 2007 [DIRS 181383], Section 6.4)	Given the differences between the MSTHM Process Model and the east-west cross-sectional Lawrence Berkeley National Laboratory Mountain-Scale TH Model, the agreement between the two models is adequate (SNL 2007 [DIRS 181383], Section 6.4). Moreover, the differences in predicted temperatures between the MSTHM Process Model and the east-west cross-sectional Lawrence Berkeley National Laboratory Mountain-Scale TH Model are within the range of temperature differences resulting from parametric uncertainty (SNL 2007 [DIRS 181383], Tables 6.3-30 and 6.3-31).
EBS Chemical Environment: PTn Pore Water	The EBS Physical and Chemical Environment Model uses pore water compositions from the TSw to represent ambient conditions for the four starting waters (SNL 2007 [DIRS 177412], Section 6.6). The ACM selects ambient pore water from the overlying formation, the PTn, and then allows this water to seep up the geothermal gradient (from 23 to 96°C) [which is downward] through the TSw to the repository horizon (SNL 2007 [DIRS 177412], Section 6.11).	This ACM was not selected for use in the TSPA-LA Model because an analysis showed that using the TSw pore water adequately captures the chemistry of representative PTn pore waters. The use of PTn starting compositions does not significantly impact the key chemical components (pH, Pco_2, Ca, K, Si) of seepage (SNL 2007 [DIRS 177412], Section 6.11.1).
EBS Chemical Environment: Treatment of Alkali Fedspar by the Near Field Chemistry Model	Within the EBS Physical and Chemical Environment Model, the mixed feldspar phase adopted to represent the volcanic feldspar observed in the Topopah Spring Tuff is treated kinetically, i.e., this phase is always undersaturated with respect to clays, zeolites, and its own end-members (SNL 2007 [DIRS 177412], Section 6.11.2). An alternate approach would be to assume that the volcanic feldspar has reached equilibrium or near equilibrium, and thus thermodynamic controls of feldspar dissolution (e.g. saturation indices) must be considered when calculating seepage water compositions.	This equilibrium ACM was not chosen because at or near ambient temperatures, the volcanic waters are usually undersaturated with respect to feldspars and the kinetic treatment of the alkali feldspar is the appropriate approach (SNL 2007 [DIRS 177412], Section 6.11.2).

Table 6.2-1. Table of Alternative Conceptual Models (Continued)

Alternative Conceptual Models	Key Assumptions	Assessment and Basis
EBS Chemical Environment: Closed System with Respect to CO_2	The IDPS Model (SNL 2007 [DIRS 177411], Section 6.5), which is a process model implemented by the EBS P&CE suite of models (SNL 2007 [DIRS 177412]) describes an ACM that assumes a closed drift system with respect to CO_2. In a closed system, there is little or no exchange of CO_2 between the solution and the atmosphere; that is, the solution is modeled as essentially isolated from the atmosphere and H_2CO_3 is treated as a non-volatile acid. What little exchange might occur in a natural system approximating a closed system would alter the fugacity of CO_2 in the atmosphere. A closed system model might be appropriate for a wetter climate; however, relative humidity would be approximately 100 percent and little or no evaporation would occur.	A closed system with respect to CO_2 is not implemented in TSPA because the expected volume ratio of air to water in the drift is so large that CO_2 degassing from, or dissolving into, seepage water in the drift will negligibly affect CO_2 fugacity compared to the uncertainty in the input value for CO_2 fugacity. However, the EBS P&CE Model incorporates the uncertainty of an open or closed system by using the maximum and minimum Pco_2 values in the abstraction for the TSPA-LA (SNL 2007 [DIRS 177412], Section 6.3.2.8 and Section 6.15.1). The minimum value assumes a completely open system and the maximum value assumes a closed system. The actual system behaves in a manner between these two end-member assumptions.
WP and DS Degradation Model Component (Section 6.3.5)		
WP and DS Degradation: Parabolic General Corrosion Rate Law for DS Degradation (SNL 2007 [DIRS 180778], Section 6.5.6)	Assumes that the increasing oxide layer thickness on diffusion of oxidizing species to the underlying metal will have an inhibiting effect on corrosion.	Model is less conservative than the primary model.
WP and DS Degradation: Decreasing Rate Law for WP Degradation (SNL 2007 [DIRS 178519], Section 6.4.3.5.1)	General Corrosion rates of metals and alloys tend to decrease with time (SNL 2007 [DIRS 178519], Section 6.4.3.5.1).	The time-dependent general corrosion behavior of the WP was not included in the TSPA-LA because the constant (time-independent) rate model (for a given temperature) is more conservative and bounds the general corrosion behavior of the WP outer shell over the repository time period.
WP and DS Degradation: General Corrosion Rate Law based on Weight-loss samples only (SNL 2007 [DIRS 178519], Section 6.4.3.5.2)	The ACM discussion for a general corrosion rate law for WP degradation based on plain weight-loss samples (rather than crevice samples) and is found in the analysis model report (SNL 2007 [DIRS 178519], Section 6.4.3.5.2). The weight-loss data were fit to a Weibull distribution using maximum likelihood estimators (i.e., using the same methods applied to the crevice sample data).	A comparison of the general corrosion rate distribution resulting from fitting the 5-year exposed weight-loss sample to the Weibull distributions based on the crevice sample data shows that this alternative conceptual model is less conservative relative to the base case general corrosion model (SNL 2007 [DIRS 178519], Figures 6-28 and 6-23).

Table 6.2-1. Table of Alternative Conceptual Models (Continued)

Alternative Conceptual Models	Key Assumptions	Assessment and Basis
Localized Corrosion Initiation: Critical Temperature-Based Localized Corrosion Initiation Model (SNL 2007 [DIRS 178519], Section 6.4.4.8.1)	The evolution of WP temperature with time, coupled with knowledge of the critical temperature for the initiation of localized corrosion, (pitting/crevice corrosion) can be used to determine when localized corrosion initiates.	Test conditions at which the required critical temperatures have been measured are not directly relevant to the potential environments on the WP surface. The model does not account for the effects of electrochemical characteristics of the solution contacting the metal.
WP and DS Degradation: Coupled Environment Fracture Model for SCC Growth Rate (SNL 2007 [DIRS 181953], Section 6.4.6)	The model, based on charge conservation, incorporates the effects of oxygen concentration, flow rate, and the conductivity of the external environment, as well as accounting for the effect of stress on crack growth.	Model underestimates the crack growth rate, as compared to the slip dissolution/film rupture model, when both models were applied to predict the crack growth rate.
Localized Corrosion Initiation: Localized Corrosion Penetration as a Time-Dependent Growth Law (SNL 2007 [DIRS 178519], Section 6.4.4.8.2)	The overall rate of localized corrosion is controlled by the rate of surface complexation reactions. Once initiated, the crevice corrosion penetration rate would decrease with increasing depth.	Data needed to apply the model can only be estimated approximately from open literature. The time-independent constant penetration rate model is more conservative.
Localized Corrosion Initiation: Passive Film Breakdown Potential for Determination of Critical Potential (SNL 2007 [DIRS 178519], Section 6.4.4.1)	An alternative technique for the determination of critical potential would be to use the passive film breakdown potential (obtained from the forward scan of the cyclic potentiodynamic polarization tests).	This criterion would not account for the (often slow) kinetics of localized corrosion initiation and may not be appropriate for modeling the long time periods involved in repository environments. Furthermore, the breakdown potential is likely to be much higher when the passive film has been formed over long time periods, allowing for a decrease in the film defect density.
Localized Corrosion Initiation: WP Surface Area Subject to Localized Corrosion (SNL 2007 [DIRS 178519], Section 6.4.4.8.3)	A distribution for the minimum area affected by localized corrosion was developed (minimum of 0.05 percent and maximum of the percent of area wetted by seepage) (SNL 2007 [DIRS 178519], Section 6.4.4.8.3).	No information is available regarding local environments on the WP; therefore, the area affected by localized corrosion due to seepage is based on the fraction of the WP surface exposed to seepage. TSPA has conservatively taken the area affected by localized corrosion to be the area wetted by seepage. Therefore, the entire surface area can potentially undergo localized corrosion.

Table 6.2-1. Table of Alternative Conceptual Models (Continued)

Alternative Conceptual Models	Key Assumptions	Assessment and Basis
Waste Form Degradation and Mobilization Model Component (Section 6.3.7)		
In-Package Chemistry: ACMs (SNL 2007 [DIRS 180506], Table 6-14).	Three ACMs were considered as alternatives to the In-Package Chemistry Abstraction (SNL 2007 [DIRS 180506], Section 6.4). The first ACM was a one-dimensional column composed of *n* cells, where the reactants in each cell represent the WP components in a vertical cross section of a WP (SNL 2007 [DIRS 180506], Section 6.4.1). The second ACM considered variable-composition seepage entering a failed WP as a function of time, changing with time-varying changes in the physical and chemical environment in the drifts and the EBS (SNL 2007 [DIRS 180506], Section 6.4.2). A third ACM considers the alternate methodologies for determining the vapor flux rate through the stress corrosion cracks in a failed WP (SNL 2007 [DIRS 180506], Section 6.4.3).	The first two ACMs and the associated screening arguments for in-package chemistry are summarized in Table 6.3.7-67. The third ACM was excluded because the abstracted relationship for the vapor flux rate into a stress corrosion cracked-failed WP provided for the TSPA-LA Model is simpler and spans the expected range by this ACM.
Cladding Degradation: ACMs (SNL 2007 [DIRS 180616], Table 6-5)	Addresses various causes of fuel failure including initial cladding failures, stainless steel clad fuels, and splitting due to dry oxidation (SNL 2007 [DIRS 180616], Table 6-5).	In the TSPA-LA compliance model, no cladding credit is taken for CSNF (SNL 2007 [DIRS 180616], Section 6.2.1.2[a]). In other words, the cladding of all CSNF is assumed to be failed upon arrival at the repository. Cladding credit for CSNF was evaluated in the PMA (Appendix C).
Waste Form Degradation: CSNF Waste Form Degradation ACMs (BSC 2004 [DIRS 169987], Section 6.4.2)	1) Electrochemical - The anodic Tafel lines can be extrapolated to the corrosion potential. The long-term corrosion behavior of spent nuclear fuel is similar to that of unirradiated UO_2. Differences between the corrosion behavior of spent nuclear fuel and unirradiated UO_2 are due to water radiolysis (BSC 2004 [DIRS 169987]).	Do not incorporate into the TSPA-LA Model; data needed to apply the model can only be estimated. Use for Nominal Scenario Class model validation-particularly for validation of long-term extrapolation (BSC 2004 [DIRS 169987]).
	Surface Complexation Model - The overall rate of CSNF corrosion is controlled by the rate of surface complexation reactions. The long-term corrosion behavior of spent nuclear fuel is similar to that of unirradiated UO_2 (BSC 2004 [DIRS 169987]).	Do not incorporate into TSPA-LA Model; data needed to apply the model can only be estimated from open literature. Use for Nominal Scenario Class model validation-particularly for validation of long-term extrapolation (BSC 2004 [DIRS 169987]).

Table 6.2-1. Table of Alternative Conceptual Models (Continued)

Alternative Conceptual Models	Key Assumptions	Assessment and Basis
Waste Form Degradation: DSNF Waste Form Degradation ACM (BSC 2004 [DIRS 172453], Section 6.3)	An ACM for DSNF waste form degradation was based on the best-estimates dissolution models presented in *DSNF and Other Waste Form Degradation Abstraction* (BSC 2004 [DIRS 172453], Section 6.3). The application of this ACM would require that the dissolution rate expression be multiplied by the "actual" effective surface area of the SNF.	This ACM was screened out of the DSNF Waste Form Degradation Submodel (Section 6.3.7.4.2) because insufficient qualified data on the corrosion rates and the surface areas of the fuel in each group are available. In addition, the upper-limit degradation model that is implemented as a surrogate for all the DSNF, other than naval SNF, is a bounding model with respect to the degradation rate.
Waste Form Degradation: HLW Glass Degradation ACMs (BSC 2004 [DIRS 169988], Section 6.4)	Diffusion-Controlled Release—Release rate of radionuclides determined by solid-state diffusion rates (BSC 2004 [DIRS 169988], Table 6-2).	Not incorporated into TSPA-LA Model, since it doesn't have a sufficient basis using the available data for waste glasses (BSC 2004 [DIRS 169988], Table 6-2).
	Composition-Independent Effective Rate Constant—Intrinsic rate constants vary over a small interval for different compositions and the very low flow rates in the repository compared to those used in the laboratory mean that the affinity term will be low (BSC 2004 [DIRS 169988], Table 6-2).	Not incorporated into TSPA-LA Model. Current approach provides a much more robust range of values for use in the TSPA-LA (BSC 2004 [DIRS 169988], Table 6-2).
Dissolved Concentration Limits: ACMs (SNL 2007 [DIRS 177418], Table 6.23-1)	Plutonium—The theoretical fO_2 model. fO_2 = 0.2 bars (SNL 2007 [DIRS 177418], Table 6.23-1).	The results of this model differ significantly from experimental measurements (SNL 2007 [DIRS 177418]).
	Plutonium—The empirical Eh model. Eh = 1.04 – 0.0592*pH (SNL 2007 [DIRS 177418], Table 6.23-1).	The results of this model are lower than experimental results (SNL 2007 [DIRS 177418]).
	Neptunium—Neptunium incorporation into uranyl secondary phases. Neptunium concentration controlled by solid solution rather than by pure phases (SNL 2007 [DIRS 177418], Table 6.23-1).	Experimental studies on whether schoepite, the critical secondary uranyl phase, can incorporate sufficient neptunium and immobilize it during spent nuclear fuel corrosion do not provide a solid basis for recommending this model for use in the TSPA-LA (SNL 2007 [DIRS 177418], Table 6.23-1).
	Thorium—Solubility control by other thorium phases included in thermodynamic modeling database including ThO_2 (thorianite), $Th_{0.75}PO_4$, $Th(SO_4)_2$, ThF_4, $ThF_4 \cdot 2H_2O$. Solubility of thermodynamically most-stable phase controls concentrations (SNL 2007 [DIRS 177418], Table 6.23-1).	Solubilities calculated with ThO_2(am) are most consistent with measured thorium solubility in pure water. Other phases may be less soluble only under certain conditions or may be based on questionable data. More soluble ThO_2(am) was chosen for (SNL 2007 [DIRS 177418], Table 6.23-1).
	Americium—Solubility control by phase with properties between $Am(OH)_3$(am) to $Am(OH)_3$. Initially formed $Am(OH)_3$(am) will invert to more stable $Am(OH)_3$ with time. $Am(OH)_3$ stability decreases with time from self irradiation (SNL 2007 [DIRS 177418], Table 6.23-1).	$AmOHCO_3$ is formed in americium solubility experiments under Yucca Mountain conditions. Under some conditions, $Am(OH)_3$ may be less soluble, but generally choosing $AmOHCO_3$ is conservative (SNL 2007 [DIRS 177418], Table 6.23-1).

Table 6.2-1. Table of Alternative Conceptual Models (Continued)

Alternative Conceptual Models	Key Assumptions	Assessment and Basis
Dissolved Concentration Limits: ACMs (SNL 2007 [DIRS 177418], Table 6.23-1) (continued)	Protactinium—Solubility is same as that of ThO_2(am). Thorium is also a good analogue to protactinium and was modeled in this report (SNL 2007 [DIRS 177418], Table 6.23-1).	Solubility of Np_2O_5 was chosen because it is higher than that of ThO_2(am) under conditions modeled, so its choice is conservative (SNL 2007 [DIRS 177418], Table 6.23-1).
	Radium—Solid solution (Ra, Ba, Sr, Ca)SO_4 (SNL 2007 [DIRS 177418], Table 6.23-1).	Chemistry of in-package and invert waters are not so far outside the normal range of natural waters to cause different radium solubilities (SNL 2007 [DIRS 177418], Table 6.23-1).
	Technetium—Technetium incorporation into epsilon or "5 metal" phases during CSNF corrosion (SNL 2007 [DIRS 177418], Table 6.23-1).	Studies on fuel corrosion indicate the formation of Epsilon particles ("5 metal particles"). Technetium in these particles may not be released when the fuel corrodes. Sparse data on this phenomenon, however, do not provide a solid basis for recommending this as a Technetium model. Therefore, no solubility was defined, and inventory release should be in control (SNL 2007 [DIRS 177418], Table 6.23-1).
	Strontium—Solubility controlled by $SrCO_3$ or $SrSO_4$ (SNL 2007 [DIRS 177418], Table 6.23-1).	No solubility was defined, and inventory release should be in control. This is a conservative approach (SNL 2007 [DIRS 177418], Table 6.23-1).
	Tin—Solubility controlled by very insoluble crystalline phase cassiterite (SnO_2) (SNL 2007 [DIRS 177418], Table 6.23-1).	Solubilities calculated with SnO_2(am) are consistent with measured Sn solubility in pure water. Other phases may form only under certain conditions (SNL 2007 [DIRS 177418], Table 6.23-1).
EBS Colloids: ACMs (SNL 2007 [DIRS 177423], Section 6.4)	Kinetic Sorption—This model provides a method for predicting sorption behavior beyond laboratory time scales. Allows interpretation of data from different time scales. Based on model developed by Painter et al. (2002 [DIRS 174071]) and extended two- and three-site model developed by Wittman et al. 2005 [DIRS 174895].	This ACM is not supported by the available data (SNL 2007 [DIRS 177423]).
	Rate of Colloid Generation (Argonne National Laboratory) (SNL 2007 [DIRS 177423], Section 6.4.2,Table 6-19)—Rate of colloid spallation depends upon the rate of waste degradation. The rate of waste degradation may be defined by the rate of release to the boron content in the alteration fluid (for DHLWG) and technetium (for CSNF).	The ACM is tailored closely to the specific experimental configuration from which the supporting data were acquired. The position of this analysis is that, while promising, the ACM is currently not sufficiently developed for application to more generalized conditions.

Table 6.2-1. Table of Alternative Conceptual Models (Continued)

Alternative Conceptual Models	Key Assumptions	Assessment and Basis
	Mechanisms of Colloid Generation in CSNF (Pacific Northwest National Laboratory) (SNL 2007 [DIRS 177423], Table 6-10)-Colloid generation at, and mobilization from, the surface of degrading waste is primarily related to flow rate at the waste surface.	The supporting concepts and data from the peer-reviewed literature were developed in the context of deposition and remobilization of existing colloids under conditions of significant groundwater flow. These conditions likely will not apply to conditions anticipated in the repository. Mechanisms of colloid generation at the surface of corroding fuel may be different from mechanisms of mobilization of a discrete deposited colloid.
EBS Flow and Transport Model Component (Sections 6.3.6 and 6.3.8)		
EBS Transport: Dual-Continuum Invert Model	Crushed tuff invert ballast is modeled as a dual-continuum material consisting of intergranular pore space and intragranular pore space. All seepage flow into the drift flows through the intergranular pore space and into the UZ fractures. Imbibition from UZ host rock into the invert flows through the intragranular pore space. Diffusion of radionuclides also occurs in both the intergranular and intragranular pore spaces, from the WP corrosion products into UZ fractures and matrix, as well as between the two invert continua (SNL 2007 [DIRS 177407], Section 6.6.3).	Insufficient data to validate diffusion coefficients in individual continua. Insufficient data to confirm whether this is a bounding approach with respect to chemical conditions in the invert for calculating solubility and colloid stability.
EBS Flow: Bathtub Flow Model	Seepage water flowing into breached WP accumulates until void volume is filled before water containing dissolved radionuclides flows out. Various cases, such as changing inflow rates and effect of solubility and dissolution rate limits are evaluated (SNL 2007 [DIRS 177407], Section 6.6.1).	For several of the most pertinent cases, the flow-through model is conservative with respect to releases of radionuclides.
EBS Transport: Constrained Water Vapor and Oxygen Diffusion Model	The rate of steel component corrosion inside a WP is compared with the rate of diffusion of water vapor and oxygen through SCCs into a WP. A continuous film of absorbed water cannot form if the consumption rate is higher, which could delay the diffusive releases until all steel is fully corroded (SNL 2007 [DIRS 177407], Section 6.6.2).	Insufficient data to validate.

Table 6.2-1. Table of Alternative Conceptual Models (Continued)

Alternative Conceptual Models	Key Assumptions	Assessment and Basis
EBS Transport: Invert Diffusion Coefficient Model with Lower Limit on Water Content	As the water content of the crushed tuff ballast decreases, the water films that connect pore spaces become disconnected, and the effective diffusion coefficient drops more rapidly than predicted by Archie's law. Below some critical water content, the diffusion coefficient becomes zero, based on models of diffusion in soils (SNL 2007 [DIRS 177407], Section 6.6.4).	Insufficient data to validate diffusive behavior at very low water contents. Nonbounding; does not provide upper bounds on diffusion coefficients.
EBS Transport: Reversible Sorption of Radionuclides onto WP Corrosion	Iron oxyhydroxide corrosion products sorb many radionuclide species. Sorption is assumed to be reversible and will not compete with other radionuclides nor compete for irreversible sorption sites (SNL 2007 [DIRS 177407}, Section 6.6.5).	Does not account for limitations on total number of sorption sites. Does not account for competition with other radionuclides for sorption sites.
EBS Transport: Plutonium Sorption from Stationary Corrosion Products and Colloids	Plutonium sorbs strongly to iron oxyhydroxide corrosion product colloids and stationary corrosion products. Sorption may be considered slowly reversible (and modeled by computing the forward and reverse rate constants for the two-site model) (SNL 2007 [DIRS 177407], Section 6.6.6).	Experiment durations are short (hours to weeks) compared to the repository time scale. The mechanisms of plutonium sorption are not well enough understood to extrapolate the results outside the experimental design.
Unsaturated Zone Transport Model Component (Section 6.3.9)		
UZ Transport: Discretization of the UZ Matrix (DFM and MINC Models)	In the dual permeability model every fracture node has a parallel rock matrix node with the gradient between the two nodes defining the matrix diffusion process. A more accurate method of representing matrix diffusion would be to further discretize the rock matrix to more accurately define the concentration gradient at the matrix-fracture interface and within the matrix. Two models that include a finely discretized matrix the Discrete Fracture Model (DFM) and MINC Model are shown to predict longer breakthrough times than the implemented dual permeability model (SNL 2008 [DIRS 184748], Section 7.2.2 and Section 7.2.2[a]). The DFM uses flow fields based on the dual permeability flow simulations and the MINC model derives its flow fields based on the finer discretization of the rock matrix. A comparison of (DFM and MINC Model results showed that the MINC Model predicts longer breakthrough times than the Discrete Fracture Model (SNL 2008 [DIRS 184748], Section 7.2.2 and Section 7.2.2[a]).	The dual porosity model used for the TSPA-LA is conservative. The DFM is readily implementable in the UZ Transport Abstraction by replacing the transfer functions. The MINC Model is not practical because of its larger computational burden (SNL 2008 [DIRS 184748], Table 6-30).

Table 6.2-1. Table of Alternative Conceptual Models (Continued)

Alternative Conceptual Models	Key Assumptions	Assessment and Basis
UZ Transport: Alternative Finite Difference Numerical Models	An alternate method of approximating radionuclide transport in groundwater based on approximating the governing equations using finite difference equations (SNL 2008 [DIRS 184748], Table 6-30) was evaluated as an ACM for the FEHM Particle Tracking model.	The FEHM Particle Tracking Transport Abstraction Model matched the results predicted by the finite difference numerical methods (SNL 2008 [DIRS 184748], Sections 7.2.2[a] and 7.2.3.1[a]). Therefore the ACM supports the results using the particle tracking method.
UZ Transport: Lateral Flow Diversion In UZ Above the Repository	Lateral flow in the PTn will divert percolating water to the faults and reduce the percolation flux at the repository (BSC 2004 [DIRS 169861], Section 6.9.2).	Generally more conservative with respect to radionuclide transport (BSC 2004 [DIRS 169861], Section 6.9.2). Note that analyses used for this conclusion are based on the original infiltration model, but the conclusions are still valid. The updated model predicts significant diversion and redistribution into faults for the PTn (SNL 2007 [DIRS 184614], Section 8.6).
UZ Transport: No Radionuclide Release into Faults	The fault zones are defined as high-permeability zones subject to fast advective transport to the the top of the TSw and to the water table (SNL 2007 [DIRS 177396], Section 6.20.2).	The effects of not allowing direct release of radionuclides into the fault zones, on the overall transport to the water table, are not significant because lateral diversion directs the radionuclides into the fault zones (SNL 2007 [DIRS 177396], Section 6.20.2).
UZ Transport: Inclusion of Drift Shadow Effects	Inclusion of drift shadow effects would approximate the influence of capillary diversion, which may cause low fracture saturation below the drift (SNL 2008 [DIRS 184748], Section 6.7).	There is insufficient data to support this effect. It is considered conservative to ignore drift shadow effects. Additionally, the increased infiltration associated with future climate states may decrease the effects (SNL 2008 [DIRS 184748], Section 6.7).
UZ Transport: Inclusion of TH, THC, and THM Effects on UZ Flow	Vaporization due to repository heat will keep the drift dry for several hundred to a few thousand years. THC and THM effects may alter transport properties of the UZ rocks (SNL 2008 [DIRS 184748], Section 6.7).	TH, THC, and THM effects are insignificant after the change to glacial-transition climate (SNL 2008 [DIRS 184748], Section 6.7).

Table 6.2-1. Table of Alternative Conceptual Models (Continued)

Alternative Conceptual Models	Key Assumptions	Assessment and Basis
UZ Transport: Alternative Fracture-Matrix Interaction Model	The TSPA-LA Model utilizes the Active Fracture Model (AFM) (Liu et al. 1998 [DIRS 105729]), which assumes that only a fraction of connected fractures are active in conducting water. The AFM is implemented by applying a fracture-matrix effective interface area reduction term or a fracture-matrix interface area adjustment factor and a fracture spacing adjustment factor. The ACM assumes that all connected fractures are active in conducting water and represents a standard methodology with no fracture-matrix effective interface area reduction term applied. The active fracture model, with its reduced effective area of diffusion between fracture and matrix, is used in the TSPA-LA Model because of its more conservative nature and its ability to explain travel times associated with ^{14}C data (SNL 2008 [DIRS 184748], Section 5, Assumption 1) and (BSC 2004 [DIRS 170035], Section 7.4.1).	Using the standard methodology would enhance diffusion between the fracture and matrix. Because the active fracture model is more conservative and has better reflected field test results, the standard methodology was not recommended for inclusion in the TSPA-LA Model.
Saturated Zone Flow and Transport Model Component (Section 6.3.10)		
SZ Transport: Minimal Matrix Diffusion	Diffusion of radionuclides into the pore space of the rock matrix in the fractured volcanic units is extremely limited due to highly channelized groundwater flow, fracture coatings, or other factors (SNL 2008 [DIRS 183750], Section 6.4).	This ACM is implicitly included in the SZ Flow and Transport Model Abstraction and the 1-D SZ Flow and Transport Submodel through the range of uncertainty in key input parameters. The uncertain input parameters influencing matrix diffusion include DCVO, FISVO, and FPVO (SNL 2008 [DIRS 183750], Table 6.3.10-1).
SZ Transport: Horizontal Anisotropy in Permeability	Alternative interpretations of pump test results in the fractured volcanic units indicate preferential permeability along structural features oriented in the NNE-SSW direction, or in the WNW-ESE direction (SNL 2008 [DIRS 183750], Section 6.4).	This ACM is implicitly included in the 3-D SZ Flow and Transport Model Abstraction and the 1-D SZ Flow and Transport Abstraction through the range of uncertainty in an input parameter. The uncertain input parameter influencing horizontal anisotropy in permeability in the volcanic units near Yucca Mountain is the ratio of N-S to E-W permeability (SNL 2008 [DIRS 183750], HAVO; Table 6.3.10-2). This continuously distributed parameter varies from less than one to greater than one with most of the realizations greater than one.
Biosphere Model Component (Section 6.3.11)		
Biosphere: Radon Release from Soil (Air Submodel)	This ACM considers radon transport in the soil and the atmosphere, which requires more input data. The ERMYN conceptual model does not include these processes and uses a simple release factor.	This ACM is from the Biosphere Model Component based on an analysis (SNL 2007 [DIRS 177399], Section 7.4.3.1) showing that the ACM and the ERMYN model produce comparable results.

Table 6.2-1. Table of Alternative Conceptual Models (Continued)

Alternative Conceptual Models	Key Assumptions	Assessment and Basis
Biosphere: Evaporative Cooler (Air Submodel)	This ACM considers an inhalation dose from aerosols generated from evaporative coolers and is based on calculating radionuclide concentrations in the air due to an increase in humidity. The ERMYN conceptual model uses a submodel based on the amount of water evaporated rather than an increase in humidity.	This ACM is from the Biosphere Model Component based on an analysis (SNL 2007 [DIRS 177399], Section 7.4.3.2) showing that this ACM and the ERMYN model produce equivalent results.
Biosphere: Direct Deposition of Irrigated Water (Plant Submodel)	This ACM considers two processes, one where the deposited radionuclide moves from external plant surfaces into the plant tissues, and then from plant tissues into the edible portion of the crop. Weathering is applied only to contaminants that remain on external plant surfaces. Food processing loss is also considered in the ACM. The ERMYN conceptual model considers the radionuclides in irrigation water to be directly translocated to the edible parts of plants with weathering and accumulation during the growing period but without food preparation loss.	This ACM is from the Biosphere Model Component based on an analysis (SNL 2007 [DIRS 177399], Section 7.4.4.1) showing that this ACM and the ERMYN model produce comparable results.
Biosphere: Direct Deposition of Airborne Particulates (Plant Submodel)	This ACM is based on the crop external contamination. This contamination factor is very similar to a soil-to-plant transfer factor. The ERMYN conceptual model considers the deposited airborne particles on crop leaves acting the same way as the intercepted irrigation water.	This ACM is from the Biosphere Model Component based on an analysis (SNL 2007 [DIRS 177399], Section 7.4.4.3) showing that this ACM and the ERMYN model produce comparable results for reasonable input values.
Biosphere: Animal Product Contamination (Animal Submodel)	Two pathways are considered in this ACM. They are animal inhalation of contaminated air and animal soil ingestion. The ERMYN conceptual model excludes the inhalation of contaminated air, but it includes animal soil ingestion.	This ACM is from the Biosphere Model Component based on an analysis (SNL 2007 [DIRS 177399], Section 7.4.5) showing that soil ingestion is important but that inhalation of contaminated air is not.
Biosphere: ^{14}C Special Submodel	This ACM considered alternate ^{14}C pathways for plant uptake. This ACM considered uptake into plants only from roots and used a very low removal rate of carbon from soil because the model did not account for gaseous release of $^{14}CO_2$.	The method used by the biosphere model was chosen because it more realistically considered uptake of $^{14}CO_2$ gas into plants, resulting in higher plant concentrations (SNL 2007 [DIRS 177399], Sections 6.3.3, 7.3.6, and 7.4.7).
Biosphere: Environment-Specific Inhalation Submodel (Inhalation Submodel)	This ACM uses average values of input parameters for inhalation exposure. The ERMYN conceptual model considers inhalation exposure as a function of the environment because many model parameters, such as mass loading, breathing rate, and exposure time, differ among environments and activities.	This ACM is from the Biosphere Model Component based on an analysis (SNL 2007 [DIRS 177399], Section 7.4.9) showing that the ACM and the ERMYN model produce comparable results. In addition, it is easier to address uncertainty in the input parameters using environment-specific values.

Table 6.2-1. Table of Alternative Conceptual Models (Continued)

Alternative Conceptual Models	Key Assumptions	Assessment and Basis
Igneous Scenario Class (Section 6.5)		
Estimating the Igneous Event Rates in the Probabilistic Volcanic Hazard Analysis	The PVHA model uses the number of identified post-Miocene era volcanic events observable at the surface plus some buried in the Yucca Mountain region. *Characterize Framework for Igneous Activity at Yucca Mountain, Nevada* (BSC 2004 [DIRS 169989], Sections 6.3.1.6 through 6.3.1.7 and Table 6-4) identifies an ACM for the PVHA in which a significant number of buried (i.e., unidentified) volcanic centers would be included in the estimation of the igneous event rates. The basis for the ACM is that aeromagnetic anomalies suggest that a significant number of unidentified volcanic events were unaccounted for in the PVHA, thus underestimating the volcanic hazard.	This ACM was not propagated into the TSPA Model because its effects on the probability of an igneous event could not be quantified without further data collection. A drilling and sampling program is underway to determine whether any of these anomalies represent Quaternary buried volcanic centers. In addition, an update to the PVHA is underway to reassess the probability of intersection and the probability of a volcanic center being located on Yucca Mountain.
Estimating the Intersection Annual Probability in the Probabilistic Volcanic Hazard Analysis	*Characterize Framework for Igneous Activity at Yucca Mountain, Nevada* (BSC 2004 [DIRS 169989], Section 6.3.1.8 and Table 6-5) identifies several ACMs for estimating the intersection probability (i.e., the annual probability of a volcanic event intersecting the repository footprint).	The ACM probabilities are captured by the probability used in the PVHA.
Dike Propagation	*Dike/Drift Interactions* (SNL 2007 [DIRS 177430], Section 6.3.8) identifies ACMs for dike propagation that use hydraulic-fracture models.	*Dike/Drift Interactions* (SNL2007 [DIRS 177430], Section 6.3.8) concluded that none of these models were appropriate for the dike propagation in the vicinity of an underground repository as none of the models has a free surface that can model the changing behavior of the dike as the surface is approached.
Effusive Magma Flow Into Drifts	*Dike/Drift Interactions* (SNL 2007 [DIRS 177430], Section 6.3.3.5) identifies ACMs for effusive or pyroclastic flow from a dike into a drift.	Simulation of these flows and their interactions with WPs is computationally intensive and, therefore, not practical for implementation within the TSPA-LA Model. Instead, the abstractions included in Waste Packages Hit accounts for the effects of these flows within the TSPA framework.
Thermal Hydrologic Effects on Zones 1 and 2 Drifts	*Dike/Drift Interactions* (SNL 2007 [DIRS 177430], Section 6.4.7) identifies ACMs for the thermal hydrologic behavior of magma-filled drifts and its effects on neighboring drifts. These ACMs involve an evaluation of additional physics, including latent heat of crystallization, host-rock saturation, and enhanced vapor diffusion, and an alternative model for heat conduction from Zone 1 to Zone 2 emplacement drifts.	Inclusion of the latent heat of crystallization and host-rock saturation in the heat transfer analyses was evaluated and is shown to have a negligible effect on the results, producing elevated temperature histories (i.e., above boiling) no more than 2 to 5 years longer than without these ACMs included in the analysis (SNL 2007 [DIRS 177430], Section 7.3.2.1).

Table 6.2-1. Table of Alternative Conceptual Models (Continued)

Alternative Conceptual Models	Key Assumptions	Assessment and Basis
Volcanic Eruption Phase Dose	An ACM for the calculation of the radiation dose received by a receptor that does not leave the region during a volcanic eruption is detailed in Section 6.5.2.4. The eruption phase of a volcanic event refers to the conditions that exist during the volcanic eruption before the deposition of volcanic ash on the ground is completed The result of this calculation is used as the basis for excluding the potential eruption phase dose in the TSPA-LA Model.	Because a high concentration of airborne radioactive particulates is expected during this phase, inhalation of airborne-contaminated ash particles is the only pathway considered (SNL 2007 [DIRS 177399], Section 6.15.2). The receptor has the same inhalation characteristics as those for the RMEI discussed in Section 6.3.11.
Seismic Scenario Class (Section 6.6)		
Alternative Modeling Approaches Evaluated for Conceptual and Computational Models of Lithophysal and Nonlithophysal Rock (SNL 2007 [DIRS 166107], Section 7.4)	A standard approach for solving excavation stability problems is the use of numerical models based on continuum mechanics. Continuum models use constitutive relations to describe the mechanical behavior of a material. The use of a constitutive model requires that the mechanical effects of fractures be lumped into the constitutive relationships.	Continuum models are unable to predict instabilities, such as fracture and rockfall (SNL 2007 [DIRS 166107], Section 7.4.1). The discontinuum approach is more suitable for representing fracture of the rock mass and separation of the intact rock mass into blocks and was therefore adopted for modeling the drift degradation processes that occur after a seismic event (SNL 2007 [DIRS 166107], Section 7.4.2).
Alternative Conceptual Model for Crack Area Density Presented in Section 6.7.4 (SNL 2007 [DIRS 181953])	The alternative model considered a circular geometry circumscribed by a single through-wall crack. The base case model combines two conceptual models based on hexagonal geometry (SNL 2007 [DIRS 181953], Section 6.7.3).	The hexagonal geometry represents a high effective density of individual cracks and the two hexagonal geometry conceptual models are considered conservative representations. The ACM analysis, which uses circular geometry, is considered a limiting realistic case (SNL 2007 [DIRS 181953], Section 6.7.2).

Table 6.2-1. Table of Alternative Conceptual Models (Continued)

Alternative Conceptual Models	Key Assumptions	Assessment and Basis
Alternative Conceptual Models for Conditional Probability Distributions Representing Damaged Areas on WP, Damaged Areas on DS, and Volume of Rockfall from Seismic Event Considered	These alternate distributions included the gamma, normal, log-normal, Weibull, and triangular distributions, as presented in Sections 6.5.1.4, 6.5.2.4, 6.6.1.4, 6.6.2.4, 6.7.1.3, 6.7.2.4, 6.9.4, and 6.10.2.8 of *Seismic Consequence Abstraction* (SNL 2007 [DIRS 176828]).	Gamma distributions generally provided simpler and more accurate representations of the statistical observations than normal, log-normal, log-triangular, and Weibull distributions. The exception to the use of gamma distributions is that the fragility analyses (for drip shield plates and framework) have used log-normal representations to simplify manipulation of products and quotients of random variables.
Alternative Damage Abstraction for Fault Displacement Damage (SNL 2007 [DIRS 176828], Section 6.11.6)	The ACM considered the probability-weighted number of waste package failures from fault displacement and the number of fault intersections with emplacement drifts. The ACM was based on the use of historical data for fault displacement in the western United States.	The results provided by the ACM are consistent with the base-case model for both the probability-weighted number of WP failures and the number of fault intersections with the emplacement drifts (SNL 2007 [DIRS 176828], Section 6.11.6).

NOTES: ANL = Argonne National Laboratory; DHLWG = defense high-level waste glass; 1-D = one-dimensional; DCVO = effective diffusion coefficient in volcanic units; FISVO = flowing interval spacing in volcanic units; FPVC = flowing interval porosity; HAVO = ratio of horizontal anisotropy (north-south over east-west) in permeability; ERMYN = Environmental Radiation Model for Yucca Mountain, Nevada; DFM = discrete fracture model; MINC = multiple interacting continua.

INTENTIONALLY LEFT BLANK

6.3 TSPA-LA MODEL FOR THE NOMINAL SCENARIO CLASS

Section 6.3 presents a description of the Nominal Scenario Class for the Total System Performance Assessment for the License Application (TSPA-LA) Model. Sections 6.3.1 to 6.3.11 describe the conceptual models, the model abstractions, and implementation of these abstractions in the TSPA-LA Model. Each subsection of Section 6.3, namely Sections 6.3.1 to 6.3.11, will be introduced by two figures that have a consistent format and type of content. The first figure in each Section 6.3 subsection will illustrate how the submodels discussed in the subsection relate to other TSPA-LA submodels. The second figure in each subsection will illustrate important information about individual submodels. In particular, the figures illustrate the principal feeds, or inputs, to the submodels, the principal outputs from the submodels, highlights of the theoretical foundation and important characteristics of the submodels, and an indication of the sources of confidence, including field and laboratory data and auxiliary modeling in the submodels, and will vary according to the contents of the individual subsections. Detailed information describing the information feeds between the submodels of the TSPA-LA Model is included on wiring diagrams presented in Appendix G. Further information regarding the areas singled out on these figures can be found in the accompanying text of the individual Section 6.3 subsections and in the supporting analysis and/or model reports that are referenced in the Section 6.3 subsections.

The TSPA-LA Model of the Yucca Mountain repository system is a combination of integrated processes that have been conceptualized and modeled as a collection of coupled model components. For the TSPA-LA Model, eight principal model components are combined to evaluate repository system performance for the Nominal Scenario Class. The model components are:

- Unsaturated Zone (UZ) Flow
- Engineered Barrier System (EBS) Environment
- Waste Package (WP) and Drip Shield (DS) Degradation
- Waste Form Degradation and Mobilization
- EBS Flow and Transport
- Unsaturated Zone (UZ) Transport
- Saturated Zone (SZ) Flow and Transport
- Biosphere.

Section 6.3 provides detailed descriptions of the TSPA-LA submodels that comprise the model components. Table 6-1 can be considered a guide that links the principal TSPA-LA Model components shown on Figure 6-1 to the TSPA-LA submodels. Each submodel description in Section 6.3 includes:

- A discussion of how the submodel is connected to other submodels and model components in the TSPA-LA Model.
- A description of the conceptual model on which the submodel is based.
- A description of the submodel abstraction.

- A description of how the abstraction is implemented in the TSPA-LA Model.

- An evaluation of the consistency and conservatism in assumptions and parameters used in the TSPA-LA Model. Assumptions and parameter values that are different among submodels in the TSPA-LA Model are documented in each section.

- A summary of alternative conceptual models (ACMs) that were considered in the development of the conceptual model.

The focus of Section 6.3 is on the TSPA-LA Model components and submodels and their implementation for the Nominal Scenario Class.

6.3.1 Mountain-Scale Unsaturated Zone Flow

UZ flow in the TSPA-LA Model refers to the percolation of groundwater through the unsaturated rocks between the land surface and the water table. The Site-Scale UZ Flow Model (SNL 2007 [DIRS 184614]) provides the flow fields for the Multiscale Thermohydrologic Model (MSTHM) and the UZ Transport Submodel (Section 6.3.9). Figure 6.3.1-1 illustrates the connections between the Site-Scale UZ Flow Model and the submodels of the TSPA-LA Model. Figure 6.3.1-1 shows that the Climate Analysis, as described in *Future Climate Analysis* (BSC 2004 [DIRS 170002]) and *Data Analysis for Infiltration Modeling: Extracted Weather Station Data Used to Represent Present-Day and Potential Future Climate Conditions in the Vicinity of Yucca Mountain* (SNL 2007 [DIRS 177081]), and the Infiltration Model, as described in *Simulation of Net Infiltration for Present-Day and Potential Future Climates* (SNL 2007 [DIRS 182145]), contribute to the Site-Scale UZ Flow Model. *Future Climate Analysis* (BSC 2004 [DIRS 170002]) provides climate analogues to be used for assessing the future mean annual temperature and precipitation in the region, including Yucca Mountain. Future climate conditions at Yucca Mountain must be predicted to determine the hydrological conditions at and near Yucca Mountain. *Data Analysis for Infiltration Modeling: Extracted Weather Station Data Used to Represent Present-Day and Potential Future Climate Conditions in the Vicinity of Yucca Mountain* (SNL 2007 [DIRS 177081]) provides climatological data based on present-day conditions in the Yucca Mountain vicinity and the climate analogues presented in *Future Climate Analysis* (BSC 2004 [DIRS 170002]). Figure 6.3.1-2 illustrates the outputs provided by the Climate Analysis to the Infiltration Model and TSPA-LA Model. *Future Climate Analysis* (BSC 2004 [DIRS 170002]) provides three climate states for use in the TSPA-LA Model: present-day, monsoon, and glacial-transition. The outputs from the *Future Climate Analysis* (BSC 2004 [DIRS 170002]) include duration (Table 6.3.1-1), climate analogues for precipitation rates, and air temperatures for each climate state. *Data Analysis for Infiltration Modeling: Extracted Weather Station Data Used to Represent Present-Day and Potential Future Climate Conditions in the Vicinity of Yucca Mountain* (SNL 2007 [DIRS 177081]) provides climatological data, such as precipitation rates and air temperatures, to the infiltration model.

Figure 6.3.1-3 illustrates and describes the main differences among the three climate states used in the TSPA-LA Model. The future climate states (i.e., monsoon and glacial-transition) were based on analogue sites with representative conditions for those periods. Figure 6.3.1-3 lists the analogue sites used to define the conditions for these future climate states. The present-day climate is based on climatic data available for the Yucca Mountain site. The monsoon climate state will have a higher precipitation rate and higher temperature than the present-day climate (BSC 2004 [DIRS 170002], Section 7.1). The glacial-transition climate state will have a higher precipitation rate but lower temperature than the present-day climate (BSC 2004 [DIRS 170002], Section 7.1). A fourth climate state is also implemented as per regulations found in *Implementation of a Dose Standard After 10,000 Years* (70 FR 53313 [DIRS 178394]). The fourth climate state (post-10,000-year climate state) extends the simulations from 10,000 years to 1,000,000 years. The implementation of the fourth climate state is based on the NRC Proposed Rule 10 CFR 63.342 (c) (2) [DIRS 178394]:

> "DOE must assess the effects of climate change. The climate change analysis may be limited to the effects of increased water flow through the repository as a

> result of climate change, and the resulting transport and release of radionuclides to the accessible environment. The nature and degree of climate change may be represented by constant climate conditions. The analysis may commence at 10,000 years after disposal and shall extend to the period of geologic stability. The constant value to be used to represent climate change is to be based on a log-uniform probability distribution for deep percolation rates from 13 to 64 mm/year (0.5 to 2.5 inches/year)."

The implementation of the fourth climate state in the Site-Scale UZ Flow Model is described in *UZ Flow Models and Submodels* (SNL 2007 [DIRS 184614]).

Net infiltration is the flux across the depth where it can no longer be withdrawn by evaporation or transpiration by plants. The Infiltration Model provides net infiltration rates of meteoric water, which are used as inputs for the upper boundary condition for the Site-Scale UZ Flow Model. Figure 6.3.1-4 schematically shows the connection between the Infiltration Model and the Site-Scale UZ Flow Model, as well as inputs to and outputs from the Infiltration Model. Figure 6.3.1-5 is a schematic illustration showing the variation of precipitation and consequent net infiltration with respect to elevation and landforms at Yucca Mountain. Net infiltration will be influenced by a number of factors (BSC 2004 [DIRS 169734], Section 7.1.3). Precipitation in the Yucca Mountain region is spatially variable and dependent on meteorological conditions, as well as elevation and surface geology (BSC 2004 [DIRS 169734], Section 7.1.3.3). There is a correlation between surface elevations and local precipitation. In the higher elevations, there are likely to be thinner surface soils and shallower fractured bedrock. In the lower elevations, especially in washes, the surface tends to be alluvium and the bedrock tends to be at a greater depth. Some of the factors that have an influence on how precipitation becomes net infiltration are the amount and rate of precipitation, evaporation, transpiration, topography, thickness of surface soils, run-on and runoff of surface water, redistribution of moisture, permeability and sorptive capacity of the soils, and the amount of vegetation, as well as fractured bedrock characteristics. In addition, these factors may change through time due to long-term climatic and geomorphologic changes.

Figure 6.3.1-6 displays principal input and output interfaces between the Site-Scale UZ Flow Model, the MSTHM (Section 6.3.2), and the UZ Transport Submodel (Section 6.3.9). As shown on Figure 6.3.1-6, outputs of the Site-Scale UZ Flow Model are passed to the MSTHM to specify the percolation flux, consisting of liquid flux in both the fracture and matrix continua, at the base of the Paintbrush nonwelded hydrogeologic (PTn) unit. The percolation flux at the base of the PTn unit, above the repository horizon, is used as an upper boundary condition, as described in *Multiscale Thermohydrologic Model* (SNL 2007 [DIRS 181383], Section 6.2.6.6). UZ hydrologic properties, such as permeability, porosity, residual saturation, van Genuchten parameters, and Active Fracture Model parameters, are also passed to the MSTHM (SNL 2007 [DIRS 181383], Table 4.1-1, Sections 6.2.6 and 6.2.6.5). These parameter values are used to generate the EBS thermal-hydrologic (TH) conditions for implementation in the TSPA-LA Model. The above parameter values are also used to generate the drift-seepage conditions, as described in *Abstraction of Drift Seepage* (SNL 2007 [DIRS 181244], Section 6.7.1.2), for implementation in the TSPA-LA Model. In addition, flow fields are passed to the UZ Transport Submodel (Section 6.3.9). The UZ flow fields provide input of fracture and matrix liquid flux

and liquid flux between fracture and matrix continua, along with liquid saturation and pressure values.

6.3.1.1 Conceptual Model

The Site-Scale UZ Flow Model uses a dual-permeability conceptual model that captures the effects of fast-flow paths and allows for fracture-matrix coupling. Flow is modeled in both fracture and matrix continua and these continua interact with one another. Both fracture and matrix continua are assigned their own hydrologic properties, such as permeability and porosity. Hydrologic properties are, in general, uniform layer-wise. Generally, fractures are modeled as part of a highly permeable continuum having low porosity, whereas the matrix is modeled as a much less permeable continuum having higher porosity than the fracture continuum. Fracture-matrix interaction is represented with an active fracture model, in which only some fractures are actively conducting water under unsaturated conditions (SNL 2007 [DIRS 184614], Section 6.1.2). Major faults are explicitly included in the Site-Scale UZ Flow Model. When compared to the same hydrologic units outside the fault zone, the fault zone fracture permeabilities are generally much higher than in the rest of the Site-Scale UZ Flow Model, enabling preferential flow paths in portions of the Site-Scale UZ Flow Model (SNL 2007 [DIRS 179545], Section 6.3.4 and Tables B1 to B4). In addition to the fault zone properties differing from the surrounding units, each hydrogeologic unit (TCw, PTn, TSw, and CHn) has a different hydrologic property set. Either the ground surface at Yucca Mountain or the tuff-alluvium contact in areas of significant alluvial cover is taken as the top model boundary and the water table is taken as the bottom model boundary of the Site-Scale UZ Flow Model. For flow simulations, the top boundary is modeled as a Dirichlet-type condition and the water flux is specified as a source term to the fracture grid blocks in the second grid layer from the top and the water table is used as the bottom boundary that is assigned a single-valued fixed water pressure, which is equivalent to specifying a constant liquid saturation (SNL 2007 [DIRS 184614], Section 6.1.3). Changes in the water table elevation at the bottom boundary because of climate-related changes in recharge are not included in the Site-Scale UZ Flow Model simulations. The basis for this implementation is that water flow through the unsaturated rock within Yucca Mountain is predominantly downward and dominated by gravity. Therefore, the elevation of the water table has little influence on the fluxes calculated for the UZ flow fields.

To approximate the effects of a rising water table on a radionuclide transport simulated by the finite element heat and mass (FEHM) transfer code (FEHM V2.24-01, STN: 10086-2.24-01-00 [DIRS 179419]), the external monsoon climate, glacial-transition, and post-10,000-year climate flow field files used in the transport model are post-processed. In the UZ flow model area, the present-day water table varies from less than 730 m to greater than 980 m above mean sea level (BSC 2004 [DIRS 169855] Figure 6.2). Within the repository footprint, the present-day water table varies from around 730 m to 850 m above mean sea level (BSC 2004 [DIRS 169855] Figure 6.2). Note that the bottom boundary for the flow models of all climate states is the present day water table. For use in conjunction with FEHM's multi-species particle tracking model, the flow-field files for the monsoon, glacial-transition, and post-10,000-year climate flow fields from the UZ Flow Model Abstraction are post-processed to approximate the affects of a rising water table. The rising water table is approximated by constraining it to a minimum elevation of 850 m above mean sea level (SNL 2008 [DIRS 184748], Section 6.4.8). For future climates, at any locations where the present-day water table is below 850 m the water table is set

to 850 m, and at any locations where the present-day water table is above 850 m, the water table is not adjusted from the present day level (BSC 2004 [DIRS 169855]). The updating of the water table is implemented in the future climate flow-field files by changing saturations to 1.0 and replacing nodal fluxes with extremely large flux values for nodes located at or below 850 m mean sea level in areas where the water-table is truncated. In the UZ Transport Submodel's FEHM multi-species particle tracking analysis, the particle exit nodes, for future climate states, become the nodes at the elevation of the new water table that have been assigned the large water flux values by FEHM. At the time of the first updating of the flow field (at the time of change to the monsoon climate), all radionuclide particles below the new water table level are instantaneously made available to the SZ. The water table then remains constant for the rest of the simulation; the monsoon, glacial-transition, and post-10,000-year climates are assumed to have a similar water table elevation. Additional information concerning the water table interface between the UZ Transport Submodel and SZ Flow and Transport Submodels, as well as the effects of water table rise on flow and the transport of radionuclides, is discussed in the subsequent sections on UZ Transport (Section 6.3.9) and SZ Flow and Transport (Section 6.3.10).

Figure 6.3.1-7 shows how the distribution of mountain-scale UZ percolation flux changes as it moves downward through the mountain due to the hydrogeologic processes and conditions within the mountain. A detailed discussion of the Site-Scale UZ Flow Model is contained in *UZ Flow Models and Submodels* (SNL 2007 [DIRS 184614]), and a summary of the processes affecting the percolation flux through the mountain is in the following discussions. Figure 6.3.1-8 shows the stratigraphic column present at a central location within the Yucca Mountain site and is useful for this discussion to visualize the thickness and order of the stratigraphic formations as they are discussed. Water flows through the densely fractured Tiva Canyon welded (TCw) unit mainly through the fractures. The high density of interconnected fractures and low matrix permeabilities in the TCw unit (SNL 2007 [DIRS 179545], Tables 6-6 through 6-9 and Section 6.3.2) are considered to give rise to significant water flow in fractures and limited matrix imbibition (water flow from fractures to the matrix). Thus, episodic infiltration pulses are expected to move rapidly through the TCw fracture networks with little attenuation by the matrix. The relatively high matrix permeabilities and porosities and low fracture densities of the PTn unit (SNL 2007 [DIRS 179545], Tables 6-6 through 6-9 and Section 6.3.2) convert the predominant fracture flow in the TCw to dominant matrix flow within the PTn. The dominance of matrix flow in the PTn and the relatively large storage capacity of the matrix, resulting from its high porosity and low saturation (under the ambient conditions), give the PTn significant capacity to attenuate infiltration pulses. Faults (or geologic structures) may cut through the entire PTn unit at some locations, leading to fast flow paths if the local PTn tuff matrix is not able to convert all of the fault flow into matrix flow. In addition, some lateral diversion of water occurs in the PTn unit owing to the capillary barrier effects (SNL 2007 [DIRS 184614], Sections 6.1.2 and 6.2.2). Unsaturated flow in the Topopah Spring welded (TSw) hydrologic unit occurs primarily through fractures. The TSw hydrologic units are the host-rock units for the entire repository footprint (Figure 6.3.2-4).

The main hydrogeologic units below the repository are the Topopah Springs welded, Calico Hills (CHn) nonwelded, and Crater Flat undifferentiated units. All of these units have vitric and zeolitic components that differ in their degree of hydrothermal alteration and subsequent hydrologic properties. The zeolitic rocks have low matrix permeability and some fracture

permeability. On the other hand, similar to the PTn unit, the vitric units in the CHn have relatively high matrix porosity and permeability. Therefore, matrix flow dominates in the vitric units. One distinctive feature below the repository is the existence of perched-water zones (SNL 2007 [DIRS 184614], Section 6.2.2.2). The occurrence of perched water suggests that certain portions of the lower TSw (e.g., the basal vitrophyre) and the upper CHn (zeolitic portion) impede vertical flow (SNL 2007 [DIRS 184614], Section 6.2.2.2). These hydrogeologic units of lower permeability act to divert the downward progression of contaminant transport by forcing path changes and increases in lateral flow components (SNL 2007 [DIRS 184614], Section 6.2.2.2).

6.3.1.2 Model Abstraction

The UZ Flow Model Abstraction is comprised of 16 steady-state flow fields generated by the three-dimensional Site-Scale UZ Flow Model (SNL 2007 [DIRS 184614], Section 6.6). The sixteen flow fields consist of four flow fields representing uncertainty for each of four climate states. The flow fields provide spatial distributions of fracture-fracture, matrix-matrix, and fracture-matrix water flow rates and moisture contents in the unsaturated zone for use in the Multiscale Thermohydrologic Model (MSTHM) Abstraction (Section 6.3.2) and the UZ Transport Submodel Abstraction (Section 6.3.9). The MSTHM utilizes the flow rates at the base of the PTn, from the 16 flow fields, to generate invert DS and WP temperature, relative humidity, drift-wall temperature, percolation flux, and saturations used by other models and submodels in the TSPA model. The UZ Transport Model Abstraction is based on FEHM's multi-species particle tracking option that uses the 16 flow fields to evaluate the movement of radionuclides from the repository to the water table. During TSPA-LA Model simulations, temporal changes in climate are approximated by changes from one steady-state flow field to another. For example, at the onset of the monsoon climate stage, a present-day climate stage flow field is replaced with a monsoon climate stage flow field.

The four climate states used in the TSPA-LA Model are the present-day climate, monsoon climate state, glacial transition climate state, and a post-10,000-year climate state. A range of durations of the first three climate states, as given in *Future Climate Analysis* (BSC 2004 [DIRS 170002], Table 6-1), are 400 to 600 years for the present-day climate, and 900 to 1,400 years for the monsoon climate. The glacial-transition climate is then predicted to last until 10,000 years after postclosure or 8,000 to 8,700 years. These durations are based on a reconstruction of climate history for the last long earth-orbital cycle from the microfossil record of cores drilled at Owens Lake (BSC 2004 [DIRS 170002], Sections 6.5.1 and 6.6.1). The range of possible durations is developed from the evaluation of the durations using alternative sedimentation rates. The minimum durations of 400 years for the present-day climate and 900 years for the monsoon climate are based on a sediment accumulation rate of 63 cm per 1000 years (BSC 2004 [DIRS 170002], Section 6.6.1 and Litwin et al. [DIRS 109440]). The maximum durations of 600 years for the present-day climate and 1,400 years for the monsoon for the glacial-transition climate are based on a sediment accumulation rate of approximately 40 cm per thousand years (BSC 2004 [DIRS 170002], Section 6.6.1 and Smith and Bishoff (1997 [DIRS 109480]). The glacial-transition climate is then based on the remaining years needed to complete the 10,000 years for the future climate analog.

The Climate Submodel is implemented in the TSPA-LA Model, using the maximum present-day and monsoon durations (i.e., the present-day climate duration is modeled as 600 years, the monsoon climate duration is 1,400 years, and the glacial-transition climate is used until 10,000 years after postclosure). The maximum present-day and monsoon climate durations were chosen based on an evaluation of the sedimentation rates used to derive the climate durations which indicated that the rate of 40 cm per thousand years is the most representative sediment-accumulation rate (BSC 2004 ([DIRS 170002], 6.6.1). As discussed in BSC 2004 ([DIRS 170002], 6.6.1), in addition to their evaluation of the 6 m to 304 m interval of borehole OL-92 on which the 40 cm per thousand years rate is based, Smith and Bishoff (1997 [DIRS 109480]) also present a sediment-accumulation rate for the upper 6 to 24 m section of borehole OL-92 of 79 cm per thousand years. Correcting for differences in porosity and density in the upper 6 to 24 m of borehole OL-92, the mass accumulation rates for the upper 6 to 24 m of borehole OL-92 and the 6 m – 304 m interval, had nearly identical mass-accumulation rates of 52.4 and 51.4 g/cm^2 per thousand years. In addition, other work by Litwin et al. (1999 [DIRS 109440]) showed that although a Holocene age silt from the borehole OL-92 had a sediment-accumulation rate of 64.2 cm per thousand years, the mass accumulation rate was 42.6 g/cm^2 per thousand years, less than the 51.4 g/cm^2 average mass-accumulation rate associated with the 40 cm per thousand years sediment-accumulation rate (Smith and Bishoff 1997 [DIRS 109480]). This shows that to be comparative, sedimentation-accumulation rates need to be corrected for the impact of compaction. This also indicates that the rates of 60 to 66 cm per thousand years (the source of 63 cm per thousand years rate used to derive the minimum duration values) presented by Litwin et al. (1999 [DIRS 109440]) may need to be adjusted. In contrast, the sediment-accumulation rate of 40.1 cm per thousand years (Smith and Bishoff 1997 [DIRS 109480]), used to derive the maximum durations, does not need to be adjusted because the 6 m to 304 m borehole interval used to develop the sediment-accumulation rate accounts for much of the impact of compaction by nature of its length. Note that the present-day climate is simulated for 550 years after closure since the simulations start at closure.

The four uncertainty cases used in the UZ Flow Model were selected from an initial set of 40 infiltration uncertainty maps for each of the first three climate states. These were generated by MASSIF, based on the LHS sampling (2 replicates of 20 realizations each) of parameters as part of the Infiltration Model Abstraction (SNL 2007 [DIRS 182145], Section 6.5.7). Parameters sampled for the Present-Day Climate State LHS simulations include the annual average of the natural logarithm of the amount of daily rainfall on days with precipitation, plant height, maximum rooting depth, soil depth for soil depth class 4, bulk saturated hydraulic conductivities of bedrock IHUs 405 and 406, holding capacity of soil group 5/7/9, readily evaporable water, minimum transport coefficient, evaporation layer depth, and the slope of the normalized difference vegetation index-basal transpiration coefficient function (SNL 2007 [DIRS 182145], Table 6.5.1.1-1, Section 6.5.1, and SNL 2007 [DIRS 184077], Section 3). Parameters sampled for the Monsoon Climate State simulations include the annual average of the probability of zero precipitation given that the previous day was dry, annual average of the natural logarithm of the amount of daily rainfall on days with precipitation, amplitude of the annual variation in the median amount of daily rainfall on days with precipitation, annual average maximum daily temperature on days with precipitation, plant height, maximum rooting depth, slope of the relationship between duration of daily precipitation and amount of daily rainfall, soil depth for soil depth class 4, bulk saturated hydraulic conductivities of bedrock IHUs 405 and 406, holding capacity of soil group 5/7/9, readily evaporable water, minimum transport coefficient,

evaporation layer depth and the slope of the normalized difference vegetation index-basal transpiration coefficient function (SNL 2007 [DIRS 182145], Section 6.5.5.2, and SNL 2007 [DIRS 184077], Section 3). Parameters sampled for the Glacial-Transition Climate State LHS simulations include the annual average of the probability of zero precipitation given that the previous day was dry, annual average of the natural logarithm of the amount of daily rainfall on days with precipitation, phase of the annual variation of the mean daily rainfall on days with precipitation, slope of the relationship between duration of daily precipitation and amount of daily rainfall, plant height, maximum rooting depth, soil depth for soil depth class 4, bulk saturated hydraulic conductivities of bedrock IHUs 405 and 406, holding capacity of soil group 5/7/9, readily evaporable water, minimum transport coefficient, evaporation layer depth, slope of the normalized difference vegetation index-basal transpiration coefficient function, and minimum precipitation duration (SNL 2007 [DIRS 182145], Section 6.5.5.3, and SNL 2007 [DIRS 184077], Section 3). The four representative infiltration maps for each climate used in the development of the associated UZ Flow Model flow fields are the 10th, 30th, 50th, and 90th percentile realization outputs of the LHS analysis. The percentile position is based on the spatially averaged mean annual net infiltration for each realization (SNL 2007 [DIRS 182145], Sections 6.5.7.1, 6.5.7.2, and 6.5.7.3).

In the development of the infiltration maps, only climate and shallow soil layer information were considered. Data from the deep UZ can provide additional information with respect to infiltration/percolation processes that can be used to indicate which scenario is closer to reality (SNL 2007 [DIRS 184614], Section 6.8.2) and derive more appropriate weighting factors. Chloride and temperature data from the Yucca Mountain site UZ are especially amenable for use in conjunction with a generalized likelihood uncertainty estimate (GLUE) methodology to determine meaningful weighting factors for the selected infiltrations maps (SNL 2007 [DIRS 184614], Section 6.8.2). Temperature profiles of the Yucca Mountain UZ are controlled by several factors including formation thermal conductivity, net infiltration rates, and surface temperatures. The temperature profiles at Yucca Mountain were used to help constrain infiltration maps because of the sensitivity to infiltration rates. Simulated temperature distributions at five boreholes, for which qualified temperature data were available, were generated using the four present-day infiltration maps to help determine weighting factors (SNL 2007 [DIRS 184614], Section 6.8.3). Results were compared to measured borehole temperature data at 50 points (40 meters or more below the ground surface) to help determine the appropriateness of the four infiltration maps. Simulated temperature distributions and comparisons to measured data are presented in *UZ Flow Models and Submodels* (SNL 2007 [DIRS 184614], Section 6.3). Chloride, which is a natural tracer for studying water movement in geologic systems, provided a second parameter that was used to constrain the infiltration maps and help generate appropriate weighting factors (SNL 2007 [DIRS 184614], Section 6.8.3). Chloride data from two horizontal tunnels and twelve vertical boreholes provided a means to compare the fit of outputs from UZ chloride submodel simulations based on the four present-day infiltration rates (SNL 2007 [DIRS 184614], Section 6.8.3). Results of the chloride simulations are presented in *UZ Flow Models and Submodels* (SNL 2007 [DIRS 184614], Section 6.5). Based on the probability of the infiltration maps from the infiltration model and the relative agreement between model simulations and the temperature and chloride data, the GLUE methodology was applied to determine the most appropriate weighting factors to be used in the TSPA-LA Model. Note that because the GLUE methodology relies on field observations for present-day conditions, the weighting factors are determined using simulations based on present-

day climate infiltration maps. The steps used in the GLUE methodology can be summarized as follows: (1) determine the prior probability values (weighting factors) for each infiltration map; (2) perform UZ flow and transport calculations for each selected infiltration map and, based on model results and observations for temperature and chloride concentrations, calculate likelihood values; and (3) determine weighting factors based on the prior weights and the likelihood values (SNL 2007 [DIRS 184614], Section 6.8.5.1). The final weighting factors presented in *UZ Flow Models and Submodels* (SNL 2007 [DIRS 184614], Section 6.8.5.3) are an average of weighting factors based on combining different likelihood functions (SNL 2007 [DIRS 184614], Section 6.8.5.1) and averaging techniques. The average weighting factors that are used in the TSPA-LA Model are presented in Table 6.3.1-2 (see also SNL 2007 [DIRS 184614], Table 6.8-1).

For the post-10,000-year period, proposed 10 CFR 63.342(c)(2) [DIRS 178394] specifies that the average percolation flux through the repository follows a log-uniform probability distribution from 13 to 64 mm/yr. Therefore, independent infiltration maps are not generated from the Infiltration Model for the post-10,000-year period. The preamble to the proposed rule (70 FR 53316 [DIRS 178394]) also states that DOE should "continue such calculations of spatial variation, subject to the constraint that, across the repository footprint, the ''average'' overall percolation rate would remain within the range and distribution specified by NRC." As for the first three climate states, four uncertainty infiltration maps are developed to be used with the UZ Flow Model. The UZ Flow Model results indicate that average infiltration at the ground surface within the projection of the repository footprint is close to the average flux through the repository at depth (SNL 2007 [DIRS 184614], Section 6.1.4). The target average infiltration values are selected from the log-uniform probability distribution of deep percolation rates from 13 to 64 mm/year. The points on the cumulative distribution are (SNL 2007 [DIRS 184614], Table 6.1-3) in cumulative form, 31 percent, 70 percent, 86 percent, and 97 percent (SNL 2007 [DIRS 184614], Figure 6.1-6), which corresponds to the cumulative probabilities derived using the GLUE methodology for the first three climate states. The average infiltration rates corresponding to these cumulative probability values are 21.29, 39.52, 51.05, and 61.03 mm/yr (SNL 2007 [DIRS 184614], Table 6.1-3). The 12 infiltration maps generated for the Present-Day, Monsoon, and Glacial Transition Climate states are used as a basis for the spatial variability for the post-10,000-year climate state (SNL 2007 [DIRS 184614], Section 6.1.4). For the 12 infiltration maps, the average infiltration through the repository footprint was calculated. The four infiltration maps with average infiltration rates that most closely matched chosen average target infiltration rates were then used as a basis for generating the flow-fields. The closest infiltration rate maps for the post-10,000-year climate state determined by the analysis were the present-day 90th percentile, the 50th percentile Glacial Transition, the 90th percentile glacial transition, and the 90th percentile monsoon for the target values of 21.29, 39.52, 51.05, and 61.03 mm/yr, respectively. The four infiltration maps were then scaled so that the average infiltration through the repository footprint would match the target values.

Implementation of uncertainty in the infiltration map for the UZ Flow Model Abstraction is then based on sampling from the set of four flow fields for each climate that was developed using the 10th, 30th, 50th, and 90th percentile infiltration maps for the respective climates. For each TSPA-LA Model epistemic realization, the infiltration scenario (10th, 30th, 50th, or 90th percentile for the present-day, monsoon, and glacial transition climates and scaled versions of the present-day 90th percentile, the 50th percentile Glacial Transition, the 90th percentile glacial

transition, and the 90th percentile monsoon) is chosen based on sampling the weighting factors presented in Table 6.3.1-2. Note that the same weighting factors are used for the present-day, monsoon and glacial transition climates. The assumption that the same weighting factors can be used for the three climate states is based the similarity in modeling methods used for infiltration and UZ Flow (SNL 2007 [DIRS 184614], Section 6.8.8). Infiltration estimates for future climates are produced using the same hydrologic parameter ranges, the same methods for modeling weather patterns and the same infiltration model as used for the present-day climate. Additionally, UZ flow estimates are generated for future climates using the same parameter sets, the same modeling assumptions and the same UZ Flow Model as for the present-day climate. Due to the similarity of modeling methods across climate states, it is expected that any deviations between UZ Flow model results for temperature and chloride, based on infiltration model results for infiltration rates under the present-day climate, are comparable for future climates and the same weighting factors can be used for present-day, monsoon and glacial transition climates (SNL 2007 [DIRS 184614], Section 6.8.8). The probabilities associated with the weighting factors are also used to select the target cases for average percolation flux through the repository footprint. This produces weighting factors consistent with the probability distribution for the post-10,000-year period, proposed in 10 CFR 63.342(c)(2) [DIRS 178394].

The UZ flow fields were abstracted using the three-dimensional Site-Scale UZ Flow Model (SNL 2007 [DIRS 184614], Section 6.2). The four present-day cases (based on 10th, 30th, 50th, or 90th percentile infiltration maps) were used for model calibration and calibrated parameters from the four calibrated cases used in conjunction with the other 12 infiltration maps to generate 12 flow fields for the future climate states (SNL 2007 [DIRS 184614], Section 6.2.5 and Table 6.2.6). The three-dimensional model calibration started with four sets of calibrated parameters generated from one-dimensional calibration analyses (DTNs: LB0611MTSCHP10.001_R0 [DIRS 178586]; LB0611MTSCHP30.001_R0 [DIRS 180293]; LB0612MTSCHP50.001_R0 [DIRS 180294]; LB0612MTSCHP90.001_R0 [DIRS 180295]); and two-dimensional site-scale calibrated fault properties (DTN: LB0612MTSCHPFT.001_R0 [DIRS 180296]) documented in *Calibrated Unsaturated Zone Properties* (SNL 2007 [DIRS 179545], Section 6.3). The four present-day cases (based on the 10th, 30th, 50th, or 90th percentile infiltration maps) were calibrated against field measured liquid saturation, water potential, perched water occurrences, and pneumatic data (SNL 2007 [DIRS 184614], Section 6.2). The calibrated parameters included the van Genuchten α parameter of tsw31, and in the perched-water zones, intrinsic permeabilities of the fracture and matrix systems and van Genuchten α and m parameters for describing the saturation-capillary pressure relationships in the fracture and matrix systems. The final calibrated three-dimensional properties for the perched-water conceptual model, which are used to generate the 16 flow fields, are documented in *UZ Flow Models and Submodels* (SNL 2007 [DIRS 184614], Appendix B, Tables B1 to B4).

Figure 6.3.1-7 shows the surface infiltration map for the 10th percentile infiltration scenario during the glacial-transition climate along with the corresponding estimated vertical percolation flux at the repository horizon level and the water table level. Comparisons of the map of the calculated repository percolation flux with that of the surface infiltration map indicate that the spatial distributions of percolation flux at the repository horizon differ significantly in the northwest from the patterns of the net infiltration rate. The surface infiltration rates and distributions are independent of faults. The major differences in the percolation flux distribution at the repository level compared to the surface infiltration patterns are: (1) flow occurs mainly

through faults in the very northern part of the model domain, north of the 237,000-m northing coordinate (see Figure 6.3.1-7 for coordinates); (2) flow is diverted into or near faults located in the model domain; and (3) a west to east shift of high infiltration zones away from the Yucca Mountain crest (SNL 2007 [DIRS 184614], Section 6.6.2.1). Overall, percolation at the repository horizon displays a very different pattern than the distribution of surface infiltration in the northern part of the modeling domain. One reason for this difference is the substantial amount of large-scale lateral flow within the PTn unit. In addition, there is a flow redistribution in the very northern part of the model domain (beyond the repository block) caused by the repository grid layer horizon laterally intersecting the CHn zeolitic and perched-water zones locally, with major flow diverted to faults. The lateral flow within the PTn unit and flow focusing into faults in the north have a large influence on percolation flux distribution at the repository horizon (SNL 2007 [DIRS 184614], Section 6.6.2.1); however, there is significantly less lateral flow and flow focusing within the repository footprint. Computations have shown that the average flux flowing to the repository is within three percent of the average flux specified at the ground surface over the projected repository area (SNL 2007 [DIRS 184614], Section 6.1.4). Hence, percolation flux patterns at the repository are similar to the patterns of infiltration flux within the repository footprint. Figure 6.3.1-7 also shows that the distribution of percolation flux at the water table level, when compared to the distribution of net infiltration rates shown at the infiltration boundary, indicates the percolation fluxes corresponding to high infiltration rate zones reduced still further from what is shown at the repository horizon level.

6.3.1.3 TSPA-LA Model Implementation

Climate Submodel Abstraction—The durations of the climate states are 600 years (550 years postclosure) for the present-day climate; 1,400 years for the monsoon climate; 8,050 years for the glacial-transition climate; and the remainder of the simulation period is simulated as a post-10,000-year climate (Table 6.3.1-1). Climate change is specified within the TSPA-LA Model by assuming climate-specific boundary conditions for UZ flow and accessing the flow field that corresponds to the selected infiltration case and climate state of the simulation period.

Infiltration Submodel—The four different infiltration cases represent epistemic uncertainty in the net infiltration rates. These scenarios are sampled in the TSPA-LA Model once per realization, based on the probability-weighting factors 61.91 percent, 15.68 percent, 16.45 percent, and 5.96 percent for the 10th percentile, 30th percentile, 50th percentile, and 90th percentile, respectively (Table 6.3.1-2) (DTN: LB0701PAWFINFM.001_R0 [DIRS 179283]). Note that the classification of 10th, 30th, 50th, and 90th percentile weighting factors is based on the infiltration maps used for the first three climates. For the post-10,000-year climate, the 10th, 30th, 50th, and 90th percentile weighting factors are associated with flow fields generated using the scaled 90th percentile present-day, 50th percentile glacial transition, 90th percentile glacial transition, and the 90th percentile monsoon infiltration maps, respectively. Because of the once per realization sampling, the infiltration cases are completely correlated across the four climate states modeled during the simulation period (e.g., during a realization in which the 10th percentile infiltration case is sampled, the 10th percentile infiltration scenario of all four climate states will be used to select the appropriate UZ flow fields). This correlation of the infiltration uncertainty across the climate transitions ensures that the full effects of the infiltration uncertainty are not dampened out of the TSPA-LA Model performance results.

UZ Flow Fields Abstraction—The 16 base-case UZ flow fields and associated information generated by the Site-Scale UZ Flow Model (Output 1 in Section 6.1.4.1) are reformatted for use by the UZ Transport Submodel to simulate the transport of radionuclides in the UZ (note that information from Output 1 is provided to the MSTHM Model, as described in Section 6.3.2).

In the UZ Transport Submodel (Section 6.3.9), changes in climate states are approximated by changes from one steady-state flow field to another and by associated changes in water-table elevation (SNL 2008 [DIRS 184748], Section 5). An instantaneous change from one steady-state flow field to another is a reasonable approximation, given the uncertainties and the inability to observe climate changes directly (SNL 2008 [DIRS 184748], Section 6.4.8). With a change to wetter conditions in the future, flow velocities will immediately be greater, and the flow path length to the water table will be shorter due to the higher water table. By applying these conditions instantaneously, there will be no model implementation-caused delay imparted to climate transition-induced changes of UZ flow and radionuclide transport conditions (SNL 2008 [DIRS 184748], Section 6.4.8).

Prior to implementation, the reformatted UZ flow fields are placed in a library of files that are read by the UZ Transport Submodel during run time. There are 16 UZ flow field files for use by the UZ Transport Submodel, one for each of the combinations of the four climate states and four possible infiltration scenarios. These files include:

- Three-dimensional, steady-state flow fields defined at each node in the FEHM UZ grid below the repository, which contain the following information used in the particle-tracking model:

  - Fracture continuum liquid flux
  - Matrix continuum liquid flux
  - Fracture continuum liquid saturation values
  - Matrix continuum liquid saturation values
  - Liquid flux between matrix and fracture continua.

  Note that the files also contain dummy pressure values (pressures are not used in the particle tracking model) and large liquid flux values of 10^{10} kg/s to indicate to FEHM which nodes are watertable release nodes.

6.3.1.4 Model Component Consistency and Conservatism in Assumptions and Parameters

To enhance understanding of the complex interactions within the TSPA-LA Model, this section presents a discussion of consistency among model components and submodels and identification of conservative assumptions in abstractions, models, and parameter sets supporting the Mountain-Scale UZ Flow Submodel.

6.3.1.4.1 Consistency of Assumptions

UZ Transport Properties—Because of the sensitivity of the matrix-diffusion process implemented in the UZ Transport Submodel to various physical parameters that are also used to define the UZ flow fields, there is an inconsistency between the Mountain-Scale UZ Flow

Submodel and the UZ Transport Model. In defining the matrix diffusion process, parameters such as the AFM values, fracture frequency and fracture porosity are sampled from stochastic distributions. However, in developing the 16 different UZ flow fields that are used in the UZ transport calculations, the parameters were held constant. A discussion of this inconsistency between Mountain-Scale UZ Flow Submodel and the UZ Transport Model parameters can be found in Section 6.3.9.4.1.

6.3.1.4.2 Identification of Conservatisms in Submodels and Abstractions

Dual-Permeability Conceptual Model—The dual-permeability conceptual model and its dual-continuum grid system are used by the Site-Scale UZ Flow Model rather than a more refined-gridding method for fracture-matrix interaction, such as the Multiple Interacting Continua method. Dual-continuum models are needed in order to model the large domain and highly fractured rock at Yucca Mountain (SNL 2007 [DIRS 184614], Section 6.1.2). For mass applied initially to the fracture domain, the dual-permeability model generates faster breakthroughs for tracer transport, as compared with Multiple Interacting Continua method, because fracture-matrix interaction is less with a dual-permeability grid (SNL 2008 [DIRS 184748], Section 7.2.2, and SNL 2007 [DIRS 177396], Section 6.19.1). In addition, the dual-permeability (dual-continuum) representation of fractures as a continuum conservatively assumes the complete interconnectivity of the fracture system (i.e., the model does not account for discontinuous fractures) (SNL 2007 [DIRS 177396], Section 6.7.8). The effects of this conservatism tend to increase flow velocity and radionuclide transport rate in the fractures, resulting in shorter radionuclide transport times to the water table.

High-Permeability Fault Pathways—Faults are modeled as high-permeability pathways from the repository to the water table. Uncertainty in fault characteristics has led to the bounding consideration that these faults are high-permeability features that extend from the ground surface to the water table (SNL 2007 [DIRS 184614], Section 5, and SNL 2007 [DIRS 177396], Section 6.7.8). High-permeability fault pathways lead to flow in faults, providing localized high-flow pathways between the ground surface and the repository as well as between the repository and the water table. High-permeability fault pathways, therefore, result in shorter radionuclide transport times to the water table.

6.3.1.5 Alternative Conceptual Model(s) for the Mountain-Scale Unsaturated Zone Flow

Section 6.2 outlines the general consideration and treatment of ACMs used to support the TSPA-LA Model. A brief description of the Mountain-Scale UZ Flow ACMs summarized in Table 6.3.1-3 is presented below. Note that the first ACM is evaluated based on analyses performed with the original infiltration model and thus references a historical model report (BSC 2004 [DIRS 169861]). The analysis is considered valid because although the infiltration model has changed, the model spatial structures including heterogeneities have not radically changed.

Lateral Flow in the PTn—Uncertainties associated with UZ conceptual flow models were analyzed using two conceptual models of the water flow in the PTn unit (i.e., the base-case UZ Flow Model and an ACM (BSC 2004 [DIRS 169861], Section 6.9). The base-case UZ Flow Model has a hydrogeologic property set for the PTn unit that favors the lateral diversion of flow

(BSC 2004 [DIRS 169861], Section 6.5.2). The ACM employs a different hydrogeologic property set for the PTn unit that does not favor large-scale lateral diversion (BSC 2004 [DIRS 169861], Section 6.5.2.2). Each of the conceptual models uses three different parameter sets that were calibrated for the lower-bound, mean, and upper-bound infiltration rates that were used in order to address uncertainties in the infiltration (DTN: SN0308T0503100.008_R0 [DIRS 165640]). Steady-state UZ flow fields were produced for each of the three infiltration cases (lower-bound, mean, and upper-bound) at each of the three climate states (present-day, monsoon, and glacial-transition). This results in nine base-case and nine alternative three-dimensional UZ flow fields. In general, the nine base-case flow fields show more lateral flow occurring within the PTn than those estimated with the ACM. Additional analyses have been performed to estimate the impact of the flow model on tracer or radionuclide transport for the nine base-case and nine alternative flow fields. A total of 40 tracer transport simulations were conducted to evaluate the impacts of infiltration rates, perched-water, PTn conceptual models, and retardations on tracer migration from the repository to the water table (BSC 2004 [DIRS 169861], Section 6.7, Tables 6.7-2 and 6.7-3). The results of the 40 three-dimensional tracer-transport simulations show a wide range of tracer-transport times from the repository to the water table. The results show that the base-case model generally provides slightly more conservative transport time estimates (BSC 2004 [DIRS 169861], Section 6.9.2). Comparative studies of chloride distributions within the UZ, simulated using the base-case and alternative flow fields, indicate consistently that the base-case flow fields provide an overall better match with the observed chloride data (BSC 2004 [DIRS 169861], Section 6.5.2.2).

Transient Infiltration Pulse—The second ACM considered in the UZ is a flow model with a transient pulse infiltration boundary condition. The appropriateness of assuming a steady-state or quasi-steady-state infiltration boundary condition, as opposed to a transient pulse infiltration boundary condition, is a key modeling issue. This assumption relies on the effect of spatial and temporal damping of transient infiltration pulses when flowing through the PTn unit. The PTn consists mainly of non- to partially-welded tuffs. Over the UZ model domain, the thickness of the PTn ranges from 150 m in the north to 30 m or less in the south. The unit can even be missing in certain areas in the south. The PTn is present over the entire repository area where it ranges from 30 m to 60 m in the repository area (SNL 2007 [DIRS 184614], Section 6.2.2). In contrast to the units above it (TCw) and below it (TSw), the PTn has high porosity and low fracture intensity, thus having a large capacity for groundwater storage. The effectiveness of the PTn unit to damp episodic flow was examined using episodic infiltration pulses on the top boundary of the model (SNL 2007 [DIRS 184614], Section 6.9). The analyses presented (SNL 2007 [DIRS 184614], Section 6.9) indicate that the steady-state flow approximation used in the UZ flow model is reasonable due to existence of the PTn unit. The impact of the thickness of the PTn unit was examined in a one–dimensional column study discussed in *UZ Flow Models and Submodels* (SNL 2007 [DIRS 184614], Section 6.9). In the column study, two model columns located at the center and south of the model, with PTn thicknesses of 81 m and 21 m respectively, were considered. Pulses of 10,080 mm/yr and a duration of 1 week were applied to the top of the model every 50 years with an ambient rate of 28.1 mm/yr over the rest of the time. The average yearly rate for the entire simulation was 32 mm/yr. Results showed strong damping effects for both columns. The 81 m column test showed only minor variations in the fluxes over time (SNL 2007 [DIRS 184614], Figure 6.9-2). The thinner (21 m) thickness column model showed relatively large fluctuations over time compared to the 81 m column model, with a maximum variance over time of 17 mm/yr and a dynamic equilibrium variation after 500 years

of 10 mm/yr (SNL 2007 [DIRS 184614], Figure 6.9-3). This is still a large dampening effect when considering the magnitude of the pulses (10,080 mm/yr). In addition, the ratio of the maximum variation in flux (17 mm/yr) to the mean infiltration rate of 32 mm/yr is 0.5, and the ratio of equilibrium variation in flux (10 mm/yr) to the mean infiltration rate of 32 mm/yr is 0.3 (SNL 2007 [DIRS 184614], Section 6.9). These ratios are small when compared to the uncertainty in surface water flux where the ratio of the range (90th percentile flux minus the 10th percentile flux) to the mean surface water flux is 1.1 for the model column associated with the 21 m PTn thickness (SNL 2007 [DIRS 184614], Section 6.9). Since the episodic variations for the 21 m thickness model are small relative to other uncertainties, the assumption of steady-state flow is considered to be valid for even the thinner column model (SNL 2007 [DIRS 184614], Section 6.9). Manepally et al. (2007 [182155]) also examined the damping influence of the PTn on episodic flow. Transient simulations were performed at three locations representative of low, medium, and high PTn and TCw thicknesses to evaluate the importance of PTn and TCw thicknesses on the assumption of steady state flow at the repository horizon. Long term transients that span up to thousands of years were included in the study. The long term transients are expected to be reflected at the repository level due to the finite storage capacity of the PTn (SNL 2007 [DIRS 184614], Section 6.9). The percolation fluxes in the study were found to fall within ± 20 percent of the long term average infiltration rate 80 percent of the time with the range in the percolation rates being 50 percent of the long term average (SNL 2007 [DIRS 182155], Section 5). When compared with the uncertainty in the fluxes implemented in the UZ Flow Model where the standard deviation in the flux implemented for the post-10,000-year climate is about 60 percent of the mean flux and the range is 127 percent of the mean flux over the repository footprint (SNL 2007 [DIRS 184614], Section 6.9), the transient fluctuations in the Manepally et al. (2007 [DIRS 182155]) study are small. Higher infiltration rate scenarios in a study by Zhang et al. (2006 [DIRS 180273]) show that the damping effect will not be weakened by high rate infiltration pulses (SNL 2007 [DIRS 184614], Section 6.9), indicating that uncertainty in infiltration magnitude for short-term transients will not affect the validity of the steady-state assumption.

Film Flow—Although cavities connected to fractures are expected to act as capillary barriers under unsaturated conditions, there is evidence at the Yucca Mountain site suggesting that film flow from fractures to cavities may occur (SNL 2007 [DIRS 184614], Section 7.8.3.3). The evidence is in the form of water release tests performed at the Yucca Mountain site and field observations of coatings in many cavities (SNL 2007 [DIRS 184614], Section 7.8.3.3). Not considering the explicit influence of cavities is a conservative approach since the cavities would retard the transport of water. Film flow on fracture surfaces as an important mechanism for fast flow in unsaturated rocks has also been examined (BSC 2004 [170035] Section 7.3 and Tokunuga and Wan 1997 [DIRS 139195]). Although the importance of film flow in the fractures is a matter of debate (BSC 2004 [170035] and Pruess 1999 [DIRS 104250]), a comparison between the AFM and a film-flow model has been performed (BSC 2004 [170035] Section 7.3). The analysis, comparing the AFM and the film-flow model, showed that the AFM could capture the fast flow behavior of water film if film flow was the major fracture flow mechanism (BSC 2004 [170035] Section 7.3.1 and Section 8.2).

Discrete Fracture Flow—An alternative modeling approach, the discrete-fracture or “weeps” type model is subject to extremely high uncertainties with respect to the fracture data needed to describe the system. In addition, the computational burden associated with this type model is

beyond present or near future resources. Therefore, this type model is not considered (SNL 2007 [DIRS 184614], Section 6.1.2).

Inclusion of TH, THC, and Thermal-Hydrologic-Mechanical Effects on UZ Flow— Vaporization due to repository heat will keep the drift dry for several hundred to a few thousand years. TH, THC and thermal-hydrologic-mechanical effects may alter flow and properties of the UZ rocks. TH, THC, and thermal-hydrologic-mechanical effects are insignificant after the change to glacial-transition climate, the period when most radionuclide transport would take place (SNL 2008 [DIRS 184748], Section 6.7). Additional conclusions with respect to TH, THC, and thermal-hydrologic-mechanical effects on UZ Flow and Transport presented in *Mountain-Scale Coupled Processes (TH/THC/THM)* include: (1) mountain-scale TH will have a large impact on fluid flow near the repository at early times but insignificant impact on UZ flow fields (BSC 2005 [DIRS 174101], Section 8.1); (2) changes in water chemistry, mineralogy, and hydrologic properties in the ambient temperature regions are minimal over the 7,000 years the THC model was simulated (BSC 2005 [DIRS 174101], Section 8.2); and (3) thermal-hydrologic-mechanical induced changes in mountain-scale hydrologic properties have no significant impact on vertical percolation through the repository horizon (BSC 2005 [DIRS 174101], Section 8.3).

INTENTIONALLY LEFT BLANK

Table 6.3.1-1. Durations of Climate States in First 10,000 Years

Climate State	Duration
Present-Day	600 years
Monsoon	1,400 years
Glacial-Transition	Remainder of 10,000 Years

Source: DTN: GS000308315121.003_R0 [DIRS 151139]
10 CFR Part 63. Energy: Disposal of High-Level Radioactive Wastes in a Geologic Repository at Yucca Mountain, Nevada [DIRS 180319].

NOTE: The TSPA-LA Model assumes that the present-day climate period begins at first emplacement and that preclosure will be the first 50 years of the present-day climate period.

Table 6.3.1-2. Net Infiltration Rates Averaged over the Unsaturated Zone Model Domain and Probability-Weighting Factors for the Infiltration Scenarios

Infiltration Case	Present-Day Climate (mm/yr)	Monsoon Climate (mm/yr)	Glacial-Transition Climate (mm/yr)	Post-10k Years (mm/yr) [a]	Probability-Weighting Factors (All Climate States)
10th Percentile	3.03	6.74	11.03	16.89	0.6191
30th Percentile	7.96	12.89	20.45	28.99	0.1568
50th Percentile	12.28	15.37	25.99	34.67	0.1645
90th Percentile	26.78	73.26	46.68	48.84	0.0596

Sources: SNL 2007 [DIRS 184614], Tables 6.1-2, 6.1-3, and LB0701PAWFINFM.001_R0 [DIRS 179283].

[a] Note that for the Post 10,000 Years data the Infiltration cases differ and represent scaled versions of the present-day 90th percentile, the 50th percentile Glacial Transition, the 90th percentile glacial transition, and the 90th percentile monsoon maps, respectively.

Table 6.3.1-3. Alternative Conceptual Models Considered for the Mountain-Scale Unsaturated Zone Flow

Alternative Conceptual Models	Key Assumptions	Screening Assessment and Basis
Lateral Flow in the PTn	Uncertainties associated with UZ conceptual flow models were analyzed using two conceptual models of the water flow in the PTn unit (i.e., the base-case UZ Flow Model and an ACM (BSC 2004 [DIRS 169861], Section 6.9)). The base-case UZ Flow Model has a hydrogeologic property set for the PTn unit that favors lateral diversion of flow (BSC 2004 [DIRS 169861], Section 6.5.2). The ACM employs a different hydrogeologic property set for the PTn unit that does not favor large-scale lateral diversion (BSC 2004 [DIRS 169861], Section 6.5.2.2).	Model best fitting the field data chosen. For the original infiltration model, the base-case UZ Flow Model description of flow in the PTn was selected because it provides better estimates of chloride concentrations and moisture content. Each of the conceptual models used three different parameter sets that were calibrated for the lower-bound, mean, and upper-bound infiltration rates that were used in order to address uncertainties in the infiltration process (DTN: SN0308T0503100.008_R0 [DIRS 165640]).
Transient Infiltration Pulse	The appropriateness of assuming a steady-state or quasi-steady-state infiltration boundary condition was examined by analyzing the effects of using a model with a transient pulse infiltration boundary condition. Effectiveness of the PTn unit to damp episodic flow was examined using episodic infiltration pulses on the top boundary of the model (SNL 2007 [DIRS 184614], Section 6.9 and Figure 6.9-3[a]).	Screened out (FEP 2.2.07.05.0A). The analyses presented (SNL 2007 [DIRS 184614], Section 6.9 and Figure 6.9-3[a]) indicate that the steady-state flow approximation used in the UZ flow model is reasonable due to existence of the PTn unit.
Film Flow	Film flow may occur between cavities and fractures (SNL 2007 [DIRS 184614], Section 7.8.3.3). Film flow may also be a process by which fast flow occurs in the fractures (BSC 2004 [170035] Section 7.3).	Film flow may occur between cavities and fractures as indicated by coatings and water release tests. Not considering the explicit influence of cavities is a conservative approach since the cavities would retard the transport of water (SNL 2007 [DIRS 184614], Section 7.8.3.3). Although the importance of film flow in the fractures is a matter of debate (BSC 2004 [170035] and Preuss 1999 [DIRS 104250]), a comparison between the AFM and a film-flow model has been performed (BSC 2004 [170035] Section 7.3). The analysis, comparing the AFM and the film-flow model, showed that the AFM would capture the fast flow behavior of water film if film flow was the major fracture flow mechanism (BSC 2004 [170035] Section 7.3.1 and Section 8.2).

Table 6.3.1-3. Alternative Conceptual Models Considered for the Mountain-Scale Unsaturated Zone Flow (Continued)

Alternative Conceptual Models	Key Assumptions	Screening Assessment and Basis
Discrete Fracture Flow	The discrete-fracture or "weeps" type model is an alternative model that explicitly defines the fractures in a fracture-flow system.	The discrete-fracture or "weeps" type model is subject to extremely high uncertainties with respect to the fracture data needed to describe the system. In addition, the computational burden associated with this type model is beyond present or near future resources. Therefore, this type model is not considered (SNL 2007 [DIRS 184614], Section 6.1.2).
Inclusion of TH, THC, and Thermal-Hydrologic-Mechanical Effects on UZ Flow	Vaporization due to repository heat will keep the drift dry for several hundred to a few thousand years. Thermal (TH), Thermal Hydrologic Chemical (THC), and thermal-hydrologic-mechanical (THM) effects may influence the flow fields used to describe flow in the UZ.	TH, THC, and thermal-hydrologic-mechanical effects are insignificant after the change to glacial-transition climate, the period when most radionuclide transport would take place (SNL 2008 [DIRS 184748], Section 6.7). Additional conclusions with respect to TH, THC, and thermal-hydrologic-mechanical effects on UZ Flow and Transport presented in *Mountain-Scale Coupled Processes (TH/THC/THM)* include: (1) mountain-scale TH will have a large impact on fluid flow near the repository at early times but insignificant impact on UZ flow fields (BSC 2005 [DIRS 174101], Section 8.1); (2) changes in water chemistry, mineralogy, and hydrologic properties in the ambient temperature regions are minimal over the 7,000 years the THC model was simulated (BSC 2005 [DIRS 174101], Section 8.2); and (3) thermal-hydrologic-mechanical induced changes in mountain-scale hydrologic properties have no significant impact on vertical percolation through the repository horizon (BSC 2005 [DIRS 174101], Section 8.3).

INTENTIONALLY LEFT BLANK

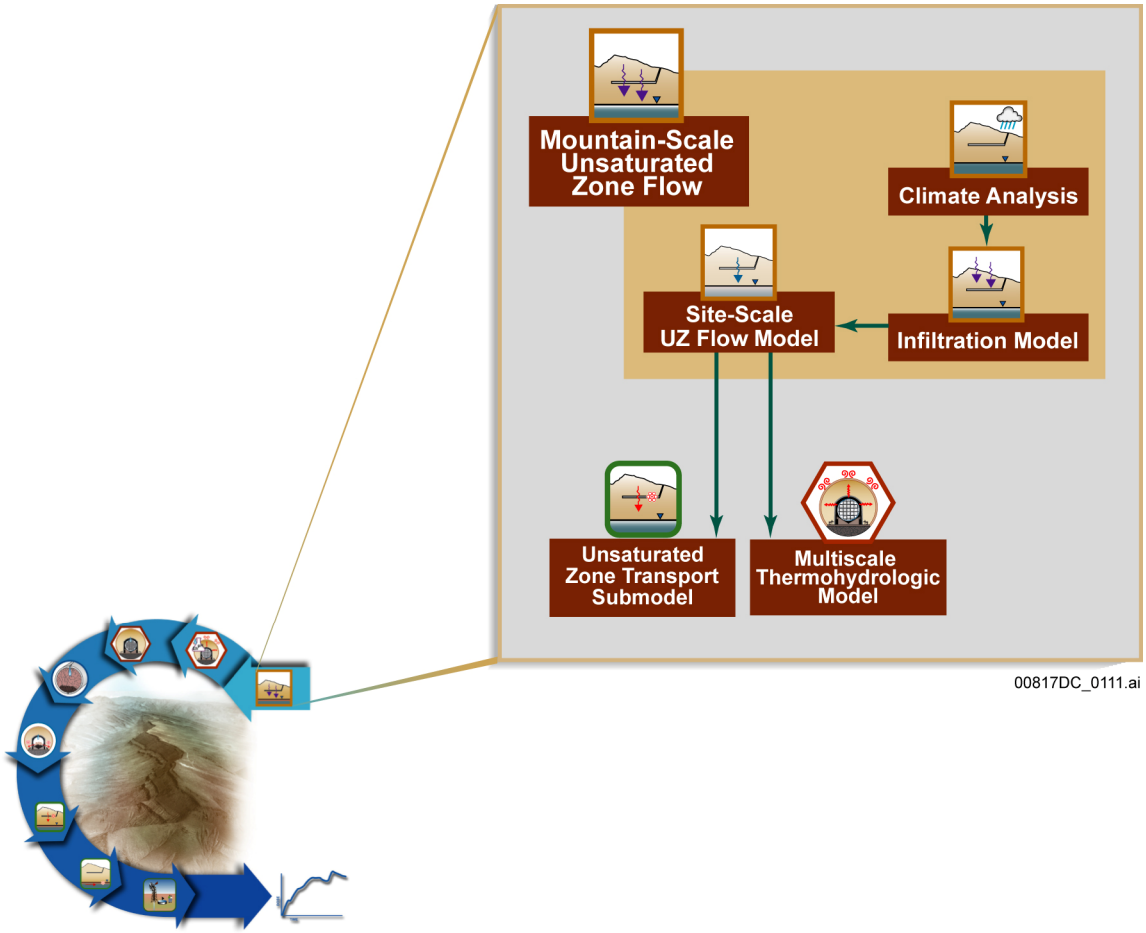

Figure 6.3.1-1. Information Flow Diagram for the Mountain-Scale Unsaturated Zone Flow

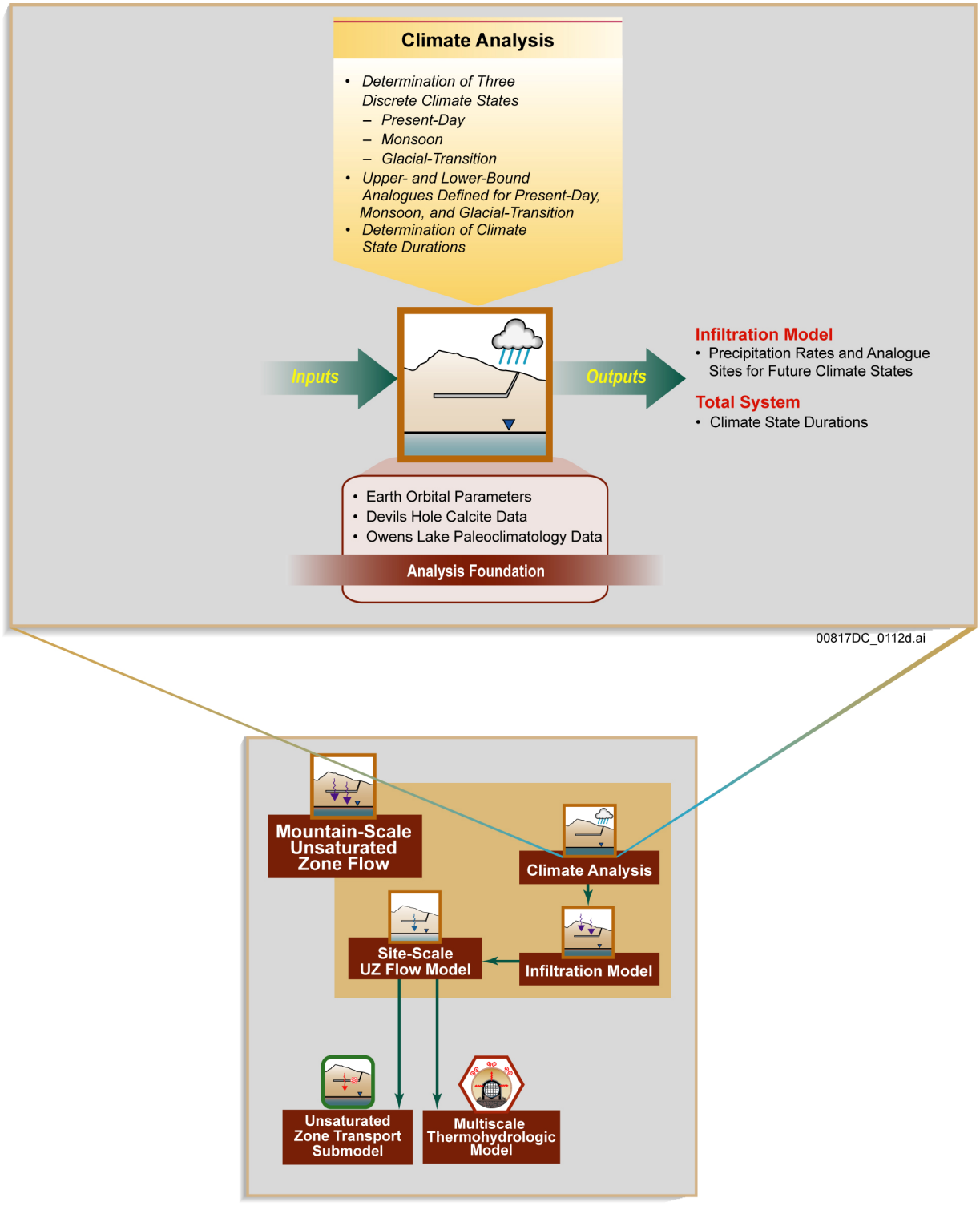

Figure 6.3.1-2. Inputs, Outputs, and Basis for Model Confidence for the Climate Analysis

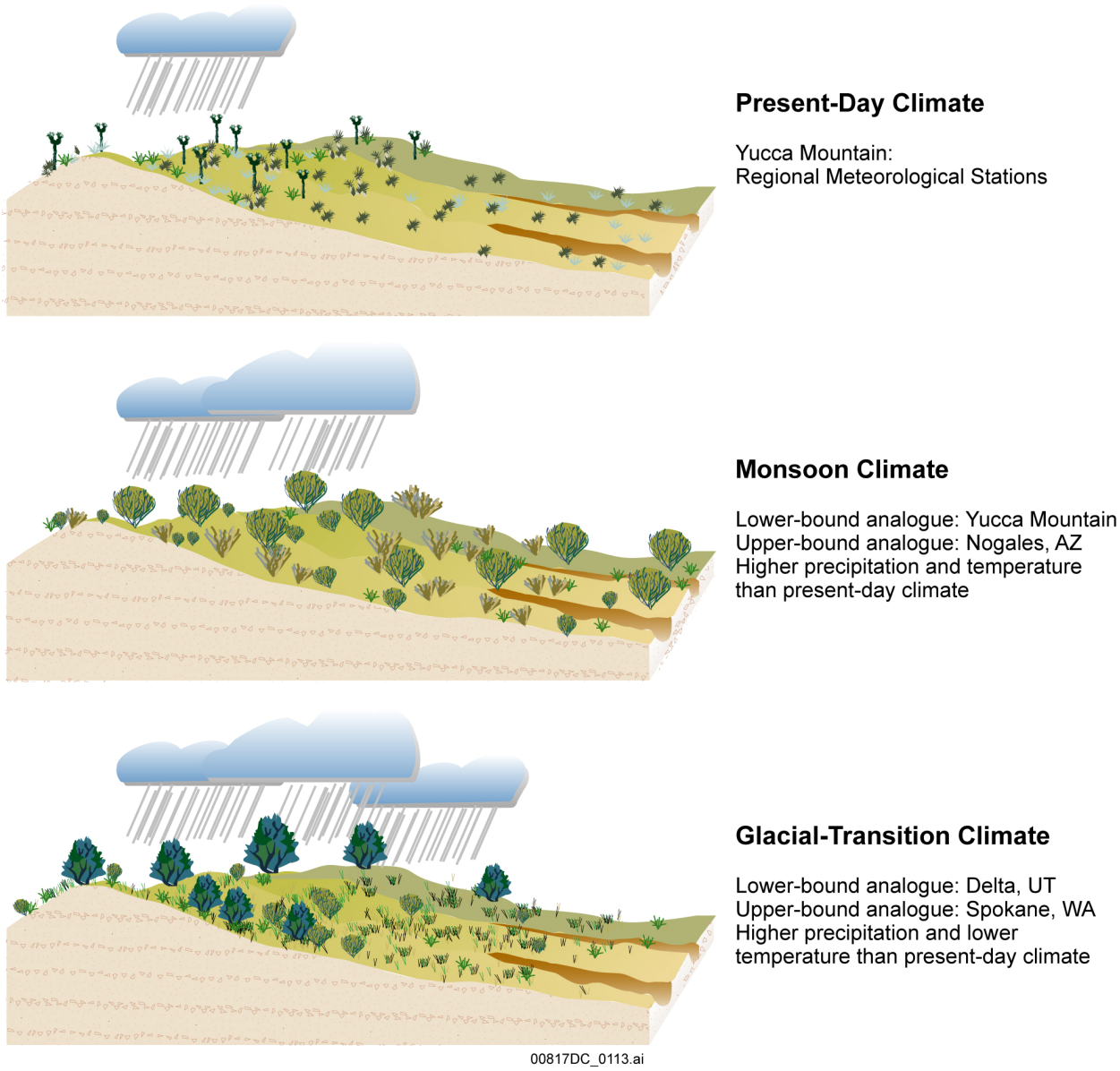

Figure 6.3.1-3. Illustration of the First Three Climate States Used in the TSPA-LA Model and the Analogues for the Monsoon and Glacial-Transition Climates

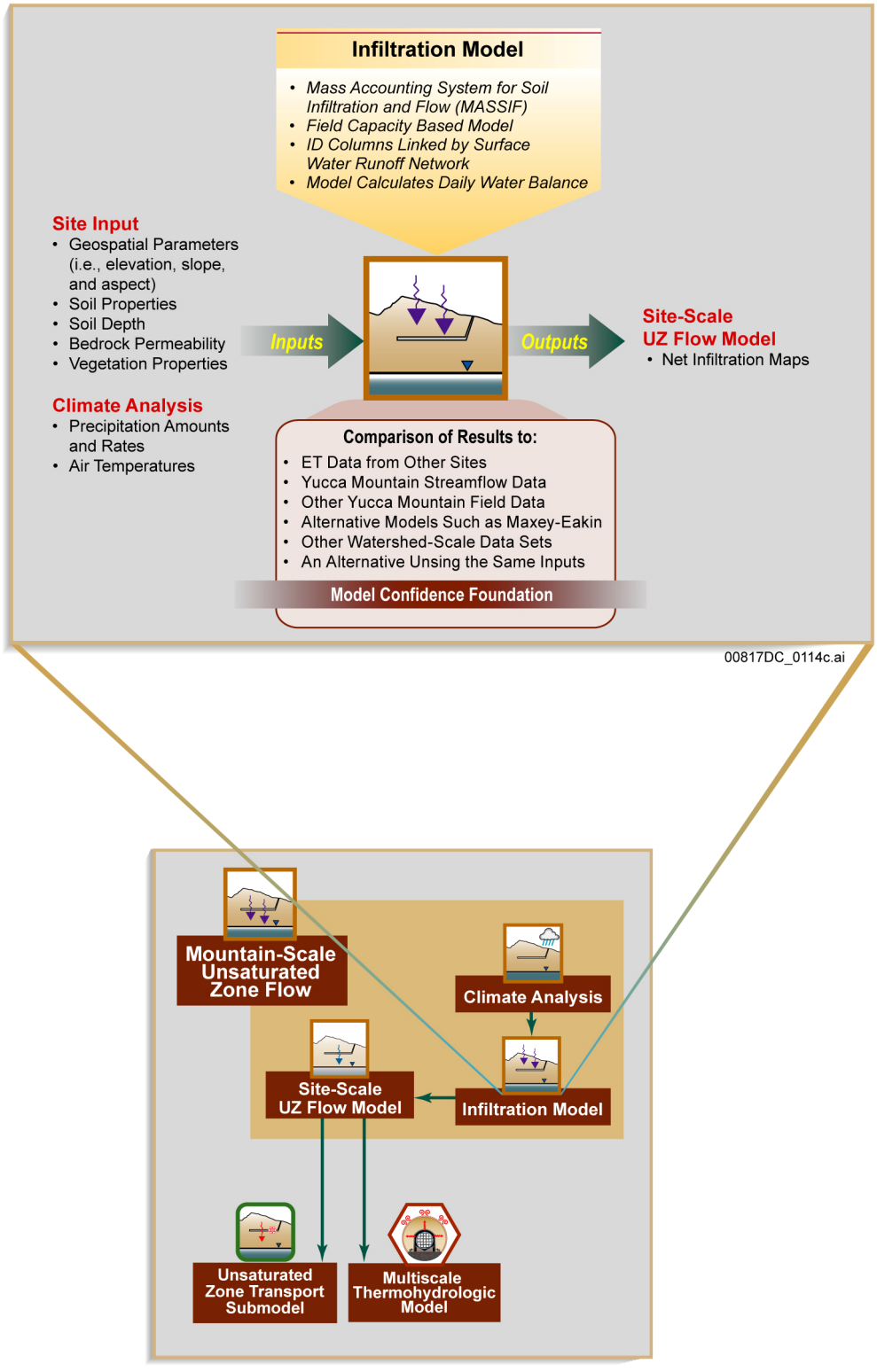

Figure 6.3.1-4. Inputs, Outputs, and Basis for Model Confidence for the Infiltration Model

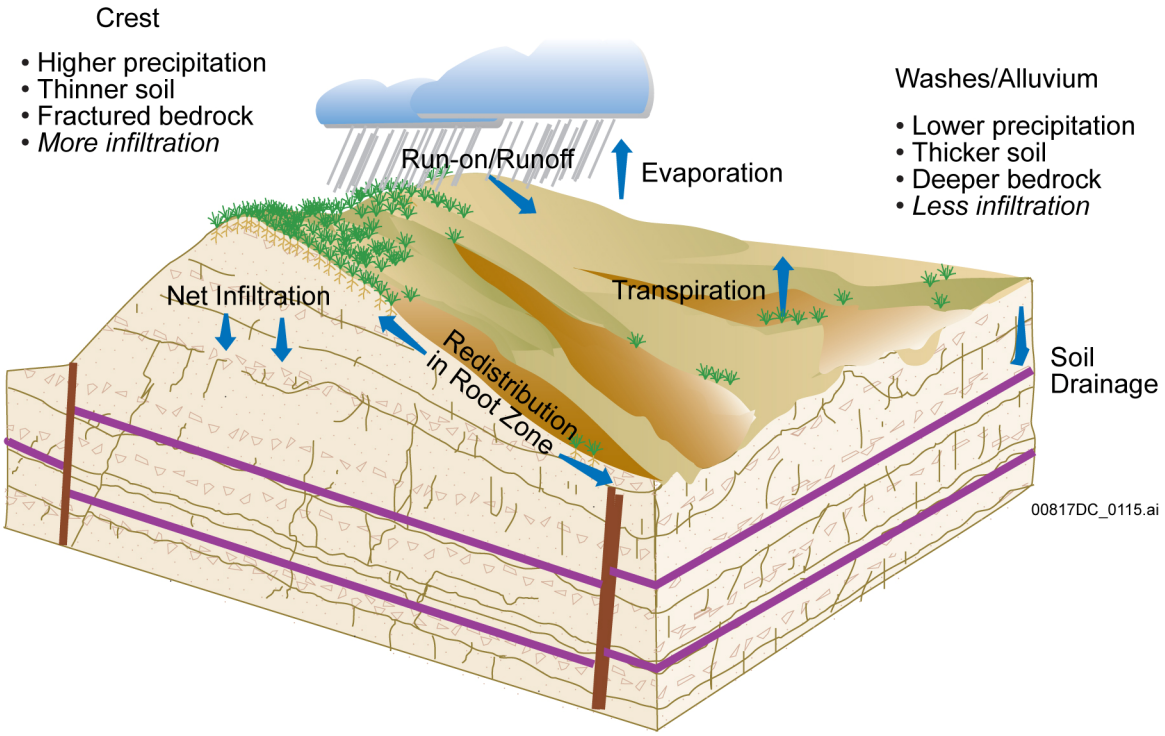

Figure 6.3.1-5. Schematic Illustration Showing the Variation of Precipitation and Consequent Infiltration with Respect to Elevation at Yucca Mountain

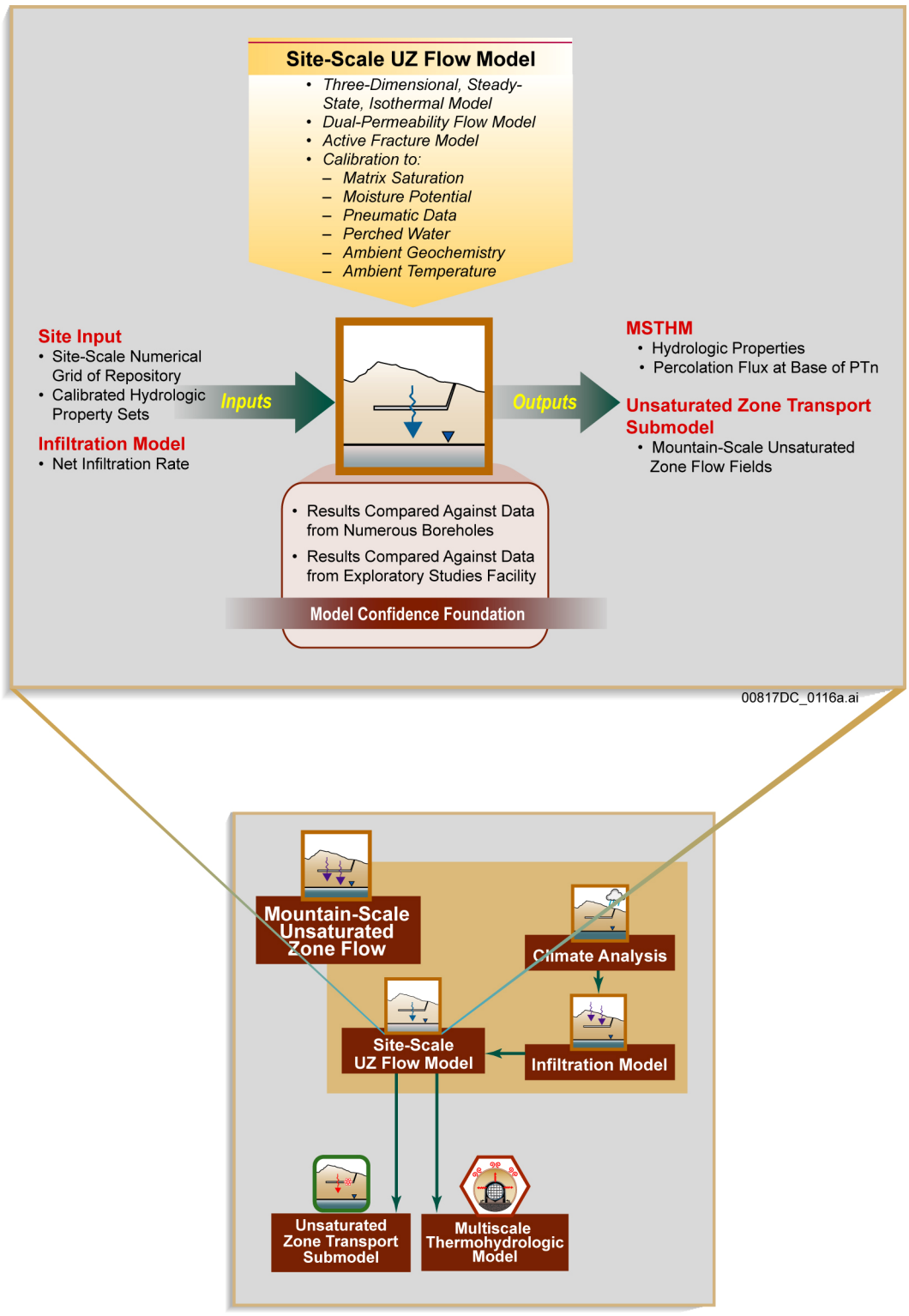

Figure 6.3.1-6. Inputs, Outputs, and Basis for Model Confidence for the Site-Scale Unsaturated Zone Flow Process Model

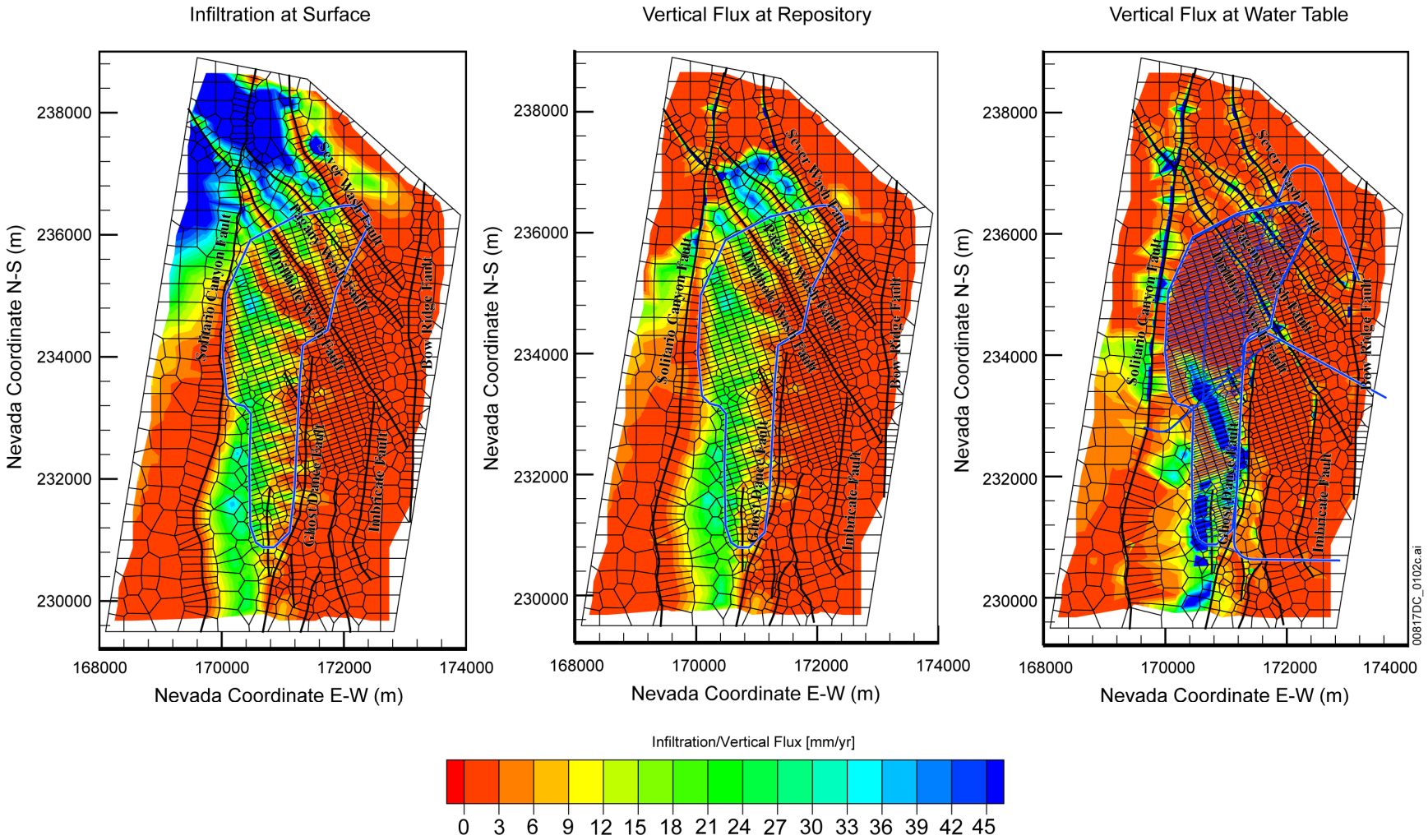

Source: Modified from SNL 2007 [DIRS 184614], Figures 6.1-4, 6.6-3, and 6.6-7

NOTE: The net infiltration boundary and water table are at varying elevations, while the repository horizon is approximated by a constant elevation of 1,080 m.

Figure 6.3.1-7. Comparison of Net Infiltration, Percolation Flux at the Repository Horizon, and Percolation Flux at the Water Table in the Tenth Percentile Infiltration Scenario During the Glacial-Transition Climate State

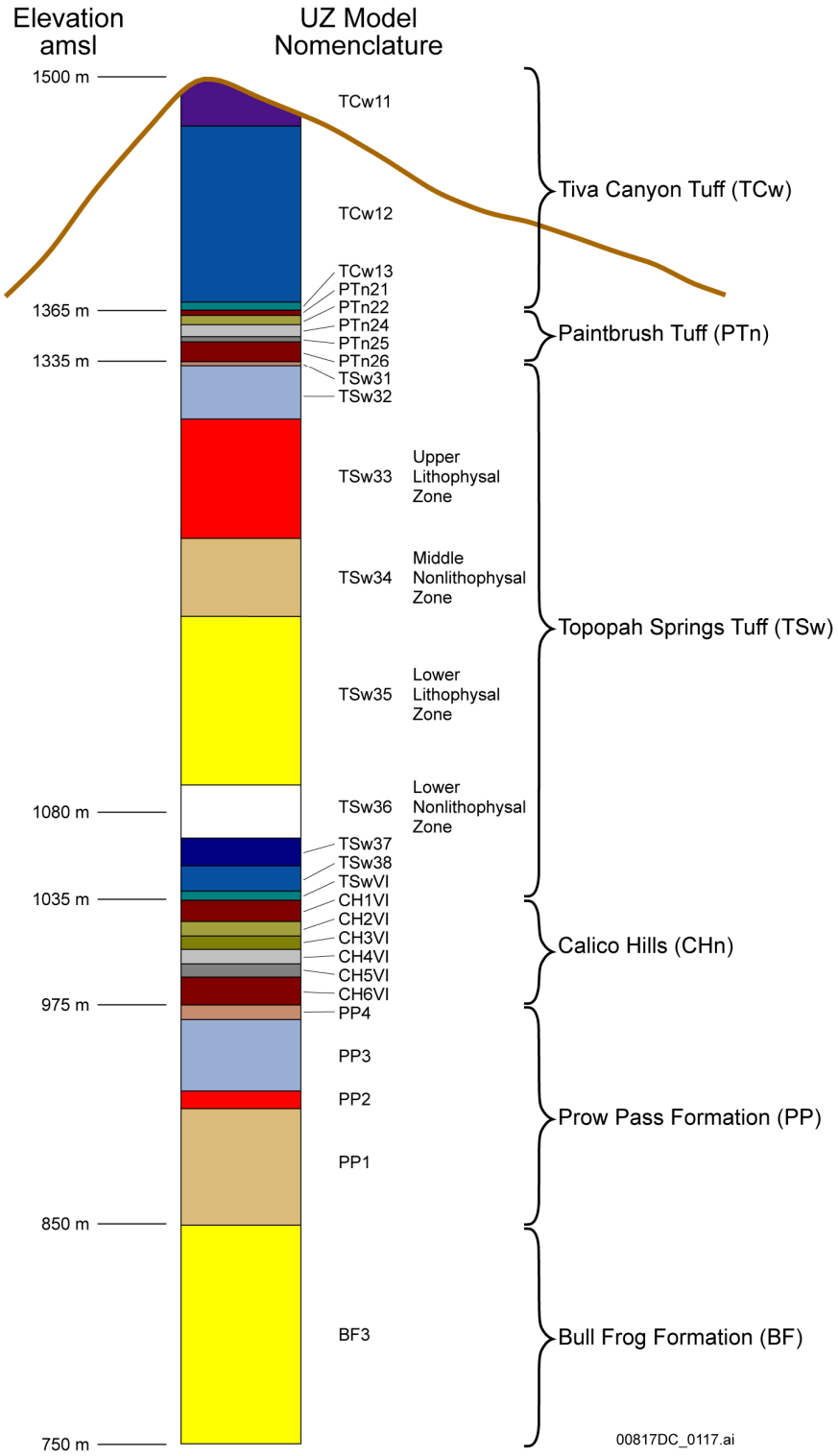

Source: DTN: LB03033DSSFF9I.001_R0 [DIRS 163047], SD-6 Borehole.

NOTE: Median elevation of the repository footprint is 1,080 m above mean sea level (amsl).

Figure 6.3.1-8. General Stratigraphy at the Yucca Mountain Site Observed at Borehole SD-6

6.3.2 Engineered Barrier System Thermal-Hydrologic Environment

After permanent closure of the repository, the heat produced by radioactive decay of the waste will influence the thermal and hydrologic conditions in the geologic formations surrounding the repository drifts, the seepage into the repository drifts, local temperature and relative humidity conditions around the WPs, and moisture movement within the drifts. For TSPA-LA Model simulations, the EBS TH Environment Model Component results are computed using results from *Multiscale Thermohydrologic Model* (SNL 2007 [DIRS 181383], Section 1 and Section 1[a]). These MSTHM Process Model results, in the form of the MSTHM Abstraction, are provided as input to the EBS TH Environment Submodel. Figure 6.3.2-1 illustrates the information flow between the Mountain-Scale UZ Flow Submodel (Section 6.3.1), the EBS TH Environment Submodel, and other TSPA-LA Model submodels.

The EBS TH Environment Model Component parameters consist primarily of time-dependent temperature and relative humidity values at various locations within the repository drifts. Other EBS TH Environment Model Component variables include percolation flux above the repository, thermally perturbed liquid saturations, and liquid-flow rates in the invert. Figure 6.3.2-1 shows these TH outputs are used by the Drift Seepage Submodel (Section 6.3.3.1), Drift Wall Condensation Submodel (Section 6.3.3.2), EBS Chemical Environment Submodel (Section 6.3.4), WP and DS Degradation Model Component (Section 6.3.5), Waste Form Degradation and Mobilization Model Component (Section 6.3.7), and the EBS Flow and Transport Model Component. The EBS Flow and Transport Model Component is composed of the EBS Flow Submodel (Section 6.3.6) and the EBS Transport Submodel (Section 6.3.8). Figure 6.3.2-2 summarizes the inputs provided to the MSTHM Process Model and the EBS TH Environment Submodel results provided by the MSTHM Abstraction (SNL 2007 [DIRS 181383], Section 8.3[a]). Figure 6.3.2-3 shows the information that the EBS TH Environment Submodel provides to other TSPA-LA submodels.

6.3.2.1 Conceptual Model

Nuclear waste emplaced in the Yucca Mountain repository will emit heat from radioactive decay. The MSTHM Process Model is used to model the effects of this decay heat on the evolution of the TH environment in the emplacement drifts. The MSTHM Process Model estimates TH conditions within the emplacement drifts and the surrounding rock as functions of time, WP type, and locations in the repository, as described in *Multiscale Thermohydrologic Model*, (SNL 2007 [DIRS 181383], Section 1). The MSTHM Process Model simulates the evolution of temperature and relative humidity for the components of the EBS. The results are abstracted for the TSPA-LA Model to provide the evolution of temperature and relative humidity on the surfaces of the DSs and WPs, temperature in the invert, temperature on the drift wall, and liquid saturation and liquid flow in the invert.

The heat output from the spent nuclear fuel (SNF) and high-level radioactive waste (HLW) will decline continuously due to the decrease in radioactive decay activity over time. After 50 years of ventilation, the repository enters its postclosure stage where ventilation will cease and the drift-wall rock temperature will be well below boiling but will increase sharply within a few years (SNL 2007 [DIRS 181383], Figure 6.2-4(c)). The maximum postclosure temperature of a WP at any location will be determined by the history of heat output, the resistance to dissipation

of heat in the host rock, heat transfer from the WP to the drift wall, and the relationship to other nearby heat sources. Peak WP temperature considered in the TSPA-LA Model for nominal performance ranges from 107.5°C to 211.0°C (SNL 2007 [DIRS 181383], Table 6.3-49[a]).

Heating of the host rock will produce movement of vapor and liquid water after permanent closure. Much of the heat will be transported away from the drifts by thermal conduction through the rock. A portion of the heat will be transported as latent heat by water that vaporizes near the drift and condenses in cooler rock farther away. Given the projected heat output of the waste and the host-rock characteristics, the near-field host rock, characterized by the drift wall temperature, will be heated to above-boiling temperatures (i.e., greater than 96°C at the repository elevation) for several centuries (SNL 2007 [DIRS 181383], Table 6.3-50[a]). Where temperature exceeds boiling, most of the water will be evaporated from the rock. The duration and extent of dry out will depend on the history of local heat generation, the percolation flux in the host rock, and host-rock properties, notably the thermal conductivity. The variability and uncertainty in host-rock hydrologic properties have an insignificant influence on host-rock dryout (SNL 2007 [DIRS 181383], Section 6.3.9). The maximum lateral extent of the dry-out zone surrounding the emplacement drifts will vary from location to location, ranging from several meters to 11.12 m, but is always expected to be much smaller than the half-drift spacing between emplacement drifts (i.e., 40.5 m) (SNL 2007 [DIRS 181383], Table 6.3-51[a]). Thermal evolution of a particular WP will also depend on its location in the repository layout (i.e., whether it is near the center or the edge of the repository). As the waste heat output decreases with time, the dry-out zone will eventually shrink back to the drift wall, cooling to below-boiling temperatures. The temperatures of the WPs will follow the evolution of the local drift-wall temperature but will be much warmer because of EBS heat transfer mechanisms between the WPs and the local drift wall. This temperature difference will approach zero at later times as the heat output declines.

The influence of heat-generation variability on WP relative humidity variability is similar to the influence on host-rock dry out (SNL 2007 [DIRS 181383], Section 6.3.9, and Section 6.3.13). Because the relative humidity at the drift wall strongly depends on the liquid-phase saturation (as well as on temperature) at the drift wall, the variability of drift-wall relative humidity is similar to that of drift-wall liquid-phase saturation. Relative humidity on a given WP depends on two factors: the drift-wall relative humidity adjacent to the WP, and the temperature difference between the WP and adjacent drift-wall surface. The relative humidity on a given WP is calculated using the relative humidity at the adjacent drift-wall surface and the temperature difference between the WP and the drift-wall surface (SNL 2007 [DIRS 181383], Section 6.1.4 and Section 6.2.4, Stage 6). WPs with higher heat-generation rates result in a greater relative humidity reduction than those with lower heat-generation rates. The differences in heat-generation rates between the eight different WP types result in differences in relative humidity histories.

6.3.2.2 Model Abstraction

The EBS TH Environment Abstraction is based on two-dimensional, drift-scale, dual-permeability TH models combined with one-, two-, and three-dimensional, thermal-conduction-only models of drift- and mountain-scale. The MSTHM Process Model combines these TH and thermal-conduction-only models in a methodology that incorporates

thermal interactions between WPs, other EBS components, and between the EBS and the surrounding hydrogeologic environment at the repository-scale, as described in *Multiscale Thermohydrologic Model* (SNL 2007 [DIRS 181383], Sections 1 and 6.2). The MSTHM Abstraction results describe heat-related responses within and among the component parts of the emplacement drifts, including the effects of repository-scale heat transfer to the surrounding environment.

The MSTHM Process Model simulates two categories of WPs: a commercial spent nuclear fuel (CSNF) WP, which includes CSNF from pressurized-water reactors (PWRs) and boiling-water reactors (BWRs), and a WP that contains both defense high-level (radioactive) waste (DHLW) and U.S. Department of Energy (DOE) owned SNF (DSNF) (SNL 2007 [DIRS 181383], Table6.2-6[a]). WPs that contain both DHLW and DSNF are referred to as DHLW/DOE SNF WPs in the *Multiscale Thermohydrologic Model* (SNL 2007 [DIRS 181383], Tables 4-1[a] and 6.2-6[a]). The TSPA-LA Model, however, refers to these DHLW/DOE SNF WPs as co-disposed (CDSP) WPs. Each waste fuel type has a different rate of heat generation over time. To develop the time histories of heat generated by the waste in the repository, the MSTHM Process Model considers a nominal WP sequence consisting of six CSNF WPs and two CDSP WPs producing results for eight distinct, local heating conditions for each repository subdomain, as described in *Multiscale Thermohydrologic Model* (SNL 2007 [DIRS 181383], Section 6.2.17[a], Table 6.2-6[a]).

The MSTHM Process Model accounts for the following natural and engineered system features:

- Repository-scale variability of percolation flux
- Temporal variability of percolation flux, as influenced by climate change
- Uncertainty in percolation flux addressed by the 10th, 30th, 50th, and 90th percentile infiltration scenarios.
- Uncertainty in thermal properties of the repository host rock using mean, high, and low values of thermal conductivity
- Variation in thermal properties between stratigraphic units in and around the repository
- Repository-scale variability of overburden thickness
- Edge-cooling effect relative to the repository footprint
- Repository design features including WPs, DSs, invert dimensions, invert material properties, drift spacing, WP spacing, and duration of preclosure ventilation
- WP-to-WP variability in heat generation rate
- Time- and distance-dependent heat removal efficiency of preclosure drift ventilation.

The effects of climate change and the resulting infiltration due to precipitation are included by changing the percolation flux boundary condition at the base of the PTn at prescribed times

during the simulations. At the beginning of the preclosure period, the climate is initially set to the present-day climate, which changes to the monsoonal climate after 600 years (of which 550 years are postclosure with present-day climate), followed by 1,400 years of a monsoonal climate, a glacial-transition climate at 2,000 years, and then a post-10,000-year climate (Section 6.3.1.2). A 50-year preclosure period with drift ventilation is included at the beginning of the MSTHM Process Model analyses and is accounted for in the input to the TSPA-LA Model (SNL 2007 [DIRS 181383], Sections 5.2.3 and 6.1.4, Table 4.1-1). However, because the TSPA-LA Model analyzes postclosure performance, the TSPA-LA Model uses the abstraction results starting at the time of closure (at the end of the ventilation period). Climate-induced changes to water table elevation are not included in the TH submodels of the TSPA-LA Model because the elevation of the water table is not expected to have a significant impact on the computed in-drift environments (SNL 2007 [DIRS 181383], Section 5.1.5).

Processes not included in the MSTHM Process Model are:

- Water vapor mixing or transport within the drifts along the drift axis caused by natural convection. See Section 6.3.3.2 for a description of how in-drift natural convection and condensation is included in the Drift Wall Condensation Submodel.

- The effects of drift degradation or collapse, due to reasons other than a seismic event, on the EBS TH responses are not included in the nominal TH abstractions. The Seismic Scenario Class includes a collapsed drift EBS TH adjustment that is limited to only a few EBS TH parameters, as described in Section 6.6.

- Changes in rock properties because of coupled thermal-hydrologic-chemical or thermal-hydrologic-mechanical processes (SNL 2007 [DIRS 181383], Section 6.2.1). The variability and uncertainty in host-rock hydrologic properties have an insignificant influence on host-rock dryout (SNL 2007 [DIRS 181383], Section 6.3.9). The influence of mechanical and chemical coupling on the TH response is demonstrated to be insignificant compared to parametric uncertainties addressed in the MSTHM Process Model (SNL 2007 [DIRS 181383], Section 8.4.1[a]).

- Changes in the TH properties of water because of dissolved solutes (SNL 2007 [DIRS 181383], Section 6.2.1).

- Flow focusing over distinct sections of emplacement drifts, though a sensitivity study was performed to analyze this exclusion (SNL 2007 [DIRS 181383], Section 6.3.2.1). See Section 6.3.3.1.2 for a description of how flow focusing is included in the Drift Seepage Submodel.

The results computed by the MSTHM Process Model are used directly in the MSTHM Abstraction for the TSPA-LA Model. The abstraction process is described below. Figure 6.3.2-4 shows the distribution of the four primary host-rock units that intersect the repository layout considered in the MSTHM Abstraction. Figures 6.3.2-5 and 6.3.2-6 show examples of the output from the MSTHM Abstraction, as described in *Multiscale Thermohydrologic Model* (SNL 2007 [DIRS 181383], Section 6.3[a]). Peak temperatures occur near the center of the repository and decreases near the edges. This spatial variability in

temperature is caused by increased lateral heat loss at the edges of the repository (i.e., the edge-cooling effect), and a reduction in heat removal efficiency due to ventilation exhaust shafts being located at the center of the repository. The location of the ventilation exhaust shafts at the center of the repository affects the spatial variability of heat in the repository because heat removal efficiency decreases with distance from the ventilation inlet (SNL 2007 [DIRS 181383], Section 6.3.1.1). Figure 6.3.2-5 shows estimated TH conditions for mean host-rock thermal conductivity and the 10th, 30th, 50th, and 90th percentile percolation flux cases, and Figure 6.3.2-6 shows estimated TH conditions for the 50th percentile percolation flux scenario combined with low, mean, and high estimates of host-rock thermal conductivity at the same location. Figures 6.3.2-5 and 6.3.2-6 show that TH conditions depend, to a moderate degree, on both the infiltration scenario and thermal conductivity of the host rock. Spatial variability of percolation flux at the repository horizon and heat transfer processes within and between drifts are two TH factors that are simulated by the MSTHM Process Model.

The MSTHM Process Model accounts for the impact of percolation-flux and host-rock thermal conductivity uncertainty on the TH environment conditions, using simulations conducted for the 10th, 30th, 50th, and 90th percentiles of percolation flux with the mean host-rock thermal conductivity values for the host-rock units. Three additional cases are used in conjunction with the four mean host-rock thermal conductivity cases to capture the impact of host-rock thermal conductivity uncertainty: 10th percentile percolation flux with low- and high-thermal conductivity, and 90th percentile percolation flux with high-thermal conductivity. The TH data sets associated with the remaining five of the 12 possible combinations of percolation flux and host-rock thermal conductivity are provided to the TSPA-LA Model as surrogates from the previously identified seven cases. These five cases use their associated values of percolation flux, but refer to one of the other seven cases for the TH data (SNL 2007 [DIRS 181383], Section 6.3.15[a]). The three thermal conductivities analyzed were assigned probability-weighting factors of 0.29, 0.37, and 0.34 for the low, mean, and high host-rock thermal conductivities, respectively (shown in Table 6.3.2-1 as a discrete distribution). The Infiltration Submodel (Section 6.3.1.2) uses weightings of 0.6191, 0.1568, 0.1645, and 0.0596 for the 10th, 30th, 50th, and 90th percentile percolation fluxes, respectively (shown in Table 6.3.1-2). Table 6.3.2-3 describes how the four probability weightings for percolation flux uncertainty and the three probability weightings for host-rock thermal conductivity uncertainty are used to determine the aggregate probability weightings for the 12 MSTHM Process Model data sets provided as input to the TSPA-LA Model. For further discussion of how the 12 combinations of host-rock thermal conductivity uncertainty and infiltration scenario uncertainties are addressed with the provided MSTHM Abstraction results, see *Multiscale Thermohydrologic Model* (SNL 2007 [DIRS 181383], Section 6.3.15[a]).

To characterize the variability in repository TH conditions, the MSTHM Process Model grid subdivides the drifts in the repository footprint into 3,264 equal-area subdomains corresponding to 20-m repository drift segments (SNL 2007 [DIRS 181383], Section 6.2.5.1 and Section 6.2.12[a]). For each of the 12 infiltration/host-rock thermal conductivity cases (Table 6.3.2-3) the MSTHM Abstraction includes the time-dependent TH variables, temperature, and relative humidity, for six different possible CSNF WPs and two different possible CDSP WPs at each of the 3,264 repository subdomains (SNL 2007 [DIRS 181383], Tables 6.2-6[a] and Section 6.2.17[a]). In addition, the MSTHM Abstraction includes time-dependent values for DS temperature and relative humidity; average drift-wall temperature, the duration of boiling at the

drift wall, the average invert temperature, the average invert saturation, and the average invert flux for each of the 3,264 repository subdomains. For the abstraction of the MSTHM Process Model data for downstream model components and submodels, two sets of output parameter analyses and organizations are performed. First, TH values and their associated repository subdomains are grouped into one of five repository percolation subregions based on the magnitude of the percolation flux at the base of the PTn. The second analysis involves determining a single 'representative' CSNF WP and a single 'representative' CDSP WP for each percolation subregion given the complete set of TH parameters at each of the repository subdomains in that percolation subregion. These output parameter analyses are summarized as follows.

6.3.2.2.1 Determination of Repository Percolation Subregions

The process used to assign each of the 3,264 MSTHM Process Model subdomains to each of the five repository percolation subregions is described in DTN: LA0702PANS02BR.001_R0 [DIRS 180322] and *Particle Tracking Model and Abstraction of Transport Processes* (SNL 2008 [DIRS 184748], Section 6.5.15[a]). Note that only the first three climate states were considered in the analysis used to find a single zone file with five sets of source nodes which best represents all the infiltration/climate combinations. The subdomains comprising each of the five repository percolation subregions were chosen based on the cumulative probability of percolation for the 12 flow fields (three different climate periods: present-day, monsoon and glacial-transition; each climate period is categorized with 4 infiltration scenarios: 10 percent, 30 percent, 50 percent and 90 percent). A 4-step binning process was applied to each of the twelve flow fields, resulting in a list of repository subdomains divided into 5 percolation subregions that share common infiltration ranges, based on the cumulative probability intervals for these subregions (SNL 2008 [DIRS 184748], Section 6.5.15[a]). The cumulative probability intervals for these five subregions of percolation rates sorted in ascending order are 0.0-0.05, 0.05-0.30, 0.30-0.70, 0.70-0.95, and 0.95-1.00 (SNL 2008 [DIRS 184748], Section 6.5.15[a]). The quantiles are shown in Table 6.3.2-2. An analysis, of the degree of similarity or difference of the results of the binning process depending on which flow field is considered, was performed. The results indicated that the bins for the 12 flow fields are quite similar to one another. As noted in SNL 2008 [DIRS 184748], Section 6.5.15[a], if a subregion is identified for a particular subdomain in the glacial-transition, 10th percentile flow field, it is very often identified as the same subregion for the other flow fields. When they are different, they almost always differ by only one subregion, that is, a 3 in one flow field becomes a 4 in another flow field, or a 2 becomes a 1. Based upon this result it was considered acceptable to use subregions from one flow field to approximate all infiltration scenarios and climate states. Therefore, the 10th percentile infiltration scenario for the glacial transition climate was used to define the five percolation subregions for all simulations including the post-10,000-year climate. The five repository percolation subregions are shown graphically on Figure 6.3.2-7. Because each of the 3,264 MSTHM Process Model subdomains are equally sized in area, 81 meters in width by 20 meters in length (SNL 2007 [DIRS 181383], Section 6.2.12[a]), the probability of an event (e.g., early failed WP) occurring in any of the five percolation subregions is the same as the quantile distribution used to define the percolation subregions (i.e., 5 percent, 25 percent, 40 percent, 25 percent, and 5 percent). The MSTHM Abstraction inputs to the TSPA-LA Model are provided in two output file sets. Both TH output file sets are indexed by subregion and waste fuel type categories.

The first file set contains WP surface temperature and relative humidity; DS surface temperature and relative humidity; and average drift-wall temperature for each of the eight WP at each repository subdomain within each percolation subregion. Because this data set from the MSTHM Abstraction is so extensive, covering eight different possible TH drift environments at each of the 3,264 repository subdomains, it is referred to as the comprehensive TH response data set. The parameter values provided in the comprehensive TH response data set are indexed by their percolation subregion and the percolation flux at each of the repository subdomains is included. Included with the comprehensive TH response data set at each of the 3,264 repository subdomains is the percolation flux experienced by that location during the simulation period. Also, included with each of the 3,264 repository subdomains are the fraction of each subdomain in lithophysal rock; the fraction of lithophysal unit value specifies whether each repository subdomain is in a lithophysal host-rock unit or not. These repository subdomain-specific TH data values and parameters are input to the WP and DS Degradation Model Component (Section 6.3.5), the Drift Seepage Submodel (Section 6.3.3.1), and the Drift Wall Condensation Submodel (Section 6.3.3.2).

A second MSTHM Abstraction file set for the TSPA-LA Model contains TH response histories for each of the five repository subregions based on a single, representative WP for each fuel type. The determination of the representative WP for each bin is described in Section 6.3.2.2.2. This data set from the MSTHM Abstraction is referred to as the representative TH response data set (Section 6.3.2.2.2). The TH information from a single representative CSNF WP and a representative CDSP WP for each repository subregion provides the following inputs: WP surface temperature and relative humidity; DS temperature and relative humidity; drift-wall temperature; invert temperature; invert saturation; and invert flux. Table 6.3.2-4 summarizes the variables estimated by the MSTHM Abstraction for the representative TH conditions at each of the five repository percolation subregions in the TSPA-LA Model. Parameter values from the representative TH response data set are used for input to the EBS Flow and Transport Model Component (Sections 6.3.6 and 6.3.8), the Waste Form Degradation and Mobilization Model Component (Section 6.3.7), the EBS Chemical Environment Submodel (Section 6.3.4), and the Drift Wall Condensation Submodel (Section 6.3.3.2).

In summary, Figure 6.3.2-1 shows the flow of MSTHM Abstraction results for the comprehensive and representative TH data sets provided to the TSPA-LA Model, consisting of TH abstractions at each of the 3,264 repository subdomains and TH abstractions at the representative WPs for each subregion. When a submodel or model component of the TSPA-LA Model requires input of TH response conditions associated with the representative CSNF or CDSP WP in a selected repository subregion, then the TH response conditions for that representative CSNF or CDSP WP are used as the TH response conditions for all CSNF or CDSP WPs in that subregion. For example, the time-dependent TH response conditions for the representative CSNF WP in a selected percolation subregion are used as the TH conditions for both the CSNF WPs in the dripping environment and the CSNF WPs in the non-dripping environment of that percolation subregion. The TH inputs to the TSPA-LA Model do not make a distinction between dripping and non-dripping environments because the TH conditions in the emplacement drifts are more strongly influenced by percolation flux and saturation in the host rock surrounding the drifts than by the flow-focusing effects associated with a dripping environment (SNL 2007 [DIRS 181383], Section 6.3.2.1). The influence of percolation flux on TH conditions is included in the MSTHM Process Model methodology. *Multiscale*

Thermohydrologic Model (SNL 2007 [DIRS 181383], Section 6.2.1) outlines the MSTHM Process Model approach and the TH processes accounted for by the model.

6.3.2.2.2 Determination of Representative Waste Packages

The representative CSNF and CDSP WPs are selected by compiling the peak WP temperature and the duration of boiling at the drift wall for each WP type in each repository percolation subregion. For each repository percolation subregion, these values are sorted from low to high, and a percentile is assigned to each WP location. For each repository percolation subregion, two representative WPs are selected, one for each WP type. Each representative WP is the one whose simulated peak WP temperature and drift-wall boiling period is closest to the calculated median value for peak WP temperature and the median boiling period duration in the selected percolation subregion, as described in *Multiscale Thermohydrologic Model* (SNL 2007 [DIRS 181383], Appendix VIII[a]). The two criteria, peak WP temperature and duration of boiling at the drift wall, that were used to select the representative CSNF and CDSP WP TH response curves were chosen because of their correlation to how dry the emplacement drifts will get and how quickly water or water vapor will return. After the process of selecting the representative WPs is completed for each waste fuel type in each percolation subregion, the TH response parameters of temperature and relative humidity values for each representative WP and associated DS, the average drift-wall temperature, the average invert temperature, the average invert saturation, and the average invert flux at each representative WP location are assembled in a representative TH response data file set. These data are accessed by the EBS TH Environment Submodel and provided as input to the Waste Form Degradation and Mobilization Model Component (Section 6.3.7), the EBS Flow and Transport Model Component (Sections 6.3.6 and 6.3.8), the EBS Chemical Environment Submodel (Section 6.3.4), and the Drift Wall Condensation Submodel (Section 6.3.3.2).

6.3.2.3 TSPA-LA Model Implementation

EBS TH Environment Submodel—Results from the MSTHM Abstraction serve as inputs to TSPA-LA Model components and submodels, as described in Section 6.3.2.2 and as follows. The TH parameters from the MSTHM Abstraction in the EBS TH Environment Submodel are time histories of:

- WP temperature
- DS Temperature
- Drift-wall temperature
- WP relative humidity
- Invert relative humidity
- Invert liquid flux (vertical component)
- Invert saturation.

An additional parameter, relative humidity of the invert, is calculated within the EBS TH Environment Submodel using the material and VanGenuchten properties of the invert (DTNs: MO0505SPAROCKM.000_R0 [DIRS 173893] and LB0610UZDSCP30.001_R0 [DIRS 179180]), the properties of water (DTN: MO0505SPAROCKM.000_R0 [DIRS 173893]), relative humidity caps (DTN: SN0706PAEBSPCE.016_R0 [DIRS 181837]),

and the methodology described in the MSTHM Process Model (SNL 2007 [DIRS 181383], Appendix XV[a]).

Two sets of TH parameter files are provided by the MSTHM Abstraction, a comprehensive set and a representative set (Section 6.3.2.2.1). The comprehensive TH response files have the TH parameter time histories (listed above) for each of the eight possible WPs at each of the 3,264 MSTHM Process Model repository subdomains, and are categorized by percolation subregion and fuel type (Figure 6.3.2-8). Included with the comprehensive TH response data set at each of the 3,264 repository subdomains is the percolation flux experienced by that location during the simulation period. Also, included for each of the 3,264 repository subdomains is a note specifying whether that repository subdomain is in a lithophysal host-rock unit or not. These comprehensive TH data values and parameters are input to the WP and DS Degradation Model Component (Section 6.3.5) and the Drift Seepage Submodel (Section 6.3.3.1). In addition, the comprehensive TH data set is used to calculate other TSPA-LA Model inputs including the average percolation flux for the drift used in the Drift Wall Condensation Submodel (Section 6.3.3.2).

The representative TH response file set has the TH parameter time histories for a single representative WP for a given fuel type in each percolation flux subregion. Each of the two sets of TH parameters is provided for the 12 infiltration/host-rock thermal-conductivity uncertainty combinations (Table 6.3.2-3). The TH parameter set containing the representative WPs is implemented into the TSPA-LA Model as a set of two-dimensional tables. Each two-dimensional table contains the TH parameter time histories for one of the 120 combinations of infiltration/thermal-conductivity uncertainty (twelve each), fuel type (two each), and percolation subregion (five each). The TH parameters from the representative WPs are used as inputs to the Waste Form Degradation and Mobilization Model Component (Section 6.3.7), EBS Flow and Transport Model Component (Sections 6.3.6 and 6.3.8), the EBS Chemical Environment Submodel (Section 6.3.4), and Drift Wall Condensation Submodel (Section 6.3.3.2). The comprehensive TH parameter set that includes each WP for a given fuel type (six CSNF WPs, two CDSP WPs) at each of the MSTHM Process Model repository subdomains (3,264 each) in a given percolation subregion (five each) is implemented as a set of externally carried model input files (DTN: MO0707PREWAPMS.000_R0 [DIRS 183002]) (see output DTN the discussion of PREWAP (PREWAP_LA V1.1, STN: 10939-1.1-00 [DIRS 181053]) output files in Appendix F-2.8), which are used by the seepage dynamically linked library (DLL) (SEEPAGEDLL_LA V.1.2.2005. Windows 2000 STN: 11076-1.2-00 [DIRS 173435]), the WP Degradation Model (WAPDEG) DLL (WAPDEG V.4.07.2003 Windows 2000. STN: 10000-4.07-00 [DIRS 181774]), and the Waste Package Localized Corrosion Initiation Analysis. In addition the representative TH data set is used to calculate the duration of boiling (e.g. time needed of drift cooling to 96°C) for each of the representative WPs which is used in the EBS Chemical Environment Submodel (Section 6.2.4).

6.3.2.4 Model Component Consistency and Conservatism in Assumptions and Parameters

To enhance understanding of the complex interactions within the TSPA-LA Model, a discussion of consistency among model components and submodels, and identification of conservative assumptions in abstractions, process models, and parameter sets supporting the EBS TH Environment Submodel are discussed below.

6.3.2.4.1 Consistency of Assumptions

In-Drift Axial Fluid Flow—The MSTHM Process Model, which provides the basis for the in-drift temperature and relative humidity abstraction of the TSPA-LA Model, does not consider the longitudinal transport of water vapor along the length of the emplacement drifts. Thus, the influence of evaporation, transport, and condensation in the heated and unheated regions of the drifts, which result in a cold-trap effect, is not fully accounted for. On the other hand, the influence of the longitudinal transport of water vapor and associated condensation on the drift walls is approximated in the In-Drift Natural Convection and Condensation Process Model (SNL 2007 [DIRS 181648], Section 6.3). Therefore, there is a conceptual difference between the MSTHM Process Model and the In-Drift Natural Convection and Condensation Process Model.

Effect on the TSPA-LA Model—Although drift-wall condensation effects have been included in the TSPA-LA Model (Section 6.3.3.2), the difference in the modeling assumptions regarding the axial transport of moisture between the MSTHM Process Model and the Drift Wall Condensation Abstraction are possibly contradictory. If longitudinal vapor transport were included in the MSTHM Process Model, condensation in the unheated regions of the repository would affect the longitudinal variation of predicted in-drift temperature and relative humidity, with the effects on relative humidity having the greater potential impact, with vapor transport resulting in drier conditions than those predicted by the MSTHM (SNL 2007 [DIRS 181383], Section 7.8[a]). The thermal effects associated with the evaporation and condensation tend to dampen longitudinal temperature and relative humidity variations because heat would more effectively move from the hotter regions in a drift where the water evaporates, and then move to the cooler regions of the drift where the water vapor condenses. Thus, the WP-to-WP variation in temperature and relative humidity could be affected. However, both model reports, *Multiscale Thermohydrologic Model* (SNL 2007 [DIRS 181383], Section 7.5.3) and *In-Drift Natural Convection and Condensation* (SNL 2007 [DIRS 181648], Section 6.3.7.2.4), indicate that these longitudinal mass/energy transfer processes have an insignificant effect on the primary MSTHM Model predictions of temperature and relative humidity.

6.3.2.4.2 Identification of Conservatisms in Submodels and Abstractions

Repository Edge Effect—Although the heat loss into the host rock due to the repository edge effect is captured in the MSTHM Process Model via thermal conduction, the thermal convection component of the heat loss into the host rock expected at the edges of the repository is not included (SNL 2007 [DIRS 181383], Section 5.2.1). The bulk permeability of the repository host rock makes thermal conductivity the dominant heat flow mechanism because mass movement, via convection, from the drifts into the host rock is impeded by the limited permeability (SNL 2007 [DIRS 181383], Section 5.2.1).

6.3.2.5 Alternative Conceptual Model(s) for Engineered Barrier System Thermal-Hydrologic Environment

An important reason for considering ACMs is to help build confidence that plausible changes in modeling assumptions or simplifications will not change conclusions regarding subsystem and total system performance. Section 6.2 outlines the general consideration and treatment of ACMs used to support the TSPA-LA Model. Conservatism at the subsystem level has been used to

select the best ACM to use rather than quantitatively propagate multiple ACMs to the TSPA-LA Model. Generally, additional uncertainty is incorporated into the selected conceptual model if more than one ACM is deemed appropriate for use rather than considering multiple ACMs in the TSPA-LA Model. If an ACM appears to be significant at the subsystem level, then an appropriate abstraction is developed for that ACM for consideration within the TSPA-LA Model. The result of the process is documented within the individual analysis and/or model reports. It is important to note that treatment of ACMs within the individual model reports may differ significantly to be consistent with available data and current scientific understanding. Therefore, a brief description of the EBS TH Environment ACM summarized in Table 6.3.2-5 is presented below.

Mountain-Scale TH Model ACM—An ACM to the MSTHM Process Model is the Mountain-Scale TH Model [DIRS 174101]. The Mountain-Scale TH Model is a monolithic TH model which used: (1) coarser grid discretization at the drift scale than the MSTHM Process Model; (2) a line-averaged approximation of the heat-generation-rate-versus-time table (whereas, the MSTHM Process Model represented the WPs as discrete heat sources); and (3) a lumped heat source that filled the entire cross section of the emplacement drift (SNL 2007 [DIRS 181383], Section 6.4).

The temperature predicted by the MSTHM Process Model is the perimeter-averaged drift-wall temperature adjacent to an "average" 21-PWR medium-heat CSNF WP. The MSTHM Process Model discretely represents the decay-heat source from individual WPs. The drift-wall gridblocks over which the drift-wall temperature is averaged extend 0.2 m to 0.5 m into the host rock surrounding the emplacement drifts (SNL 2007 [DIRS 181383], Section 6.4). The temperature prediction in the east-west cross-sectional Mountain-Scale TH Model is for a gridblock that occupies the entire cross section of a drift; therefore, it is a lumped representation of the drift temperature (SNL 2007 [DIRS 181383], Section 6.4). Moreover, because the east-west cross-sectional Mountain-Scale TH Model uses a line-averaged heat source, it axially smears out the differences between 'hot' and 'cold' WP locations along the drift (SNL 2007 [DIRS 181383], Section 6.4).

During the post-boiling period, the temperatures predicted by both the MSTHM Process Model and the ACM modeling approach are in good agreement (SNL 2007 [DIRS 181383], Section 6.4). During the early-time heat-up period, the coarse (lateral and axial) grid-block spacing in the east-west cross-sectional Mountain-Scale TH Model does not capture the rapid drift-wall temperature rise that the more finely gridded MSTHM Process Model predicts. Because of the coarse lateral grid block spacing in the east-west model, it smears out the lateral temperature gradient between the drift and the mid-pillar location. Therefore, it tends to overpredict the temperature at the mid-pillar location, thereby preventing condensate from shedding between drifts (SNL 2007 [DIRS 181383], Section 6.4). The fine lateral grid-block spacing in the MSTHM Process Model captures the influence that the lateral temperature gradient has on allowing condensate to shed between drifts. The tendency for the east-west cross-sectional Mountain-Scale TH Model to under represent condensate shedding results in a more substantial condensate buildup above the repository horizon (SNL 2007 [DIRS 181383], Section 6.4). Also, the line-averaged heat-source approximation smears out differences in temperature between otherwise 'hot' and 'cold' WP locations, thereby preventing condensate from breaking through 'cold' WP locations along the emplacement drifts (SNL 2007

[DIRS 181383], Section 6.4). Altogether, the under prediction of condensate shedding between drifts and condensate breakthrough at 'cold' WP locations causes the east-west cross-sectional Mountain-Scale TH Model to build up more condensate above the repository horizon that leads to episodic heat-pipe behavior.

The MSTHM Process Model and the east-west cross-sectional Mountain-Scale TH Model are in agreement (SNL 2007 [DIRS 181383], Section 6.4). Moreover, the differences in predicted temperatures between the MSTHM Process Model and the east-west cross-sectional Mountain-Scale TH Model are within the range of temperature differences resulting from parametric uncertainty (SNL 2007 [DIRS 181383], Tables 6.3-30 and 6.3-31).

No ACMs related to the EBS TH Environment Submodel were recommended for inclusion in the TSPA-LA Model.

Table 6.3.2-1. Parameter Distribution for Host-Rock Thermal-Conductivity Uncertainty

Parameter Name in TSPA-LA Model	Description	Distribution
Thermal_Conductivity_Uncert_a	Uncertainty between the three host-rock thermal-conductivity scenarios (1=low, 2=mean, and 3=high).	Discrete (p, v) [(0.29, 1), (0.37, 2), (0.34, 3)]

Sources: *Multiscale Thermohydrologic Model* (SNL 2007 [DIRS 181383], Table 6.3-47[a]); and DTN: LL0703PA026MST.013_R0 [DIRS 179981].

Table 6.3.2-2. Percolation-Based Probability Subregion Quantile Ranges

Subregion Index	Quantile Range
1	$p < 0.05$
2	$0.05 \leq p < 0.30$
3	$0.30 \leq p < 0.70$
4	$0.70 \leq p < 0.95$
5	$p \geq 0.95$

Source: DTN: MO0505SPAROCKM.000_R0 [DIRS 173893].

Table 6.3.2-3. Probability Weighting for the 12 Percolation Flux and Host-Rock Thermal-Conductivity Combinations

Percolation Flux Case	Probability			
	Host-Rock Thermal-Conductivity			
	All	Low	Mean	High
All	1.0000	0.29	0.37	0.34
10%	0.6191	0.1795	0.2291	0.2105
30%	0.1568	0.0455	0.0580	0.0533
50%	0.1645	0.0477	0.0609	0.0559
90%	0.0596	0.0173	0.0220	0.0203

Source: *Multiscale Thermohydrologic Model* (SNL 2007 [DIRS 181383], Table 6.3-47[a]).

Table 6.3.2-4. List of Thermal-Hydrologic Variables Predicted by the MSTHM Process Model and Used in the TSPA-LA Model

Thermal-Hydrologic Variable	Drift-Scale Location
Temperature	Drift wall (perimeter average)
	Drip shield (upper surface)
	Waste package (surface average)
	Invert (average)
Relative humidity	Waste package (surface average)
	Drip Shield (average)
Liquid-phase saturation (intragranular)	Invert (average)
Liquid-phase flux	Invert (average)

Table 6.3.2-5. Alternative Conceptual Model Considered for the Engineered Barrier System Thermal-Hydrologic Environment

Alternative Conceptual Models	Key Assumptions	Screening Assessment and Basis
Mountain-Scale TH Model	An ACM to the MSTHM Process Model is a mountain-scale TH model developed by Lawrence Berkeley National Laboratory (DIRS 174101)). The Lawrence Berkeley National Laboratory model is a monolithic TH model. The Lawrence Berkeley National Laboratory TH model used: (1) coarser grid discretization at the drift scale than the MSTHM Process Model; (2) a line-averaged approximation of the heat-generation-rate-versus-time table (whereas the MSTHM Process Model represented the WPs as discrete heat sources); and (3) a lumped heat source that filled the entire cross section of the emplacement drift (SNL 2007 [DIRS 181383], Section 6.4).	Screened out. Given the differences between the MSTHM Process Model and the east-west cross-sectional Lawrence Berkeley National Laboratory Mountain-Scale Model, the agreement between the two models is adequate (SNL 2007 [DIRS 181383], Section 6.4). Moreover, the differences in predicted temperatures between the MSTHM Process Model and the east-west cross-sectional Lawrence Berkeley National Laboratory Mountain-Scale Model are within the range of temperature differences resulting from parametric uncertainty (SNL 2007 [DIRS 181383], Tables 6.3-30 and 6.3-31).

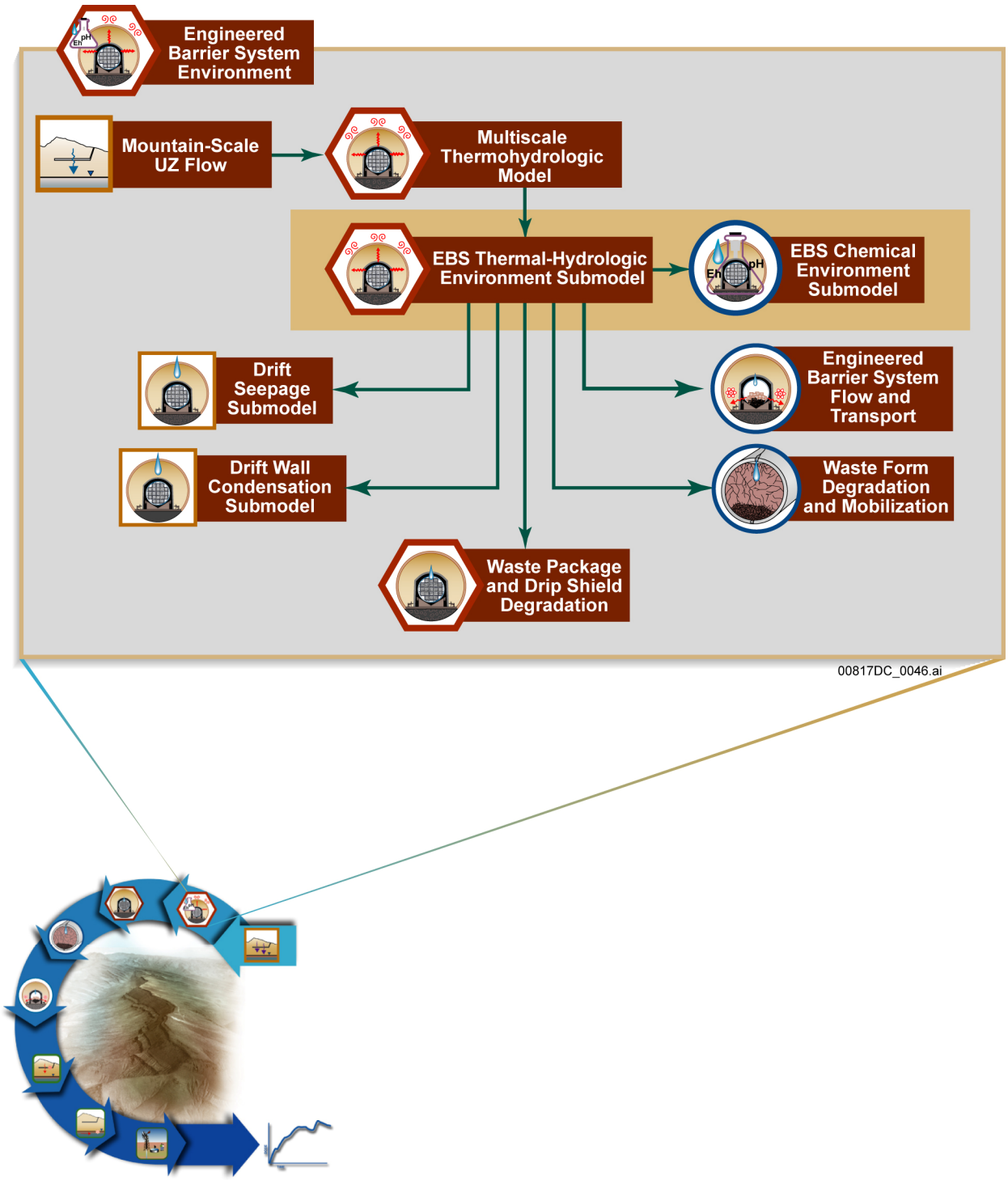

Figure 6.3.2-1. Information Flow Diagram for the EBS Thermal-Hydrologic Environment Submodel

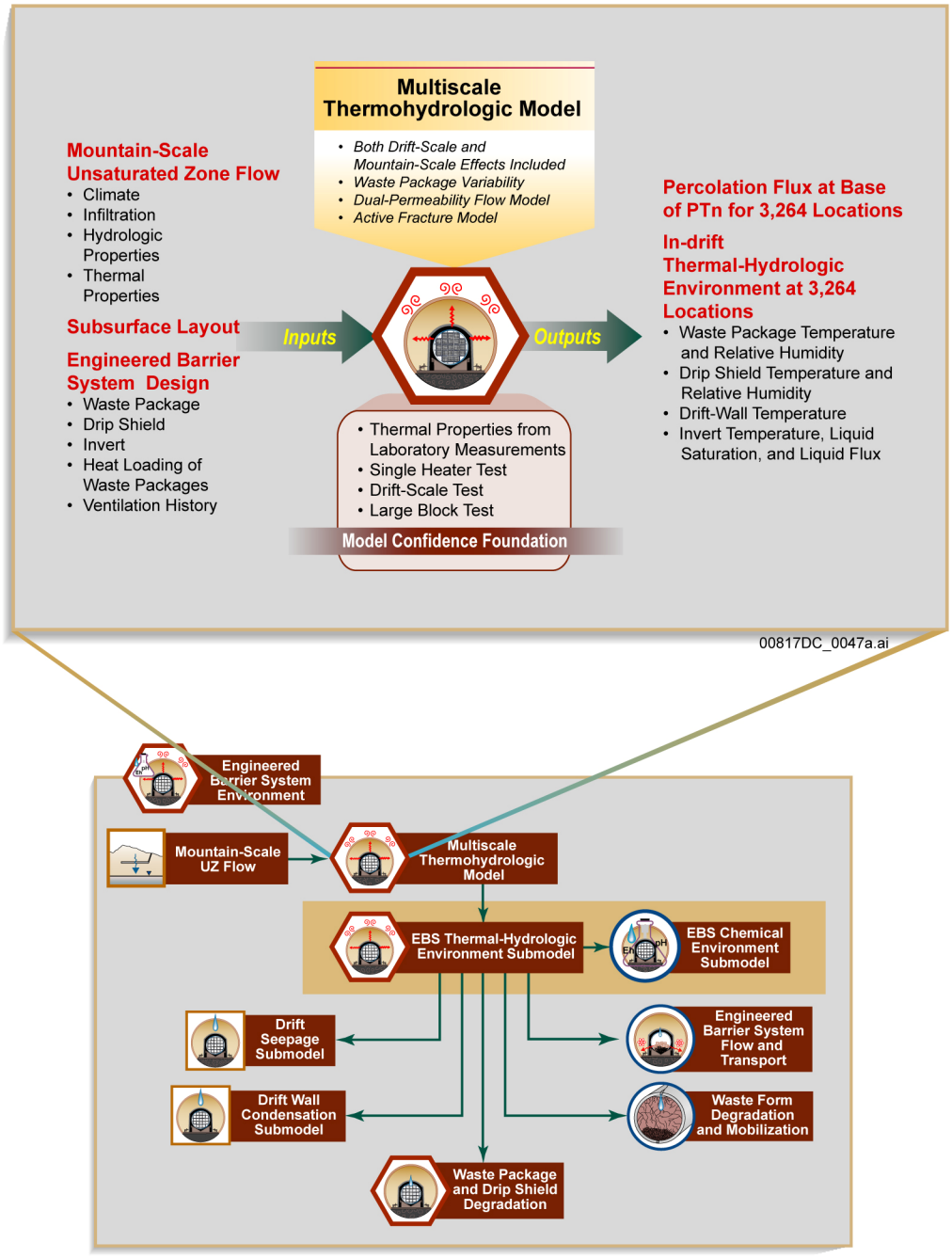

Figure 6.3.2-2. Inputs, Outputs, and Basis for Model Confidence for the Multiscale Thermohydrologic Process Model

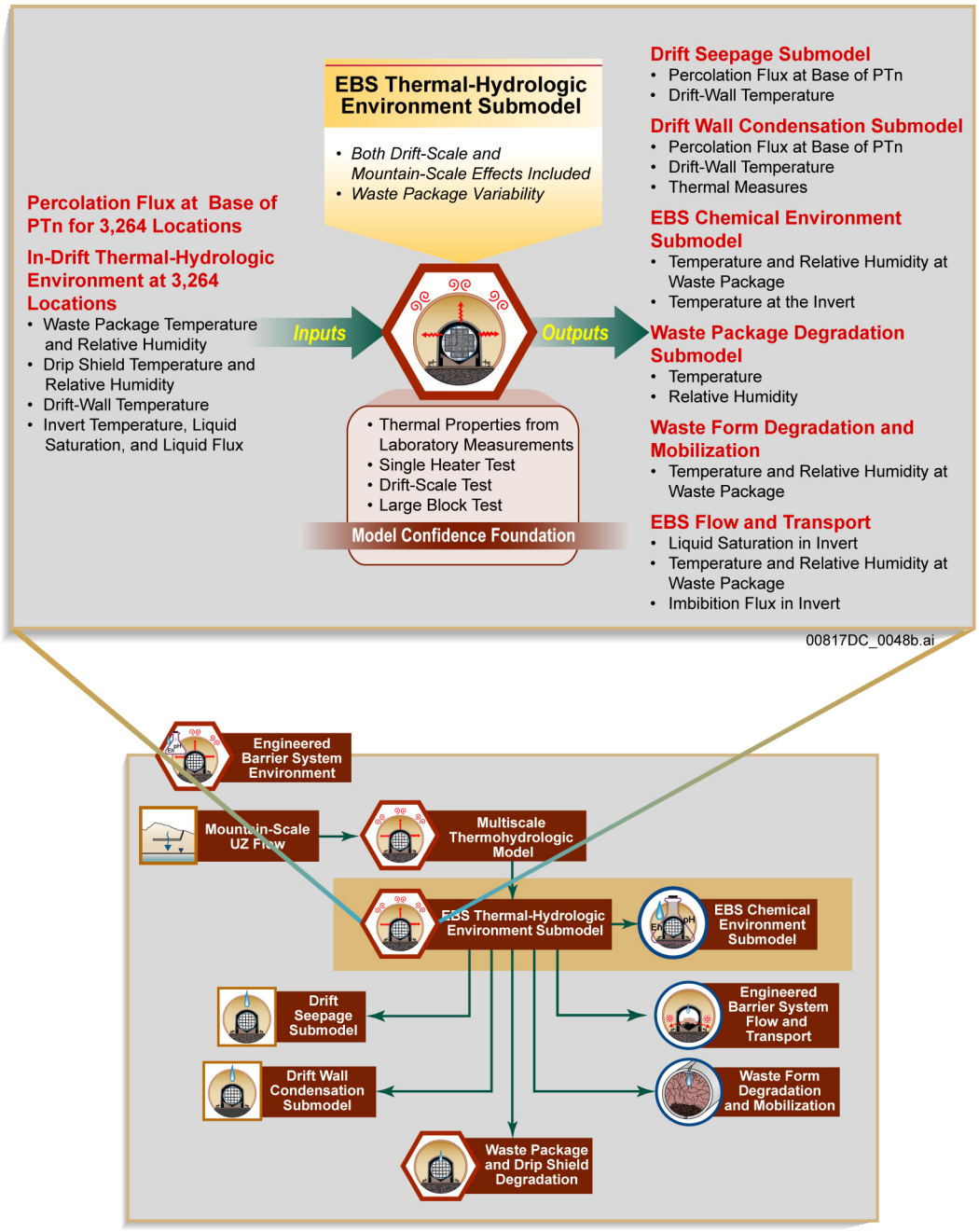

Figure 6.3.2-3. Inputs, Outputs, and Basis for Model Confidence for the EBS Thermal-Hydrologic Environment Submodel

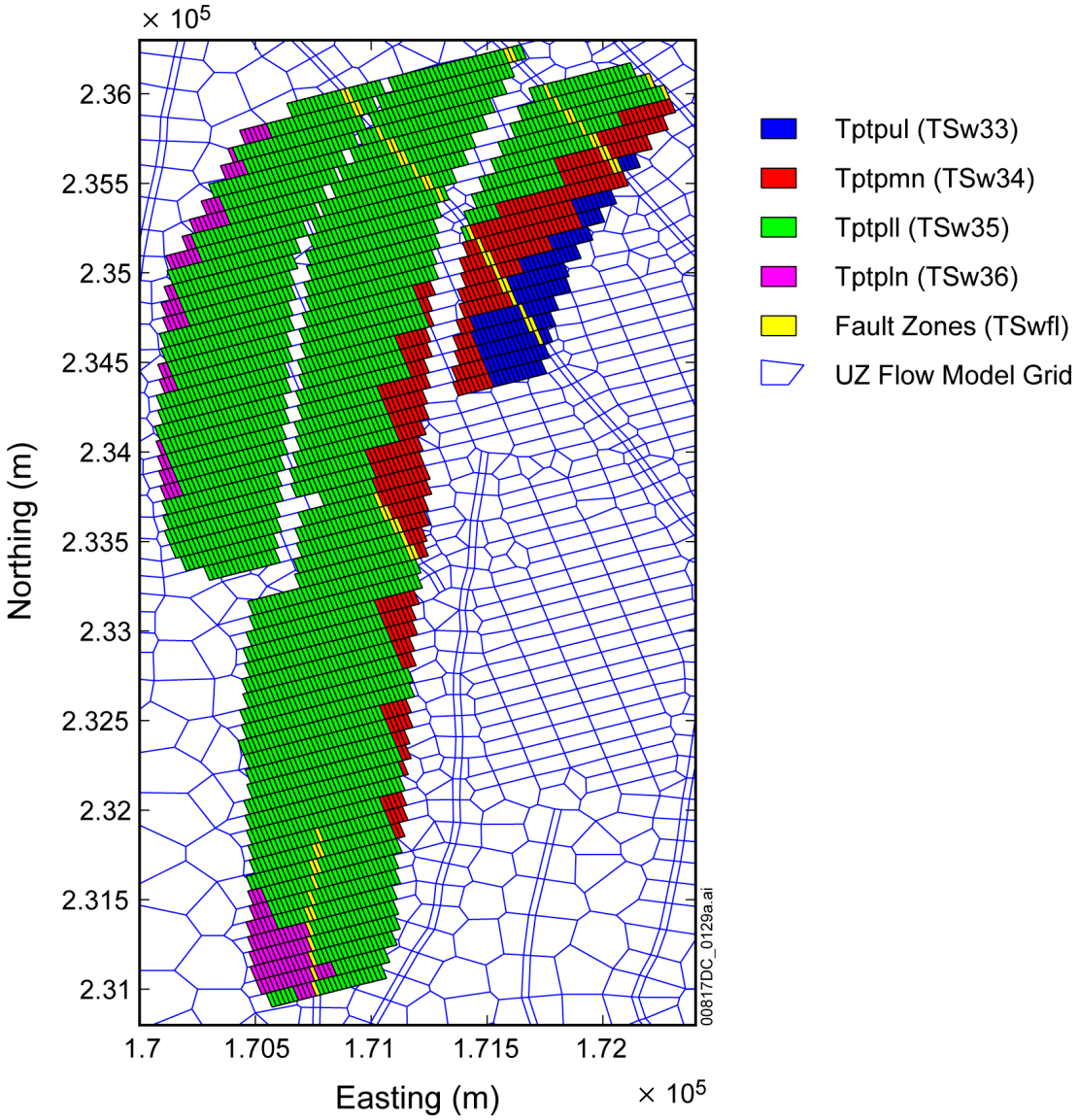

Source: SNL 2007 [DIRS 181383], Figure 6.2-18[a].

NOTES: Also shown are the five representative locations (indicated by circles) that were selected to examine thermal-hydrologic conditions in the four primary host-rock units.

Tptpul = Topopah Spring Tuff crystal-poor upper lithophysal zone; Tptpmn = Topopah Spring Tuff middle nonlithophysal zone; Tptpll = Topopah Spring Tuff crystal-poor lower lithophysal zone; Tptpln = Topopah Spring Tuff lower nonlithophysal zone.

Figure 6.3.2-4. The Distribution of the Four Primary Host-Rock Units is Shown for the Repository Layout Considered in the Multiscale Thermohydrologic Model Calculations for the TSPA-LA Model

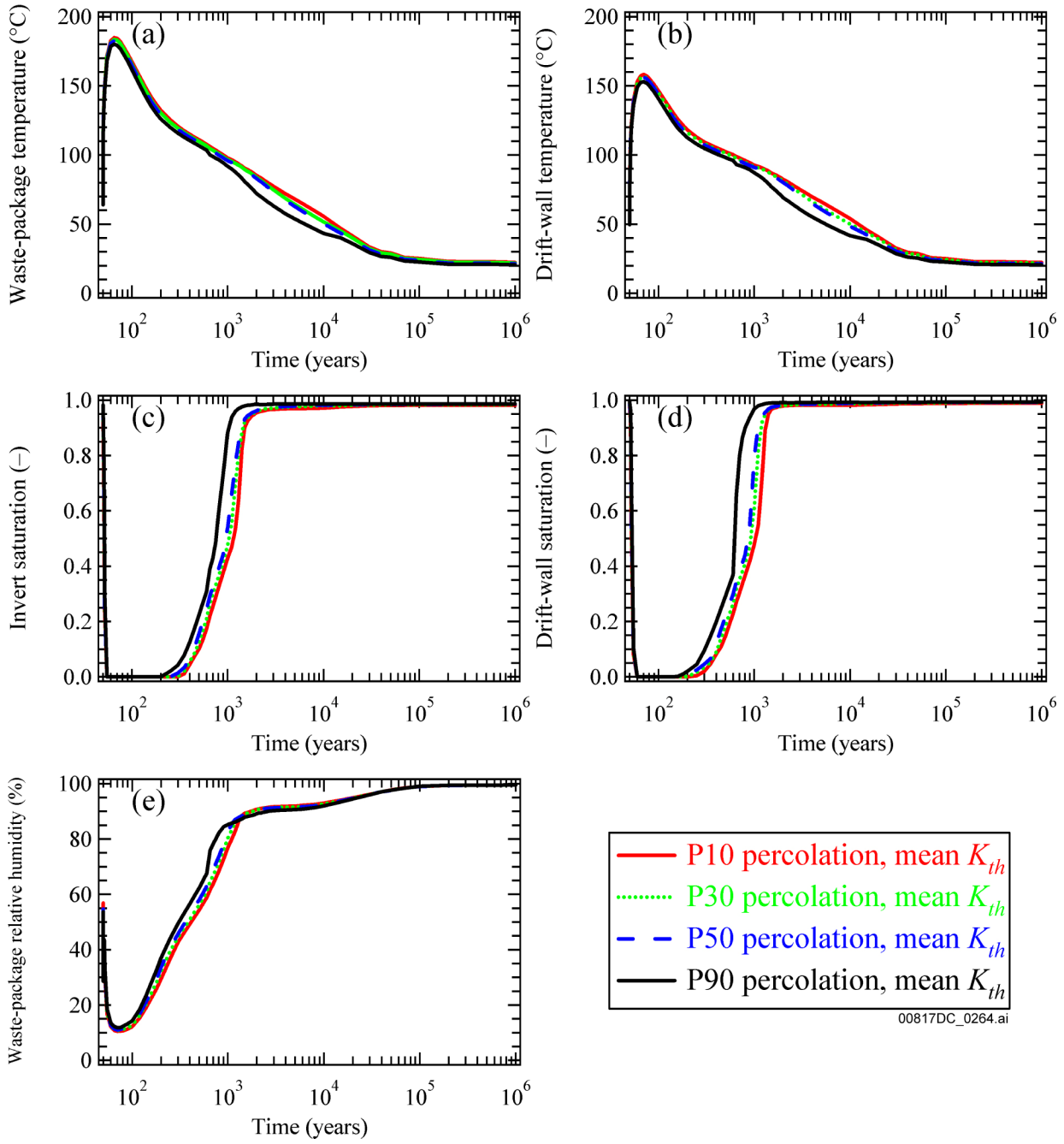

Source: DTNs: LL0703PA011MST.006_R0 [DIRS 179853]; LL0703PA012MST.007_R0 [DIRS 179854]; LL0703PA013MST.008_R0 [179855]; and LL0703PA014MST.009_R0 [DIRS 179856].

NOTE: Plotted thermal-hydrologic variables are: (a) waste-package temperature; (b) drift-wall temperature; (c) invert liquid-phase saturation; (d) drift-wall liquid-phase saturation; and (e) waste-package relative humidity.

Figure 6.3.2-5. Thermal-Hydrologic Conditions for the PWR1-2 Waste Package Plotted for 10th, 30th, 50th and 90th Percentile Percolation-Flux Cases at a Location near the Center of the Repository

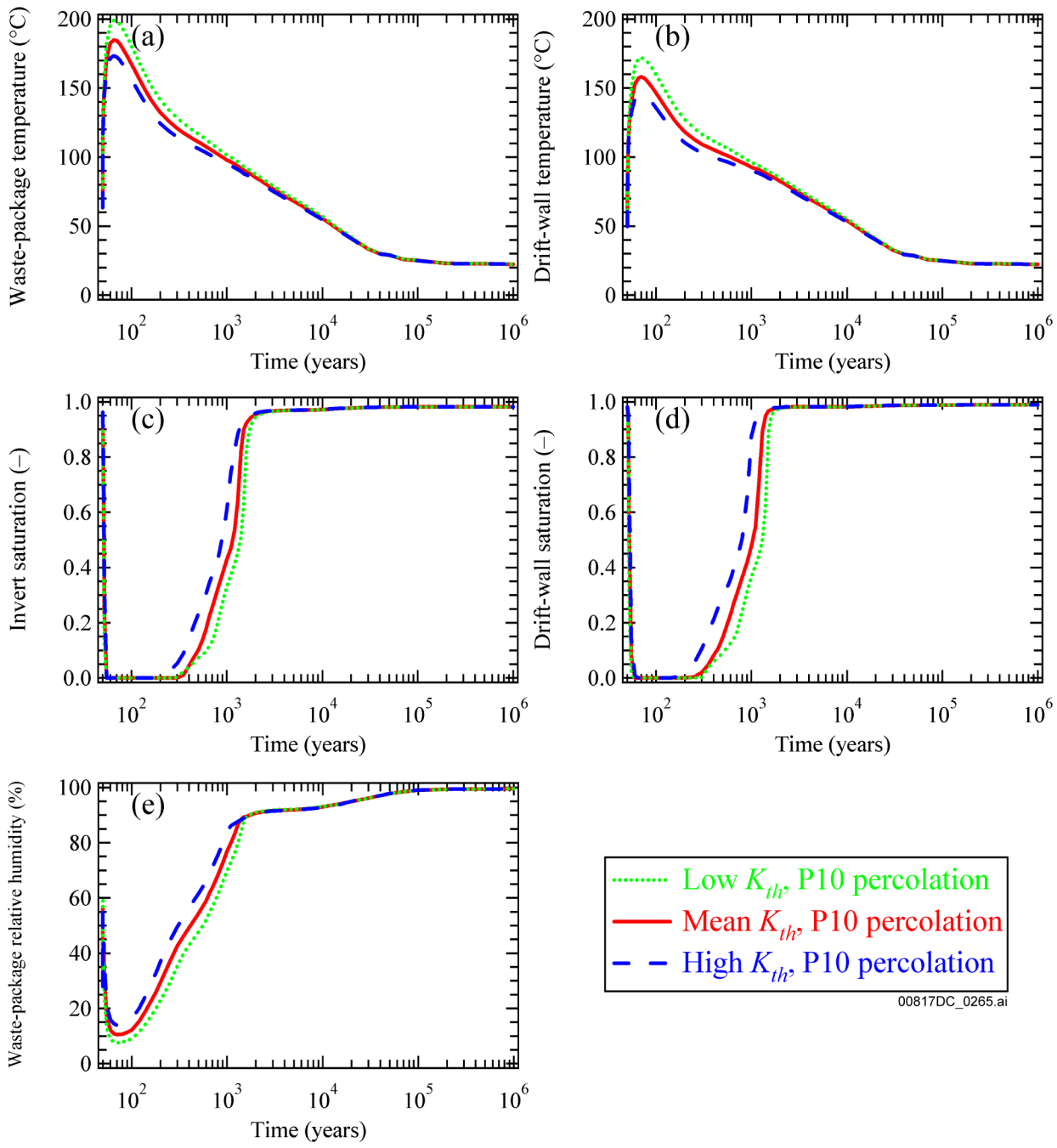

Source: DTNS: LL0703PA011MST.006 _R0 [DIRS 179853]; LL0703PA015MST.010_R0, [DIRS 179857]; and LL0703PA017MST.012_R0 [DIRS 179859].

NOTE: The plotted thermal-hydrologic variables are: (a) waste-package temperature; (b) drift-wall temperature; (c) invert liquid-phase saturation; (d) drift-wall liquid-phase saturation; and (e) waste-package relative humidity.

Figure 6.3.2-6. Thermal-Hydrologic Conditions for the PWR1-2 Waste Packages Plotted for 10th Percentile Percolation Flux Case at a Location Near the Center of the Repository

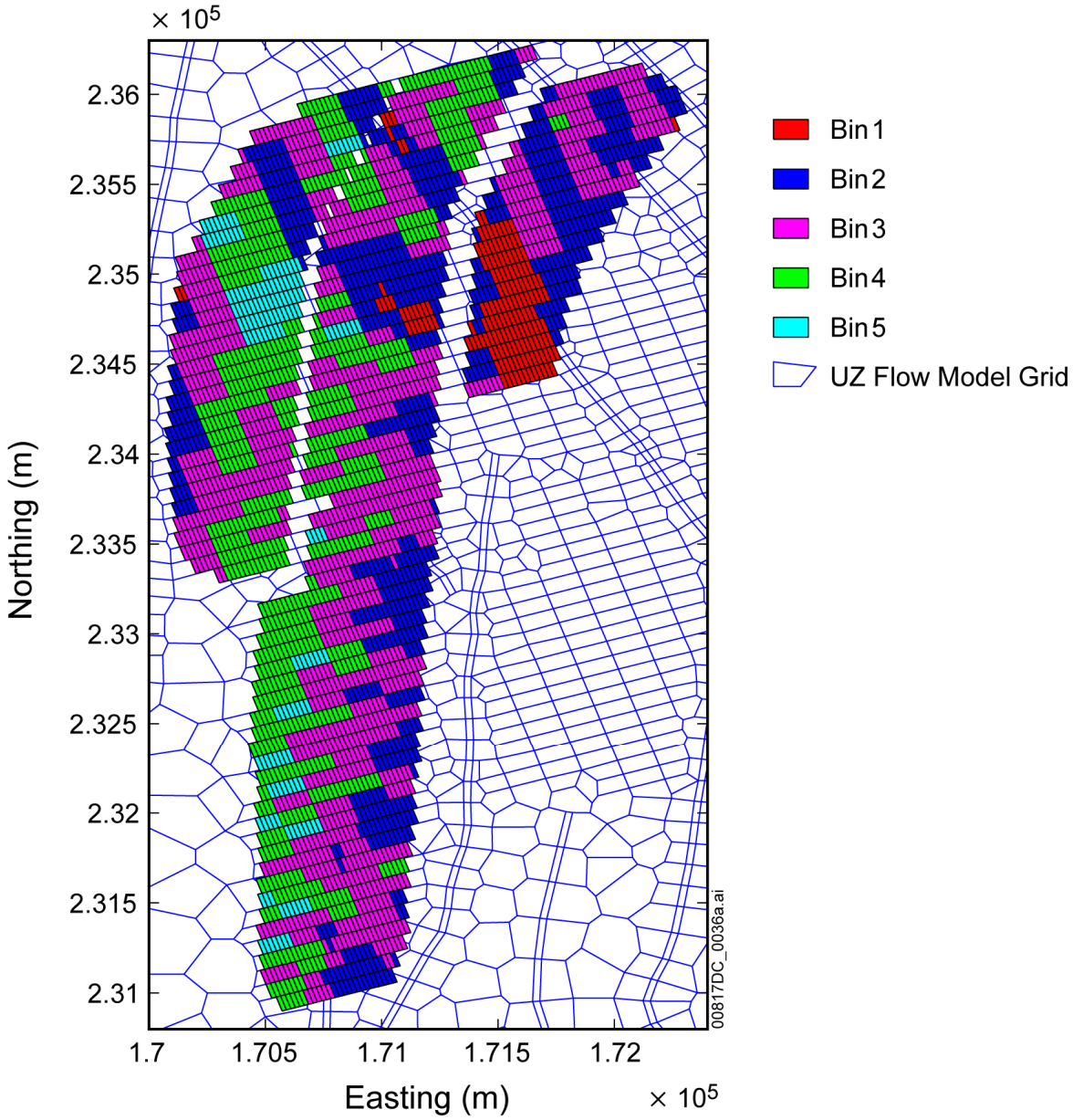

Sources: SNL 2007 [DIRS 181383], Figure VIII-1[a].

Figure 6.3.2-7. Repository Percolation Subregions Used in the TSPA-LA Model (based upon the 30th percentile infiltration case, glacial-transition period)

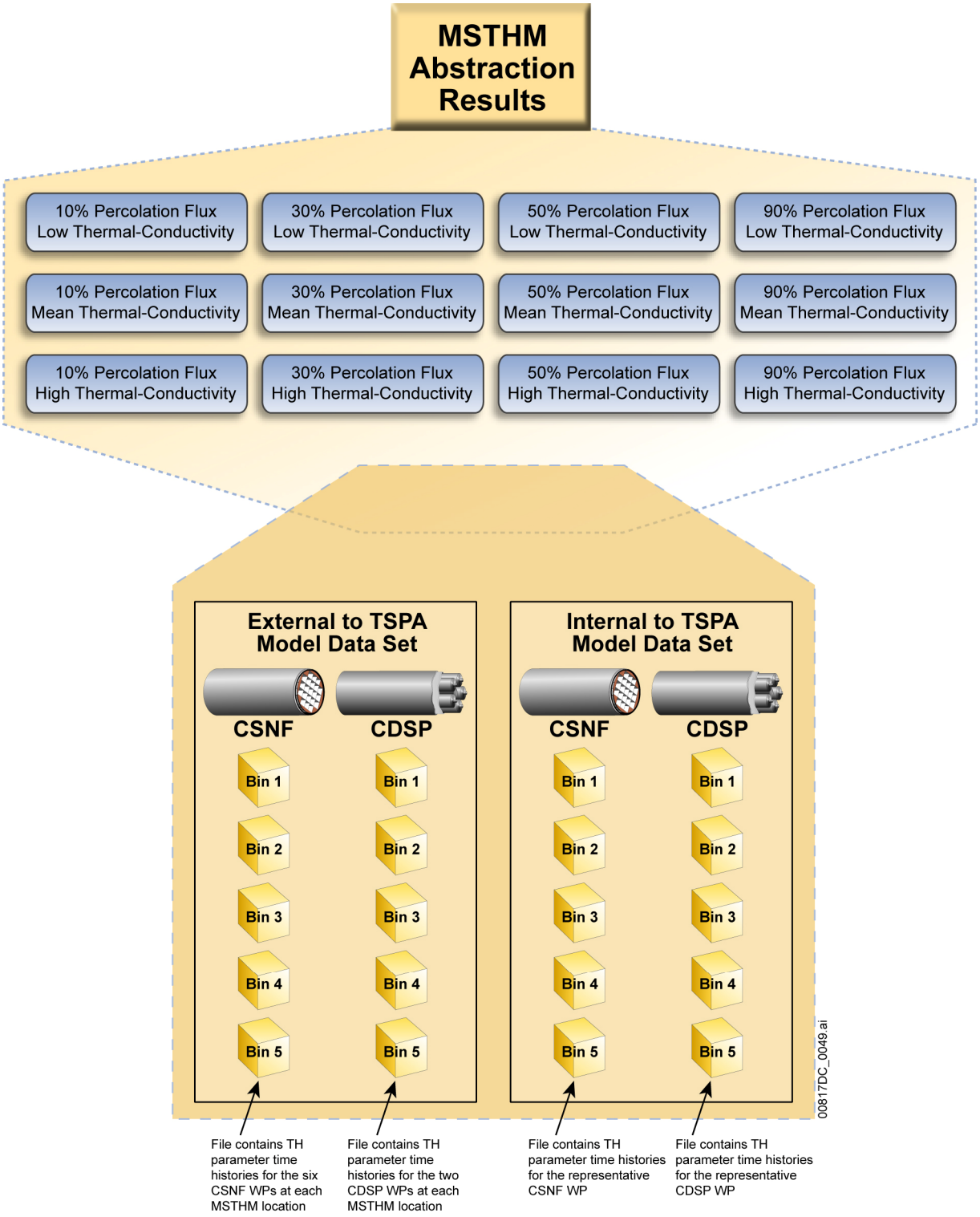

Figure 6.3.2-8. Thermal-Hydrologic Time History Parameter Inputs to the TSPA-LA Model